

博士論文

**Study on improvement of indoor thermal environment of traditional
dwellings based on subdivision of climatic region**

気候地域の細分化に基づく伝統的住居の室内温熱環境改
善に関する研究

2023 年 6 月

鲁 子良

ZILIANG LU

Study on Improvement of Indoor Thermal Environment of Traditional Dwellings based on Subdivision of Climatic Region

ABSTRACT

Under China's requirement to attain a carbon peak by 2030, and in the face of energy consumption dilemmas and environmental crises, decreasing building energy use has gained a widespread concern. Passive design is a climate adaptive design method that can save energy and reduce carbon emissions without using artificial energy resources and effectively improve the building's indoor thermal comfort. And climate conditions are a critical factor in determining the passive design scheme. Climate zoning helps formulate building energy conservation standards and adapt building energy conservation technology according to the region. In addition, as China has a considerable number of rural regions, which occupies 34% of the building area and consumes 22% of the total building energy consumption up to 2020. With a large number of rural dwellings and the ongoing rise of demands for thermal comfort and energy consumption, improving the indoor thermal comfort and reducing building energy consumption in traditional rural dwellings by utilizing their climate adaptability (passive strategies) is of great significance.

CHAPTER 1, RESEARCH BACKGROUND AND PURPOSE OF THE STUDY.

In this chapter, the research discussed China's urbanization process and associated carbon emissions, the current state of energy consumption in rural residential buildings, the principles of ecological architecture and passive design strategies, and the climate adaptability of traditional dwellings. Given the large number of rural dwellings and the growing demand for residents' thermal comfort, as well as the pressing need to reduce building energy consumption, leveraging the climate adaptability of traditional dwellings through passive strategies represents a promising approach for improving indoor thermal comfort and reducing energy use in rural areas. This has significant implications for addressing China's energy consumption and environmental challenges.

CHAPTER 2, LITERATURE REVIEW. This chapter provides a comprehensive review of the relevant research pertaining to this paper, including the literature review on climatic subdivision, thermal comfort, and passive design strategy. Previous studies have mainly focused on existing climate zones and single aspects such as residential thermal environment, thermal comfort, and energy consumption. However, there has been limited research on behavior adjustment methods in thermal adaptation,

particularly in the relationship between climate adaptation and thermal comfort renovation. Hence, it is important to investigate the improvement of indoor thermal comfort in traditional residential buildings in the Qinba mountainous area based on a thorough investigation of thermal comfort in the context of climate subdivision.

CHAPTER 3, RESEARCH METHODOLOGY. The main work of this paper is Qinba mountainous area's climatic subdivision, residents' thermal comfort investigation, and dwellings' passive strategy optimization. Therefore, the methodologies employed in this research, including spatial interpolation method, field survey method, computer simulation method, statistical analysis method, and multi-objective optimization method, are summarized in Chapter 3. These methods can help us organize and classify the meteorological data, calculate the thermal comfort indicators, simulate building energy consumptions before and after renovation of passive strategies, and ultimately obtain the optimal optimization solutions for each climatic sub-region.

CHAPTER 4, CLIMATIC SUBDIVISIONS IN QINBA MOUNTAINOUS AREA. In this chapter, the research utilized Co-Kriging spatial interpolation and computer simulation methods to subdivide the Qinba mountainous area into 5 climatic sub-regions and classified the supplementary climatic elements to describe the region's climatic characteristics. Firstly, based on Co-Kriging spatial interpolation method, by applied the value of HDD18 and CDD26 in the past decade, the Qinba mountainous area are divided in 5 climatic sub-regions. In addition, the Co-Kriging method was applied to add supplementary meteorological information, including relative humidity, wind speed, and solar radiation, to the 5 climatic sub-regions. Subsequently, the climatic conditions and annual thermal loads of buildings in representative counties within each sub-region were analyzed. The findings indicate that the variation trends of meteorological elements and annual thermal loads of buildings in each climatic sub-region are consistent with the climate subdivision logic of the Qinba mountainous area.

CHAPTER 5, FIELD SURVEY AND TRADITIONAL DWELLING' ENVIRONMENTAL MEASUREMENT IN THE CLIMATIC SUB-REGIONS. In this chapter, the research summarized the characteristics of traditional settlements, courtyards, and residential dwellings by using the field survey method, and conducted the environmental parameter measurements in the 5 climatic sub-regions. Firstly, based on the mountainous topography and location of settlements in the study area, 3 types of settlements were identified, including the settlement in the gully, settlement leaning against the mountain, and settlement on the mountain slope. Then, the building layout of traditional dwellings was categorized into 4 types: "I"-shaped, "L"-shaped, "U"-shaped, and "□"-shaped dwelling. Additionally, courtyards were classified into 3

types: open, semi-open, and closed courtyard. Lastly, the research team conducted multiple investigations on traditional dwellings during winter and summer in the 5 climatic sub-regions, revealing that the study area experiences low temperature with high humidity in winters and moderate temperatures with high humidity in summers.

CHAPTER 6, THERMAL COMFORT INVESTIGATION OF THE CLIMATIC SUB-REGIONS. This chapter aims to compare the indoor thermal environment of traditional dwellings in the 5 climatic sub-regions of Qinba mountainous area, as well as investigate the thermal sensation of residents, by utilizing field survey, statistical analysis, and computer simulation methods. Firstly, the study conducted outdoor and indoor environmental parameter measurements along with thermal sensation questionnaires from residents. Then, the obtained data was used to calculate thermal comfort equations for each climatic sub-region using linear regression analysis of mean thermal sensation voting (MTS) and indoor operating temperature (T_{op}). From these equations, the neutral temperatures and thermal comfort ranges were calculated. Finally, the annual building thermal loads of typical traditional dwellings in the 5 climatic sub-regions were simulated based on both standard requirements and the measured neutral temperature. It was found that the annual thermal loads based on the measured neutral temperature were significantly lower than those based on standard requirements.

CHAPTER 7, EFFECTIVENESS STUDY OF PASSIVE DESIGN PARAMETERS FOR TRADITIONAL DWELLING. In this chapter, by using computer simulation, statistical analysis, and orthogonal arrays method, the effectiveness of passive design parameters was evaluated in each sub-region, and the single-objective optimization approaches to enhance the building energy efficiency of the passive design strategies were obtained. Firstly, for the single controlled variable study, the 4 effective passive renovation parameters (the sunroom depth, the heat transfer coefficient of exterior wall, roof, and window) for traditional dwellings were selected based on energy consumption analysis and relative sensitivity coefficient calculation. Then, for the multi controlled variable study, this research utilized orthogonal arrays analysis to assess the effectiveness of 4 parameters and obtain the optimal combination, resulting in a significant reduction in the building's annual thermal load.

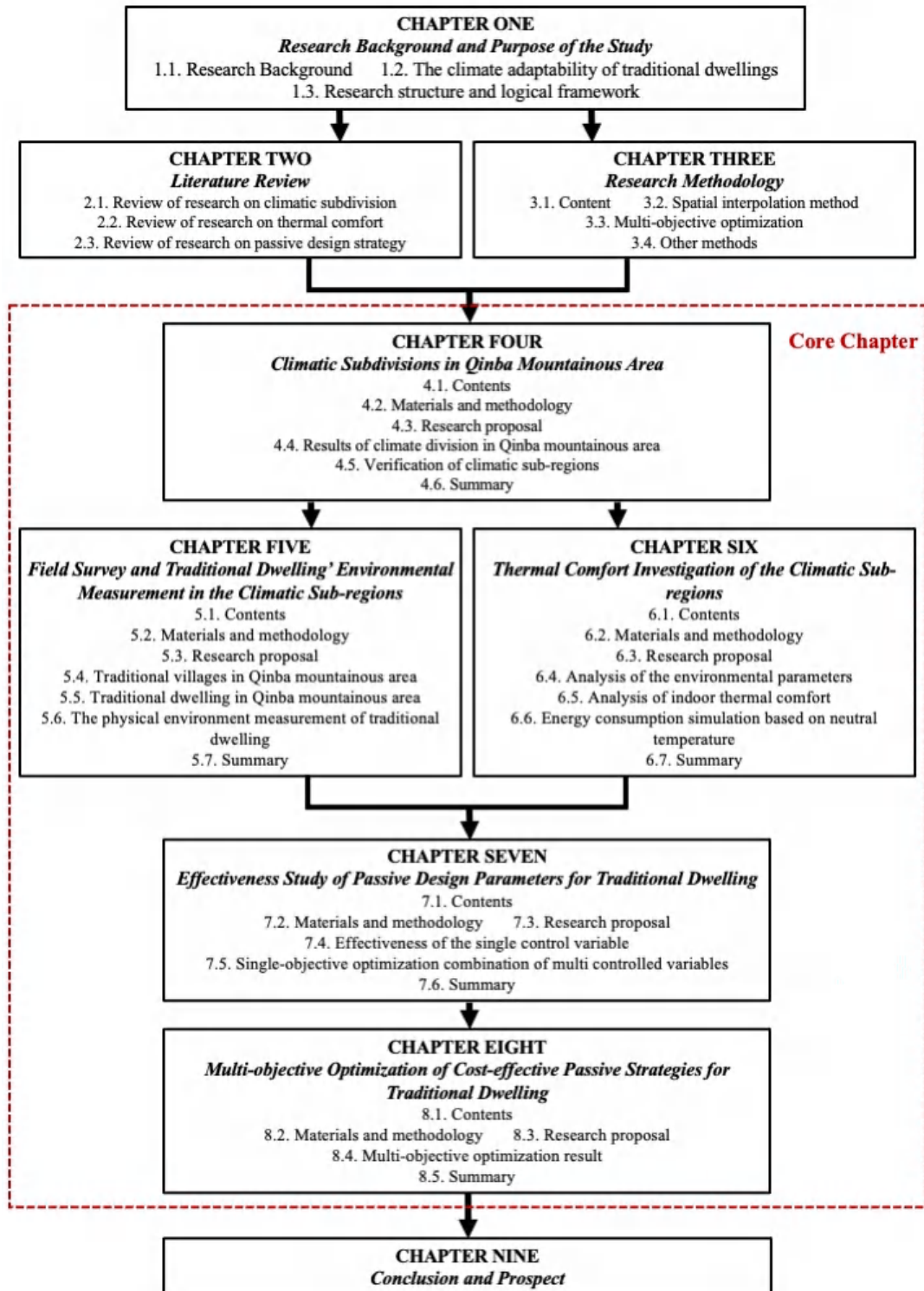
CHAPTER 8, MULTI-OBJECTIVE OPTIMIZATION OF COST-EFFECTIVE PASSIVE STRATEGIES FOR TRADITIONAL DWELLING. This chapter employs computer simulations, statistical analysis, NSGA-2, and TOPSIS method to optimize passive design strategies for traditional dwellings in the 5 climatic sub-regions with 3 objectives of improving building energy efficiency, thermal comfort,

and cost-effectiveness using multi-objective optimization approaches. To begin with, the study fitted multiple regression equations based on 4 effective passive design parameters to determine the building's annual thermal load, proportion of uncomfortable hours, and renovation investment for each sub-region. Then, by using the NSGA-2 method, we identified a set of Pareto optimal solutions based on a multi-regression equation with the 3 objectives in each sub-region. In addition, the research employed the TOPSIS method to calculate the Euclidean distance and obtain 20 optimal solutions in each sub-region. Finally, the study simulated the building's annual thermal loads and indoor comfort values for the optimal renovated dwelling in each of the climatic sub-regions. The optimal combination leads to a noteworthy decrease in the building's annual thermal load.

CHAPTER 9, CONCLUSION AND PROSPECT. The conclusion of whole thesis is deduced, and the future work has been discussed.

Keywords: Qinba mountainous area, climatic subdivision, thermal comfort, thermal load, passive strategy, multi-objective optimization

Study on Improvement of Indoor Thermal Environment of Traditional Dwellings in Qinba Mountainous Area based on Subdivision of Climatic Region



CONTENTS

ABSTRACT	I
STRUCTURE OF THIS PAPER	V

CHAPTER 1: RESEARCH BACKGROUND AND PURPOSE OF THE STUDY

1.1. Research background	1-1
1.1.1. Energy consumption in China’s construction industry	1-1
1.1.2. The current energy consumption status of rural residential buildings in China	1-4
1.2. The climate adaptability of traditional dwellings	1-5
1.2.1. Overview of climate adaptability research on traditional dwellings	1-5
1.2.2. Passive design strategies.....	1-10
1.2.3. The case study of building climate adaptability	1-12
1.2.4. Qinba mountainous area	1-15
1.2.5. The research gap	1-16
1.3. Research structure and logical framework	1-16
1.3.1. Research purpose and significance.....	1-16
1.3.2. Research content.....	1-18
1.3.2. Chapter content overview and related instructions.....	1-19
Reference	1-23

CHAPTER 2: LITERATURE REVIEW

2.1. Review of research on climatic subdivision	2-1
2.1.1. Overview of climatic subdivision.....	2-1
2.1.2. Main evaluation indicators for climatic subdivision	2-4
2.1.3. China’s current climate zoning standards.....	2-5
2.1.4. Research prospect	2-7
2.2. Review of research on thermal comfort	2-8
2.2.1. Overview of thermal comfort	2-9
2.2.2. Thermal comfort index	2-13
2.2.3. Research prospect	2-18
2.3. Review of research on passive design strategy	2-18
2.3.1 Overview of passive design strategy	2-19
2.3.2 Research prospect	2-22
Reference	2-23

CHAPTER 3: RESEARCH METHODOLOGY

3.1. Content	3-1
3.2. Spatial interpolation method	3-2
3.2.1. Overview of spatial interpolation method	3-2
3.2.2. Classification of spatial interpolation method	3-3
3.2.3. Kriging spatial interpolation method	3-4
3.2.4. The application of spatial interpolation method in the research	3-7
3.3. Multi-objective optimization	3-8
3.3.1. Overview of multi-objective optimization	3-8
3.3.2. Multi-objective optimization (NSGA-2)	3-8
3.3.3. Multi-objective decision-making (TOPSIS)	3-11
3.3.4. The application of multi-objective optimization in the research	3-12
3.4. Other methods	3-12
3.4.1. Data statistics method	3-13
3.4.2. Field survey method	3-16
3.4.3. Computer energy consumption simulation	3-19
Reference	3-21

CHAPTER 4: CLIMATIC SUBDIVISIONS IN QINBA MOUNTAINOUS AREA

4.1. Content	4-1
4.2. Materials and methodology	4-1
4.2.1. Research background	4-1
4.2.2. Study area	4-2
4.2.3. Motivation	4-6
4.2.4. Method and data source	4-7
4.3. Research proposal	4-8
4.3.1. Climatic subdivision	4-8
4.3.2. Supplementary elements of climatic sub-regions	4-8
4.3.3. Verification of climatic sub-regions	4-9
4.4. Results of climate division in Qinba mountainous area	4-9
4.4.1. Climatic sub-regions in Qinba mountainous area	4-9
4.4.2. Supplementary elements of climatic sub-regions in Qinba mountainous area	4-14
4.5. Verification of climatic sub-regions	4-21
4.5.1. The climate conditions of the 5 climatic sub-regions	4-21
4.5.2. Building energy simulation in each climatic sub-region	4-31
4.6. Summary	4-34
Reference	4-36

CHAPTER 5: FIELD SURVEY AND TRADITIONAL DWELLING' ENVIRONMENTAL MEASUREMENT IN THE CLIMATIC SUB-REGIONS

5.1. Contents	5-1
5.2. Materials and methodology	5-1
5.2.1. Research background.....	5-1
5.2.2. Research scope	5-2
5.2.3. Method.....	5-3
5.3. Research proposal	5-3
5.4. Traditional villages in Qinba mountainous area	5-4
5.4.1. Settlements' site selection and characteristics	5-4
5.4.2. Case study.....	5-5
5.4.3. The settlement climate suitability strategy in Qinba mountainous area	5-8
5.5. Traditional dwelling in Qinba mountainous area	5-9
5.5.1. Courtyard form	5-10
5.5.2. Building function and form	5-12
5.5.3. Building structure	5-16
5.5.4. Building construction	5-17
5.6. The physical environment measurement of traditional dwelling	5-19
5.6.1. Traditional dwelling in climatic sub-region A1	5-20
5.6.2. Traditional dwelling in climatic sub-region A2.....	5-24
5.6.3. Traditional dwelling in climatic sub-region B1	5-28
5.6.4. Traditional dwelling in climatic sub-region B2.....	5-32
5.6.5. Traditional dwelling in climatic sub-region C.....	5-36
5.7. Summary	5-41
Reference	5-43

CHAPTER 6: THERMAL COMFORT INVESTIGATION OF THE CLIMATIC SUB-REGIONS

6.1. Contents	6-1
6..2. Materials and methodology	6-1
6.2.1. Research background.....	6-1
6.2.2. Motivation	6-2
6.2.3. Summary of traditional dwellings	6-2
6.2.4. Method.....	6-5
6.3. Research proposal	6-6

6.3.1. Measurement of environmental parameters	6-7
6.3.2. Questionnaire research	6-7
6.4. Analysis of the environmental parameters	6-8
6.4.1. Temperature	6-9
6.4.2. Relative humidity	6-10
6.5. Analysis of indoor thermal comfort	6-11
6.6.1. Thermal environment evaluation index	6-11
6.6.2. Residents' thermal adaptive behavior analysis	6-12
6.6.3. Residents' indoor thermal sensation vote	6-13
6.6.4. Neutral temperature	6-15
6.6.5. Thermal comfort range	6-17
6.6.6. The relationship of MTS and PMV	6-17
6.6. Energy consumption simulation based on neutral temperature in climatic sub-regions	6-20
6.6.1. Energy consumption simulation	6-20
6.6.2. Simulation result analysis	6-21
6.6.3. Suggestion on improving indoor thermal environment	6-22
6.7. Summary	6-23
Reference	6-25

CHAPTER 7: EFFECTIVENESS STUDY OF PASSIVE DESIGN PARAMETERS FOR TRADITIONAL DWELLING

7.1. Contents	7-1
7.2. Materials and methodology	7-1
7.2.1. Research background.....	7-1
7.2.2. Method.....	7-3
7.3. Research proposal.....	7-3
7.4. Effectiveness of the single control variable	7-4
7.4.1. Passive design parameters	7-4
7.4.2. Single control variable analysis.....	7-4
7.4.3. Effectiveness identification of single control variable	7-22
7.5. Single-objective optimization combination of multi controlled variables	7-29
7.5.1. Single-objective optimization.....	7-29
7.5.2. Evaluation of the optimal combination of the multi controlled variables by orthogonal method	7-30
7.5.3. Simulation of the optimization model of traditional dwellings.....	7-32
7.5.4. Temperature and humidity simulation of the traditional dwelling before and after optimization	7-33

7.6. Summary	7-35
Reference	7-37

CHAPTER 8: MULTI-OBJECTIVE OPTIMIZATION OF COST-EFFECTIVE PASSIVE STRATEGIES FOR TRADITIONAL DWELLING

8.1. Contents	8-1
8.2. Materials and methodology	8-1
8.2.1. Method	8-2
8.2.2. Model setting	8-3
8.3. Research proposal	8-3
8.3.1. Multi-objective optimization model.	8-3
8.3.2. The multi-objectives	8-4
8.3.3. Multiple regression model	8-5
8.3.4. NSGA-2 genetic algorithm	8-6
8.3.5. The TOPSIS decision-making method	8-6
8.4. Multi-objective optimization result	8-7
8.4.1. The fitting of multiple regression equations.	8-7
8.4.2. Decision-making of the passive design strategy	8-8
8.4.3. Thermal loads simulation of the optimized dwelling	8-16
8.4.3. Thermal comfort improvement of the optimized dwelling	8-17
8.5. Summary	8-24
Reference	8-26

CHAPTER 9: CONCLUSION AND PROSPECT

9.1. Conclusion	9-1
9.2. Prospect	9-5

Chapter 1

***RESEARCH BACKGROUND AND PURPOSE OF
THE STUDY***

CHAPTER ONE: RESEARCH BACKGROUND AND PURPOSE OF THE STUDY

<i>RESEARCH BACKGROUND AND PURPOSE OF THE STUDY</i>	1
1.1. Research background.....	1
1.1.1. Energy consumption in China’s construction industry	1
1.1.2. The current energy consumption status of rural residential buildings in China	4
1.2. The climate adaptability of traditional dwellings	5
1.2.1. Overview of climate adaptability research on traditional dwellings	5
1.2.2. Passive design strategies.....	10
1.2.3. The case study of building climate adaptability	12
1.1.5. Qinba mountainous area	15
1.2.4. The research gap	16
1.3. Research structure and logical framework	16
1.3.1. Research purpose and significance	16
1.3.2. Research content.....	18
1.3.3. Chapter content overview and related instructions.....	19
Reference	23

1.1. Research background

1.1.1. Energy consumption in China’s construction industry

China is presently experiencing a crucial phase of rapid urbanization. In 2012, China’s urbanization rate surpassed 50% for the first time, reaching 58.52% in 2017. Projections indicate that it is expected to reach 70% by 2030 [1]. However, the energy consumption structure dominated by coal has directly led to the environmental pollution and emission-intensive characteristics of China’s urbanization process. Urbanization and industrialization are closely intertwined, and the energy-intensive and expansive economic growth model that emerged during China’s rapid urbanization and industrialization inherently limits the significant reduction of carbon emissions in the short term [2].

Meanwhile, China is actively formulating and implementing effective policies and approaches to achieve peak carbon dioxide emissions by 2030 and is committed to being carbon neutral by 2060 [3]. Since 2020, China is responsible for 26.1% of world greenhouse gas emissions, and has been the world’s greatest energy consumer and carbon emitter [4]. In China, the building sector accounts for approximately 40% of energy consumption and 36% of carbon dioxide emissions, which could be a real challenge to the Chinese construction industry to increase energy efficiency and reduce energy consumption, while it is an opportunity for research academics [5].

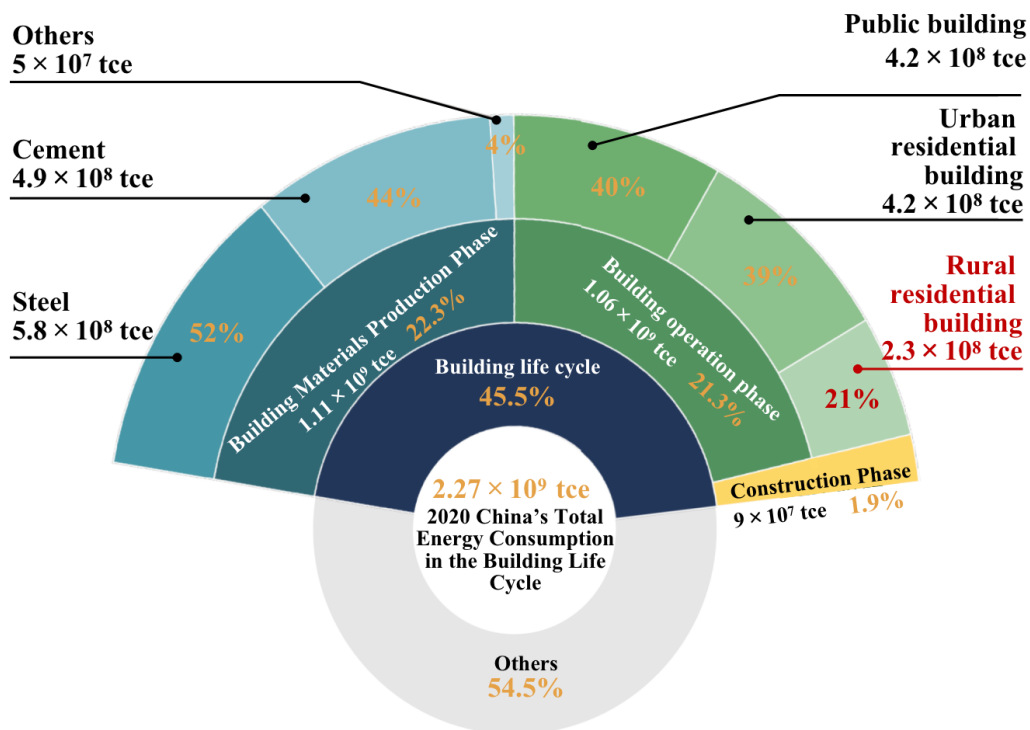


Figure 1-1. The total energy consumption and proportion of China’s building life cycle in 2020

Source: 2022 Research Report of China Building Energy Consumption and Carbon Emissions

As shown in Figure 1-1, in 2020, the total energy consumption of China’s building life cycle was 2.27 billion metric tons of standard coal(tce), accounting for 45.5% of the country’s total energy consumption. Among them, the energy consumption in the building materials production phase, construction phase, and building operation phase were 1.1 billion tce, 0.09 billion tce, and 1.06 billion tce, respectively, accounting for 22.3%, 1.9%, and 21.3% of the country’s total energy consumption. Specifically, the energy consumption of urban residential buildings and rural residential buildings were 0.42 billion tce and 0.23 billion tce, respectively, accounting for 39% and 21% of the energy consumption in the building operation phase [6].

As shown in Figure 1-2, the total carbon emissions from China’s building life cycle were 5.08 billion metric tons of CO₂ (tCO₂), accounting for 50.9% of the country’s total carbon emissions. Among them, the carbon emissions from the building materials production phase, construction phase, and building operation phase had similar proportions to the building energy consumption, accounting for 28.2%, 1.0%, and 21.7% of the country’s total carbon emissions, respectively. Specifically, the carbon emissions from urban residential buildings and rural residential buildings were 0.83 billion tCO₂ and 0.43 billion tCO₂, respectively, accounting for 38% and 20% of the carbon emissions in the building operation phase [6].

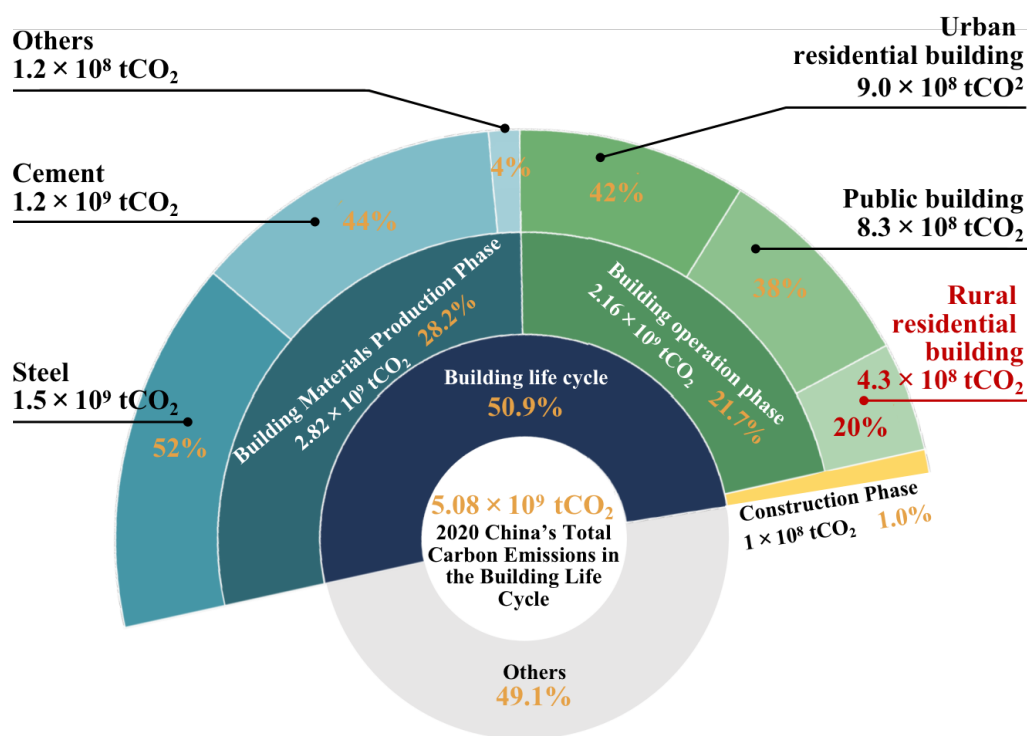


Figure 1-2. The total carbon emissions and proportion of China’s building life cycle in 2020
 Source: 2022 Research Report of China Building Energy Consumption and Carbon Emissions

As a result, the construction industry plays a significant role in energy consumption and carbon emissions. In terms of the trends in operational energy consumption and carbon emissions of buildings, shown in Figure 1-3, from 2005 to 2020, the energy consumption during

the operation stage of buildings increased by 0.58 billion tce, with an average annual growth rate of 5.4%. The carbon emissions during the operation stage increased by 1.07 billion tCO₂, with an average annual growth rate of 4.7% [6]. The energy consumption in building operations has shown a gradual increase over the years. Although the growth rate has slowed down, it remains a crucial factor in overall energy consumption.

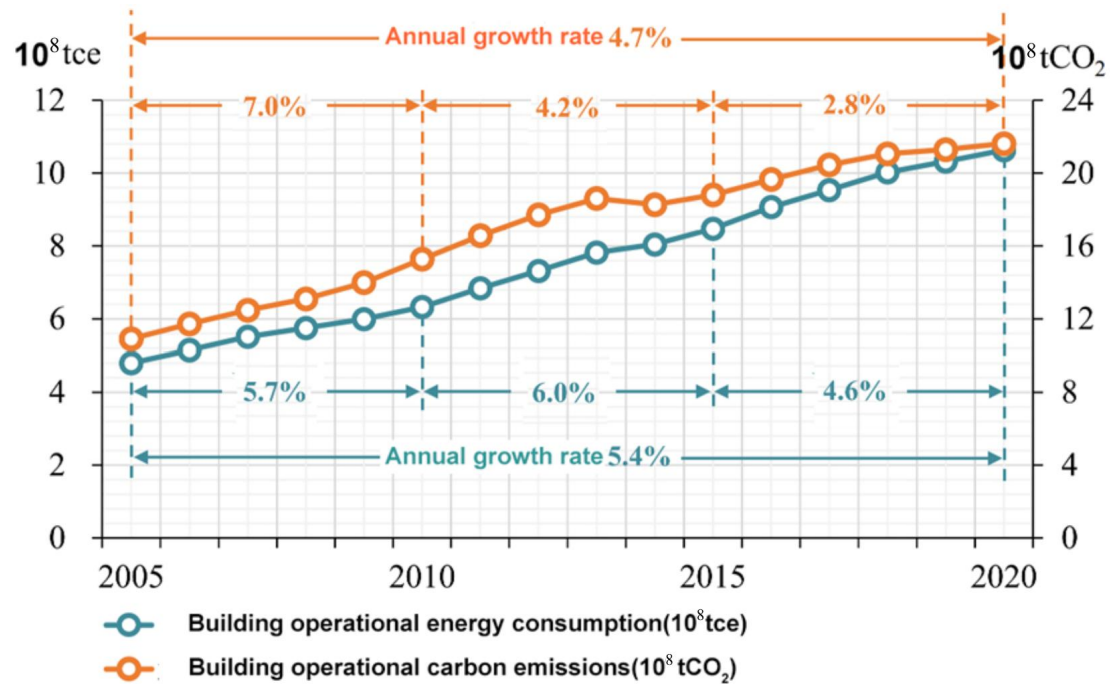


Figure 1-3. Trends in operational energy consumption and carbon emissions of buildings
 Source: 2022 Research Report of China Building Energy Consumption and Carbon Emissions

The energy consumption in building operations is closely related to the building area and energy consumption per unit area. As shown in Figure 1-3 and 1-4, according to the data from the seventh national census of China, the total building area in China in 2020 was estimated to be 69.6 billion square meters, of which 80% were residential buildings and 20% were public buildings. Among them, rural residential buildings accounted for 23.3 billion square meters, which is 34% of the total building area, and the corresponding building energy consumption and carbon emissions accounted for 22% and 20%, respectively. Urban residential buildings accounted for 32 billion square meters, which is 39% of the total building area, and the corresponding building energy consumption and carbon emissions accounted for 46% and 42%, respectively. The data shows that the per unit area energy consumption and carbon emissions of rural residential buildings are lower than those of urban residential buildings (5, 6).

Furthermore, maintaining a comfortable indoor environment in most contemporary buildings necessitates significant energy consumption. Residential buildings' heating and cooling load accounts for roughly 10% of the world's total energy consumption [7]. In this context, traditional dwellings located in the rural areas, using local materials and traditional construction

techniques, could be explored as a potential solution for reducing energy consumption while still maintaining a comfortable indoor thermal environment [8, 9]. However, despite their potential benefits, many traditional buildings have been self-built based on the traditional experience without scientific and technical guidance, which according to some research, fails to meet residents' requirements [10-12]. As a result, there is growing scholarly interest in developing energy-saving design strategies combined with the climate adaptive solutions of traditional dwellings that can improve thermal comfort.

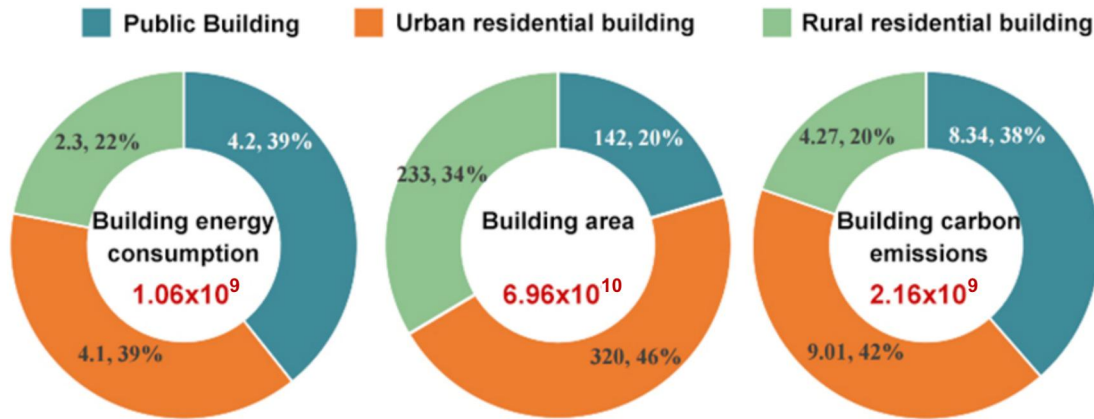


Figure 1-4. Building operational energy consumption and carbon emissions in 2020

Source: 2022 Research Report of China Building Energy Consumption and Carbon Emissions

1.1.2. The current energy consumption status of rural residential buildings in China

The acceleration of urbanization has had a certain impact on the development of traditional rural dwellings. With the improvement of people's living standards, the enthusiasm of residents for rural construction has also been further strengthened. From 2001 to 2012, the per capita building area in the rural of China increased from 25.7m² to 37.1m². In 2010, the building area in rural region of China accounted for more than 50% of the total building area in the country, with a total rural building area of approximately 23 billion square meters [13].

China has a considerable number of rural regions, which consume 22% of the total building energy consumption up to 2020 [6]. With the improvement of residents' living standards, the unit energy consumption of rural residential buildings has been steadily increasing. As shown in Figures 1-5, from 2000 to 2017, the energy consumption of rural residential buildings in China increased year by year, and the unit energy consumption of rural areas increased from 3.51kgce/m² to 10.20kgce/m², with an annual growth rate of nearly 6.47% [14]. It can be seen that the energy consumption growth rate has accelerated after 2015, and the form of residential energy consumption has become more severe [14]. In 2010, the energy consumed by burning plant straw, wood, and other biomass for winter heating in rural areas, excluding coal consumption, was about 139 million tce [15]. Therefore, it is urgent to explore passive design

techniques suitable for the climate of various regions of Chinese dwellings to guide rural construction. It is necessary to study and determine the effectiveness and optimization range of the passive techniques applied, and to organize a scientific rural construction system. In addition, suitable designs should be combined with local economies and materials, and renewable energy should be fully utilized to create a comfortable living environment.

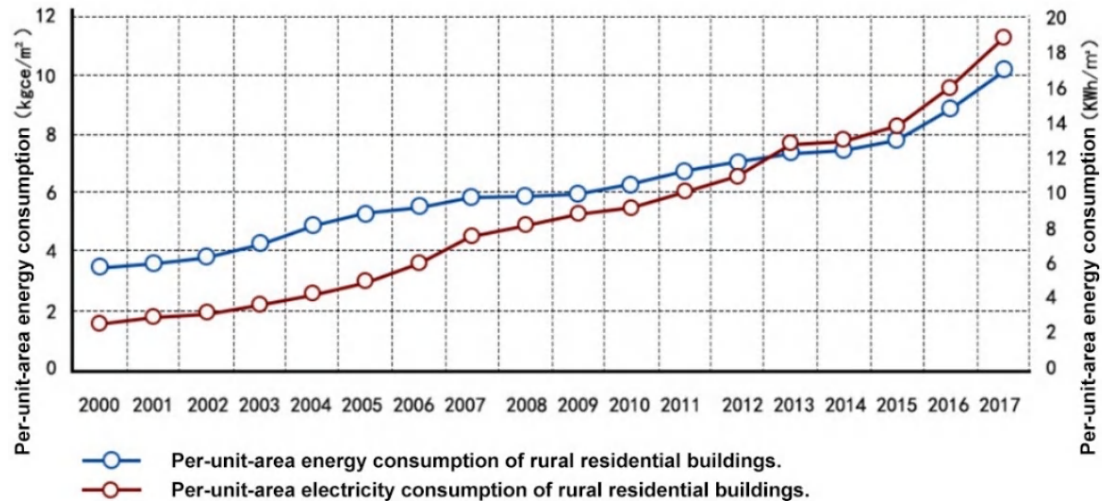


Figure 1-5. Trends in energy consumption of rural buildings in China

Source: 2019 China Building Energy Consumption Research Report

1.2. The climate adaptability of traditional dwellings

In rural residential buildings, there are numerous locally adopted construction techniques that have been tested over a long period in the local climate, exhibiting strong ecological climate adaptability in traditional dwellings [16]. Climate-adaptive traditional dwellings refer to traditional dwellings that considers local climate conditions during the design and construction process. These dwellings, shaped by extensive practice and accumulated experience, employ a range of design and technological approaches to adapt to diverse climatic characteristics and provide comfortable indoor environments [17, 18]. The influence and elements of traditional dwellings can still be observed in a significant number of rural residential buildings, and modern rural residential architecture can draw from the design principles and climate-adaptive technologies of traditional dwellings to enhance living conditions. Therefore, analyzing the relationship between traditional architectural forms and climatic environments and uncovering their climate adaptability mechanisms are prerequisites for the development of low-energy consumption housing in rural areas.

1.2.1. Overview of climate adaptability research on traditional dwellings

Traditional dwellings refer to the buildings that have been constructed using traditional materials, techniques, and styles of a particular region or culture. They are an essential part of

a region's cultural heritage and reflect the lifestyle, values, and social structure of the people who lived in them. Traditional dwellings can be found in different regions of the world. In general, traditional dwellings have certain common characteristics that make them suitable for their specific environments. In recent times, traditional dwellings have faced various challenges such as modernization, urbanization, and changing lifestyles. Many traditional dwellings have been abandoned or replaced by modern structures, leading to a loss of cultural heritage and knowledge. However, there is growing recognition of the value of traditional dwellings, and efforts are being made to preserve and adapt them to modern living requirements while retaining their cultural and environmental significance.

(1) Overview of climate adaptability research on traditional dwellings in global scale

Vernacular architecture, characterized by its regional specificity, functionality, everyday use, and distinctive features, is closely related to the research scope of Chinese traditional dwellings. Scholars and researchers have extensively investigated diverse facets of vernacular dwellings in the global scale, encompassing architectural design, construction techniques, cultural significance, and their ability to adapt to local climates.

In the late 19th century, western countries began to pay attention to the study of vernacular architecture. In the early stages, research on vernacular architecture primarily focused on fields such as anthropology and archaeology, mainly exploring the social population and living environment. In the latter half of the 20th century, as interdisciplinary studies became more mature, research on local architecture expanded from multiple perspectives. The accumulation of social, historical, and technical knowledge deepened, gradually forming a diversified framework. Disciplines such as anthropology, geography, and architecture have contributed to the study of vernacular architecture from various angles, including human culture and history, spatial geography, typology, and physical environment. The climate adaptability of dwellings is an important branch of research in the architectural discipline, particularly in the study of traditional dwellings. The research process can be broadly divided into the following stages:

1) Architecture and Climate (Before the 20th century)

Architects have been paying attention to climate factors since the inception of architecture. In the 1st century BC, the Roman architect Vitruvius mentioned the relationship between architecture and climate in his work "De Architectura", which can be regarded as one of the earliest documents on architectural climate adaptation. The book presents specific requirements for how architectural structures should adapt to climate conditions [19]. It was not until the mid-20th century that technological equipment began to control the indoor environment of buildings. Prior to this, the architectural design process consistently emphasized the consideration of local natural climate characteristics and employed various architectural techniques to adapt to the climate [20]. However, with the advent of the industrial age, technological advancements have led to the widespread application of machinery and equipment, resulting in significant energy consumption and environmental pollution in the

process of improving indoor environments. As a result, the feasibility and long-term sustainability of climate adaptation in traditional dwellings have once again become a focal point of attention. Subsequently, a series of literature related to the climate adaptability of traditional dwellings has been published [21].

2) Climate adaptability of traditional dwellings (During the 20th century)

In the mid-20th century, with the concept “No climate, no architecture” being introduced, architects began to pay attention to research on climate-responsive energy-saving measures [22]. From this period onwards, mainstream residential architectural design shifted from focusing solely on architectural form, economy, and materials, to incorporating traditional construction techniques and materials [23]. Strategies such as courtyard forms, orientation, openings, thermal mass walls, wind-capturing windows, and adaptable living patterns were employed to adapt to outdoor climatic conditions [24]. During the 1950s to 1970s, regionalism in architectural theory triggered a growing interest and research into the climatic adaptation of dwellings. Categorization studies on residential roof forms in different climate regions globally demonstrated the significant impact of climate factors on vernacular architectural forms. During this period, scholars published numerous groundbreaking theoretical works, with bioclimatic design methods emerging as the fundamental theory for climate-responsive architectural research and design, providing new tools and frameworks for the study of climatic adaptation in dwellings. Research in practice mainly focused on summarizing applicable architectural plans and climate strategies for various climate regions based on traditional dwellings [25]. From the 1970s to the 1990s, environmental issues and energy crises prompted the study of the environmental adaptability features of dwellings as an independent research topic, leading to the emergence of multidisciplinary approaches and comprehensive studies on residential buildings, including the assessment of architectural physics performance and human thermal comfort technologies.

3) Passive design strategies in Traditional Dwellings (After 2000)

After the year 2000, with the emergence of the concept of sustainability, there has been a significant amount of research on passive architectural strategies suitable for different climate types in traditional dwellings. The development of building physics theories and advancements in testing methods have laid the foundation for the rapid development of research on climate adaptation in traditional dwellings. Passive design technologies began to be widely disseminated around 2000, accompanied by the emergence of numerous computer analysis software tools for building energy efficiency and environmental analysis. These tools have facilitated the integration of climate adaptation in traditional dwellings with passive design strategies through computer simulations, making research and design more scientific and forward-looking. Around 2000, architects compiled and organized passive strategies in buildings, drawing inspiration from traditional architectural techniques for natural ventilation and daylighting, and utilizing modern technology to optimize the implementation of passive

strategies in practical projects [26]. Subsequently, scholars shifted their research focus on climate adaptation in traditional dwellings from empirical induction to absorption and reutilization [27]. They combined the climate adaptation experiences of traditional dwellings with modern construction methods to create green, energy-efficient, and locally reflective new vernacular architecture. Several books have been published explaining the differences in construction approaches between modern vernacular architecture and traditional vernacular architecture, providing classic case studies and passive design techniques for buildings adapted to the environment.

In the past decade, scholars have employed advanced research methods such as computer simulation and genetic algorithms to quantitatively analyze the impact of passive strategies on indoor thermal comfort and building energy consumption, aiming to find optimal solutions. A detailed exploration of these quantitative studies holds significant guiding significance for this research. In 2014, Susanne et al. divided traditional Nepalese vernacular architecture into 4 different climate zones and designed traditional houses based on local climate conditions. Different passive solar measures were determined for the four climate zones [28]. In 2017, Maria et al. conducted extensive research on rural vernacular dwellings in coastal, lowland, and mountainous areas of Cyprus, analyzing that vernacular architecture successfully addressed the special challenges brought about by local conditions [29]. In 2019, Mady et al. compared the advantages and disadvantages of traditional building's materials and modern building's materials, and the results showed that the performance of vernacular houses was better. Even if new concrete houses were used, passive strategies were still important [30]. In 2020, May et al. designed traditional multi-level roofs for vernacular architecture in Myanmar and investigated their performance when building parameters, such as building form, ventilation, and materials, changed. The research results showed that Myanmar's multi-level roofs can improve indoor comfort in tropical regions. In 2021, Kerstin et al. evaluated the drawbacks of traditional sandstone slabs and discussed restoration solutions, proposing selection criteria for appropriate alternative materials [31]. In 2021, João et al. studied the characteristics of several vernacular buildings in Leiria, Portugal, by surveying and inspecting them, which helps to effectively preserve and use vernacular architecture in Leiria [32]. In 2021, Barbara et al. evaluated the thermal comfort conditions of vernacular dwellings in six low-tech building types in the western Sahel region of sub-Saharan Africa [33]. In 2022, Inês et al. evaluated the thermal comfort of vernacular houses based on a Portuguese environmental adaptation thermal comfort model [34]. In 2023, Sudhir et al. used a multi-objective optimization method to combine the building modeling tool EnergyPlus with non-dominated sorting genetic algorithm II (NSGAI) to find the best combination of different passive cooling functions. The research results showed that using passive cooling components can optimize the indoor thermal environment to the greatest extent [35].

(2) Overview of climate adaptability research on traditional dwellings in China

Research on Chinese traditional dwellings began in 1929 with the establishment of the “China Architectural Society,” and has since yielded fruitful results. After more than a century of accumulation and development, research on Chinese traditional dwellings can be broadly categorized into 5 areas: the dwellings’ mapping research, the traditional culture of dwellings, the construction technology of dwellings, the preservation of traditional dwellings, and the climate adaptability of traditional dwellings.

Extensive and in-depth research has been conducted by numerous universities and research institutions in China to address the challenges encountered in the ecological and climatic design strategies of traditional dwellings. In the 1920s to 1950s, the influence of climate characteristics on the roof forms of vernacular dwellings was described from a meteorogeographical perspective. From the 1950s to the 1970s, the use of shading, insulation, ventilation, and other building climate adaptation technologies in vernacular practices across different climatic regions was discussed, gradually establishing the mechanisms and applications of traditional building climate adaptation techniques, forming the foundation of climate adaptability theory. In the 1970s to the 1990s, the adaptive mechanisms of traditional dwellings to local climates were systematically explored from an ecological perspective. In the late 1990s, there were significant research and practical achievements in traditional building climate adaptability [36]. Liu et al. made significant contributions in research on low-energy and green building models in western China, as well as the regeneration and development of regional traditional architecture. He led the completion of various types of low-energy building demonstration projects in Shaanxi, Yunnan, Tibet, Sichuan, Qinghai, Ningxia, and other regions.

Since 2000, with the application of computer simulation technology, the research methods, levels, and fields of traditional dwellings have been continuously expanded, leading to the more in-depth and detailed studies on traditional dwellings in different regions of China. Researchers have employed quantitative methods to conduct detailed investigations on the thermal environment, thermal comfort, climate suitability, and energy efficiency of traditional vernacular dwellings.

Scholars have conducted extensive research on thermal environment and thermal comfort in traditional residential architecture. In 2021, Liu et al. conducted actual measurements of the indoor thermal environment of traditional residential architecture in Guilin during winter, and the result shows that the interstitial space and attic space had insulation effects, which could inhibit indoor heat dissipation and reduce heat loss [37]. In 2023, Guo et al. deduced the evaluation model of thermal comfort for traditional residential architecture in summer, and obtained the neutral temperature and thermal comfort range of the traditional residential architecture in the ancient city of Handan [38]. In 2023, Yan et al. conducted a subjective questionnaire survey and objective data measurement of the indoor thermal environment and thermal comfort characteristics of traditional residential architecture in Hebei Province. The

measured data showed that the thermal environment quality of old traditional residential architecture was poor, but the thermal adaptation of residents was strong [39].

The research on the climate adaptability of traditional dwellings is also a major focus of quantitative studies on traditional dwellings. In 2019, Xu et al. studied the climate adaptability characteristics of traditional residential architecture in the Qinba Mountain regions and summarized the advantages and disadvantages of residential architecture's physical environment in response to climate characteristics. The results showed that traditional adobe residential architecture was well adapted to the local climate in the summer season, but the indoor thermal comfort in the winter season was not entirely satisfactory [40]. In 2020, He et al. used the building climate analysis software to compare and analyze meteorological data in Qingdao and Dalian, and found that local residential architecture had formed building and living habits that were adapted to the climate from the aspects of building layout, building materials, and lifestyle [41]. In 2023, He et al. summarized the climate adaptability strategies of traditional residential architecture in Tulufan Township, and the multi-layer space and comprehensive building envelope structure are the most effective climate strategies [42].

At the same time, many scholars have conducted extensive research on building energy efficiency. In 2019, Chi et al. studied the optimal orientation of buildings of traditional dwelling in Zhejiang Province, and the results showed that the difference in annual total electricity consumption between the best and worst orientations of buildings was about 80 kWh [43]. In 2021, Chi et al. deduced the distribution characteristics of the plane energy consumption coefficient of traditional dwellings in Zhejiang Province at the macro level, and calculated the plane energy consumption coefficient of different forms of dwellings in each sub-region for evaluating the energy efficiency of different plane layout [44]. In 2022, Li et al. conducted energy consumption simulation and analyzed the energy-saving transformation of the envelope structure of traditional Huizhou residential architecture. After the transformation, the cumulative energy consumption of the building was reduced by 66.4% during its service life [45].

1.2.2. Passive design strategies

Passive strategies play a crucial role in enhancing the climate adaptability of buildings. Through thoughtful architectural design and layout, passive strategies can maximize the utilization of natural climatic conditions, such as sunlight, and ventilation to provide a comfortable indoor environment [46]. Therefore, passive strategies are instrumental in achieving building climate adaptability. They not only reduce reliance on mechanical equipment and energy consumption but also enhance the sustainability and environmental-friendliness of buildings [47]. By fully utilizing and integrating passive strategies, buildings can better adapt to local climate and environmental conditions, offering comfortable, energy-efficient, and sustainable living and working spaces.

Traditional residential buildings have achieved the maximum harmony between human and nature through the extensive use of locally suitable “passive design” strategies. Passive technology mainly refers to the use of basic principles of building environmental control technology, such as building form, structure, and regional climate, to organize and process various building elements in a reasonable manner without air conditioning or other equipment systems [48]. This strategy maximizes the improvement of indoor environmental conditions and ensures that the indoor thermal environment meets the needs of human comfort.

The construction wisdom of Chinese traditional dwellings responds to various climate environments through passive design techniques, which creates the diversity of traditional residential buildings and maximizes their adaptation to nature [40]. In the mid-20th century, the emergence and maturity of heating equipment made it possible for buildings to rely entirely on artificial adjustment, ignoring the use of building design to respond to climate. Rural residential buildings were gradually covered by high-energy-consumption and low-ecological concrete jungles, and the unsustainable relationship between nature and architecture caused climate deterioration, extreme cold and hot weather becoming the norm [49]. Faced with the increasingly deteriorating environment, it is essential to rethink how traditional dwellings respond to nature, how to use architectural climatology to study passive technology adapted to the site, and how to make our rural areas healthier and more updated.

Previously, the academic community focused more on the evolution of local culture and architectural styles in traditional residential buildings, neglecting the micro-level climate. The computer simulation technology has helped architects to actively interpret local climate language, focusing on the interaction between architectural form, space, and climate research. Through computer simulation, it is possible to quantitatively analyze the relationship between building construction methods and physical environments such as climate, energy, and thermal comfort, and optimize the scope of passive technology to meet the comfort needs of human habitats. By quantifying the passive design strategies of traditional residential buildings, their effectiveness in local architectural design can be evaluated, providing important theoretical guidance for the development of passive technology in traditional residential buildings.

Currently, countries around the world are actively formulating low-energy building development goals and technical policies, establishing low-energy or even ultra-low-energy building standards and corresponding technical systems suitable for their own characteristics. Building energy conservation in China has gone through a difficult process. Gradual building energy conservation can no longer meet China’s energy needs for economic development. Improving building energy efficiency and achieving sustainable development is the inevitable trend of green building development. Proposing low-energy consumption technologies for different climate zones is the most effective way to achieve low-energy consumption goals.

1.2.3. The case study of building climate adaptability

Table 1-1. Climate adaptability strategies of world traditional dwellings

Tropical Monsoon Climate Zone	Subtropical and Temperate Climate Zones
 <p data-bbox="349 792 687 826">Thailand vernacular dwelling</p> <ol data-bbox="252 875 783 1016" style="list-style-type: none"> 1. The open courtyard is conducive to ventilation and heat dissipation. 2. The raised ground floor is conducive to flood prevention, moisture-proofing, ventilation, and cooling. 3. The sloping roof is conducive to drainage. 	 <p data-bbox="924 792 1225 826">Korea vernacular dwelling</p> <ol data-bbox="810 875 1342 1003" style="list-style-type: none"> 1. Changing doors and windows forms are used to adapt to different climates. 2. Wide eaves are conducive to shading. 3. Sandwich walls are conducive to heat preservation and insulation.
Cold Temperate Climate Zone	Polar Climate Zone
 <p data-bbox="371 1503 663 1536">Finland wooden dwelling</p> <ol data-bbox="252 1581 783 1753" style="list-style-type: none"> 1. The thick wooden enclosure structure has good insulation properties. 2. The small size of the door and window openings reduces heat loss. 3. The dark outer surface increases heat absorption. 4. The steep sloping roof prevents snow accumulation. 	 <p data-bbox="994 1503 1155 1536">Inuit ice room</p> <ol data-bbox="810 1581 1342 1753" style="list-style-type: none"> 1. The spherical architectural form can reduce the surface area of heat dissipation, which is beneficial for insulation. 2. The sphere shape helps the building resist cold winds. 3. The semi-underground space reduces the penetration of cold air.

Image source: <https://www.snaphome.asia/blog/thailand-houses-architecture>; <https://www.hostelsclub.com/en/magazine/try-a-traditional-korean-guest-house>; <https://aarch.dk/en/basp-studentwork-finland/>; <https://www.outsideonline.com/outdoor-gear/hiking-gear/what-do-i-need-build-igloo/>

Since the beginning of human architectural activities, the construction of houses has been closely related to the local climate and environment. The active response to regional climate

and environment has become a natural habit in architecture. Traditional architecture is a living space that our ancestors obtained using the most economical materials available in the local area to achieve maximum comfort, while the architectural form reflects the regional characteristics and meets the needs of the villagers' production and life.

Although residential buildings in different regions and different periods have different characteristics, their overall construction form and basic style are preserved as regional features. Traditional dwellings, which have been formed over hundreds of years to adapt to specific conditions such as climate, region, and culture, have achieved a combination of application and defense in the face of local climate and environmental conditions. The external characteristics of each traditional dwelling are the result of adaptation to the climate, making traditional dwellings in harmony with nature and able to meet human comfort needs for most of the time.




(1) The case study of building climate adaptability in global scale

Due to different climatic conditions, different natural environments, different cultural backgrounds, and different resource supplies, practice has proved that the architecture in different regions reflects the characteristics that match the local climate conditions, natural environment, geographical features, cultural background, and resource supply, and carries a distinct natural mark. Table 1-1 lists the main forms of traditional dwellings in the world's climatic zones and how they adapt to local climate through passive strategies. In tropical regions, traditional dwellings mainly focus on ventilation, heat insulation, moisture-proofing, and rain-proofing. In temperate regions with distinct seasons, both winter insulation and summer heat insulation need to be considered. In cold climates, such as in the Han Dynasty region, the primary task of traditional dwellings is winter insulation.

(2) The case study of building climate adaptability in China

China has a vast territory and a long history. In the long history of agricultural civilization, various forms of traditional dwellings have been nurtured. These dwellings often use passive design strategies to respond to climate, improve indoor thermal comfort, reduce building energy consumption, and achieve sustainable development. However, these passive strategies have been simplified or abandoned in recent years. In the context of the new era, although modern means can be used to build a comfortable indoor environment, it cannot escape various problems such as increased energy consumption and climate warming, similar to those in cities. At the same time, blindly borrowing the design and construction methods of urban buildings will lead to a lack of characteristics in traditional dwellings and a homogenization of their appearance. Therefore, the renovation and construction of rural residential buildings using the principles of climate adaptability, along with indigenous building materials and construction methods, are crucial aspects of sustainable development in rural areas. Table 1-2 summarizes the architectural forms and climate adaptation strategies of traditional dwellings in different climatic regions of China.

Table 1-2. Climate adaptability strategies of Chinese traditional dwellings

Tropical monsoon climate zone	Subtropical monsoon climate zone
	
<p>Yunnan bamboo dwelling</p>	<p>Sichuan timber dwelling</p>
<p>1. Elevated ground floor to prevent moisture. 2. Large windows with low air tightness for better ventilation. 3. Sloping roof for efficient drainage. 4. Using pillars as building materials according to local conditions.</p>	<p>1. Sloping roof for efficient drainage. 2. Using bamboo clay walls, and timber walls as building materials according to local conditions. 3. Storage space is set up under the roof for insulation and heat preservation.</p>
Temperate monsoon climate zone	Temperate continental climate zone
	
<p>Beijing quadrangle courtyard</p>	<p>Shaanxi cave dwellings</p>
<p>1. Enclosed courtyard, providing shade in summer and introducing sunlight in winter. 2. Enclosed courtyard resists cold winds in winter.</p>	<p>1. Facing the sun and backing against the mountain, with an open field in front. 2. Free form of windows and doors to introduce natural light into the interior. 3. Good insulation and heat preservation walls and roof materials.</p>
Plateau mountain climate zone	
	
<p>Qiang's stone tower dwelling</p>	

1. Skylights on the roof of the building for ventilation, lighting, and smoke exhausting. 2. Using stone as building material according to local conditions, with good insulation performance. 3. Due to less rainfall in the area, a flat roof is adopted.

Image source: <https://baijiahao.baidu.com/s?id=1680064404961873762&wfr=spider&for=pc>; photographed by the author; <https://www.ks5u.com/down/2012-4/4/770486.Shtml>; <https://baijiahao.baidu.com/s?id=1709682098500422720&wfr=spider&for=pc>; <https://www.51yuansu.com/sc/lqshudogpx.html>

Yunnan bamboo dwellings are located in the tropical monsoon climate zone, characterized by high average temperatures and abundant rainfall. These dwellings elevate the foundation to prevent moisture, use large windows with low air tightness for better ventilation, employ sloping roofs for efficient drainage, and utilize bamboo and pillars as building materials based on local conditions. Sichuan timber dwellings are situated in the subtropical monsoon climate zone, characterized by cold and humid winters and hot and humid summers. These dwellings feature sloping roofs for efficient drainage, incorporate storage spaces under the roof for insulation and heat preservation, and utilize bamboo clay walls and timber walls as building materials according to local conditions. Beijing quadrangle courtyard are located in the temperate monsoon climate zone, characterized by cold and dry winters. These dwellings have enclosed courtyards that provide shade in summer and introduce sunlight while blocking cold winds in winter. Shaanxi cave dwellings are situated in the temperate continental climate zone, characterized by cold and dry winters and pleasant summers. These dwellings are positioned against mountains, facing the sun, and have open spaces in front. They employ a free form of windows and doors to introduce natural light, and utilize high-quality local insulation and heat preservation materials for walls and roofs. Qiang's stone tower dwellings are found in the plateau mountain climate zone, characterized by cold winters, cool summers, and low rainfall. These dwellings have skylights on the roof for ventilation, lighting, and smoke exhausting. They adopt a flat roof design for simplicity and use local stone as building material, offering good insulation performance.

1.1.5. Qinba mountainous area

The Qinba mountainous area is a boundary area for China's climate and geography, with numerous small basins and valleys connecting the mountains. It is also a convergence area for many ethnic groups such as Qin, Ba, Chu, and Shu, and has the climate characteristics of both hot summers and cold winters and cold regions. The summer is hot and humid, and the winter is wet and cold, which includes various lifestyles and residential patterns under special climatic conditions. The area is inhabited by many ethnic groups, with a rich cultural heritage. The architecture exhibits regional characteristics of white walls, blue tiles, hanging beams, deep eaves, and small courtyards. The residential buildings adopt self-organizing construction forms that are adaptable to the environment, using limited low technology and passive construction technique. Traditional cooking and heating methods lead to serious indoor pollution, and poor airtightness can cause the indoor air temperature to be too low in winter. There is a certain

deviation between the degree of climate regulation that traditional building techniques can achieve and the comfort requirements.

1.2.4. The research gap

Through recent research on the climate adaptability and energy-efficient buildings in traditional architecture, it has been found that: in terms of geographical distribution, there is a significant amount of research conducted in China, which exhibits good continuity and comprehensiveness; in terms of climate zones covered, the majority of studies focus on humid temperate climates, followed by arid climates and equatorial humid climates; in terms of research focus, the emphasis is primarily on analyzing data related to the thermal environment, thermal comfort, wind environment, and energy consumption of individual dwellings; in terms of research content, the main focus is on the renovation of traditional dwellings. There are still several research gaps in previous studies.

1) Traditional ecological research on residential buildings mainly classifies them according to different regions or cultures, and there is less research conducted from the perspective of national building thermal zoning. Moreover, there are differences in the forms of traditional residential buildings within the same thermal zone, and more detailed climate zoning should be established to analyze the construction techniques and intelligent building methods of traditional residential buildings in more detail.

2) The issue of indoor thermal comfort in traditional residential buildings. Research on the thermal comfort of traditional residential buildings is relatively general and lacks a systematic study on climate zoning, residential forms, and thermal comfort investigation. Therefore, the three should be considered together.

3) Passive strategies for the renovation of traditional residential buildings often do not consider thermal comfort investigation. Considering the passive renovation strategies for local residents' thermal comfort can set the indoor cooling and heating set points based on the local residents' neutral temperature, which can save energy to a certain extent.

4) In the simulation stage of passive renovation strategies for traditional residential buildings, only a single energy consumption target is often considered, without comprehensive consideration of indoor comfortable hours, renovation costs, and other factors. Therefore, a multi-objective optimization model should be established to comprehensively balance the relationships between various goals.

1.3. Research structure and logical framework

1.3.1. Research purpose and significance

(1) Research purpose

This study is based on the national conditions of rural revitalization in China. It studies and interprets residential buildings from the perspective of conforming to nature, inheriting culture,

improving living quality, and protecting the ecological environment. It analyzes the relationship between residential building forms and climate environment, reveals the mechanism of climate adaptation, and further evaluates the effectiveness of existing climate adaptation technologies. At the design stage, it proposes building design methods and technologies that are adapted to the climate. This is the premise for the development of low-energy consumption buildings in Qinba Mountain area, and it is also a national development strategy and rural construction needs. The results and conclusions have important theoretical value for rural revitalization and the development of regional low-energy consumption buildings, and promote the application of basic research results. Therefore, improving living quality through low-energy consumption is an urgent need for rural revitalization in Qinba Mountain area.

This article takes the climate zoning of Qinba Mountain area as the starting point, subdivides the area into sub-climatic regions with more similar climate characteristics, and calculates the thermal comfort range of each sub-climatic region to apply more reasonable passive design strategies. The effectiveness of each passive strategy is determined through single-factor analysis, and then an ideal residential passive strategy optimization model that meets energy consumption, comfort, and economic goals is selected through multi-objective optimization genetic algorithm.

(2) Research significance

In the long-term development of traditional architecture, a clear adaptation relationship has been formed with the local environment. On the one hand, it is necessary to critically absorb the climate adaptability features in the traditional construction system. On the other hand, it is necessary to respond to contemporary life requirements and form a sustainable and beneficial development system with the context and social environment, proposing adaptive architecture with regional characteristics and cultural continuity based on modern technology and materials.

1) The lack of systematic meteorological data and complete investigation materials on residential buildings in the Qinba mountainous area. This research can serve as basic data for similar studies and provide reference for the analysis of the impact of climate on residential buildings, expanding the vision and methods of climate adaptability research on residential buildings through investigation of climate characteristics, regional environment, settlement space, building form, and testing of indoor physical environment.

2) The current thermal zoning cannot describe the climate characteristics of the Qinba mountainous area in detail. This research subdivides the sub-climate zones of the Qinba mountainous area, proposes indoor thermal comfort parameters and ranges for sub-climate zones, and can serve as a basis for building design adapted to the climate by proposing low-energy consumption building indoor thermal comfort parameters that meet basic thermal comfort conditions. This is helpful in analyzing the relationship between buildings and indoor and outdoor climate environments, providing theoretical basis and technical support for determining indoor thermal environmental control parameters and adapting building design to

the climate.

3) Improving the theoretical basis for the scientific design of traditional residential buildings, revealing the climate adaptation mechanism of residential buildings in the Qinba mountainous area, establishing the theory of climate adaptability for residential buildings, laying the foundation for the scientific design of residential buildings through understanding the relationship between climate characteristics and building forms, as well as building characteristics, physical environment, material properties, and construction methods. Through graphic and tabular forms, further demonstrating the methods and technical strategies of climate-adapted residential design in the Qinba mountainous area.

1.3.2. Research content

Under China's requirement to attain a carbon peak by 2030, and in the face of energy consumption dilemmas and environmental crises, decreasing building energy use has gained a widespread concern. Passive design is a climate adaptive design method that can save energy and reduce emissions without using artificial energy resources and effectively improve the building's indoor thermal comfort. And climate conditions are a critical factor in determining the passive design scheme. Climate zoning helps formulate building energy conservation standards and adapt building energy conservation technology according to the region. As a result, it is essential to conduct research on passive strategies optimization based on detailed climatic subdivision and thermal comfort investigations.

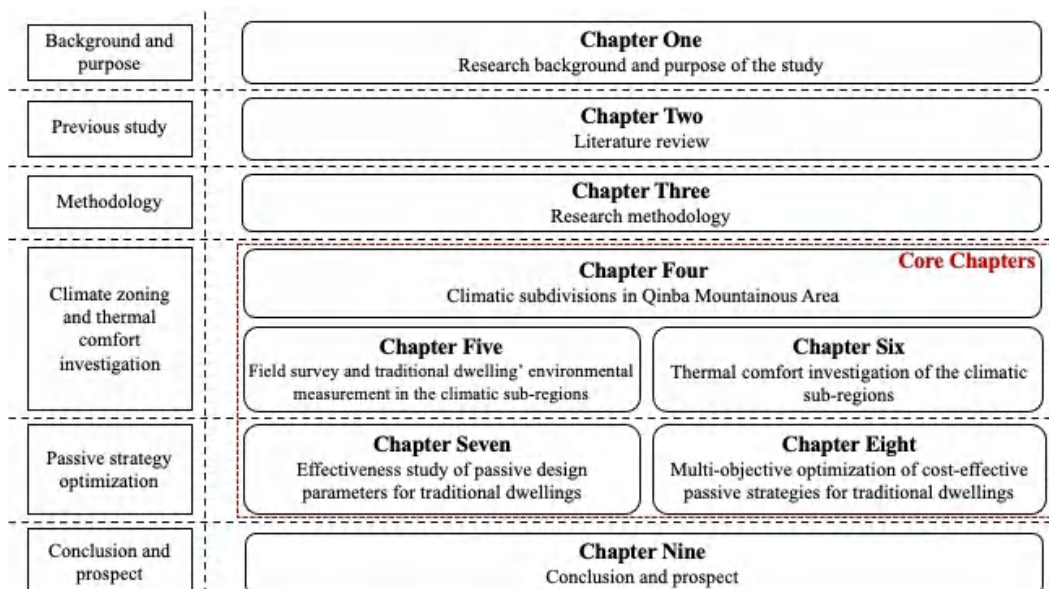


Figure 1-6. The research flowchart

This study mainly focuses on the application of passive strategies in the sub-climate zoning of the Qinba mountainous area. The main research content is shown in Figure 1-6, and the core chapters research content can be summarized as follows:

(1) Sub-climate zoning in the Qinba mountainous area

Collecting meteorological data from the past decade in the Qinba mountainous area and using the Kriging spatial interpolation method, the sub-climate zones of the Qinba mountainous area are divided based on the main control conditions of HDD18 and CDD26 (temperature). Relative humidity, wind speed, and solar radiation are used as auxiliary meteorological factors to describe the meteorological characteristics of each county.

(2) Field research and problem summary of traditional residential buildings in the Qinba mountainous area

Taking traditional residential buildings in the Qinba mountainous area as the research object, the problems of traditional residential buildings in the Qinba mountainous area are summarized and analyzed through literature review, questionnaire survey, and indoor physical environment testing, including both qualitative and quantitative aspects.

(3) Research on indoor thermal comfort of traditional residential buildings in sub-climate zones

Using subjective questionnaires and physical environment measurements, a mathematical model for predicting indoor thermal comfort of residents is obtained through linear regression analysis. Based on the PMV-PPD equation, the neutral temperature and thermal comfort range of indoor environments in sub-climate zones are calculated.

(4) Determining the effectiveness of passive technologies in traditional residential buildings

Using computer energy consumption simulation analysis for different passive strategies and combining mathematical statistics methods, the effectiveness of passive strategies in the Qinba mountainous area is evaluated and optimized, and the effectiveness of each passive strategy is determined.

(5) Proposing a multi-objective optimization model for passive renovation of traditional residential buildings

Establishing a multi-objective optimization genetic algorithm model with “energy consumption”, “economy”, and “comfort” as goals, selecting the optimal design strategy combination through iteration based on simulation results, and further simulating the indoor comfort level of the optimal results through software.

1.3.3. Chapter content overview and related instructions

The brief introduction of chapters schematic is shown in Figure 1-7. Here are the related instructions for each chapter.

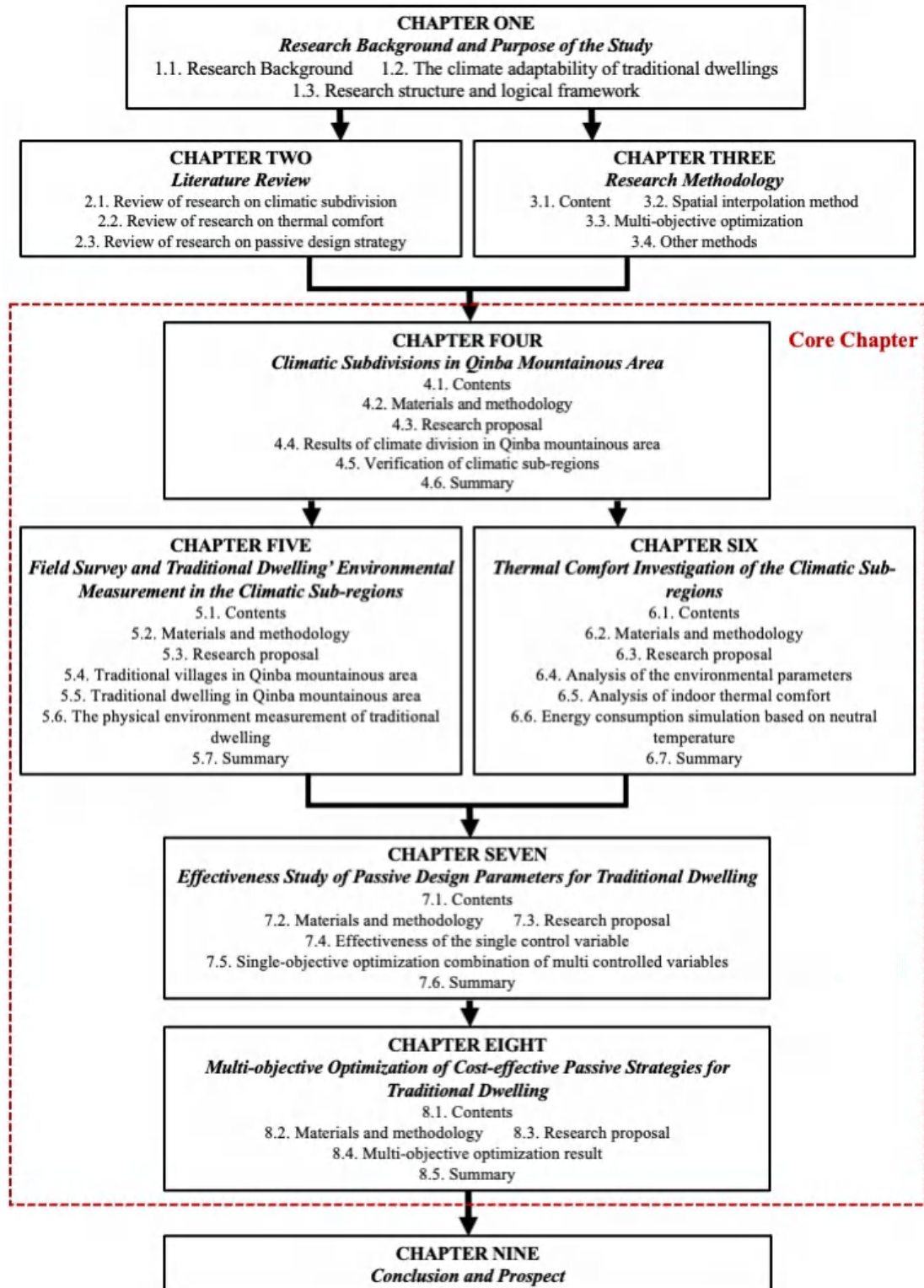


Figure 1-7. Brief chapter introduction

CHAPTER 1, RESEARCH BACKGROUND AND PURPOSE OF THE STUDY

This chapter provides an overview of the research background, including China's urbanization process and its carbon emissions, the energy consumption status of rural residential buildings, the principles of ecological architecture and passive design strategies, and the climate adaptability of traditional dwellings. With the increasing demand for comfortable living conditions in rural areas and the urgent need to reduce energy consumption, it is necessary to explore effective approaches to improve indoor thermal comfort and energy efficiency in traditional dwellings using passive strategies.

CHAPTER 2, LITERATURE REVIEW

This chapter provides a comprehensive review of the related research for this paper, which includes the literature review of climatic subdivision, thermal comfort, and passive design strategy. The climatic subdivision section discusses previous studies of climatic subdivision and China's current climate zoning standards. The thermal comfort section reviews previous studies and evaluation indicators of thermal comfort, while the passive design strategy section describes previous studies and various types of passive design parameters. The content of these three parts can help this study derive research directions for the climate-adaptive renovation of traditional dwellings under the background of climate zoning.

CHAPTER 3, RESEARCH METHODOLOGY

This chapter provides a summary of the various methodologies employed in this research, which include spatial interpolation, field survey, computer simulation, statistical analysis, and multi-objective optimization. These methods were used to achieve the climatic subdivision of Qinba mountainous area, the calculation of residents' thermal comfort, and the optimization of passive design strategies for traditional dwellings. These methodologies were employed to organize and classify meteorological data, calculate thermal comfort indicators, simulate building energy consumption pre and post passive strategy renovation, and ultimately obtain the optimal solutions for each climatic sub-region.

CHAPTER 4, CLIMATIC SUBDIVISIONS IN QINBA MOUNTAINOUS AREA

To begin with, the Qinba mountainous area was divided into the climatic sub-regions based on the values of HDD18 and CDD26 in the past decade, using the Co-Kriging spatial interpolation method. Moreover, supplementary meteorological information, such as relative humidity, wind speed, and solar radiation, was added to the climatic sub-regions using the Co-Kriging method. Finally, the climatic conditions and annual thermal loads of buildings in representative counties within each sub-region were analyzed.

CHAPTER 5, FIELD SURVEY AND TRADITIONAL DWELLING' ENVIRONMENTAL MEASUREMENT IN THE CLIMATIC SUB-REGIONS

Firstly, based on the mountainous topography and location of settlements in the study area, 3 types of settlements were identified, including the settlement in the gully, settlement leaning against the mountain, and settlement on the mountain slope. Then, the building layout of

traditional dwellings was categorized into 4 types: “I”-shaped, “L”-shaped, “U”-shaped, and “□”-shaped dwelling. Additionally, courtyards were classified into 3 types: open, semi-open, and closed courtyard. Lastly, the research team conducted multiple investigations of outdoor and indoor physical environmental measurements on traditional dwellings during winter and summer in the 5 climatic sub-regions to investigate the indoor thermal environment.

CHAPTER 6, THERMAL COMFORT INVESTIGATION OF THE CLIMATIC SUB-REGIONS

Firstly, the research team measured the outdoor and indoor environmental parameters, collected thermal sensation questionnaires from residents, and analyzed the data. Then, by using linear regression analysis of mean thermal sensation voting (MTS) and indoor operating temperature (T_{op}), the research calculated the thermal comfort equations for each climatic sub-region. From these equations, the neutral temperatures and thermal comfort ranges can be obtained. Finally, the research simulated the annual building thermal loads of a typical traditional dwelling in the 5 climatic sub-regions according to both the standard requirements and the measured neutral temperature.

CHAPTER 7, EFFECTIVENESS STUDY OF PASSIVE DESIGN PARAMETERS FOR TRADITIONAL DWELLING

To begin with, in the single-variable controlled study, this research identified the 4 effective passive design parameters for traditional dwellings, including the sunroom depth, and the heat transfer coefficient of the exterior wall, roof, and window. These parameters were selected through energy consumption analysis and calculation of the relative sensitivity coefficient. Then, in the multi-variable controlled study, this research utilized orthogonal arrays analysis to evaluate the effectiveness of the four parameters and determine the optimal combination.

CHAPTER 8, MULTI-OBJECTIVE OPTIMIZATION OF COST-EFFECTIVE PASSIVE STRATEGIES FOR TRADITIONAL DWELLING

Initially, this study employed multiple regression equations based on four effective passive design parameters to determine the annual thermal load, proportion of uncomfortable hours, and renovation investment for each sub-region. Then, the research applied the NSGA-2 method to identify a set of Pareto optimal solutions based on a multi-regression equation with three objectives. Furthermore, the research utilized the TOPSIS method to select the 20 optimal solutions in each sub-region. Ultimately, the research simulated the annual thermal loads and indoor comfort values for the optimal renovated dwelling in each climatic sub-region.

CHAPTER 9, CONCLUSION AND PROSPECT

The conclusion of whole thesis is deduced, and the future work has been discussed.

Reference

- [1] "Notice of the State Council on the Issuance of the National Population Development Plan (2016-2030)," *The Bulletin of the State Council of the People's Republic of China*, no. 06, pp. 24-35, 2017.
- [2] S. shao, M. Fan, and H. Huang, "Urbanization Process and Carbon Emission Peaking Pathway in China: 1995-2035," *journal of China Economics*, no. 01, pp. 83-117+372-374, 2022.
- [3] J. Xi, "Address at the General Debate of the seventy-fifth Session of the United Nations General Assembly," in *People's Daily*, ed. Beijing, China: People's Daily Press, 2020.
- [4] "China Building Energy Consumption Annual Report 2020," *Building Energy Efficiency*, vol. 49, no. 02, pp. 1-6, 2021.
- [5] X. Li and C. W. J. I. Yu, "China's building energy efficiency targets: challenges or opportunities?," *Indoor and Built Environment*, vol. 21, no. 5, pp. 609-613, 2012.
- [6] C. A. o. B. E. Efficiency, "2022 Research Report of China Building Energy Consumption and Carbon Emissions," *China Association of Building Energy Efficiency* 2022.
- [7] C. Beckett, R. Cardell-Oliver, D. Ciancio, and C. Huebner, "Measured and simulated thermal behaviour in rammed earth houses in a hot-arid climate. Part B: Comfort," *Journal of Building Engineering*, vol. 13, pp. 146-158, 2017.
- [8] M. K. Singh, S. Mahapatra, and S. Atreya, "Bioclimatism and vernacular architecture of north-east India," *Building and Environment*, vol. 44, no. 5, pp. 878-888, 2009.
- [9] F. Wang, S. Wang, B. Cheng, and W. Wang, "To inhabit, retain or abandon? Adaptive utilization of energy-efficient sunken buildings by rural households in Shanzhou, China," *Energy and Buildings*, vol. 255, p. 111668, 2022.
- [10] T. Shao and H. Jin, "A field investigation on the winter thermal comfort of residents in rural houses at different latitudes of northeast severe cold regions, China," *Journal of Building Engineering*, vol. 32, p. 101476, 2020.
- [11] D. H. C. Toe and T. Kubota, "Comparative assessment of vernacular passive cooling techniques for improving indoor thermal comfort of modern terraced houses in hot-humid climate of Malaysia," *Solar energy*, vol. 114, pp. 229-258, 2015.
- [12] X. Dong, V. Soebarto, and M. Griffith, "Achieving thermal comfort in naturally ventilated rammed earth houses," *Building and Environment*, vol. 82, pp. 588-598, 2014.
- [13] N. B. o. S. o. China, *China Statistical Yearbook*. Beijing, China: China Statistics Press, 2013.
- [14] C. S. Council, "2019 China Building Energy Consumption Annual Report," *Construction and Architecture*, no. 07, pp. 30-39, 2020.
- [15] T. U. R. C. f. B. E. Efficiency, "Annual Development Research Report on Energy Efficiency in Chinese Buildings 2012," Beijing, China 2013.
- [16] P. Motealleh, M. Zolfaghari, and M. Parsaee, "Investigating climate responsive solutions in vernacular architecture of Bushehr city," *HBRC journal*, vol. 14, no. 2, pp. 215-

223, 2018.

[17] X. Juan and L. Jiaping, "Ecological Exploration and Practice of Tradition Residential Buildings in Qinba Mountain District," *Information Technology Journal*, vol. 12, no. 24, p. 8505, 2013.

[18] W. Yang, J. Xu, Z. Lu, J. Yan, and F. Li, "A systematic review of indoor thermal environment of the vernacular dwelling climate responsiveness," *Journal of Building Engineering*, vol. 53, p. 104514, 2022.

[19] L. Bianco, "Architecture, Engineering and Building Science: The Contemporary Relevance of Vitruvius's *De Architectura*," *Sustainability*, vol. 15, no. 5, p. 4150, 2023.

[20] X. Zhang, "Study on climate adaptability of traditional residential buildings in the Luzhong Mountain Area," Master Thesis Master Thesis, Qingdao University of Technology, Doctoral thesis, 2021.

[21] M. Košir, *Climate Adaptability of Buildings*. Springer, 2019.

[22] S. Wang, "Exploration of Climate adaptability Trend of Traditional Residential Houses in Different Regions," Master Thesis Master Thesis, North China University of Water Resources and Electric Power, 2022.

[23] J. Xu and X. Huo, "Study on strategy of inheritance and development of traditional building in Qinba Mountains Region," *Industrial Construction*, vol. 44, no. 09, pp. 40-44, 2014.

[24] J. Xu and X. Huo, "Study of ecological design on rural building in Qinba Mountain Regions," *Journal of Architecture and Civil Engineering*, vol. 31, no. 03, pp. 132-136, 2014.

[25] S. Chen, M. S. Mehmood, S. Liu, and Y. Gao, "Spatial Pattern and Influencing Factors of Rural Settlements in Qinba Mountains, Shaanxi Province, China," *Sustainability*, vol. 14, no. 16, p. 10095, 2022.

[26] L. You, "The Study of Parametric Design with Sustainable Strategies," Master Thesis Master Thesis, Tianjin University, 2012.

[27] Y. Gao, "Research on Passive Design Strategy of Library in Hot Summer and Cold Winter Area," Master Thesis Master Thesis, South China University of Technology, 2019.

[28] S. Bodach, W. Lang, and J. Hamhaber, "Climate responsive building design strategies of vernacular architecture in Nepal," *Energy and Buildings*, vol. 81, pp. 227-242, 2014.

[29] M. Philokyprou, A. Michael, E. Malaktou, A. Savvides, and Environment, "Environmentally responsive design in Eastern Mediterranean. The case of vernacular architecture in the coastal, lowland and mountainous regions of Cyprus," *Building and Environment*, vol. 111, pp. 91-109, 2017.

[30] M. Mohamed, A. Klingmann, and H. Samir, "Examining the thermal performance of vernacular houses in Asir Region of Saudi Arabia," *Alexandria Engineering Journal*, vol. 58, no. 2, pp. 419-428, 2019.

[31] M. Zune, C. A. J. Pantua, L. Rodrigues, and M. Gillott, "A review of traditional multistage roofs design and performance in vernacular buildings in Myanmar," *Sustainable*

Cities and Society, vol. 60, p. 102240, 2020.

[32] K. Elert, E. G. Baños, A. I. Velasco, and P. Bel-Anzué, "Traditional roofing with sandstone slabs: Implications for the safeguarding of vernacular architecture," *Journal of Building Engineering*, vol. 33, p. 101857, 2021.

[33] J. L. Parracha, J. Lima, M. T. Freire, M. Ferreira, and P. Faria, "Vernacular earthen buildings from Leiria, Portugal—Architectural survey towards their conservation and retrofitting," *Journal of Building Engineering*, vol. 35, p. 102115, 2021.

[34] I. Costa-Carrapiço, J. N. González, R. Raslan, C. Sánchez-Guevara, and M. D. R. Marrero, "Understanding thermal comfort in vernacular dwellings in Alentejo, Portugal: A mixed-methods adaptive comfort approach," *Building and Environment*, vol. 217, p. 109084, 2022.

[35] S. K. Gupta, P. R. Chanda, and A. Biswas, "A 2E, energy and environment performance of an optimized vernacular house for passive cooling-Case of North-East India," *Building and Environment*, vol. 229, p. 109909, 2023.

[36] L. Zhang, J. Liu, J. Zhao, and F. An, "Test study of the indoor thermal environment in winter of herdsman settlement residential building in China's western mountain grassland area," *Chemical Engineering Transactions*, vol. 46, pp. 703-708, 2015.

[37] H. Liu and M. Tang, "Field Study on Indoor Thermal Environment of Zhuang Traditional Dwellings in Northwest Guangxi in Winter," *Building Science*, vol. 37, no. 06, pp. 113-121, 2021.

[38] H. Guo, Y. Wang, F. Fei, C. Xu, and L. Wang, "Research on the Indoor Thermal Environment of Traditional Houses in Handan Guangfu Ancient City in Summer," *Building Science*, vol. 39, no. 04, pp. 90-96+192, 2023.

[39] Y. Wang et al., "Indoor thermal comfort evaluation of traditional dwellings in cold region of China: A case study in Guangfu Ancient City," *Energy and Buildings*, vol. 288, p. 113028, 2023.

[40] X. Juan, L. Ziliang, G. Weijun, Y. Mengsheng, and S. Menglong, "The comparative study on the climate adaptability based on indoor physical environment of traditional dwelling in Qinba mountainous areas, China," *Energy and Buildings*, vol. 197, pp. 140-155, 2019.

[41] Q. He, X. Wang, S. Xu, and H. Li, "Analysis of Climate Adaptability of Buildings in the Bohai Rim Region, Taking Qingdao and Dalian as Examples," *Building Science*, vol. 36, no. 10, pp. 68-76, 2020.

[42] W. He, Z. Wu, R. Jin, and J. Liu, "Organization and evolution of climate responsive strategies, used in Turpan vernacular buildings in arid region of China," *Frontiers of Architectural Research*, 2023.

[43] J. Zhang, G. Li, Z. Zhu, and D. Bart, "An investigation of the impact of Building Azimuth on energy consumption in sizhai traditional dwellings," *Energy*, vol. 180, pp. 594-614, 2019.

[44] F. a. Chi, L. Xu, and C. Peng, "Derivation and application of coefficient of building plane energy consumption: based on the case of Sizhai Village," *Industrial Construction*, vol. 51, no. 04, pp. 31-39, 2021.

[45] X. Li and Y. Li, "Comprehensive benefit analysis of energy saving transformation of Hui-style residential buildings in southern Anhui," *Journal of Xi'an University of Technology*, vol. 38, no. 04, pp. 500-506+569, 2022.

[46] Y. Elaouzy and A. El Fadar, "Energy, economic and environmental benefits of integrating passive design strategies into buildings: A review," *Renewable Sustainable Energy Reviews*, vol. 167, p. 112828, 2022.

[47] H. Chang, Y. Hou, I. Lee, T. Liu, and T. D. Acharya, "Feasibility study and passive design of nearly zero energy building on rural houses in Xi'an, China," *Buildings*, vol. 12, no. 3, p. 341, 2022.

[48] B. Song, "Study on Passive Design Strategies and Energy Saving Performance for Wannan Vernacular Dwellings," *Master Thesis Master Thesis*, Xi'an University of Architecture and Technology, 2015.

[49] J. Zhang, "Research on morphological characteristics and optimization of traditional buildings in Hanzhong based on indoor thermal environment," *Master Thesis Master Thesis*, Chang'an University, 2022.

Chapter 2

LITERATURE REVIEW

CHAPTER TWO: LITERATURE REVIEW

<i>LITERATURE REVIEW</i>	1
2.1 Review of research on climatic subdivision	1
2.1.1 Overview of climatic subdivision.....	2
2.1.2 Main evaluation indicators for climatic subdivision	4
2.1.3 China’s current climate zoning standards.....	5
2.1.4 Research prospect.....	7
2.2. Review of research on thermal comfort	8
2.2.1 Overview of thermal comfort	9
2.2.2 Thermal comfort index	13
2.2.3 Research prospect.....	18
2.3. Review of research on passive design strategy	18
2.3.1 Overview of passive design strategy	19
2.3.2. Research prospect.....	22
Reference	23

2.1 Review of research on climatic subdivision

Climate refers to the long-term average weather conditions and their variation characteristics in a specific location or region. It is formed by the long-term interaction of factors such as solar radiation, atmospheric circulation, geographical environment, and human activities [1]. Climate zoning refers to the division of the Earth’s surface based on differences in climate conditions, grouping regions with similar climates into one climate zone [2]. The study of climate zoning can help us better understand and predict climate change, formulate policies to address climate change, and plan and manage areas such as energy, agriculture, water resources, and the environment. Climate zoning can assist in understanding and predicting the impact of climate change on human activities in different regions. It can also aid in the development of policies and measures to address climate change, such as promoting energy conservation and emission reduction, strengthening forest conservation, and developing building codes [3]. For the construction industry, climate conditions are one of the key factors determining passive design solutions [4]. Climate zoning helps provide guidance for the regional applicability of various construction technologies and is the basis for developing policies, standards, and regulations related to building energy efficiency.

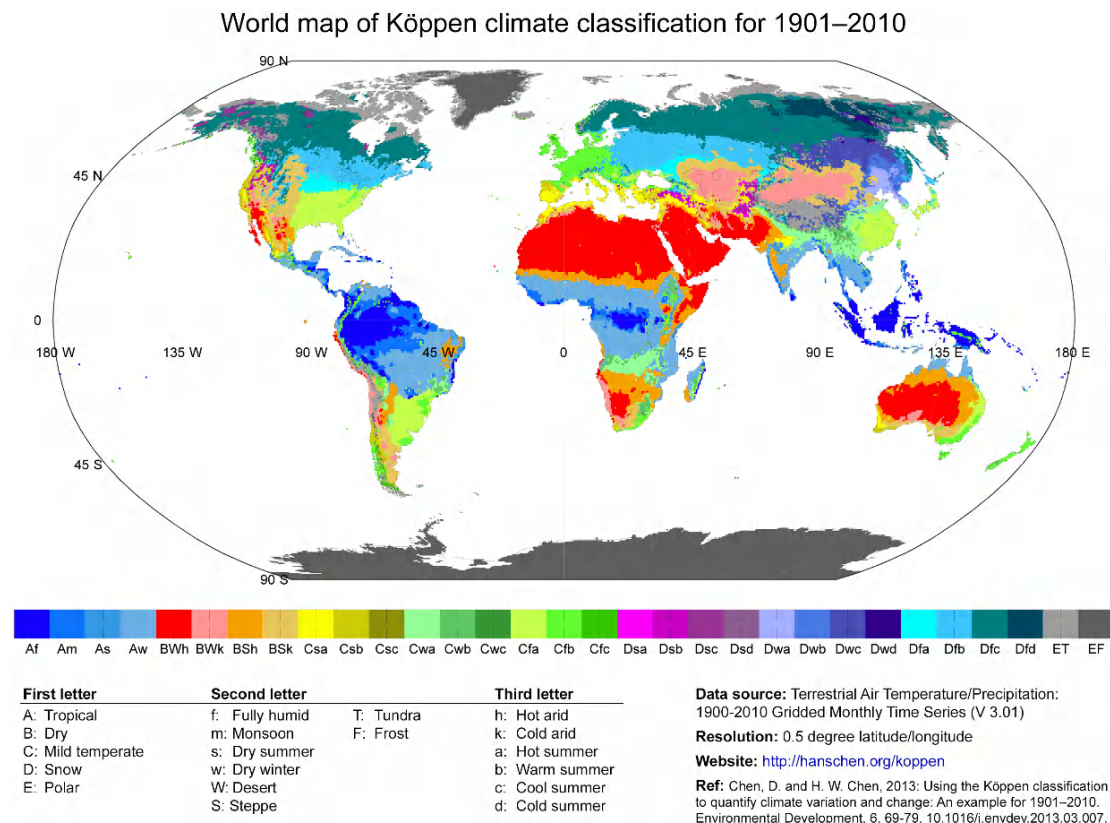


Figure 2-1. Köppen climate classification system

Source: <http://hanschen.org/koppen>

2.1.1 Overview of climatic subdivision

(1) Climatic subdivision research on a global scale

With the continuous development of social production and life, the regional characteristics of climate are increasingly recognized by humans. Scholars use a comprehensive evaluation index system to group similar climate zones and establish a reasonable climate zoning system. Many countries around the world consider climate zoning as a necessary step in the development of building thermal design standards.

As shown in Figure 2-1, in the early 20th century, Köppen divided the world into 5 climate zones, which are Tropical (A), Dry (B), Mild Mid-Latitude (C), Continental (D), and Polar (E), based on temperature and precipitation, and each primary zone is further subdivided based on additional climatic factors, such as temperature and precipitation seasonality, which results in a more detailed classification system. The map has been widely used worldwide and is known as the Köppen climate classification system [5, 6]. The impact of climate on buildings has led architects and researchers of indoor thermal environment to pay attention to the local climate characteristics of buildings. Therefore, building climate zoning has gradually been widely established to provide guidance for the thermal design of buildings and the adaptability of passive design strategies.

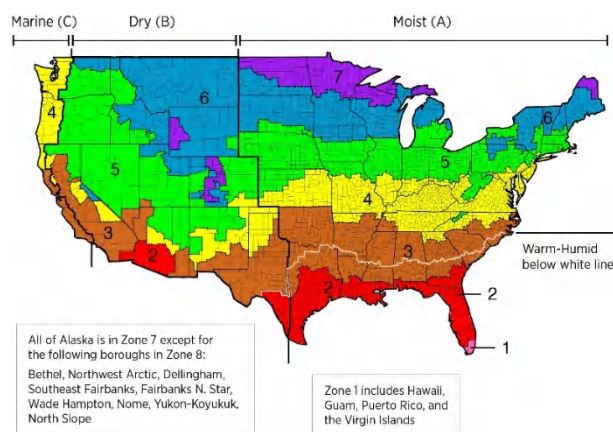


Figure 2-2. The climate zones of the United States

Source: <https://basc.pnnl.gov/images/iecc-climate-zone-map>

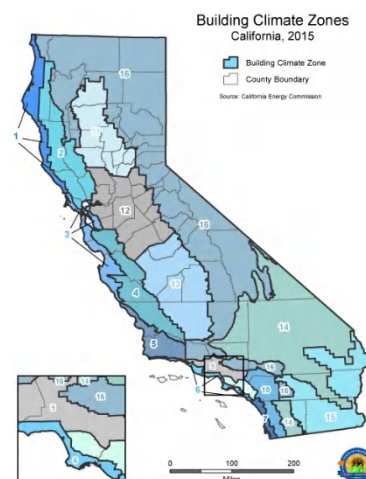


Figure 2-3. The climate zones of the California

Source: <https://eecoordinator.info/cecs-updated-climate-zone-map/>

Some standards and regulations have detailed climate zoning for their respective countries. In 1984, France divided the country into 3 climatic zones based on degree-hours (with a critical temperature of 11°C). The heating degree-hours for each zone are H1 (63,000 h°C), H2 (52,000 h°C), and H3 (37,000 h°C). The climatic zoning also takes into consideration the administrative divisions, ensuring that a province does not span across two zones [1]. In 1989, the ASHRAE90.1-1989 standard used clustering algorithms to divide the world into 58 climate zones based on various solar radiation, HDD, and CDD indicators for each orientation [7]. The standard was revised in 1993 and 2001 to modify HDD and CDD and further zone division. In

2011, Morocco selected 11 representative cities and conducted heating and cooling demand energy consumption simulations based on local climate conditions. The country was then divided into 6 climate zones based on the simulation results [8]. In 2013, Spain used regression analysis of HDD20, CDD20, and sunshine hours to obtain a climatic severity index, and divided the country into 4 zones in summer and 5 zones in winter. After combination classification, a total of 16 climate zones were generated [9-11]. In 2016, the ASHRAE90.1-2016 standard used HDD18 and CDD10 to divide the United States into nine hot climate zones and three humid climate zones, and generated 19 climate zones after combination classification, shown in Figure 2-2 [12]. In 2016, Australia used indicators such as water vapor pressure, average daily maximum temperature in January, average temperature in July, and heating degree days to divide the country into eight climate zones [13]. Japan uses the value of HDD18 to divide the country into 8 climatic zones [14]. Some researchers have also conducted climate zoning studies. In 2007, Manoj Kumar divided India into six climate zones based on daytime and nighttime temperatures in summer and winter [15]. In 2009, Joseph divided Madagascar into three zones based on average temperatures in January and July, and described the passive design of buildings [16].

At the same time, some countries and regions have also subdivided the main climate zones. Climate zone subdivision can provide more specific guidance for the selection of building heating and air conditioning technology solutions and the evaluation of energy-saving effects. In 2016, the Australian government further subdivided the country into 69 sub-climate zones and developed different energy efficiency levels for each sub-climate zone [17]. In 1995, the state of California in the United States used the average summer and winter temperatures from 600 weather stations to further divide the state into 16 climate zones and developed local building regulations to guide energy-saving work in buildings, shown in Figure 2-3 [18].

(2) Climatic subdivision research in China

Currently, there are 2 national standards for building climate zoning and thermal design zoning, as well as one recommended standard for energy-efficient design of residential buildings in China. The “Standard of climatic regionalization for architecture (GB 50178-93)” divides China into 7 primary zones and 20 secondary zones [19]. The “Thermal design code for civil building (GB 50176-2016)” divides China into 5 thermal zones, and “Energy-saving Design Standard for Residential Buildings in Hot-Summer and Cold-Winter Areas (JGJ134-2010)” divides China into 11 sub-climate zones to control air conditioning energy consumption [20, 21].

Apart from standards, scholars have studied the relationship between architecture and climate, the applicability of passive strategies in building design, and the application of heating, ventilation, and air conditioning systems. In 2003, Yang analyzed the relationship between indoor environmental conditions and outdoor climate conditions in typical Chinese cities based on Givoni’s climate analysis chart, and studied the climate analysis methods for building design [22]. In 2006, Dong et al. used hierarchical clustering analysis to identify meteorological factors that control the effect of natural ventilation for cooling, and developed a design zoning map for natural ventilation and cooling [23]. In 2006, Xie established a calculation model based on steady-state heat transfer theory, using outdoor meteorological factors that affect passive building construction, and proposed a zoning index for passive solar building design and regional division for passive solar building heating [24]. In 2008, Fu et al. divided China into

8 building climate zones based on the spatial variation coefficient of meteorological indicators, using HDD18 and CDD26 as primary indicators and winter solar radiation and summer relative humidity as secondary indicators [25]. In 2008, Xia Wei used Kriging spatial interpolation to obtain zoning maps for passive design potential and effectiveness of passive strategies, and revised the zoning based on a combination of standard deviation and maximum value [1]. In 2009, Liu et al. proposed the use of degree days, relative humidity, and clear sky index as climate zoning factors, and divided China into five climate zones using cluster analysis, addressing the deficiencies in existing standards [26]. In 2017, Xu et al. used the cluster analysis method to re-divide China into 8 climate zones on the basis of the mean air temperature in January and July, but the scope of climate division is still too large, and the specific indicators HDD18 and CDD26 that affect building energy consumption are not considered [27]. In 2019, Xiong et al. also used the cluster analysis method to sub-divide the hot summer and cold winter area of China's thermal region into 7 zones based on the value of HDD18 and CDD26, but the zoning resolution is only accurate to the municipal administrative division and does not consider the impact of climate zoning on the passive design of buildings [3]. In 2021, Yang et al. uses cluster analysis method to partition the urban climate of Xi'an city, Nanjing city and study their impact on building energy consumptions. The accuracy of the partition is very high, but it is limited to the analysis of flat urban areas and does not involve the vast rural areas with complex terrain [28, 29]. In 2022, Zhang et al. utilized daily data from 1902 highly dense ground meteorological stations in Chongqing to divide the region into five climate zones. The improved building climate zoning will to some extent improve the building energy efficiency and reduce emissions in Chongqing [30].

2.1.2 Main evaluation indicators for climatic subdivision

(1) Air temperature

The outdoor air temperature under climate zoning is the main factor affecting the heating and cooling energy consumption. By setting the temperature for air conditioning cooling and heating, the number of days when equipment is activated is determined, and cooling degree days (CDD) and heating degree days (HDD) are used as the main evaluation indicators for climate zoning.

(2) Relative humidity

Air humidity has a significant impact on human thermal comfort. In winter, under the same temperature conditions, high humidity can increase the sensation of coldness. Under suitable outdoor relative humidity conditions, natural ventilation can help to remove excess indoor moisture. For areas with extremely high relative humidity, some additional dehumidification measures are necessary to ensure indoor thermal comfort.

(3) Wind speed

Wind speed can effectively improve the indoor humid and thermal environment of buildings and is one of the clustering variables in climate zoning. For areas with high wind speeds, ventilation conditions are better, which can increase the potential for natural ventilation in summer, increase the heat exchange frequency between the building surface and air, and take away excess heat. However, compared to winter, high wind speeds can easily cause cold air to penetrate through the gaps in the building envelope, increasing the indoor heating energy consumption. For areas with low wind speeds, insufficient air circulation is not conducive to

zones (Zone I, II, III, IV, V, VI, and VII) based on the primary reference standards such as the average temperature in January and July, and the average relative humidity in July, and the secondary reference standards such as annual precipitation, the number of days with an average temperature of $\leq 5^{\circ}\text{C}$ and $\geq 25^{\circ}\text{C}$. Furthermore, within each primary zone, the map is further subdivided into 20 sub-climatic zones considering factors like average temperatures in January and July, permafrost characteristics, maximum wind speed, and annual precipitation [19]. For each sub-climatic zone, corresponding architectural requirements and technical measures are proposed. Currently, the building climate zoning uses meteorological data from national standard stations, which have a long statistical time and accurate data, mainly for large-scale research objects. However, there is still a lack of research on climate in certain complex geographic regions.



Figure 2-5. China thermal zoning map

Source: *Thermal design code for civil building (GB 50176-2016)*

From the perspective of building thermal design, the “Thermal design code for civil building (GB 50176-2016)” divides the whole country into 5 thermal zones, shown in Figure 2-5 [20]. The purpose is to ensure that the thermal design of civil buildings is compatible with the regional climate, meets the basic indoor thermal environment requirements, and complies with national energy-saving guidelines, shown in Table 2-1. The primary indicators for zoning are the average temperature in the coldest month (January) and the hottest month (July), and the secondary indicators are number of days with an average temperature of $\leq 5^{\circ}\text{C}$ and $\geq 25^{\circ}\text{C}$. The 5 thermal zones in China include the severely cold region, the cold region, the hot summer and cold winter region, the hot summer and warm winter region, and the mild region [20]. In addition, due to the significant impact of climate factors on building energy consumption, “Design standard for energy efficiency of residential buildings in hot summer and cold winter

zone (JGJ 134-2010)” uses heating degree days (HDD18) and cooling degree days (CDD26) to measure the degree of cold and heat in the area and divides China into 11 sub-climate zones for controlling air conditioning energy consumption [21].

Table 2-1. China thermal zoning and design requirements
Source: *Thermal design code for civil building (GB 50176-2016)*

Thermal zone	classification indicators		Design requirements
	Primary indicators	Secondary indicators	
Severely cold region	${}^1T_{ATC} \leq -10^\circ\text{C}$	${}^3T_{DAT} \leq 5^\circ\text{C}, \geq 145\text{d}$	Buildings must adequately meet winter heating requirements, and generally, summer heat prevention may not be a primary consideration.
Cold region	$-10^\circ\text{C} \leq T_{ATC} \leq 0^\circ\text{C}$	$T_{DAT} \leq 5^\circ\text{C}, 90-145\text{d}$	Buildings should meet winter insulation requirements, and in some regions, they should also consider summer heat prevention.
Hot summer & cold winter region	$0^\circ\text{C} \leq T_{ATC} \leq 10^\circ\text{C};$ $25^\circ\text{C} \leq {}^2T_{ATH} \leq 30^\circ\text{C}$	$T_{DAT} \leq 5^\circ\text{C}, 0-90\text{d};$ $T_{DAT} \geq 25^\circ\text{C}, 50-110\text{d}$	Buildings must meet summer heat prevention requirements while also appropriately considering winter insulation.
Hot summer & warm winter region	$T_{ATC} > 10^\circ\text{C};$ $25^\circ\text{C} \leq T_{ATH} \leq 29^\circ\text{C}$	$T_{DAT} \leq 25^\circ\text{C}, 100-200\text{d}$	Buildings must adequately meet summer heat prevention requirements, and generally, winter insulation requirements may not be a primary consideration.
Mild region	$0^\circ\text{C} \leq T_{ATC} \leq 13^\circ\text{C};$ $28^\circ\text{C} \leq T_{ATH} \leq 25^\circ\text{C}$	$T_{DAT} \leq 5^\circ\text{C}, 0-90\text{d}$	In some regions, buildings should consider winter insulation, while generally, summer heat prevention may not be a primary consideration.

Note: ${}^1T_{ATC}$ refers to the average temperature of the coldest month; ${}^2T_{ATH}$ refers to the average temperature of the hottest month; T_{DAT} refers to the daily average temperature.

Due to the consistent criteria used for building climate zoning and thermal zoning, these two classifications are compatible and fundamentally consistent with each other.

2.1.4 Research prospect

As can be seen from above, researchers mainly focus on two issues: the selection of zoning indicators, and the integration of mathematical methods and actual zoning problems. In addition to national and industry standards, scholars have conducted research on energy-saving zoning for building climates, passive solar design zoning, natural ventilation design zoning, etc., according to the adaptability of building climates in different professional fields. In terms of the selection of climate zoning indicators, both domestic and foreign researchers mainly use temperature as the main indicators, combined with other climate factors such as relative humidity, wind speed, and solar radiation. In terms of zoning methods, climate zoning research mostly uses climate analysis, clustering methods, spatial interpolation, etc., but different

methods have different purposes, resulting in vastly different climate zoning results. From the above research, China's climate division across the country is still relatively rough. In the world, there are few studies on sub-climatic zones at the provincial administrative region scale, and the climate zoning does not integrate the thermal comfort temperature range and passive design strategy for the region. Based on the literature review, the following 4 topics can be focused on in future research.

(1) Updating meteorological data. Future research needs to update the old data used for meteorological zoning. In the global environment of climate warming, the observation capabilities and technologies of meteorology have improved, resulting in improved accuracy of related data records. Currently, China's building climate regional division mainly relies on data recorded from 1971-2000, and there is an urgent need to update climate data to improve building climate zoning.

(2) Increasing the sample size of meteorological zoning data. The original zoning standards were based on a small sample of climate data. The increase in meteorological stations continuously improves the blank and discontinuity of meteorological data between regions, and requires more detailed zoning. The existing building climate zoning and thermal zoning standards were established early, based on a sample size of less than 200 groups of meteorological station data, which has a certain impact on the accuracy and coherence of zoning boundaries.

(3) Considering comprehensive meteorological factors for zoning. The selection of meteorological factors that affect each other directly affects the accuracy of zoning. The comprehensive impact of meteorological elements that interact with each other affects the climate characteristics of the region. Therefore, it is crucial to screen and assign weights to meteorological elements for the scientific and rationality of climate zoning.

(4) Considering comprehensive disciplinary needs for zoning. Different disciplines and research have different focuses on meteorological zoning, and the meteorological factors and weights used are also different. Detailed climate zoning should be carried out for subdivided disciplinary fields to guide disciplinary development.

2.2. Review of research on thermal comfort

The American Society of Heating, Refrigerating and Air-Conditioning Engineers (ASHRAE) defines thermal comfort as "the mental state in which satisfaction is expressed with the thermal environment". Therefore, thermal comfort is subject to personal variations influenced by factors such as mood, culture, and individual, organizational, and social aspects. It is important to note that comfort is not merely a physical state but a subjective perception. The definition of thermal comfort acknowledges that it involves the cognitive process of evaluating various inputs influenced by physical, physiological, psychological, and other factors [31]. Even in the same environment, individuals can have different thermal sensations. While sensors may yield consistent results regardless of the geographical location of measurement, this is not the case for individuals. In fact, people occupying very similar spaces, experiencing the same climate, and sharing a common culture may express diverse opinions on thermal comfort due to a multitude of factors influencing human perception [32]. Therefore, the assessment of subjects is essential in achieving a comprehensive evaluation of the study parameters. Thermal comfort is generally experienced when the body temperature remains within a narrow range, skin

moisture is low, and the physiological effort required for thermoregulation is minimized. Additionally, comfort is influenced by behavioral actions such as adjusting clothing, modifying activities, changing posture or location.

Currently, the comfort zone recommended in the ASHRAE and ISO 7730 standards is widely used worldwide as a benchmark for assessing thermal comfort. These standards were developed based on research conducted on healthy young individuals primarily from European and American countries, using the human heat balance equation as a foundation and established through experimental studies. In laboratory research, environmental parameters remain constant over time, and the human body is considered a passive recipient of external thermal stimulation. However, the increasing comparison between laboratory research and field test results has shown that the human body is not merely a passive recipient of the external environment. The various adaptabilities of the human body have a significant influence on thermal comfort. As a result, numerous field investigations on thermal comfort have been conducted worldwide. Due to the variations in dietary patterns, human metabolism, climate and cultural backgrounds, economic development levels, lifestyle habits, and differences in architectural design techniques and standards across countries, there exist substantial differences in physiological adaptation and psychological expectations. These differences lead to varying thermal sensations. Therefore, it is essential to conduct on-site investigations of human thermal comfort in architectural indoor environments for different regions, functional purposes, and even different building operational modes [33]. Therefore, there are two distinct approaches to defining thermal comfort, each with its own strengths and limitations: the rational (heat-balance) approach and the adaptive approach. The rational approach, exemplified by the research of Fanger, relies on data from climate chamber studies to develop its theoretical framework [34]. The adaptive approach draws upon data from field studies conducted with individuals in real building environments [35].

2.2.1 Overview of thermal comfort

(1) Thermal comfort research on a global scale

With the development and progress of human society, the increasing economic and living standards have led to higher demands for living environments. In 1919, with the establishment of the Pittsburgh Indoor Climate Laboratory by the American Society of Heating and Ventilating Engineers (ASHVE), a milestone was reached in the scientific study of thermal comfort. Subsequently, numerous scholars conducted extensive indoor experimental research on thermal comfort and proposed a series of standards for evaluating and predicting the indoor thermal environment [33]. In 1923, through a substantial number of experiments, Houghton determined the comfort boundary of semi-nude males as a function of air temperature and humidity under stationary air conditions, proposing the index of Effective Temperature (ET). The numerical value of ET is the same as the air temperature in a static saturated air environment with the same thermal sensation [36]. In the 1960s, scholars began to pay attention to people's thermal comfort sensations in actual building environments and developed more indicators and methods related to subjective evaluation. Scholars have determined the 6 factors that affect thermal sensation: 4 physical variables (air temperature, air velocity, relative humidity, mean radiant temperature) and 2 personal variables (clothing resistance and metabolic rate) [37]. These factors are crucial in determining thermal comfort standards, as they

have a significant impact on energy consumption in a building's environmental systems and contribute to building sustainability [38]. In 1971, Gagge introduced a new index called New Net Effective Temperature (ET*) that integrates the effects of temperature and humidity on human thermal comfort. It is specifically applicable to individuals wearing standard clothing and engaged in seated work. Subsequently, the Standard Effective Temperature (SET) index was proposed, which considers the influence of different activity levels and clothing thermal resistance [39]. Meanwhile, in the 1970s, Fanger conducted extensive research on climate chambers, established the thermal comfort equation, Predicted Mean Vote (PMV) index, and Predicted Percentage Dissatisfied (PPD) index. This index comprehensively considers 6 factors: air temperature, humidity, air velocity, mean radiant temperature, metabolic rate, and clothing thermal resistance. It is developed based on the subjective thermal sensation levels derived from psychological and physiological considerations. As the most comprehensive evaluation index, it takes into account various factors related to human thermal comfort [31]. The International Organization for Standardization (ISO) developed the ISO 7730 standard in 1984, and the American Society of Heating, Refrigerating and Air-Conditioning Engineers (ASHRAE) established the ASHRAE 55-1992 standard in 1992. Both standards were based on the PMV-PPD indices and became widely adopted indoor thermal environment evaluation standards at that time. As a result, the establishment of thermal comfort standards allowed for the development of a separate discipline dedicated to the study of human thermal comfort.

Indeed, the thermal comfort standards that evaluate and predict indoor thermal environments were initially developed based on studies conducted on healthy young individuals from European and American countries. These studies were conducted in controlled laboratory settings, utilizing steady-state conditions and the human heat balance equation, with the requirement of maintaining stable environmental parameters. However, it is important to acknowledge that human adaptability to thermal environments varies, making these standards potentially less applicable to other countries and regions. With the advancement of on-site research on thermal comfort, a significant amount of field-testing results has emerged. These findings have demonstrated notable discrepancies between the actual thermal sensation experienced by individuals in indoor environments and the predicted results based on the international thermal comfort standards such as ASHRAE 55-1992 and ISO 7730. Therefore, in the 1970s, scholars have conducted on-site investigations of indoor thermal environments in different regions, as well as research on human thermal comfort. Howell et al. conducted on-site investigations of staff in public buildings such as office buildings, libraries, and teaching buildings [40, 41]. In 1970, Humphreys compared field survey results with laboratory research findings and observed that the thermal neutral temperature obtained from field measurements through regression models better matched human actual thermal sensation compared to predicted results from models. He attributed this difference to the adaptability of individuals to climate conditions and introduced the concept of "thermal adaptation" for the first time, and provided a regression equation that relates human thermal sensation to outdoor average air temperature [42, 43]. Since then, on-site research has become an important way of studying thermal comfort. In 1980s, research gradually focused on the impact of individual differences on thermal comfort, such as age, gender, physique, and other factors [44-46]. 1990s, scholars began to consider the adaptive capacity of buildings and people's adaptive capacity to thermal environments, proposed the adaptive methods. In 1998, Richard and Brager developed

adaptation models for air-conditioned rooms and naturally ventilated rooms based on a sample dataset from 21,000 field studies conducted in various climatic regions around the world [47, 48]. Humphreys, Richard, and other scholars have proposed the concept of thermal adaptation in relation to human thermal comfort based on field investigations from recent decades. They suggest that human thermal sensation, thermal satisfaction, and thermal acceptability are influenced by the interaction between people's expectations of a specific indoor climate and the actual thermal environment. This indicates that individuals can adapt and adjust their thermal perception and preferences based on their experiences and the specific conditions they encounter [49]. In 1995, ASHRAE completed a survey and test of global building thermal environments and thermal comfort and established a human adaptation model applicable to future building thermal comfort research, of which the PMV steady-state model is the most commonly used [50]. In 1998, Brager et al. constructed an adaptive model for air-conditioned rooms and naturally ventilated rooms based on sample data obtained from field research in various global climate regions. More and more laboratory research and field test results show that the human body is not a passive recipient of external environments, and various adaptabilities of the human body have a significant impact on thermal comfort [51]. As a result, two fundamental research approaches emerged in the field of thermal comfort. One approach is based on the human heat balance and relies on artificial laboratory studies, where individuals are considered passive recipients of controlled environmental changes rather than active adaptors in real-world conditions. The comfort indices derived from this approach are referred to as "rational approach" in academia. The other approach is based on adaptive research conducted through field investigations. It recognizes that humans are not merely passive recipients of environmental stimulation but also active adaptors. It acknowledges that thermal comfort is part of the human body's self-regulating system, taking into account behavioral, physiological, and psychological adjustments. This approach views thermal comfort as a dynamic system, and the comfort indices derived from it are known as "adaptive approach".

Since the beginning of the 21st century, people's evaluation and assessment of indoor environments have continuously improved. Researchers have conducted studies on human thermal comfort in different age groups, regions, and seasons. In 2013, Mendes et al. conducted on-site thermal comfort research on hundreds of elderly people in a nursing home in Portugal [52]. In 2016, Singh et al. found that family composition, building envelope, and occupant activities and preferences have a significant impact on indoor thermal comfort by comparing the indoor thermal environment testing and thermal comfort investigation of traditional Belgian buildings [53]. In 2017, Sutida et al. conducted field investigations on the thermal comfort of medical staff in a hospital building in Bangkok, Thailand, and verified the availability of the Predicted Mean Vote (PMV) model [54]. In 2017, Ivan et al. conducted on-site thermal comfort research in the four main climate zones of Mexico and obtained an adaptive thermal comfort model applicable to these regions. They also determined the upper limit of indoor air temperature for passive cooling and the lower limit for active cooling [55]. In 2017, Antonio et al. evaluated the thermal comfort conditions of a primary school in Spain by conducting subjective thermal comfort assessments on teachers and students and calculating the Predicted Mean Vote (PMV) and Percentage of Dissatisfied (PPD) to assess the difference in subjective opinions between students and teachers. They found that children have a higher threshold for indoor thermal comfort and are more difficult to satisfy [56]. In 2018, Aradhana et al.

investigated the indoor thermal environment and thermal comfort of a naturally ventilated classroom in a school in Ambala, India. Through questionnaire analysis and measurements, they obtained a neutral temperature of 27.1°C [57]. In 2019, Atmaca et al. measured the indoor thermal comfort levels and energy consumption of two mosques and proposed design and air conditioning system recommendations for future mosques [58]. In 2019, Veronica found no significant differences in thermal sensation, comfort, and acceptability between elderly and young participants.[59] In 2020, Forcada et al. conducted a questionnaire survey on 623 elderly residents and staff in a nursing home in the Mediterranean climate region during summer. They found that the comfortable temperature for the elderly was 24.4°C, and for non-elderly was 23.5°C. The elderly were more tolerant of high temperatures than non-elderly [60]. In 2021, Pablo et al. investigated the thermal comfort of a school building in southwestern Spain and collected 64 thermal questionnaires. They observed a neutral temperature at an average indoor temperature of 24-27°C, which is larger than the international standard range for thermal comfort [61]. In 2023, Molina et al. investigated the thermal comfort of residential buildings in high-altitude rural areas in southern Peru and calculated the energy required to maintain thermal comfort inside the buildings [62]. In 2023, Niveditha et al. determined the thermal comfort range for elderly people in warm and humid summer climates in India. They used linear regression analysis to obtain a comfortable temperature of 30°C for residents, with a comfort range of 28.5°C-31.5°C, which is smaller than that of young people [63].

(2) Thermal comfort research in China

Due to slower social and economic development, research on indoor thermal comfort in China did not begin until the 1980s. Wei et al. conducted the first study on indoor thermal comfort in 1980, focusing on the influencing factors. Since then, Chinese scholars have conducted extensive research on indoor thermal comfort. This study focuses on thermal comfort research in rural areas of China. Due to the imbalance in urban and rural economic development, there are significant differences in living standards and habits among residents, resulting in considerable variations in people's behavior, physiological adaptation, and psychological expectations regarding the thermal environment. Although some scholars in China have conducted research on the indoor thermal environment of residential buildings in some cities, the conclusions drawn from these studies may not be applicable to the research on thermal comfort in rural residential buildings. Moreover, rural settlements in China are often located in areas with complex natural and geographical features. Therefore, investigations of thermal comfort should consider the influence of climate and geographical characteristics. And large geographic units or administrative regions should be subdivided into climate zones for the investigation of thermal comfort. Additionally, the distribution of rural dwellings is not centralized, making thermal comfort research relatively challenging. The current research on rural indoor thermal comfort in China mainly focused on severe and cold regions, and scholars analyzed indoor thermal environment indicators from different perspectives.

In 2002, Wang et al. investigated the indoor thermal environment and thermal comfort of rural homes near Harbin in winter. The results showed that the neutral temperature in winter was 14.4°C, and 90% of the acceptable temperature range was 8.8°C [64]. In 2006, Jin et al. studied the indoor thermal environment of rural homes in severely cold regions and proposed a thermal comfort range of 15-18°C [65]. In 2010, Zhu et al. surveyed the indoor thermal comfort of farmers in Yinchuan and found that the optimal comfort temperature for farmers should be

greater than 15°C [66]. In 2011, Huang et al. studied the thermal comfort of rural homes during the heating season in Beijing and found that the neutral temperature of rural dwellings was 18.4°C, the acceptable temperature lower limit was 10.9°C, and the comfortable temperature was related to the dressing habits and lifestyle of farmers [67]. In 2011, Yang et al. conducted the environmental measurement and questionnaire survey on the residential dwelling in Guangzhou, and the result showed that the thermal neutral temperature of rural residents was 11.7°C, 80% of residents' acceptable temperature range lower limit was 8.0°C, and the expected temperature was 12.7°C [68]. In 2012, Gao et al. conducted field tests and questionnaire surveys on the thermal comfort of rural homes in cold regions. The results showed that the average indoor temperature in winter was only 11.7°C, and the comfortable temperature that satisfied residents was 15.26°C [69]. In 2019, Lei et al. studied the local thermal comfort of college students in Taiyuan, and found that the PMV model overestimated the students' thermal sensation. The lower limit of acceptable temperature for 80% of students was 19°C, and students preferred a cooler environment [70]. In 2020, Fu et al. studied the adaptive thermal comfort of office spaces in Guangzhou and found that the comfortable temperature in summer and winter was 26.2°C and 21.1°C, respectively [71]. In 2020, Yu et al. conducted a field study on the adaptive thermal comfort of elderly people in the hot summer and cold winter region of China and found that the acceptable temperature range for elderly people was 14.4~19.4°C in winter, 23.8~27.0°C in summer, and 20.6~31.7°C in transition seasons [72]. In 2021, Jia et al. conducted a field survey on transportation buildings and found that passengers were more adaptable to indoor thermal environments than the PMV-PPD model predicted [73]. In 2022, Chang et al. studied the differences in indoor thermal environment and human comfort among residential buildings in urban, suburban, and rural areas. The results showed that the acceptable working temperature ranges for residents in urban, suburban, and rural areas were 20.9~28.0°C, 17.7~23.3°C, and 15.1~21.6°C, respectively [74]. In 2022, Zheng et al. analyzed the thermal response of residents in Xi'an to seasonal climate change. The results showed that clothing adjustment during transition seasons was the most sensitive to temperature changes, and the neutral temperatures in winter, transition seasons, and summer were 19.4°C, 22.6°C, and 24.1°C, respectively [75]. In 2022, Zhao et al. studied large shopping malls in cold regions of China and found that the indoor thermal environment was overheated in winter and too cold in summer. The neutral temperatures in spring, summer, autumn, and winter were 21.3°C, 25.4°C, 19.0°C, and 17.4°C, respectively [76]. In 2023, Wang et al. conducted a survey on the thermal environment characteristics of large and small classrooms during the heating period in winter. The results showed that the average air temperature in large lecture halls was about 3°C lower than that in small classrooms. In addition, the vertical height difference of the large lecture hall resulted in different air temperature and relative humidity distribution in different locations [77].

2.2.2 Thermal comfort index

(1) Human thermal comfort

1) Human thermal sensation

Thermal sensation is a subjective description of whether a person feels “cold” or “hot” in the surrounding environment, and it cannot be measured directly by any method. The study of thermal sensation belongs to the field of psychology. Weber began to study the psychology of sensation. The human body's thermal sensation cannot be fully demonstrated, and a person's

perception of thermal sensation cannot be simply predicted by the temperature of the stimulus alone. It also includes the effects of many other factors, such as the body surface area, body posture, duration of external thermal stimulation, the body's original thermal state, and people's subjective feelings in their minds. Therefore, the human body's sense of hot and cold not only includes the physiological sensation of hot and cold stimulation but also includes people's subjective descriptions of hot and cold sensations.

2) Human thermal comfort

Human thermal comfort is defined in the ASHRAE 55-92 standard as a conscious state reflecting a person's satisfaction with the thermal environment, and in the ISO 7330 standard as a thermal environment that subjectively feels comfortable. Human thermal comfort is a feeling of whether or not one is comfortable, which is obtained by synthesizing one's own thermal balance and perceived environmental conditions. It is determined by both physiological and psychological factors, but it is more heavily influenced by psychological factors. Human thermal comfort is obtained by studying the subjective thermal response of the human body to the thermal environment, and thereby obtaining the optimal combination range and allowable range of environmental parameters that affect human thermal comfort, as well as a series of control and adjustment measures to achieve this condition. Parameters that affect human thermal comfort include environmental parameters such as air temperature, air humidity, air velocity, mean radiant temperature, and human parameters such as clothing thermal resistance and metabolic rate.

a. Thermal neutral temperature. The thermal neutral temperature refers to the theoretical temperature at which the human body feels most comfortable (neither cold nor hot) in the environment. The thermal neutral temperature can be divided into measured thermal neutral temperature and predicted thermal neutral temperature. By conducting a linear regression analysis between the thermal sensation votes obtained from the survey participants and the corresponding environmental temperatures, the measured neutral temperature can be determined. The predicted thermal neutral temperature is obtained by using Fanger's PMV index to predict the average voting value of human thermal sensation obtained through laboratory studies as the dependent variable, and the linear relationship between PMV and temperature: $PMV = a \cdot t + b$, setting $PMV = 0$, the predicted thermal neutral temperature can be obtained. By using Fanger's PMV index to predict the voting values of human thermal sensation under experimental conditions, and conducting a linear regression analysis between the predicted voting values and the environmental temperature, the predicted thermal neutral temperature can be obtained.

b. Expected temperature. The calculation of the expected temperature uses the probability method, that is, within a certain temperature range, the linear regression curve of the hot dissatisfaction rate (thermal sensation voting value of 3, 2) with the change of indoor air temperature and the cold dissatisfaction rate (thermal sensation voting value of -3, -2) with the change of indoor air temperature are statistically calculated, and the two regression curves are plotted on the same graph. The air temperature corresponding to the intersection of the two regression curves is the expected temperature.

(2) Factors influencing human thermal comfort

There are 6 main factors that influence human thermal comfort, including air temperature, relative humidity, air velocity, mean radiant temperature, metabolic rate, and clothing insulation.

The specific descriptions of each influencing factor are as follows:

1) Environmental factors

a. Air temperature. Air temperature is the main parameter that affects human thermal sensation and comfort. It is also the primary factor that affects human thermal comfort. Various factors such as local climate, window size, and building materials can affect indoor air temperature. When indoor air temperature drops slightly, people will feel slightly cold, and their bodies will generate some heat through physiological processes to achieve thermal equilibrium. When indoor air temperature rises slightly, people will feel slightly warm, and their bodies will dissipate excess heat through sweating. Therefore, when the human body is in a relatively stable thermal environment, it can maintain thermal balance through its own physiological processes, allowing people to feel comfortable. However, large temperature changes cannot be balanced by the body's physiological processes. Studies have shown that the most comfortable indoor temperature range is approximately 20°C to 24°C. When indoor air temperature drops below 15°C, fingers become stiff and unable to write or perform normal work. When indoor air temperature exceeds 33°C, it can lead to an increase in body temperature and adverse physical conditions.

b. Mean radiant temperature. In order to maintain a constant body temperature, the human body undergoes various heat exchanges with the surrounding environment, and radiant heat exchange is a type of heat exchange that is always present. Mean radiant temperature is an important parameter for radiant heat exchange between the human body and the surrounding environment. It is defined as the average temperature of the surfaces around the environment that radiate heat to the human body. The radiant heat exchange between the human body and the interior surfaces of the building envelope depends on the temperature of each surface and the relative position between the human body and the surface. Currently, the mean radiant temperature of the environment is often calculated by measuring the black globe temperature.

$$t_{MRT} = t_g + 2.44\sqrt{v}(t_g - t_a) \quad (2-1)$$

Where t_{MRT} is mean radiant temperature, °C; t_g is the black globe temperature, °C; v is the air velocity, m/s; t_a is the indoor air temperature, °C.

c, Relative humidity. The size of relative humidity indirectly affects the evaporation of water on the surface of the skin and the amount of sweating in the human body. If the relative humidity is too high, the rate of evaporation of water on the skin surface decreases and the amount of sweating decreases, causing a feeling of dampness. If the relative humidity is too low, the rate of evaporation of water on the skin surface increases and the amount of sweating increases, causing a feeling of dryness. According to relevant research, the most suitable indoor temperature in winter is 18°C~25°C, and the relative humidity is 30%~70%. At this time, most people will feel comfortable.

d, Airflow velocity. Airflow velocity affects the skin's perception of the outside world, and people often refer to the uncomfortable feeling caused by airflow velocity as "draft". Airflow velocity is an important factor affecting human thermal comfort. Research has shown that in cold environments, drafts can disrupt the body's thermal balance and make people feel cold. In contrast, in warm environments, drafts may promote heat dissipation in the body, but if the

airflow is too fast, it may cause uncomfortable feelings. Therefore, in summer, a higher airflow velocity often increases human thermal comfort, while in winter, if the indoor airflow velocity is too high, it will make people feel cold.

2) Human factors

a. Metabolic rate. The human metabolic rate refers to the amount of heat generated per unit of time on the surface of the human body, which is the process of converting other forms of energy within the body into heat. The metabolic rate of the human body is influenced by many factors. For example, when a person is stimulated and experiences high levels of mental stress, the metabolic rate will increase significantly. Additionally, the metabolic rate gradually decreases with age. A healthy adult in their 20s having a maximum metabolic rate of 12 met, while a person in their 70s will have a metabolic rate that decreases to 7 met. Furthermore, the metabolic rate of females is 6% to 10% lower than that of males. The unit of measurement for metabolic rate is met ($1\text{met}=58.2\text{W/m}^2$). The normal metabolic rate of an adult is shown in Table 2-2.

Table 2-2. Metabolic rate of the human body

Source: *Thermal design code for civil building (GB 50176-2016)*

Type of activity	W/m ²	met	Type of activity	W/m ²	met
Sitting	40	0.7	Walking, 0.9m/s	115	2.0
Standing	70	1.2	Walking, 1.2m/s	150	2.6
Lying down	46	0.8	Walking, 1.8m/s	220	3.8
Sleeping	40	0.7	Walking, 2.37m/s	366	6.29
Cooking	94-115	1.6-2.0	going up the stairs	707	12.1
Reading	55	1.0	going down the stairs	233	4.0
Working in office	65	1.1	lifting heavy objects	120	2.1
Organizing documents	80	1.4	strolling	123	2.1

b. Clothing thermal resistance. The clothing thermal resistance represents the sensible heat resistance of the clothing itself, with units of $\text{m}^2\cdot\text{K}/\text{W}$ and clo ($1\text{ clo} = 0.155\text{ m}^2\cdot\text{K}/\text{W}$). The thermal resistance of 1 clo clothing refers to the thermal resistance of a person wearing long-sleeved shirts, long pants, regular clothing, or outdoor clothing that can withstand heat in a comfortable environment where the air velocity is less than 0.05 m/s, the relative humidity is less than 50%, and the air temperature is 21°C. Relevant studies have shown that the thermal resistance of summer clothing is 0.5 clo, while the thermal resistance of winter clothing is 1.5 clo to 2.0 clo.

(3) Evaluation Indicators of Indoor Thermal Environment

There are various indicators for evaluating indoor thermal environment, such as Effective Temperature (ET), Standard Effective Temperature (SET), New Effective Temperature (ET*), and predicted mean votes (PMV) etc. Now, a brief overview of the thermal environment evaluation indicators relevant to this study will be provided.

1) PMV-PPD Index

PMV (Predicted Mean Vote) is an index recognized by the International Organization for Standardization (ISO) for evaluating indoor thermal environment. Due to individual differences that exist among people in some aspects, it represents the thermal sensation of the vast majority of people in the same thermal environment. Currently, PMV is a comprehensive index that can

be used to evaluate thermal comfort. The PMV index uses a 7-level scale, as shown in Table 2-3.

Table 2-3. Thermal sensation voting questionnaire

Thermal sensation	Cold	Cool	slightly cool	comfortable temperature	slightly warm	warm	Hot
PMV	-3	-2	-1	0	1	2	3

Subsequently, Fanger proposed the Predicted Percent Dissatisfied (PPD) based on the PMV index, which represents the percentage of people who are dissatisfied with their thermal environment. In the 1980s, the International Organization for Standardization (ISO) proposed a new standard, ISO 7730, for evaluating indoor and outdoor environmental parameters. This standard indicates that in a thermal environment, 10% of people may feel uncomfortable, and the recommended value of the corresponding PMV-PPD index is between -0.5 and 0.5. The following Figure 2-6 shows the relationship curve between PMV and PPD.

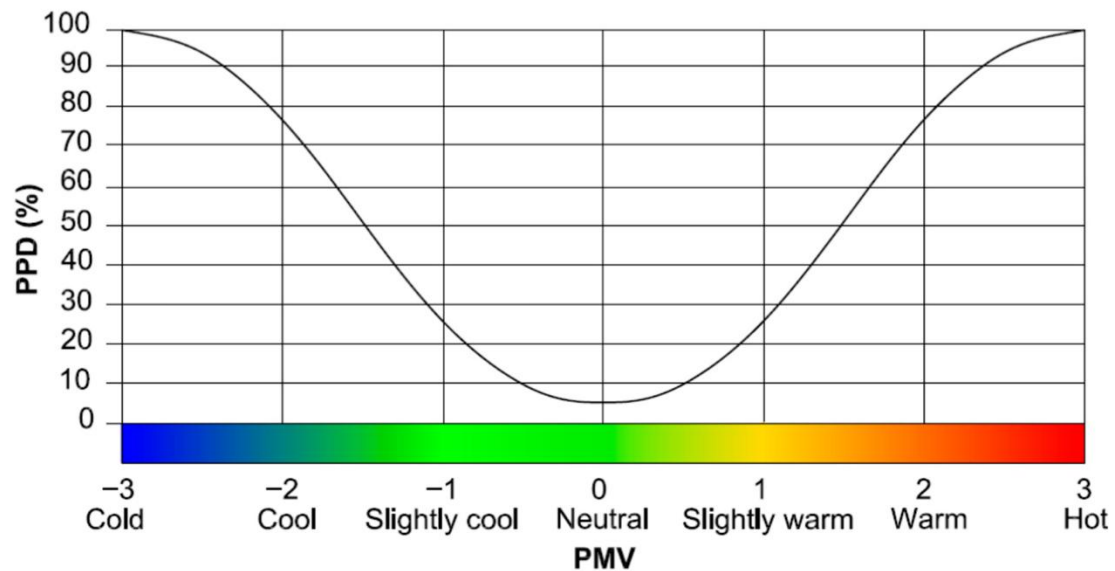


Figure 2-6. The relationship curve between PMV and PPD [78]

2) Operative Temperature

The operative temperature (T_{op}) considers the combined effects of air temperature and mean radiant temperature on human thermal sensation, resulting in a more precise physical interpretation of thermal comfort for occupants. The calculation formula for operative temperature (T_{op}) is as follows:

$$T_{op} = \frac{h_r \cdot T_{mr} + h_c \cdot T_a}{h_r + h_c} \quad (2-2)$$

Where h_r is the radiation heat transfer coefficient, $W/(m^2 \cdot K)$; h_c is the convective heat transfer coefficient, $W/(m^2 \cdot K)$, and its value is determined based on ASHRAE 55-2013; T_a is the indoor air temperature, $^{\circ}C$; T_{mr} is the mean radiant temperature in the indoor environment, $^{\circ}C$.

2.2.3 Research prospect

As can be seen from above, the biggest achievement in worldwide research on thermal comfort is the proposal of a series of relevant indicators for evaluating thermal environment that are still in use today, and the establishment of universal standards for global thermal environment through experiments. In addition, through extensive questionnaire surveys and on-site thermal environment testing, the thermal comfort range of different regions, genders, ages, and building types has been explored. Research on thermal comfort in China started relatively late. Currently, China has conducted a large number of on-site investigations and research on human thermal comfort in different thermal zones, and has established an adaptive thermal comfort model. However, there is little research on thermal comfort in residential buildings in mountainous rural areas, especially traditional dwellings, and the indoor thermal comfort of traditional dwellings urgently needs to be improved. Future research can focus on the following aspects:

1) Study the environmental characteristics, climate adaptability of rural areas. Rural residential buildings are often located in areas with harsh natural environments, such as the hot south and cold north. Researchers can investigate local environmental characteristics and climate adaptability to explore the key influencing factors of thermal comfort in rural residential buildings.

2) Study the thermal comfort evaluation indicators of rural residential buildings. According to different climate zones, corresponding thermal comfort evaluation indicators for rural residential buildings can be developed, thereby optimizing the indoor thermal environment while reducing building energy consumption.

2.3. Review of research on passive design strategy

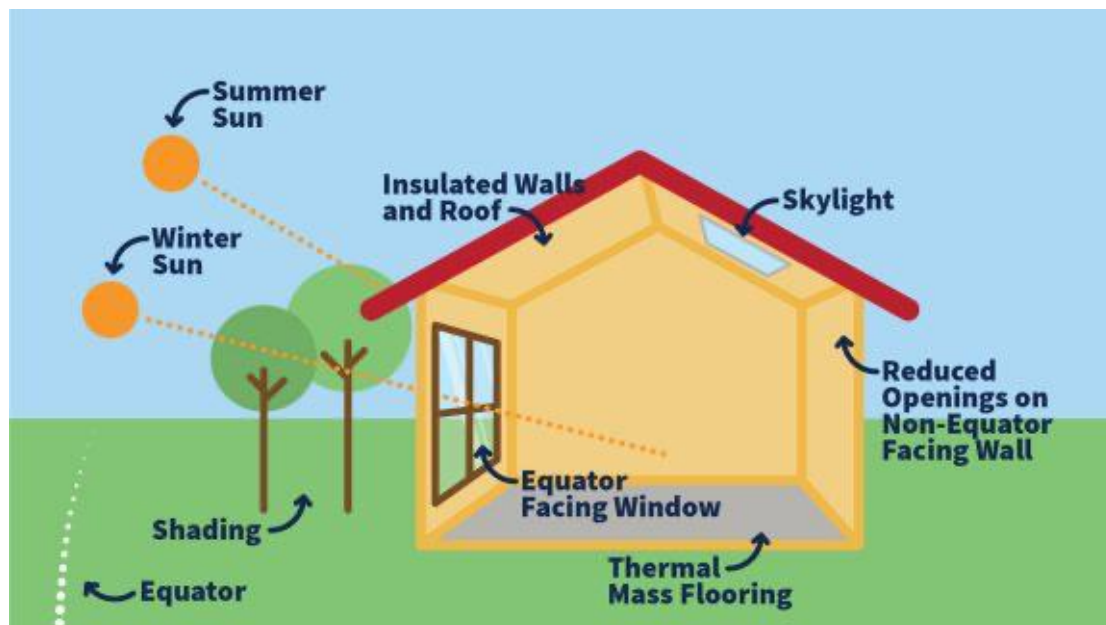


Figure 2-7. Passive design strategies diagram

Source: <https://www.bradpettitt.com/blog/effective-house-design-for-passive-heating-and-cooling/>

Passive strategies refer to the strategies that use the characteristics of the building itself and environmental factors to achieve energy-saving purposes. These strategies do not rely on the operation of mechanical or electrical equipment, but rather achieve energy-saving through the design, construction, and operation of the building. The design of passive strategies involves multiple aspects, such as building orientation, wall thickness and insulation performance, window size and orientation, indoor thermal comfort, natural ventilation, and lighting, shown in Figure 2-7. The main purpose of these strategies is to reduce the building's energy demand, lower operating costs, and reduce environmental impact.

2.3.1 Overview of passive design strategy

(1) Passive design strategy research on a global scale

Passive design has been inherent in vernacular architecture for centuries, with a history spanning thousands of years. There is evidence to suggest that ancient people considered various factors when constructing buildings, such as orientation towards the sun, utilizing materials with thermal inertia, natural ventilation, etc.

Since the 1960s and 1980s, a series of problems caused by industrial civilization, such as resource shortage, air pollution, and water scarcity, have gradually emerged. The Western academic community began to seek corresponding solutions and advocate for low-energy, environmentally friendly, and regionally appropriate building groups to solve these problems. In 1963, American scholar Olgyay first proposed a systematic analysis method for building climate in his book "Design with Climate," advocating for more consideration of climate factors in the building design process [79]. In 1976, Baruch improved Olgyay's bioclimatic method by considering people, climate, and architecture, analyzed climate conditions from the perspective of thermal comfort, and provided powerful references for designers in the design strategies that could be adopted [80]. The global oil crisis in the 1970s made developed countries realize the importance of non-renewable resources and energy conservation. Subsequently, various countries launched a series of energy-saving research work and began to focus on the research of passive solar buildings in the construction field, attempting to use solar energy resources for low-energy building design. In 1984, Kato et al. summarized the passive solar design techniques in the practice of passive solar building design based on multiple cases he participated in Japan [81]. In 1986, Sodha et al. introduces the fundamentals of solar passive building science and architecture, including thermal comfort, climate factors, passive design concepts and components, heat transmission, mathematical models, performance evaluation, cooling systems, design patterns, and appendices with relevant tables and tools [82].

In 1990s, the concept of passive building design was introduced. In 1994, Bansal et al. first proposed the concept of "passive building design." He believed that "passive building design" refers to the design method that, under the premise of relying as little as possible on conventional energy consumption, relies on the planning layout, building design, and environmental configuration of the building itself, adapts to and utilizes the regional climate characteristics, and creates a healthy and comfortable indoor thermal environment [83]. The definition not only pointed out the direction for other researchers' efforts but also provided important guidance for promoting energy conservation, environmental protection, and comfortable building design. After 1994, scholars began to study passive building design from a technical perspective. Baruch et al. discussed passive cooling of buildings from a technical

perspective and cited a large number of experimental data to explain that temperature control of buildings can be effectively achieved through technical means, which has important significance for building design in hot summer regions [84]. In 1999, Glauser discussed various passive cooling strategies in detail in his research and illustrated them with examples.

In recent years, scholars have begun to pay attention to the application of passive strategies and their relationship with building energy consumption accompanied by the emergence of numerous computer analysis software tools. Through computer simulations, the result of research and design would be more scientific and forward-looking. In 2014, Laurent et al. studied the application of air heating technology in passive buildings in cold climate zones. The research results showed that it is better to combine air heating technology with other heating methods and optimize system operation through load feedback control [85]. In 2014, Agnieszka et al. studied the performance of ground-source heat exchangers in passive building ventilation systems in cold regions using experimental and simulation methods. It is suggested that ground-source heat exchangers operating in passive building ventilation systems in cold climate zones can use the thermal capacity of the ground for heating and effectively suppress external temperature fluctuations [86]. In 2016, Dan et al. built an energy-saving house and compared its feasibility with a reference house designed according to Romania's energy efficiency requirements from the perspectives of energy consumption and lifecycle cost analysis [87]. In 2018, Fatima et al. conducted comprehensive research on the passive optimization design of residential buildings and obtained the best climate-based passive design strategy, which improved indoor thermal comfort while reducing building energy consumption [88]. In 2018, Jurgen et al. simulated Tokyo, Shanghai, Las Vegas, Abu Dhabi, and Singapore as representative cities to prove that passive buildings are feasible in all climate zones worldwide [89]. In 2019, Tajda et al. studied the influence of building orientation on the optimal window size of passive buildings in different climate zones in Europe. The research results showed that the south-facing facade allowed the highest percentage of glass [90]. In 2019, Haider et al. and Ascione et al. conducted research in Australia and Italy, respectively, where passive design strategies were used for the renovation of existing residential houses and industrial buildings, improving energy efficiency rates by 58% and 81%, respectively [91, 92]. In 2020, Zahiri et al., and Pajek et al. discussed the use of passive strategies in different types of buildings and simulated the improvement of the indoor thermal environment [93-95]. In the past several years, scholars have started using multi-objective optimization algorithms to optimize indoor thermal comfort through passive strategies while reducing energy consumption and saving costs. In 2021, Jung et al. conducted the multi-objective optimization of passive design strategy for multi-story residential buildings in South Korea. The results showed significant improvements in energy efficiency, environmental impact, and economic feasibility through optimized passive design factors, such as airtightness, occupants, and window-to-wall ratio [96]. In 2021, Abdou et al. assesses the feasibility of achieving net zero energy buildings in the Moroccan housing stock through a combination of architectural energy efficiency practices and renewable energy sources. the application of the multi-objective study conclusions combined with an efficient use of renewable energies makes it possible to achieve zero energy building throughout all Moroccan housing stock [97].

(2) Passive design strategy research in China

Research on passive house building theory in China started relatively late compared to

western countries. In 1970, universities represented by Tsinghua University began to study passive solar house theory. Gao from Tsinghua University introduced the “Arcology” theory of Italian architect in 1985. Since then, China has had a theoretical understanding of ecological architecture. From around 2000, research on passive building theory gradually became more abundant in China.

In 1999, Liu et al. proposed a renovation strategy for traditional cave dwellings in Shaanxi, combining passive solar energy, natural ventilation, and rammed earth insulation structures. This approach significantly improved the thermal environment of the indoor cave dwellings [98]. In 2003, Yang explores the relationship between Chinese climate and architecture, as well as the analysis methods for passive design adapted to climate conditions. she proposed a novel approach to passive design zoning and provide corresponding guidelines and design strategies that are tailored to China’s climatic characteristics. The aim is to achieve energy efficiency through passive design techniques during the architectural design phase. This research introduces the concept of passive design zoning based on climate considerations, offering valuable insights and principles for effective design strategies [22].

Then, scholars explored the feasibility and effectiveness of passive strategies from actual projects. In 2007, Yin proposed a passive building design strategy suitable for Wuhan and modified the shortcomings in planning and architectural design through software verification, discussing the feasibility of passive building design development and promotion in Wuhan [99]. In 2012, Lin used passive design methods such as building orientation, natural ventilation, shading measures, and insulation to effectively reduce building energy consumption in the energy-saving demonstration apartment of Fuzhou University [100]. In 2013, Li et al. optimized buildings based on the climate characteristics of Wuhan, including planning and layout of building groups, regional greening, water design, building orientation, shape coefficient, window-to-wall ratio, and ventilation and shading design, to improve the microclimate of building areas [101].

Subsequently, scholars began to quantitatively analyze passive design strategies using software and established an evaluation system for passive strategies. In 2013, Peng explored the relationship between climate, passive design, and thermal comfort, used Climate Consultant and Design Builder simulation software to discuss the best passive design strategies for office buildings in specific climates [102]. In 2014, Yin summarized the basic concepts, characteristics, and technical points of passive buildings, considered economic, social, ecological, and technical factors, established an evaluation system for passive buildings, and constructed an efficiency evaluation model based on comprehensive evaluation method, using actual projects to verify the scientificity and effectiveness of the system and model [103]. In 2015, Zhou et al. used simulation software to numerically simulate the energy-saving and natural ventilation effects of passive house projects based on the climatic characteristics of Hefei, analyzing and verifying the feasibility of passive design strategies [104]. In 2015, Xing determined the evaluation standards for indoor thermal comfort of residential buildings in Chengdu through thermal comfort investigation, and provided a passive design technical solution through numerical simulation and economic analysis [105]. In 2016, Lyu et al. applied simulation software to simulate the energy consumption of an office building in cold region, and summarized passive energy-saving design strategies suitable for cold and severe cold regions in China [106]. Residential buildings in rural regions have also been the subject of certain

academic discussions in China. Liu et al., Ge et al., Chi et al., and Peng, focused on the single passive parameter of traditional dwelling, simulated and analyzed its impact on building energy consumption, then quantitative evaluated and provided the best passive approach [107-110]. Gao, and Zhao et al. tested the indoor thermal environment of traditional houses in specific areas such as the western humid and cold mountainous region and western Henan cold region, and proposed the architectural design principles and strategies suitable for the local climate [111, 112]. Zhang et al. simulated the total energy usage of traditional dwellings in rural areas, and studied the value of passive technologies that could minimize the energy consumption [113]. According to the literature review, the effectiveness of passive techniques could vary depending on building types, usage patterns and climate areas.

2.3.2. Research prospect

Through literature review, scholars have focused on optimizing building energy consumption through single or combined passive strategies in existing research on passive strategies. Future research can focus on the following aspects:

1) Combining passive strategies with sustainable design. With the increasing awareness of environmental protection and sustainable development, future research on passive strategies will pay more attention to the application of sustainable design, such as using natural light and natural ventilation to reduce energy consumption and using regional materials or renewable energy to improve building energy efficiency.

2) Combining passive strategies with human thermal comfort research. Human thermal comfort is an important consideration factor in passive design. Future research will focus more on optimizing passive strategies based on human thermal comfort, such as determining the intensity of passive strategies based on the measured thermal neutral temperature.

3) Multi-objective optimization of passive design strategies. Many scholars have applied passive strategies to reduce building energy consumption in various regions of the world, but the economic and acceptability factors have not been considered in the application stage of passive strategies. Multi-objective optimization of passive design strategies will provide designers with the optimal solution to meet other optimization goals while reducing energy consumption.

Reference

- [1] W. Xia, "Study of climate classification Based on Passive Design strategies," doctoral thesis doctoral thesis, Tsinghua University, 2009.
- [2] A. Walsh, D. Cóstola, and L. C. Labaki, "Performance-based climatic zoning method for building energy efficiency applications using cluster analysis," *Energy*, vol. 255, p. 124477, 2022.
- [3] J. Xiong, R. Yao, S. Grimmond, Q. Zhang, and B. Li, "A hierarchical climatic zoning method for energy efficient building design applied in the region with diverse climate characteristics," *Energy and Buildings*, vol. 186, pp. 355-367, 2019.
- [4] J. Xiong et al., "Subdivision of hot summer and cold winter zone for building thermal performance," *Journal of HV&AC*, vol. 49, no. 04, pp. 12-18, 2019.
- [5] W. Köppen, "Klassifikation der klimate nach Temperatur, Niederschlag und Jahreslauf," *Pet. Mitt.*, vol. 64, pp. 193-203,243-248, 1918.
- [6] H. E. Beck, N. E. Zimmermann, T. R. McVicar, N. Vergopolan, A. Berg, and E. F. Wood, "Present and future Köppen-Geiger climate classification maps at 1-km resolution," *Scientific data*, vol. 5, no. 1, pp. 1-12, 2018.
- [7] ASHRAE/IESNA, "ASHRAE/IES Standard 90.1–1989 Energy Efficient Design of New Buildings Except Low-rise Residential Buildings," ed: ASHRAE Atlanta, GA, 1989.
- [8] M. E. H. D. Lamrhari, "Comportement thermique et économie d'énergie dans un appartement avec différentes mesures d'efficacité énergétique dans les six zones climatiques du Maroc," *Université Cadi Ayyad Marrakech (Maroc)*, 2018.
- [9] J. Terés-Zubiaga, A. Campos-Celador, I. González-Pino, and C. Escudero-Revilla, "Energy and economic assessment of the envelope retrofitting in residential buildings in Northern Spain," *Energy and Buildings*, vol. 86, pp. 194-202, 2015.
- [10] C. Diaz-Lopez, K. Verichev, J. A. Holgado-Terriza, and M. Zamorano, "Evolution of climate zones for building in Spain in the face of climate change," *Sustainable Cities Society*, vol. 74, p. 103223, 2021.
- [11] M.-M. Fernandez-Antolin, J. M. del Río, V. Costanzo, F. Nocera, and R.-A. Gonzalez-Lezcano, "Passive design strategies for residential buildings in different Spanish climate zones," *Sustainability*, vol. 11, no. 18, p. 4816, 2019.
- [12] Thermal Environmental Conditions for Human Occupancy: ANSI/ASHRAE Standard 55-2017 (Supersedes ANSI/ASHRAE Standard 55-2013) Includes ANSI/ASHRAE Addenda Listed in Appendix N, 2017.
- [13] National Construction Code NCC 2016 Building Code of Australia—Volume One (BCA), 2016.
- [14] J. Yuan, C. Farnham, K. Emura, and Buildings, "Optimal combination of thermal resistance of insulation materials and primary fuel sources for six climate zones of Japan," *Energy and Buildings*, vol. 153, pp. 403-411, 2017.
- [15] M. K. Singh, S. Mahapatra, and S. Atreya, "Development of bio-climatic zones in north-east India," *Energy and Buildings*, vol. 39, no. 12, pp. 1250-1257, 2007.
- [16] O. Rakoto-Joseph, F. Garde, M. David, L. Adelard, Z. Randriamanantany, and Management, "Development of climatic zones and passive solar design in Madagascar," *Energy Conversion*, vol. 50, no. 4, pp. 1004-1010, 2009.
- [17] "Nation House Energy Rating Scheme - Climate Zone Map (accessed March 16,

2017)," ed: Department of the Environment and Energy, 2012.

[18] C. e. commission, "Building climate zones," in California energy maps, ed: California energy commission, 2020.

[19] Standard of climatic regionalization for architecture (GB 50178-93), 1993.

[20] Thermal design code for civil building (GB 50176-2016), 2016.

[21] Design standard for energy efficiency of residential buildings in hot summer and cold winter zone (JGJ 134-2010), 2010.

[22] L. Yang, "Climatic analysis and architectural design strategies for bio-climatic design," Doctoral thesis Doctoral thesis, Xi'an University of Architecture and Technology, 2003.

[23] H. Dong, "Climate mapping of natural ventilative cooling," Master Thesis 硕士, Xi'an University of Architecture and Technology, 2006.

[24] L. Xie, "Climate division for passive solar buildings," Master Thesis Master Thesis, Xi'an University of Architecture and Technology, 2006.

[25] X. Fu, H. Zhang, and G. Huang, "Discussion of climatic regions of building energy efficiency in China," Journal of HV&AC, no. 02, pp. 44-47+17, 2008.

[26] D. Liu, J. Liu, L. Yang, and W. Wang, "Research of building climatic region division in China," Journal of HV&AC, vol. 39, no. 05, pp. 93-96, 2009.

[27] X. Xu, "Research of building climate classification based on cluster analysis and energy-saving control," Master Thesis, Xi'an University of Architecture and Technology, 2017.

[28] Y. Yang, "Research on climate zoning evaluation of urban building and its effect on building energy consumption," Master Thesis, Xi'an University of Architecture and Technology, 2021.

[29] X. Yang et al., "Impact of urban heat island on energy demand in buildings: Local climate zones in Nanjing," Applied Energy, vol. 260, p. 114279, 2020.

[30] T. Zhang et al., "A Case Study of Refined Building Climate Zoning under Complicated Terrain Conditions in China," International Journal of Environmental Research Public Health, vol. 19, no. 14, p. 8530, 2022.

[31] N. Djongyang, R. Tchinda, and D. Njomo, "Thermal comfort: A review paper," Renewable sustainable energy reviews, vol. 14, no. 9, pp. 2626-2640, 2010.

[32] S. Cao, X. Li, B. Yang, and F. Li, "A review of research on dynamic thermal comfort," Building Services Engineering Research & Technology, vol. 42, no. 4, pp. 435-448, 2021.

[33] Q. Yang, "Study on the indoor thermal comfort in the cold zone," Master Thesis, Xi'an University of Architecture and Technology, 2010.

[34] T. Doherty and E. A. Arens, "Evaluation of the physiological bases of thermal comfort models," ASHRAE Transactions, 1988.

[35] A. G. Kwok and N. B. Rajkovich, "Addressing climate change in comfort standards," Building and Environment, vol. 45, no. 1, pp. 18-22, 2010.

[36] F. C. HOUGHTEN, "Determining lines of equal comfort," ASHVE Transactions, vol. 29, pp. 163-176, 1923.

[37] Z. Lin and S. Deng, "A study on the thermal comfort in sleeping environments in the subtropics—developing a thermal comfort model for sleeping environments," Building and Environment, vol. 43, no. 1, pp. 70-81, 2008.

[38] R. Yao, B. Li, and J. Liu, "A theoretical adaptive model of thermal comfort—Adaptive Predicted Mean Vote (aPMV)," Building and Environment, vol. 44, no. 10, pp. 2089-2096,

2009.

[39] A. P. Gagge, "An effective temperature scale based on a simple model of human physiological response," *Ashrae Trans.*, vol. 77, no. 1, pp. 247-262, 1971.

[40] W. C. Howell and P. A. Kennedy, "Field validation of the Fanger thermal comfort model," *Human factors*, vol. 21, no. 2, pp. 229-239, 1979.

[41] W. C. Howell and C. Stramler, "Contribution of psychological variables to the prediction of thermal comfort judgments in real world settings," *ASHRAE Trans*, vol. 87, no. 5, 1981.

[42] M. Humphreys, F. Nicol, and S. Roaf, *Adaptive thermal comfort: foundations and analysis*. Routledge, 2015.

[43] J. F. Nicol and M. A. Humphreys, "Adaptive thermal comfort and sustainable thermal standards for buildings," *Energy and Buildings*, vol. 34, no. 6, pp. 563-572, 2002.

[44] J. A. Wagner and S. M. Horvath, "Influences of age and gender on human thermoregulatory responses to cold exposures," *Journal of Applied Physiology*, vol. 58, no. 1, pp. 180-186, 1985.

[45] K. Collins and E. Hoinville, "Temperature requirements in old age," *Building Services Engineering Research Technology*, vol. 1, no. 4, pp. 165-172, 1980.

[46] T. Chung and W. Tong, "Thermal comfort study of young Chinese people in Hong Kong," *Building and Environment*, vol. 25, no. 4, pp. 317-328, 1990.

[47] R. De Dear and G. S. Brager, "Developing an adaptive model of thermal comfort and preference," 1998.

[48] R. J. De Dear, "A global database of thermal comfort field experiments," *ASHRAE transactions*, vol. 104, p. 1141, 1998.

[49] G. S. Brager, R. J. J. E. De Dear, and buildings, "Thermal adaptation in the built environment: a literature review," vol. 27, no. 1, pp. 83-96, 1998.

[50] W. Yang, J. Xu, Z. Lu, J. Yan, and F. Li, "A systematic review of indoor thermal environment of the vernacular dwelling climate responsiveness," *Journal of Building Engineering*, vol. 53, p. 104514, 2022.

[51] G. S. Brager and R. J. De Dear, "Thermal adaptation in the built environment: a literature review," *Energy and Buildings*, vol. 27, no. 1, pp. 83-96, 1998.

[52] A. Mendes et al., "Indoor air quality and thermal comfort—Results of a pilot study in elderly care centers in Portugal," *Journal of Toxicology Environmental Health, Part A*, vol. 76, no. 4-5, pp. 333-344, 2013.

[53] M. K. Singh, S. Attia, S. Mahapatra, and J. Teller, "Assessment of thermal comfort in existing pre-1945 residential building stock," *Energy*, vol. 98, pp. 122-134, 2016.

[54] S. Sattayakorn, M. Ichinose, and R. Sasaki, "Clarifying thermal comfort of healthcare occupants in tropical region: A case of indoor environment in Thai hospitals," *Energy and buildings*, vol. 149, pp. 45-57, 2017.

[55] I. Oropeza-Perez, A. H. Petzold-Rodriguez, and C. Bonilla-Lopez, "Adaptive thermal comfort in the main Mexican climate conditions with and without passive cooling," *Energy and Buildings*, vol. 145, pp. 251-258, 2017.

[56] A. Martinez-Molina, P. Boarin, I. Tort-Ausina, and J.-L. Vivancos, "Post-occupancy evaluation of a historic primary school in Spain: Comparing PMV, TSV and PD for teachers' and pupils' thermal comfort," *Building and Environment*, vol. 117, pp. 248-259, 2017.

[57] A. Jindal, "Thermal comfort study in naturally ventilated school classrooms in composite climate of India," *Building and Environment*, vol. 142, pp. 34-46, 2018.

[58] A. Atmaca and G. Z. Gedik, "Evaluation of mosques in terms of thermal comfort and energy consumption in a temperate-humid climate," *Energy and Buildings*, vol. 195, pp. 195-204, 2019.

[59] V. Soebarto, H. Zhang, and S. Schiavon, "A thermal comfort environmental chamber study of older and younger people," *Building and Environment*, vol. 155, pp. 1-14, 2019.

[60] N. Forcada, M. Gangoellis, M. Casals, B. Tejedor, M. Macarulla, and K. Gaspar, "Summer thermal comfort in nursing homes in the Mediterranean climate," *Energy and Buildings*, vol. 229, p. 110442, 2020.

[61] P. Aparicio-Ruiz, E. Barbadilla-Martin, J. Guadix, and J. Munuzuri, "A field study on adaptive thermal comfort in Spanish primary classrooms during summer season," *Building and Environment*, vol. 203, p. 108089, 2021.

[62] J. R. Molina, G. Lefebvre, and M. M. Gómez, "Study of the thermal comfort and the energy required to achieve it for housing modules in the environment of a high Andean rural area in Peru," *Energy and Buildings*, vol. 281, p. 112757, 2023.

[63] N. Sudarsanam and D. Kannamma, "Investigation of Summertime Thermal Comfort at the residences of Elderly People in the Warm and Humid Climate of India," *Energy and Buildings*, p. 113151, 2023.

[64] Z. Wang, X. Fang, and L. Lian, "Field experiments on occupant thermal comfort in Harbin," *Journal of Harbin Institute of Technology*, no. 04, pp. 500-504, 2002.

[65] h. Jin, H. Zhao, and X. Wang, "Research on the indoor thermal comfort environment of rural housing in winter in super-cold region," *Journal of Harbin Institute of Technology*, no. 12, pp. 2108-2111, 2006.

[66] Y. Zhu and J. Liu, "Research on the indoor thermal environment of rural architecture in winter in northwestern areas," *China Civil Engineering Journal*, vol. 43, no. S2, pp. 400-403, 2010.

[67] L. Huang, Y. Zhu, Q. Ouyang, and B. Cao, "Indoor thermal comfort in rural houses around Beijing in heating season," *Journal of HV&AC*, vol. 41, no. 06, pp. 83-85+115, 2011.

[68] L. Yang, Q. Yang, H. Yan, and J. Liu, "Field study on thermal comfort of rural houses in winter in the Guanzhong region, Shaanxi Province," *Xi'an University of Architecture and Technology (Natural Science Edition)*, vol. 43, no. 04, pp. 551-556, 2011.

[69] Y. Gao, "Study on the Indoor Comfortable Index And Energy Efficiency Evaluation Technology of the Rural House in Cold Areas," Master Thesis 硕士, Tianjin University, 2012.

[70] S. Jing, Y. Lei, H. Wang, C. Song, and X. Yan, "Thermal comfort and energy-saving potential in university classrooms during the heating season," *Energy and Buildings*, vol. 202, p. 109390, 2019.

[71] C. Fu, C. M. Mak, Z. Fang, M. O. Oladokun, Y. Zhang, and T. Tang, "Thermal comfort study in prefab construction site office in subtropical China," *Energy and Buildings*, vol. 217, p. 109958, 2020.

[72] Y. Jiao, H. Yu, Y. Yu, Z. Wang, and Q. Wei, "Adaptive thermal comfort models for homes for older people in Shanghai, China," *Energy and Buildings*, vol. 215, p. 109918, 2020.

[73] X. Jia, B. Cao, Y. Zhu, and Y. Huang, "Field studies on thermal comfort of passengers in airport terminals and high-speed railway stations in summer," *Building and Environment*,

vol. 206, p. 108319, 2021.

[74] S. Chang, W. He, H. Yan, L. Yang, and C. Song, "Influences of vernacular building spaces on human thermal comfort in China's arid climate areas," *Energy and Buildings*, vol. 244, p. 110978, 2021.

[75] W. Zheng, T. Shao, Y. Lin, Y. Wang, C. Dong, and J. Liu, "A field study on seasonal adaptive thermal comfort of the elderly in nursing homes in Xi'an, China," *Building and Environment*, vol. 208, p. 108623, 2022.

[76] S. Zhao, L. Yang, S. Gao, M. Li, H. Yan, and Y. Zhai, "Field investigation on the thermal environment and thermal comfort in shopping malls in the cold zone of China," *Building and Environment*, vol. 214, p. 108892, 2022.

[77] L. Wang, Y. Wang, F. Fei, W. Yao, and L. Sun, "Study on winter thermal environment characteristics and thermal comfort of university classrooms in cold regions of China," *Energy and Buildings*, p. 113126, 2023.

[78] B. Cakó et al., "An efficient method to compute thermal parameters of the comfort map using a decreased number of measurements," *Energies*, vol. 14, no. 18, p. 5632, 2021.

[79] K. Yeang, J. Reynolds, V. Olgyay, and D. Lyndon, "Design with Climate: Bioclimatic Approach to Architectural Regionalism-New and expanded Edition," 2015.

[80] B. Givoni, *Human·Building·Climate*. Beijing, China: China Architecture & Building Press, 1982.

[81] Y. Kato and S. Tanabe, "House with solar chimney and the house with rock tower: three passive solar houses at north latitude 35 degrees in Japan," in *Unknown Host Publication Title: American Solar Energy Soc Inc*, 1984, pp. 143-148.

[82] M. S. Sodha, N. Bansal, P. Bansal, A. Kumar, and M. A. Malik, *Solar passive building*. United States, 1986.

[83] N. K. Bansal, G. Hauser, and G. Minke, *Passive building design: a handbook of natural climatic control*. Elsevier science BV Amsterdam, The Netherlands, 1994.

[84] B. Givoni, *Passive low energy cooling of buildings*. John Wiley & Sons, 1994.

[85] L. Georges, M. Berner, and H. M. Mathisen, "Air heating of passive houses in cold climates: Investigation using detailed dynamic simulations," *Building and Environment*, vol. 74, pp. 1-12, 2014.

[86] A. Flaga-Maryanczyk, J. Schnotale, J. Radon, and K. Was, "Experimental measurements and CFD simulation of a ground source heat exchanger operating at a cold climate for a passive house ventilation system," *Energy and Buildings*, vol. 68, pp. 562-570, 2014.

[87] D. Dan et al., "Passive house design—An efficient solution for residential buildings in Romania," *Energy for Sustainable Development*, vol. 32, pp. 99-109, 2016.

[88] F. Harkouss, F. Fardoun, and P. H. Biwole, "Passive design optimization of low energy buildings in different climates," *Energy*, vol. 165, pp. 591-613, 2018.

[89] J. Schnieders, W. Feist, and L. Rongen, "Passive Houses for different climate zones," *Energy and Buildings*, vol. 105, pp. 71-87, 2015.

[90] T. P. Obrecht, M. Premrov, and V. Ž. Leskovar, "Influence of the orientation on the optimal glazing size for passive houses in different European climates (for non-cardinal directions)," *Solar Energy*, vol. 189, pp. 15-25, 2019.

[91] H. Albayyaa, D. Hagare, and S. Saha, "Energy conservation in residential buildings

by incorporating Passive Solar and Energy Efficiency Design Strategies and higher thermal mass," *Energy and Buildings*, vol. 182, pp. 205-213, 2019.

[92] F. Ascione et al., "A real industrial building: Modeling, calibration and Pareto optimization of energy retrofit," *Journal of Building Engineering*, vol. 29, p. 101186, 2020.

[93] S. Zahiri and H. Altan, "Improving energy efficiency of school buildings during winter season using passive design strategies," *Sustainable Buildings*, vol. 5, p. 1, 2020.

[94] S. Zahiri and H. Altan, "The effect of passive design strategies on thermal performance of female secondary school buildings during warm season in a hot and dry climate," *Frontiers in built environment*, vol. 2, p. 3, 2016.

[95] L. Pajek, J. Potočnik, and M. Košir, "The effect of a warming climate on the relevance of passive design measures for heating and cooling of European single-family detached buildings," *Energy and Buildings*, vol. 261, p. 111947, 2022.

[96] Y. Jung, Y. Heo, and H. Lee, "Multi-objective optimization of the multi-story residential building with passive design strategy in South Korea," *Building and Environment*, vol. 203, p. 108061, 2021.

[97] N. Abdou, Y. E. Mghouchi, S. Hamdaoui, N. E. Asri, and M. Mouqallid, "Multi-objective optimization of passive energy efficiency measures for net-zero energy building in Morocco," *Building and Environment*, vol. 204, p. 108141, 2021.

[98] J. Liu and L. Yang, "Thermal design of a zero energy cave-dwelling solar house," *Acta Energetica Solaris Sinica*, no. 03, pp. 302-310, 1999.

[99] C. Yin, "Design Strategies for the Passive Building Design (PBD) used in regions of hot in summer and cold in winter ——based on the design of Wuhan artists village," Master Thesis, Huazhong University of Science and Technology, 2007.

[100] J. Lin, "Investigation of passive energy efficiency design in subtropical region, a case study of the energy efficiency demonstration apartment in Fuzhou University," *Fujian Architecture & Construction*, no. 09, pp. 21-24, 2012.

[101] J. Li, C. Wu, W. Qu, and W. Li, "Passive design strategies based on climatic characteristics in Hot-Summer and Cold-Winter Zone , taking Wuhan City for example," *Building Energy Saving*, vol. 41, no. 07, pp. 54-56+73, 2013.

[102] Y. Peng, "The research on the passive design of office building based on software simulation in the hot summer and cold winter zone," Master Thesis, Hunan University, 2013.

[103] B. Yin, "Benefit Evaluation and policy support of Passive building," Master Thesis, Xi'an University of Architecture and Technology, 2014.

[104] B. Zhou and W. Zhang, "Simulation and analysis of energy saving effect in hot summer and cold winter area of passive demonstration room," *Journal of Anhui Jianzhu University*, vol. 23, no. 03, pp. 52-55, 2015.

[105] Y. Xing, "Passive technology and energy performance analysis of Chengdu residential building," Master Thesis, Xi'an University of Architecture and Technology, 2015.

[106] D. Lyu, Z. Zhang, X. Kang, Z. Yang, and X. Shen, "Analysis of energy consumption of passive office building in North China," *Journal of Hebei University of Engineering (Natural Science Edition)*, vol. 33, no. 03, pp. 76-79, 2016.

[107] J. Liu, L. Wang, Y. Yoshino, and Y. Liu, "The thermal mechanism of warm in winter and cool in summer in China traditional vernacular dwellings," *Building and Environment*, vol. 46, no. 8, pp. 1709-1715, 2011.

[108] X. Ge, J. He, W. Wang, H. Shen, L. Zhang, and H. Xiong, "Energy saving optimization design of typical rural residential buildings in cold zones of western Henan," *Building Energy Efficiency*, vol. 49, pp. 53-58, 2021.

[109] F. a. Chi, Y. Wang, R. Wang, G. Li, and C. Peng, "An investigation of optimal window-to-wall ratio based on changes in building orientations for traditional dwellings," *Solar Energy*, vol. 195, pp. 64-81, Jan 1 2020.

[110] M. Peng, "Application of key technology and materials in the building envelop of passive house and low energy buildings," *New Building Materials*, vol. 42, pp. 77-82, 2015.

[111] Y. Gao, "Research on Suitable Ecological Construction Modes of Rural Residence in Hot-humid and Cold-wet Mountain Area in Western of China," Ph.D. Thesis, Xi'an University of Architecture and Technology, 2014.

[112] Y. Zhao, "Suitable Technologies for Climate Adaptability: A Case Study of Fujian Architecture," *South Architecture*, no. 03, pp. 54-59, 2019.

[113] G. Zhang, Q. Zhang, F. Wang, Q. Wang, and R. Liang, "Study on Influencing Factors of Energy Consumption in Traditional Rural Dwellings of Kangding Prefecture Based on DesignBuilder," *BUILDING SCIENCE*, vol. 35, no. 06, pp. 108-115, 2019.

Chapter 3

RESEARCH METHODOLOGY

CHAPTER THREE: RESEARCH METHODOLOGY

<i>RESEARCH METHODOLOGY</i>	1
3.1. Content.....	1
3.2. Spatial interpolation method.....	2
3.2.1. Overview of spatial interpolation method	2
3.2.2. Classification of spatial interpolation method	3
3.2.3. Kriging spatial interpolation method	4
3.2.4. The application of spatial interpolation method in the research.....	7
3.3. Multi-objective optimization	7
3.3.1. Overview of multi-objective optimization	7
3.3.2. Multi-objective optimization (NSGA-2)	8
3.3.3. Multi-objective decision-making (TOPSIS).....	11
3.3.4. The application of multi-objective optimization in the research	12
3.4. Other methods.....	12
3.4.1. Data statistics method.....	13
3.4.2. Field survey method	16
3.4.3. Computer energy consumption simulation.....	19
Reference.....	21

3.1. Content

The main objective of this paper is to examine the climatic divisions within the Qinba mountainous area, evaluate the thermal comfort experienced by residents in each climatic sub-region, and enhance passive design approaches for local dwellings. As shown in Figure 3-1, this chapter presents an overview of the methodologies employed in this study, encompassing the spatial interpolation method, field survey method, data statistics method, computer simulation, and multi-objective optimization method. These various methods were utilized to organize and categorize meteorological data, calculate indicators of thermal comfort, simulate the energy consumption of buildings both before and after implementing passive design strategies, and ultimately derive optimal solutions for each specific climatic sub-zone. By leveraging these methodologies, the research successfully optimized passive design strategies, leading to improved energy efficiency and thermal comfort in dwellings across the Qinba mountainous area.

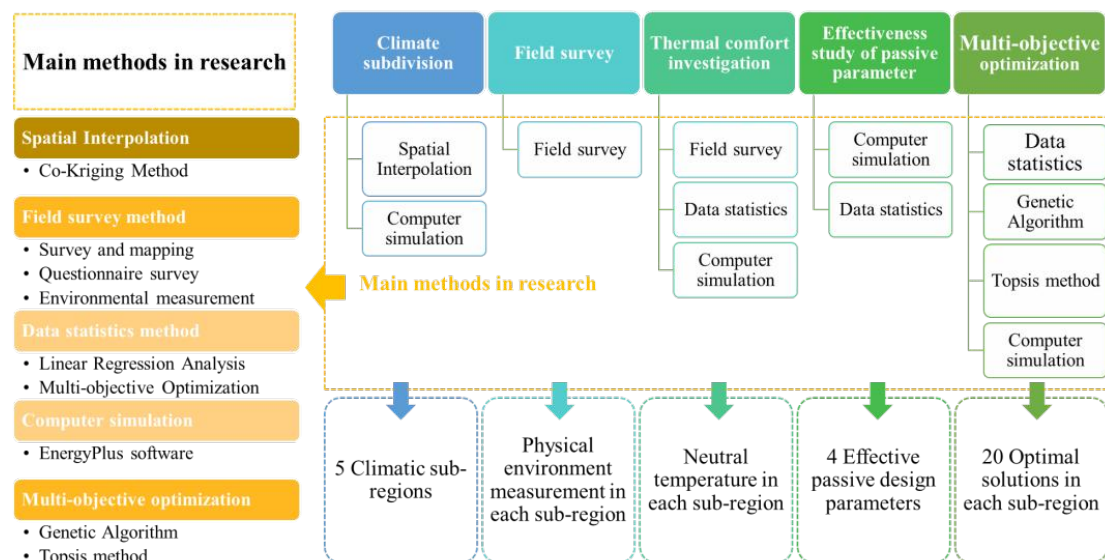


Figure 3-1. The methods employed in this research

For the climatic subdivision of the Qinba mountainous area discussed in Chapter 4, this study utilized the spatial interpolation method to integrate discrete meteorological data into a continuous spatial surface and obtained climate data contour lines, providing a basis for the climatic subdivision of the Qinba mountainous area. In Chapter 5, the traditional dwellings in the Qinba mountainous area were investigated and analyzed from three aspects: settlements, courtyards, and traditional dwellings, using the field survey method. In Chapter 6, the on-site investigation of thermal comfort in the sub-regions was conducted using the field survey method, data statistical method, and energy consumption simulation method. The neutral temperature and thermal comfort temperature range for each climatic sub-region were calculated, and the energy consumption was compared between the use of standard and

measured thermal comfort temperatures as set points for building heating and cooling. In Chapter 7, the effectiveness analysis of passive design strategies was carried out by quantitatively analyzing the impact of various passive design strategies on energy consumption using computer simulation method and data statistical method, and effective passive design strategies for the Qinba mountainous area were selected. In Chapter 8, the multi-objective optimization of passive design strategies was conducted using various approaches such as data analysis method, genetic algorithm, Topsis multi-objective decision-making method, and energy consumption simulation. The optimal combination of passive design strategies for each climatic sub-region in the Qinba mountainous area was selected, and the energy consumption before and after the optimal combination was calculated.

3.2. Spatial interpolation method

The spatial interpolation method is a model construction method that converts scattered point data into surface data. The essence of spatial interpolation is to fit a functional equation based on the characteristic values and spatial positions of a given set or multiple sets of discrete points. This functional equation reflects the mathematical relationship between the characteristic values of the given points and their spatial positions, thereby inferring the characteristic values of other spatial points within a certain range [1, 2]. Figure 3-2 shows the spatial interpolation method diagram. In the processing of meteorological data, spatial interpolation can transform discrete meteorological station data into continuous spatial data surfaces, thereby obtaining meteorological parameters for unmeasured areas [3].

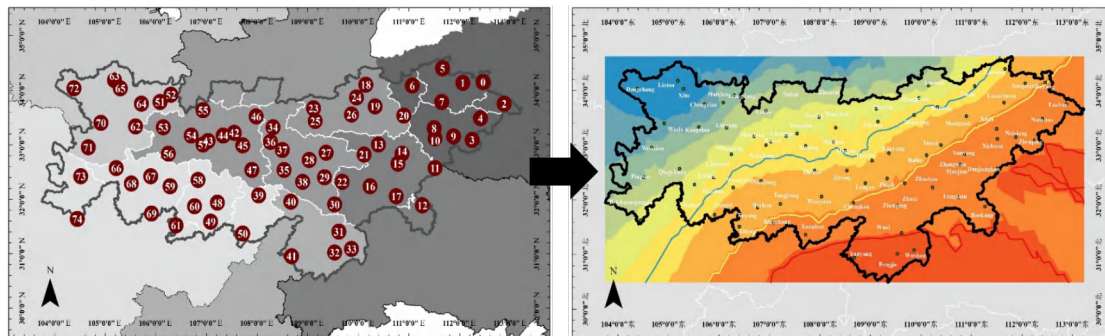


Figure 3-2. Spatial interpolation method diagram

3.2.1. Overview of spatial interpolation method

Currently, the spatial interpolation method is widely utilized in various disciplines' research. Zhang et al. developed a data processing procedure for public transportation passenger flow using passenger flow data collected from bus card swipers. They employed GIS spatial interpolation methods to visualize the spatial and temporal distribution of public transportation passenger flow. This research aimed to provide decision-making insights for public transportation operation and scheduling [4]. Li et al. proposed a comprehensive index method

for the health of the bay ecosystem based on basic GIS, indicating the spatial interpolation in nutrient levels in Daya Bay, and providing scientific basis for environmental governance in Daya Bay [5]. Lin et al. used the spatial interpolation method to quickly update the grid benchmark land price in Shenzhen, and obtained a spatial interpolation-based land price update method that meets the accuracy requirements of land price updates [6]. Antal et al. compared different spatial interpolation methods for estimating daily precipitation in Portugal [7]. Ebrahim et al. utilized data from 3825 stations from 2002 to 2016 to analyze the spatial structure of the mean annual temperature and annual average precipitation in Iran. It divided Iran into 24 sub-climatic zones [8]. Zhang et al. utilized a Bayesian Kriging regression method to model and estimate monthly air temperature using satellite-derived land surface temperature [9]. Li et al. introduces a space-time regression-kriging model and applies it to monthly average temperature data, resulting in a significant enhancement in interpolation accuracy compared to alternative methods [10].

The above research shows that spatial interpolation methods can scientifically and rigorously visualize data based on existing data, with strong practicality, objective and accurate results and vivid images. Among the research, the spatial interpolation methods are widely used in environmental management research. Environmental data collected through field surveys usually represent point sources. Yet, for effective decision-making, environmental managers require spatially continuous data that cover the entire region of interest, while scientists need accurate and well-distributed spatial data to make sound interpretations [3]. Scholars have done a lot of research on optimizing and utilizing spatial interpolation methods, making them low-cost, widely applicable, and without temporal and spatial limitations. Studies using spatial interpolation methods to obtain air temperature raster data often focus on larger areas. Jone et al. used data from 1584 stations worldwide to generate global raster data through direct interpolation methods [11]. Pan et al. combined elevation DEM data and used 726 meteorological stations nationwide from 1961 to 2000 to obtain temperature raster data for mainland China using interpolation methods [12].

Common spatial interpolation methods based on ArcGIS software include trend surface method, natural neighbor method, spline function method, etc., but these methods lack the introduction of covariates and are not suitable for analyzing temperature changes in mountainous areas. However, the co-Kriging interpolation method allows the introduction of multiple factors as covariates for spatial interpolation of climate elements (such as DEM elevation data, as temperature changes regularly with altitude), greatly improving the interpolation accuracy, and is an important method supporting this research [3].

3.2.2. Classification of spatial interpolation method

The premise of spatial interpolation is that the estimated objects are spatially correlated. By measuring the scattered sampling positions or measuring relatively smaller planned areas, real

test data is obtained. Then, the method of calculating other unknown objects or all point data within the region is used to estimate missing data at other point locations through interpolation, which improves data density and can grid the data, interpolating missing spatial data into regular distributed spatial data.

Spatial interpolation methods are generally divided into non-geostatistical interpolation methods and geostatistical methods. non-geostatistical interpolation methods assign values to locations based on surrounding measured values and specified mathematical formulas used to determine the smoothness of the generated surface, without considering spatial correlation and variability. The commonly used non-geostatistical interpolation methods are natural neighbor interpolation, spline interpolation, trend surface interpolation, and inverse distance weighting interpolation. Geostatistical methods employ geostatistical principles and models, taking into account spatial correlation and variability. Examples include Kriging, Kernel Density Estimation, and other geostatistical techniques.

Kriging interpolation, named after French geostatistician D.G. Krige, is an optimal interpolation method. Kriging not only considers the relative positions between the observation points and estimated points, but also takes into account the relative spatial relationships between the observation points [13]. This allows the Kriging method to have high accuracy and reliability in estimating missing values or values at unsampled points. Kriging spatial interpolation method is a widely used interpolation technique that offers high accuracy, stability, interpretability, and the ability to assess uncertainty in the estimated values. It finds extensive applications in geographic spatial data analysis, environmental modeling, resource management, and decision support [14]. Therefore, in this study, the Kriging interpolation method was chosen as the basis for climate zoning.

3.2.3. Kriging spatial interpolation method

Kriging interpolation, also known as spatial local interpolation, is an unbiased optimal estimation method for regional variables within a limited area based on the theory of variogram through structural analysis. The Kriging interpolation method was first used by South African mining engineer Krige in the 1950s to estimate the best possible average grade of a mining block based on the different ore samples within and outside the ore block. French statistician Matheron subsequently theorized and systematized the method, naming it Kriging or the Kriging method [15].

Kriging takes into account various factors of the information samples, such as the original shape, size, spatial distribution of the evaluated objects, and the spatial structure information of the variables, in order to achieve linear, unbiased, and minimum variance estimation. To accomplish this, Kriging assigns a certain weight coefficient to each sample, and finally evaluates the unknown quantity of the evaluated object using a weighted average method. Kriging has been continuously developed and improved, and different Kriging methods can be

used for various situations and purposes. Depending on different conditions, the Kriging method can be divided into 8 types, such as ordinary Kriging, universal Kriging, co-Kriging, disjunctive Kriging, regression Kriging, and so on, the application ranges are shown in Table 3-1 [16].

Table 3-1. Classification and application ranges of Kriging methods [3]

Type	Application ranges
Ordinary Kriging	Satisfying the intrinsic hypothesis, the average value of the regionalized variable is an unknown constant
Simple Kriging	Satisfying the second-order stationary hypothesis, the mean value of the variable is a known constant
Universal Kriging	The mathematical expectation of the regionalized variable is an unknown varying value
Indicator Kriging	Used when there are genuine outliers, and the data does not follow a normal distribution
Probability Kriging	Used to calculate the probability of a certain variable content
Disjunctive Kriging	Used to calculate the recoverable reserves
Co-Kriging	Applicable to interrelated multivariate regionalized variables
Logistic Normal Kriging	Used when data follows a normal distribution

(1) The derivation process of Kriging method

The estimation process of almost all spatial interpolation methods involves calculating weighted averages of sampled data. These methods commonly employ a general estimation formula, which can be expressed as follows:

$$\hat{Z}(x_0) = \sum_{i=1}^n \lambda_i Z(x_i) \quad (3-1)$$

Where \hat{Z} is the estimated value of an attribute at the point of interest x_0 , Z is the observed value at the sampled point x_i , λ_i is the weight assigned to the sampled point, and n represents the number of sampled points used for the estimation [17]. The attribute is usually called the primary variable, especially in geostatistics.

All Kriging estimators are variants of the basic equation (3-2), which is a slight modification of equation (3-1), as follows:

$$\hat{Z}(x_0) - \mu = \sum_{i=1}^n \lambda_i [Z(x_i) - \mu(x_0)] \quad (3-2)$$

Where μ is a known stationary mean, assumed to be constant over the whole domain and calculated as the average of the data [18]. The parameter λ_i is kriging weight; n is the number of sampled points used to make the estimation and depends on the size of the search window; and $\mu(x_0)$ is the mean of samples within the search window.

The kriging weights are estimated by minimizing the variance, as follows:

$$\begin{aligned} \text{var}[\hat{Z}(x_0)] &= E \left[\{\hat{Z}(x_0) - Z(x_0)\}^2 \right] \\ &= E \left[\left(\hat{Z}(x_0) \right)^2 + \left(Z(x_0) \right)^2 - 2\hat{Z}(x_0)Z(x_0) \right] \\ &= \sum_{i=1}^n \sum_{j=1}^n \lambda_i \lambda_j C(x_i - x_j) + C(x_i - x_0) - 2 \sum_{i=1}^n \lambda_i C(x_i - x_0) \end{aligned} \quad (3-3)$$

Where $Z(x_0)$ is the true value expected at point x_0 , n represents the number of observations to be included in the estimation, and $C(x_i - x_j) = \text{Cov}[Z(x_i), Z(x_j)]$ [19].

(2) The characteristics of Kriging method

The Kriging method has the following characteristics in the analysis and evaluation of environmental factors such as meteorological elements: 1) It can handle irregular sampling intervals and missing data. In temperature and humidity monitoring, the distribution of sampling points is usually irregular, and there may be missing data. Kriging can interpolate between irregular sampling points, and interpolation can be performed even if there is missing data. 2) It is robust to outliers. Temperature and humidity data may contain outliers, which may have a significant impact on the interpolation results. Kriging can adjust the covariance function to reduce the influence of outliers and improve the interpolation accuracy. 3) It can provide an estimate of interpolation error. Kriging can estimate the interpolation error through the semivariance function, thereby providing a reliable evaluation of the interpolation results. 4) It can provide interpolation results with different spatial resolutions: Kriging can control the spatial resolution of interpolation results by adjusting the interpolation distance, thereby providing interpolation results with different spatial resolutions. 5) It can select the best interpolation parameters through cross-validation: Kriging can select the best interpolation parameters through cross-validation, thereby improving the interpolation accuracy. In temperature and humidity monitoring, selecting the best interpolation parameters can improve the accuracy and reliability of estimation. Therefore, in this study, Kriging interpolation method was used for the climatic subdivision in Qinba mountainous area [3].

3.2.4. The application of spatial interpolation method in the research

In this study, 75 meteorological stations in the study zone were used to collect the meteorological observation factors, such as the air temperature, relative humidity, wind speed, solar radiation intensity, etc., in the past ten years [20]. The Kriging was used to divide climatic sub-regions [21, 22]. The main steps of the climate subdivision based on the Kriging spatial interpolation method are shown in Figure 3-3. The first step is collecting meteorological data from 75 climate stations in the study area for 10 years. The meteorological data includes the daily air temperature, monthly relative humidity, wind speed, and solar radiation intensity. And the values of HDD18 and CDD 26 of each climate station according to the daily air temperature were calculated. The second step is importing the meteorological data and geographic information into Arch Map 10.8 software. The third step is applying the HDD18 and CDD26 values as the primary variables and elevation as the co-variables, for the Co-Kriging analysis. The fourth step is visualizing the spatial interpolation results as the continuous spatial surfaces and contour maps.

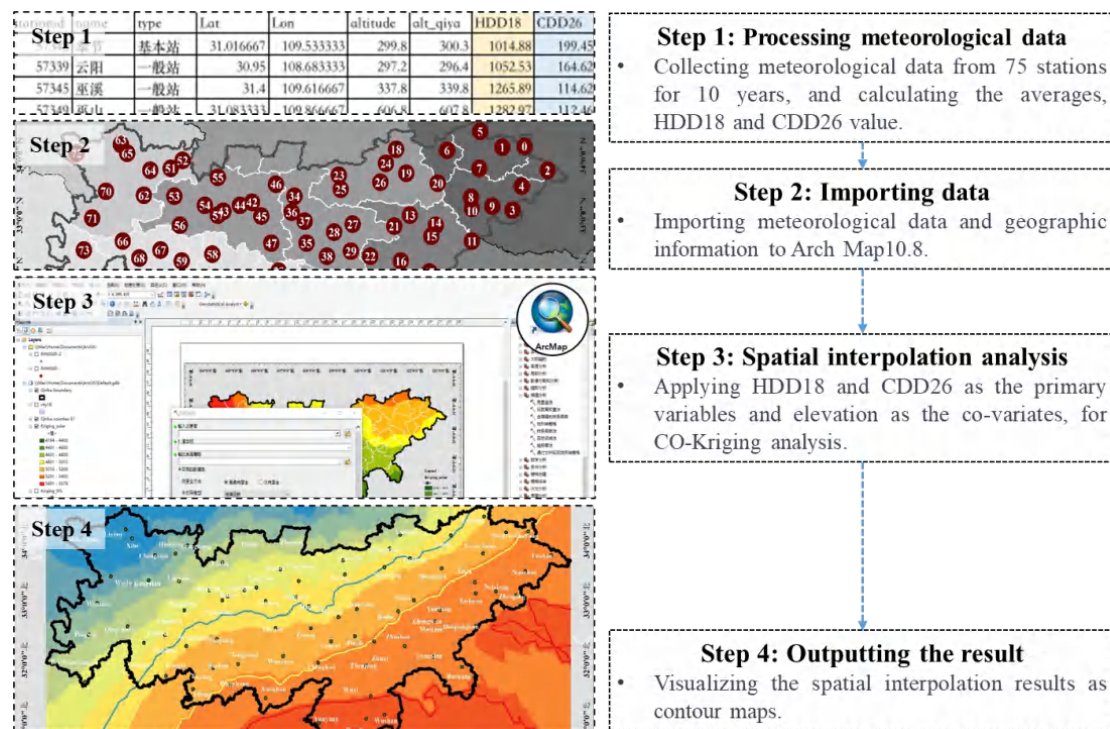


Figure 3-3. The application of spatial interpolation methods in this research

3.3. Multi-objective optimization

3.3.1. Overview of multi-objective optimization

Multi-objective optimization is a technique used to address optimization problems with multiple conflicting objectives. Unlike traditional single-objective optimization that focuses on optimizing a single objective, multi-objective optimization aims to find a set of solutions that

strike a balance and trade-off among multiple objectives. The goal is not to find a single optimal solution, but rather a set of non-dominated solutions known as the Pareto optimal solution set. Multi-objective optimization involves considering multiple decision variables and constraints, aiming to identify the best compromise solution.

Various methods are available for multi-objective optimization, including evolutionary algorithms, multi-objective genetic algorithms, and particle swarm optimization. These methods iteratively search for solutions, gradually approaching the Pareto optimal solution set. They provide decision-makers with a range of alternatives, enabling them to make informed decisions and trade-offs among different objectives. Multi-objective optimization finds applications in diverse fields such as engineering design, economics, and environmental management. It assists decision-makers in making rational choices among multiple objectives and identifying optimal solutions for complex problems. NSGA-2 (Nondominated Sorting Genetic Algorithm 2) is a popular multi-objective optimization algorithm. NSGA-2 uses a genetic algorithm approach, which involves the use of selection, crossover, and mutation operators to evolve a population of candidate solutions.

Then the research conducts multi-objective decision-making with the aim of selecting the top 20 optimal solutions from the Pareto solution set. These solutions will be used for energy consumption and thermal comfort simulations before and after the renovation of traditional residential buildings. Topsis (Technique for Order of Preference by Similarity to Ideal Solution) is a commonly used method for multi-objective decision-making, which determines the optimal solution by comparing the similarity between the candidate solutions and the ideal solution.

3.3.2. Multi-objective optimization (NSGA-2)

(1) The principle of multi-objective optimization

The essence of multi-objective optimization is to pursue the maximum or minimum values of multiple objectives under the same set of constraints. Taking the minimization as an example, the mathematical formulation can be represented as:

$$\begin{cases} \text{Minimize } F_1(x) \\ \text{Minimize } F_2(x) \\ \text{Minimize } F_3(x) \end{cases} \quad (3-4)$$

However, due to the interdependencies and trade-offs among multiple objectives in multi-objective optimization, the direct application of single-objective optimization methods, which solve each objective function individually to obtain the optimal value, is not applicable.

The most effective approach for solving multi-objective optimization problems is multi-objective evolutionary algorithms, such as non-dominated sorting genetic algorithm (NSGA),

NSGA-II, Pareto archived evolution strategy (PAES), strength Pareto evolutionary algorithm (SPEA), and SPEA2. Multi-objective evolutionary algorithms could approximate the Pareto optimal solution set using their global optimization principles without requiring prior knowledge of the detailed information of each objective. Multi-objective evolutionary algorithms are widely recognized as one of the primary methods for solving multi-objective optimization problems due to their strong objectivity, global search capabilities, and the ability to obtain a well-distributed Pareto set.

(2) The Pareto set

The Pareto set refers to the collection of solutions in multi-objective optimization that cannot be improved in any one objective without sacrificing the performance in other objectives [23]. This means that each solution in the Pareto set is considered the optimal solution without any better solutions across all objectives [24]. The Pareto set is an important concept in multi-objective optimization as it represents multiple optimal solutions that may involve trade-offs or compromises among different objectives. By analyzing the Pareto set, decision-makers can gain insights into multiple optimal solutions of the problem and make choices based on specific needs and preferences.

(3) NSGA-2

Genetic algorithms draw inspiration from the principles of biological evolution, allowing data to evolve from an initial state of random chaos to reasonable solutions based on certain rules. They are based on Darwin's theory of natural selection and concepts from genetics, simulating processes such as inheritance, variation, selection, and adaptation found in nature to find the optimal solution to a problem. The workflow of genetic algorithms is as follows: firstly, a set of initial solutions is randomly generated as a population; then, based on the objective function, each individual is evaluated for fitness, and superior individuals are selected as parents; in addition, new offspring individuals are created through crossover and mutation between parents, and they replace some individuals in the original population, forming a new generation of the population. The process of selection and variation is repeated until the optimal solution is obtained.

In 1994, Srinivas and Deb proposed the Non-dominated Sorting Genetic Algorithm (NSGA) [25]. NSGA performs non-dominated sorting on the chromosomes of the population, dividing them into several levels. The first level represents the non-dominated chromosomes, and the corresponding second level is dominated by the first level. This process continues, with each subsequent level being dominated by the previous level. The solutions in the first level are Pareto non-dominated solutions [25]. However, NSGA has drawbacks such as long computation time and high complexity during the non-dominated sorting process, resulting in slow iteration speed, low evolutionary efficiency, which led to a significant amount of subsequent research aiming to improve and extend it.

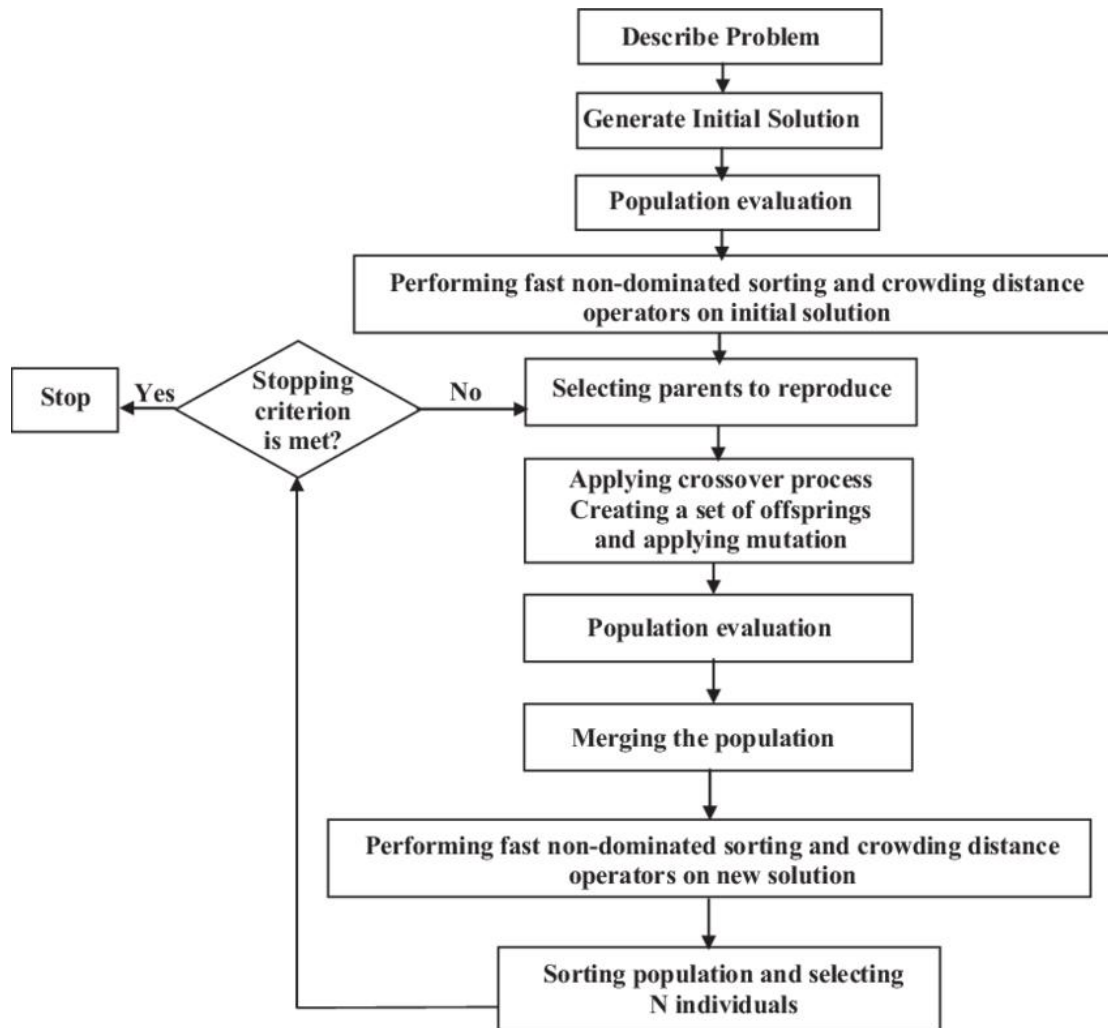


Figure 3-4. The NSGA-II algorithm flowchart [26]

In 2002, Deb et al. proposed the NSGA-II algorithm based on their previous work on the NSGA algorithm [27]. Compared to NSGA, NSGA-II has several advantages, including lower algorithm complexity, faster execution speed, and better uniformity of the solution set. Figure 3-4 shows the flowchart of the NSGA-II algorithm. NSGA-II improves upon NSGA in the following aspects: It reduces the computational complexity of the algorithm based on NSGA. It introduces a crowding distance comparison operator based on the niche technique, which helps maintain the diversity of the population. It employs an elitist preservation strategy to retain the elite individuals from the parent population. Before generating the new parent population, the parent population and the offspring population are combined, and then hierarchical sorting and crowding distance calculation are performed on the intermediate population. Individuals are selected to enter the next generation's evolution process, allowing individuals with excellent genes to have the opportunity to pass down their genes and improve the convergence speed of the population [27].

3.3.3. Multi-objective decision-making (TOPSIS)

Multi-objective decision-making refers to the decision-making process that considers multiple objectives or criteria and selects the optimal solution by evaluating and comparing different alternatives. In this study, multi-objective decision-making aims to select the best 20 solutions from the Pareto set. Technique for Order of Preference by Similarity to Ideal Solution (TOPSIS) is a commonly used multi-objective decision-making method. TOPSIS determines the optimal solution by comparing the similarity between the alternative solutions and the ideal solution.

The TOPSIS method is based on two key concepts, which are the ideal solution and the negative ideal solution. The ideal solution represents the solution that performs the best on all objective criteria, while the negative ideal solution represents the solution that performs the worst on all objective criteria. Using these ideal and negative ideal solutions, the TOPSIS method calculates the distances and closeness measures between each alternative solution and the ideal solution to determine their rankings. As illustrated in Figure 3-5, the solution with the shortest Euclidean distance to the positive ideal solution is the best solution. D_1 represents the Euclidean distance between each solution and the ideal solution, and D_2 represents the Euclidean distance between each solution and the negative ideal solution [28-30]. The green point represents the negative ideal solution, the orange point represents the positive ideal solution, and the grey points indicate all other alternatives in the Pareto solution set. The best option, represented by the red point, is the one closest to the green point. Cao et al.[31] and Delgarm et al.[32] provide further details on the computation procedure.

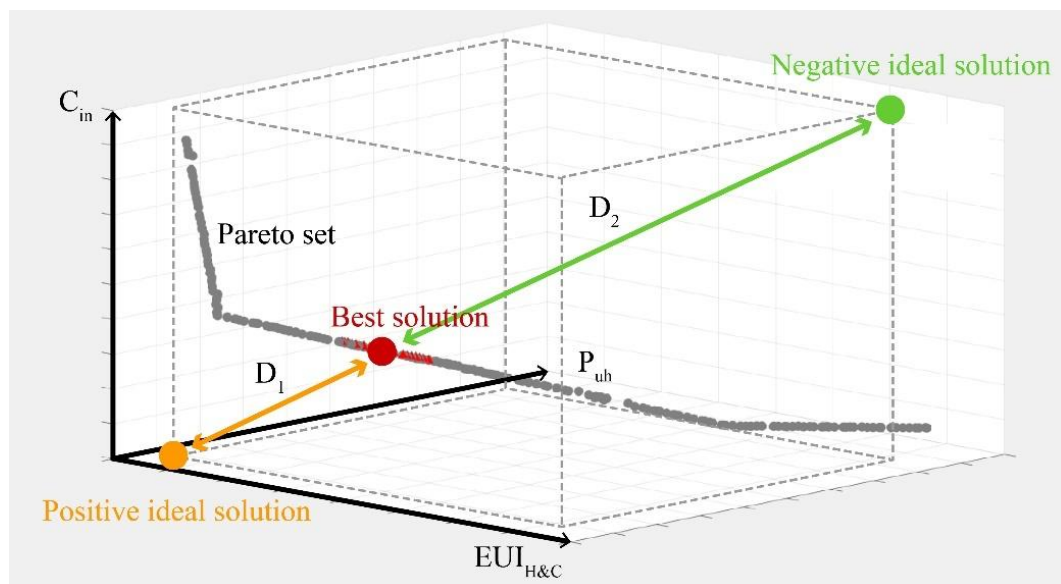


Figure 3-5. Schematic diagram of TOPSIS

3.3.4. The application of multi-objective optimization in the research

Figure 3-6 illustrates the workflow of the multi-objective optimization in this study. In this section, a multi-objective optimization model was developed, incorporating the NSGA-2 method and the TOPSIS method, based on the objectives of “building energy consumption”, “human comfort”, and “economy”. The model aims to derive the optimal solution for renovating traditional dwellings using passive strategies. The first step involves energy simulation, where the values of the three objectives can be obtained by modifying passive design parameters. To facilitate subsequent linear regression analysis, a minimum of 100 sets of simulated data is required. Furthermore, a multiple linear regression equation is fitted, considering the independent variables (4 passive design parameters) and dependent variables (3 objectives). Subsequently, the NSGA-2 system incorporates the 3 equations for each sub-region to obtain the Pareto set, which represents a set of optimal solutions selected by NSGA-2. However, the Pareto set still contains a large number of solutions. Hence, employing the TOPSIS method based on the Euclidean distance, 20 optimal solutions for the three-objective optimization within the Pareto set are obtained.

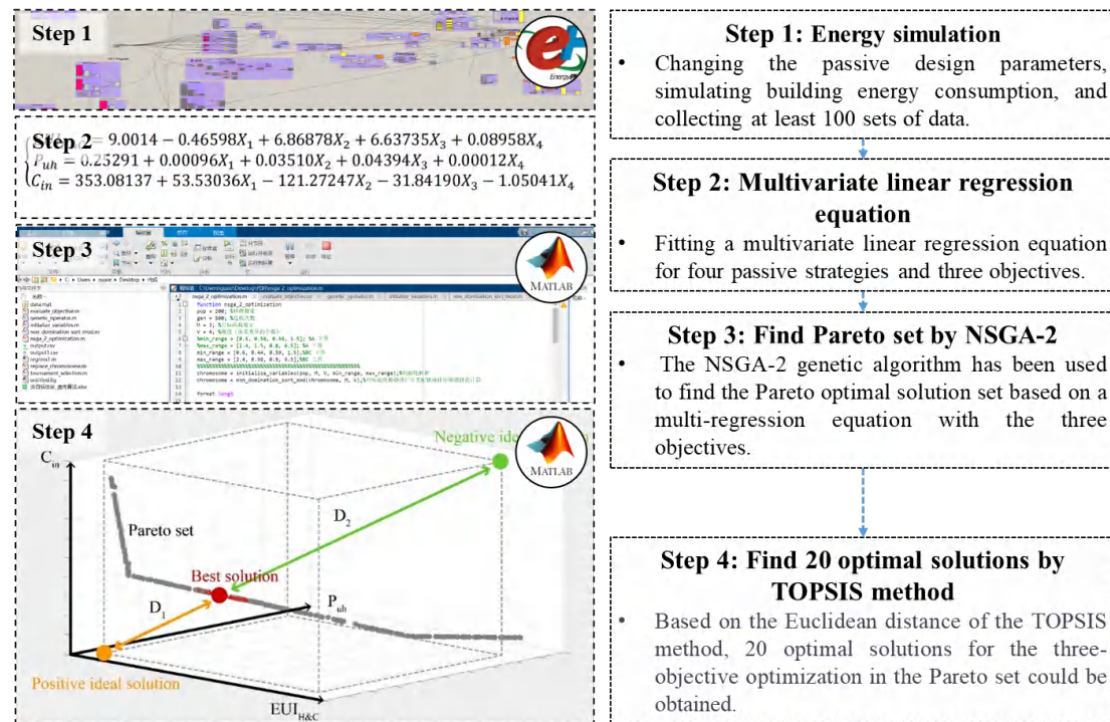


Figure 3-6. The application of multi-objective optimization in this research

3.4. Other methods

This study incorporated additional research methods, namely the data statistics method, field surveys method, and computer simulations, to enhance the comprehensiveness of the investigation.

and thus derive more accurate and reliable conclusions. Data analysis methods can be divided into 3 categories: descriptive analysis, inferential analysis, and predictive analysis. Descriptive analysis is based on data collection, and its purpose is to describe and summarize the characteristics of the data through statistical indicators such as mean, median, and standard deviation. Inferential analysis attempts to analyze the correlations and patterns in the data through these characteristics and make inferences and predictions. Predictive analysis uses existing data to establish mathematical models and predict what will happen in future data. The method used in this study is inferential analysis, including linear regression analysis and multiple regression analysis.

The statistical methods used in this study mainly include linear regression analysis and multiple linear regression analysis. Linear regression analysis is primarily applied in Chapter 6 for thermal comfort investigations, aiming to fit a linear equation between indoor temperature and residents' thermal sensation votes, and subsequently obtain the neutral temperature and thermal comfort range for traditional dwellings during winter and summer. Multiple linear regression analysis is primarily used in Chapter 8 for multi-objective optimization, aiming to fit a mathematical model between 3 objectives and 4 passive strategies.

(2) Linear Regression Analysis

Linear regression analysis was proposed by the British statistician Francis Galton in the late 19th century. He used this method to study the hereditary laws of human height, which was the first application of linear regression analysis. The role of linear regression analysis is to establish a linear model by modeling the relationship between independent and dependent variables to predict the value of the dependent variable [34]. In practice, linear regression analysis is usually used to study the relationship between two or more variables and to establish a mathematical model between these variables [35].

Simple linear regression refers to a linear relationship model between only one independent variable and one dependent variable. The basic idea is to establish a linear equation and solve the slope and intercept through the method of least squares to describe the relationship between the independent variable and the dependent variable. The formula for this method is:

$$y = e_0 + e_1x + \varepsilon \quad (3-4)$$

Where y represents the value of the dependent variable; x represents the value of the independent variable; e_0 represents the intercept, which represents the value of the dependent variable when the independent variable is 0; e_1 represent the coefficients of the model, also known as regression coefficients or slopes; ε represents the error term [35].

Simple linear regression requires a linear relationship between the independent variable and the dependent variable, and independence between the independent variables. In practical

applications, data preprocessing, model verification and other steps are also required to ensure the accuracy and reliability of the model.

(3) Multiple regression analysis

Multiple linear regression analysis is an extended form of linear regression analysis used to explore the statistical method of the relationship between multiple independent variables and one dependent variable. It can describe the relationship between independent variables and dependent variables by establishing a linear equation, thereby predicting future outcomes.[36] The development of multiple linear regression analysis can be traced back to the late 19th and early 20th centuries when the statistician Francis Galton used linear regression to study the relationship between height and intelligence. However, its practical application did not become popular until the mid-20th century, when the development of computer technology provided convenience and possibility for analyzing large amounts of data, making multiple linear regression analysis widely used [36]. Nowadays, multiple linear regression analysis has become one of the most commonly used data analysis methods in fields such as statistics and economics. Since the 21st century, with the development of big data, artificial intelligence, and other technologies, multiple linear regression analysis combined with other data analysis methods for comprehensive analysis has provided important support for decision-making in various industries. The multiple linear regression model can be expressed as:

$$y = e_0 + e_1x_1 + e_2x_2 + \dots + e_nx_n + \varepsilon \quad (3-5)$$

Where y represents the value of the dependent variable; x_1 to x_n represent the values of independent variables; e_1 to e_n represent the coefficients of the model, also known as regression coefficients or slopes; e_0 represents the intercept, which represents the value of the dependent variable when all independent variables are 0; ε represents the error term [37].

(4) The application of data statistics method in the research

In Chapter 6, the thermal comfort investigation was conducted in both winter and summer, collecting subjective thermal sensation questionnaires from participants residing in traditional dwellings. Simultaneously, indoor temperature and humidity conditions were recorded during the questionnaire completion. To ensure the accuracy of the regression equation, over 100 thermal sensation questionnaires were collected in each climatic sub-region. The bin method was employed to divide the collected questionnaires and measured temperatures into temperature intervals of 0.5°C. The average values of operative temperature (T_{op}) and thermal sensation votes were calculated for each temperature interval within each sub-climatic region. By plotting scatter plots on a two-dimensional coordinate axis, with T_{op} in x-axis and mean thermal sensation votes (MTS) in y-axis, a linear regression analysis was performed. This analysis yielded the fitted equation for T_{op} and MTS, as shown in Equation 3-6. Using the fitted

equation, the neutral temperature of the climatic sub-region could be determined when $MTS=0$. Additionally, the thermal comfort range for 90% of the residents could be obtained when $MTS=\pm 0.5$.

$$MTS = a \cdot T_{op} + b \quad (3-6)$$

In Chapter 8, multiple linear regression analysis was employed to fit a mathematical model that incorporates 4 passive strategies and 3 objectives. By randomly varying the parameter values of the 4 passive strategies within their specified ranges, the energy simulation software was used to obtain the corresponding values of the building annual thermal load ($EUI_{H\&C}$) and the proportion of discomfort hours (P_{uh}). Additionally, the initial renovation investment (C_{in}) was calculated for each set of parameter values. At least 100 sets of data were simulated for each sub-climatic region to facilitate the fitting of the multiple linear regression equations. By using statistical software such as Origin, the 3 objectives were set as the parameters for the y-axis, while the 4 passive strategies were set as the parameters for the x-axis. By performing multiple linear regression analyses for each objective, mathematical models were derived for the 4 passive strategies and 3 objectives in each sub-climatic region, as shown in Equation 3-7. These mathematical models would be used for subsequent multi-objective optimization analyses.

$$\begin{cases} EUI_{H\&C} = a_0 + a_1 \cdot x_1 + a_2 \cdot x_2 + a_3 \cdot x_3 + a_4 \cdot x_4 \\ P_{uh} = b_0 + b_1 \cdot x_1 + b_2 \cdot x_2 + b_3 \cdot x_3 + b_4 \cdot x_4 \\ C_{in} = c_0 + c_1 \cdot x_1 + c_2 \cdot x_2 + c_3 \cdot x_3 + c_4 \cdot x_4 \end{cases} \quad (3-7)$$

3.4.2. Field survey method

(1) Overview of field survey method

Field survey involves conducting on-site observations, interviews, and data collection to obtain detailed and comprehensive research data, and it is a research method widely employed in social sciences [38]. It emphasizes direct observation and communication with the target individuals or groups to gain in-depth understanding of their behaviors, attitudes, values, and social interactions. Field survey is a valuable method that allows researchers to study individuals and social phenomena in real-life contexts [39]. It involves studying the actual environments and social backgrounds using various data collection techniques such as observation, interviews, and surveys to gather qualitative and quantitative data. This method can be applied in various disciplines, including sociology, anthropology, psychology, education,

among others, to gain in-depth insights into social phenomena, human behavior, and social relationships.

In this study, the field survey method was primarily applied in Chapter 5 for investigating the traditional settlements and dwellings in Qinba mountainous area, and in Chapter 6 for conducting indoor thermal comfort investigations. The field surveys were divided into 3 main parts: the surveying and mapping, the environmental measurement, and the thermal sensation questionnaire survey. The main process of conducting field surveys is illustrated in Figure 3-7.

(2) Research scope

The site investigations are conducted in term of the climatic sub-regions. Including 3 main parts, the traditional settlement, courtyard, and dwellings. Figure 3-8 shows the research scope of the field survey. The map highlights the villages visited by the research team, represented by darker colors. The green labels indicate the case study villages selected for the settlement analysis. The red labels denote the specific dwellings where indoor and outdoor physical environment measurements were conducted.

According to the climatic sub-division of the Qinba mountainous area and considering the distribution of traditional villages, accessibility to transportation, and other factors, the research team conducted comprehensive on-site surveys and research activities in selected counties within the 5 climatic sub-regions from July 2020 to January 2023. The research work involved various tasks, including surveying and mapping, questionnaire surveys, and environmental measurements. A total of 24 counties and 63 villages in the Qinba mountainous area were investigated, with particular emphasis on 21 key villages.



Figure 3-8. The research scope

(3) Research content

The field survey was conducted in the designated traditional villages within the Qinba mountainous area. The survey comprised 4 main components, namely traditional villages, courtyards, traditional dwellings, and residents' information. The key research topics and their corresponding details are presented in Table 3-2.


Table 3-2. Research Content of the research

Category	Research content
Village	Geographic environment, climatic environment, settlement planning, regional culture
Courtyard	Site information, Courtyard form, landscape
Dwelling	Orientation, plane layout, function, structure, construction, elevation information, outdoor and indoor physical environment measurement
Resident	Lifestyle, custom and habit, thermal sensation

(4) Measuring setting and instrument

The thermal environment measurement of rural dwellings was carried out continuously for 48 hours during winter (January) and summer (July) in the 5 climatic sub-regions. The data were recorded every 30 minutes, resulting in a total of 96 data sets. To ensure accuracy, a set of 24-hour data was selected for analysis. The key parameters measured included the outdoor and indoor air temperature, the outdoor and indoor relative humidity, the outdoor and indoor black ball temperature, as well as the outdoor and indoor wind speed. The indoor measurement point was positioned at the room's center and 1.4 meters above the ground. Details about the instruments used are provided in Table 3-3.

Table 3-3. The instruments' parameters

Meteorological Parameters	Instrument	Images	Measuring range	Precision
Air temperature	TP3207.2		-40~100°C	1/3DIN
Relative humidity	TP3207.2R		0~100%	±2%
Wind velocity	AP3203.2		0.05~5 m/s	± (0.05+0.5%)
Black globe temperature	TP3276.2		-30~120°C	1/3DIN

3.4.3. Computer energy consumption simulation

Energy simulation is utilized in Chapters 4, 6, 7, and 8 to conduct building energy consumption simulations for traditional dwellings in different climatic regions, building envelope structures, and combinations of passive strategies. This allows for the analysis of the impact of different climatic conditions, air conditioning set points, and passive strategies on building energy consumption. Due to the research focus on the thermal environment of buildings, the energy simulation in this study specifically emphasizes the thermal load of buildings, which includes the heating and cooling loads.

(1) Simulation software

To assess the heating and cooling loads of the buildings, this research utilized EnergyPlus simulation software [40]. The version of EnergyPlus the study used is integrated into the Grasshopper plug-in of Rhinoceros, a 3D modeling software [41]. On the Grasshopper platform, using EnergyPlus simulation engine, the heating and cooling loads of traditional dwellings in each climatic sub-region will be computed with appropriate meteorological documents. This will be achieved by utilizing standardized weather files in EnergyPlus weather (EPW) file format. By utilizing the available weather data, the thermal load of the target buildings in the study area will be analyzed. The workflow of Grasshopper and EnergyPlus can be visualized in Figure 3-9 [42].

EnergyPlus is an advanced software tool used for building energy simulation. It is widely applied in the fields of building design and energy analysis to evaluate various aspects of a building's energy consumption, thermal comfort, and indoor environmental quality [43]. Based on physical principles and models for heat transfer, thermal radiation, and air movement, EnergyPlus enables comprehensive simulation and analysis of a building's thermal, moisture, lighting, and electrical energy consumption.

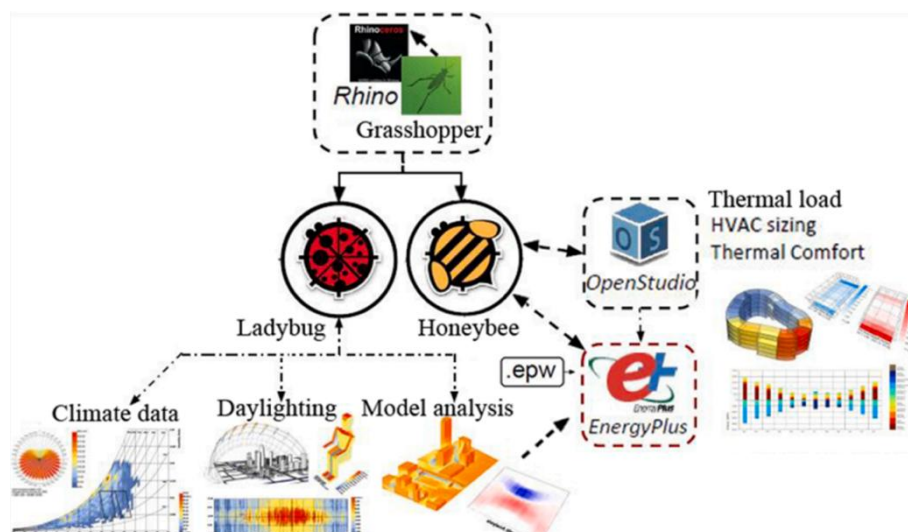


Figure 3-9. Algorithm mode of thermal load in Grasshopper with plug-ins of Honeybee and Ladybug [42]

(2) Simulation setting

In the climate zone analysis section of Chapter 4, the simulation settings aim to validate the climate zone results. The simulations involve using the same building envelope and indoor conditions specified in the regulations for hot-summer and cold-winter regions. The energy consumption of the models is compared by only varying the outdoor climatic conditions. In the thermal comfort survey section of Chapter 6, the simulations aim to compare the building annual thermal loads based on the cooling and heating set points based on the measured neutral temperature and the standard requirement. The simulations use the actual building envelope within each climatic sub-region for accurate representation. In the passive strategy optimization sections of Chapters 7 and 8, the simulations involve using the actual building envelope within the climatic sub-region and incorporating different passive strategies. The energy consumption simulations are conducted based on the real-life scenarios with the additional passive strategies.

Since the energy simulation settings vary for each chapter, a detailed explanation will be explained in each respective chapter.

Reference.

- [1] L. Mitas and H. Mitasova, "Spatial interpolation," *Geographical information systems: principles, techniques, management applications*, vol. 1, no. 2, 1999.
- [2] D. E. Myers, "Spatial interpolation: an overview," *Geoderma*, vol. 62, no. 1-3, pp. 17-28, 1994.
- [3] J. Li and A. D. Heap, *A review of spatial interpolation methods for environmental scientists*. Geoscience Australia, 2008.
- [4] J. Zhang, J. Wang, and M. Du, "Visualization Analysis of Bus Passenger Flow Distribution Based on Spatial Interpolation Method," *Bulletin of surveying and mapping*, no. 04, pp. 38-41+52, 2015.
- [5] C. Li et al., "Establishment of integrated methodology for bay ecosystem health assessment and its application in Daya Bay," *Acta Ecologica Sinica*, vol. 33, no. 06, pp. 1798-1810, 2013.
- [6] Y. Lin, Y. Peng, W. Hu, and R. Li, "Research on Urban Standard Land Price Updating and Application Based on Spatial Interpolation," *Geospatial Information*, vol. 17, no. 02, pp. 75-78+10, 2019.
- [7] A. Antal, P. M. Guerreiro, and S. Cheval, "Comparison of spatial interpolation methods for estimating the precipitation distribution in Portugal," *Theoretical Applied Climatology*, vol. 145, no. 3-4, pp. 1193-1206, 2021.
- [8] E. Asadi Oskouei et al., "Mapping Climate Zones of Iran Using Hybrid Interpolation Methods," *Remote Sensing*, vol. 14, no. 11, p. 2632, 2022.
- [9] Z. Zhang and Q. Du, "A bayesian kriging regression method to estimate air temperature using remote sensing data," *Remote Sensing*, vol. 11, no. 7, p. 767, 2019.
- [10] S. Li, D. A. Griffith, and H. Shu, "Temperature prediction based on a space-time regression-kriging model," *Journal of Applied Statistics*, vol. 47, no. 7, pp. 1168-1190, 2020.
- [11] P. Jones, S. Raper, and T. Wigley, "Southern Hemisphere surface air temperature variations: 1851-1984," *Journal of Applied Meteorology Climatology*, vol. 25, no. 9, pp. 1213-1230, 1986.
- [12] Y. Pan, D. Gong, L. Deng, J. Li, and J. Gao, "Smart distance searching-based and DEM-informed interpolation of surface air temperature in China," *ACTA Geographica Sinica*, no. 03, pp. 366-374, 2004.
- [13] M. R. Holdaway, "Spatial modeling and interpolation of monthly temperature using kriging," *Climate research*, vol. 6, no. 3, pp. 215-225, 1996.
- [14] T. Wu and Y. Li, "Spatial interpolation of temperature in the United States using residual kriging," *Applied Geography*, vol. 44, pp. 112-120, 2013.
- [15] R. Franke, "Scattered data interpolation: tests of some methods," *Mathematics of computation*, vol. 38, no. 157, pp. 181-200, 1982.
- [16] M. Brauer, C. Lencar, L. Tamburic, M. Koehoorn, P. Demers, and C. Karr, "A cohort

study of traffic-related air pollution impacts on birth outcomes," *Environmental health perspectives*, vol. 116, no. 5, pp. 680-686, 2008.

[17] R. Webster and M. A. Oliver, *Geostatistics for environmental scientists*. John Wiley & Sons, 2007.

[18] H. Wackernagel, *Multivariate geostatistics: an introduction with applications*. Springer Science & Business Media, 2003.

[19] E. H. Isaaks and R. M. J. N. Y. Srivastava, *Applied geostatistics*. New York: Oxford University Press, 1989.

[20] H. Li, Y. Yang, K. Lv, J. Liu, and L. Yang, "Compare several methods of select typical meteorological year for building energy simulation in China," *Energy*, vol. 209, p. 118465, 2020.

[21] A. Sekulić, M. Kilibarda, D. Protić, M. P. Tadić, and B. Bajat, "Spatio-temporal regression kriging model of mean daily temperature for Croatia," *Theoretical Applied Climatology*, vol. 140, pp. 101-114, 2020.

[22] J. Xiong et al., "Subdivision of hot summer and cold winter zone for building thermal performance," *Journal of HV&AC*, vol. 49, no. 04, pp. 12-18, 2019.

[23] K. Deb, M. Mohan, and S. Mishra, "A fast multi-objective evolutionary algorithm for finding well-spread pareto-optimal solutions," *KanGAL report*, vol. 2003002, pp. 1-18, 2003.

[24] E. Zitzler and L. Thiele, "Multiobjective evolutionary algorithms: a comparative case study and the strength Pareto approach," *IEEE transactions on Evolutionary Computation*, vol. 3, no. 4, pp. 257-271, 1999.

[25] N. Srinivas and K. Deb, "Multiobjective optimization using nondominated sorting in genetic algorithms," *Evolutionary computation*, vol. 2, no. 3, pp. 221-248, 1994.

[26] M. Pouraliakbarimamaghani, M. Mohammadi, and A. Mirzazadeh, "A multi-objective location-allocation model in mass casualty events response," *Journal of Modelling in Management*, vol. 13, no. 1, pp. 236-274, 2018.

[27] K. Deb, A. Pratap, S. Agarwal, and T. Meyarivan, "A fast and elitist multiobjective genetic algorithm: NSGA-II," *IEEE transactions on evolutionary computation*, vol. 6, no. 2, pp. 182-197, 2002.

[28] H.-Q. Nguyen, V.-T. Nguyen, D.-P. Phan, Q.-H. Tran, and N.-P. Vu, "Multi-criteria decision making in the PMEDM process by using MARCOS, TOPSIS, and MAIRCA methods," *Applied sciences*, vol. 12, no. 8, p. 3720, 2022.

[29] B. Ceballos, M. T. Lamata, and D. A. Pelta, "A comparative analysis of multi-criteria decision-making methods," *Progress in Artificial Intelligence*, vol. 5, pp. 315-322, 2016.

[30] P. Kumar and P. Sarkar, "A comparison of the AHP and TOPSIS multi-criteria decision-making tools for prioritizing sub-watersheds using morphometric parameters' analysis," *Modeling Earth Systems Environment*, vol. 8, no. 3, pp. 3973-3983, 2022.

[31] X. Cao et al., "Energy-quota-based integrated solutions for heating and cooling of residential buildings in the Hot Summer and Cold Winter zone in China," *Energy and Buildings*,

vol. 236, p. 110767, 2021.

[32] N. Delgarm, B. Sajadi, and S. Delgarm, "Multi-objective optimization of building energy performance and indoor thermal comfort: A new method using artificial bee colony (ABC)," *Energy and Buildings*, vol. 131, pp. 42-53, 2016.

[33] R. L. Ott and M. T. Longnecker, *An introduction to statistical methods and data analysis*. Cengage Learning, 2015.

[34] D. C. Montgomery, E. A. Peck, and G. G. Vining, *Introduction to linear regression analysis*. John Wiley & Sons, 2021.

[35] G. A. Seber and A. J. Lee, *Linear regression analysis*. John Wiley & Sons, 2003.

[36] W. D. Berry, W. D. Berry, S. Feldman, and D. Stanley Feldman, *Multiple regression in practice* (no. 50). Sage, 1985.

[37] L. S. Aiken, S. G. West, and S. C. Pitts, "Multiple linear regression," *Handbook of psychology*, pp. 481-507, 2003.

[38] G. Guan, "Investigation Study Spatially Of Dong-Traditional-Village In Qiandongnan Region," *Master Thesis*, Xi'an University of Architecture and Technology, 2015.

[39] T. Kane, "Indoor temperatures in UK dwellings: investigating heating practices using field survey data," © Tom Kane, 2013.

[40] R. Kamal, F. Moloney, C. Wickramaratne, A. Narasimhan, and D. Goswami, "Strategic control and cost optimization of thermal energy storage in buildings using EnergyPlus," *Applied Energy*, vol. 246, pp. 77-90, 2019.

[41] A. Eltaweel and Y. Su, "Controlling venetian blinds based on parametric design; via implementing Grasshopper's plugins: A case study of an office building in Cairo," *Energy and Buildings*, vol. 139, pp. 31-43, 2017.

[42] F. a. Chi et al., "Prediction of the total day-round thermal load for residential buildings at various scales based on weather forecast data," *Applied Energy*, vol. 280, p. 116002, 2020.

[43] S. El Ahmar, F. Battista, and A. Fioravanti, "Simulation of the thermal performance of a geometrically complex Double-Skin Facade for hot climates: EnergyPlus vs. OpenFOAM," in *Building Simulation*, 2019, vol. 12, pp. 781-795: Springer.

Chapter 4

***CLIMATIC SUBDIVISIONS IN QINBA
MOUNTAINOUS AREA***

CHAPTER FOUR: CLIMATIC SUBDIVISIONS IN QINBA MOUNTAINOUS AREA

<i>CLIMATIC SUBDIVISIONS IN QINBA MOUNTAINOUS AREA</i>	1
4.1. Content.....	1
4.2. Materials and Methodology.....	1
4.2.1. Research background.....	1
4.2.2. Study area	2
4.2.3. Motivation	6
4.2.4. Method and data source.....	7
4.3. Research proposal.....	8
4.3.1. Climatic subdivision.....	8
4.3.2. Supplementary elements of climatic sub-regions.....	8
4.3.3. Verification of climatic sub-regions.....	9
4.4. Results of climatic subdivision in Qinba mountainous area.....	9
4.4.1. Climatic sub-regions in Qinba mountainous area.....	9
4.4.2. Supplementary elements of climatic sub-regions in Qinba mountainous area.....	14
4.5. Verification of climatic sub-regions.....	21
4.5.1. The climate conditions of the 5 climatic sub-regions.....	21
4.5.2. Building energy simulation in each climatic sub-region	31
4.6. Summary.....	34
Reference	36

4.1. Content

Climate condition is an essential aspect in determining the passive design scheme. The Qinba mountainous area is vast in area and has diverse terrain. It is also dotted with a large number of rural settlements. A single climate zoning cannot meet the diverse climatic conditions of this area. More detailed climatic subdivisions can serve as a foundation for building energy conservation specifications and building passive design, which can aid in improving indoor thermal comfort and lowering building thermal loads.

In this section, using the spatial interpolation method, the Qinba mountainous area is divided into 5 climatic sub-regions, A1, A2, B1, B2, and C, based on the values of HDD18 and CDD26 calculated through the annual daily average air temperature. In addition, the relative humidity, wind speed, and solar radiation intensity were used as supplementary elements for sub-climate zoning.

Furthermore, in order to verify the rationality of the climate subdivision scheme, the daily meteorological data of the typical counties in the 5 climatic sub-regions in the Qinba mountainous area were selected to analyze the differences in meteorological characteristics. Based on these meteorological data, EnergyPlus is used to simulate the energy consumptions of the target dwelling, and the correlations between its energy consumption levels and climate zoning scheme is analyzed. According to the annual thermal loads, it shows an upward trend from region A1 to C, with the value of 14.31 kWh/m², 16.46 kWh/m², 26.11 kWh/m², 28.43 kWh/m², and 30.64 kWh/m², respectively. The simulation results are consistent with the climatic sub-regions' expected energy consumption level.

4.2. Materials and Methodology

4.2.1. Research background

In light of China's goal to achieve a carbon peak by 2030 and the pressing challenges of energy consumption and environmental crises, there has been a growing focus on reducing building energy consumption [1]. Passive design strategies, as a climate-responsive approach, can effectively enhance indoor thermal comfort, save building energy consumption, and lower carbon emissions without relying on artificial energy sources [2-4]. And climate conditions are a critical factor in determining the passive design scheme [5]. Through climate zoning, it becomes possible to establish building energy efficiency standards and tailor energy-saving techniques to suit specific regions [6].

Governments and scholars worldwide are actively engaged in climate zoning research and have developed technical regulations for building energy efficiency based on the climate characteristics of their respective countries [7-10]. The specific details of these zoning approaches and regulations are elaborated in the literature review of Chapter 2. Scholars typically employ a set of climate zoning indicators for their studies, including air temperature,

heating degree days and cooling degree days calculated based on air temperature, relative humidity, solar radiation, wind speed, etc. Depending on the requirements of their respective disciplines, scholars select appropriate zoning indicators to conduct detailed investigations into climate zoning [8, 11-14].

4.2.2. Study area

(1) Overview of Qinba mountainous area

Qinba mountainous region situated at the center of China, the entire region is between $103^{\circ}44' \sim 113^{\circ}14'E$ and $30^{\circ}29' \sim 34^{\circ}38'N$, mainly including the Qinling Mountain, the Daba Mountain, and their hinterland, stretching more than 1,000 kilometers from east to west, with a total area of about 225,000 km². Figure 4-1 shows the location of Qinba mountainous area.



Figure 4-1. The location of Qinba mountainous area

By 2018, the overall population was 37.65 million, with 30.516 million living in rural areas [15]. Qinba mountainous area includes 17 cities, 81 counties, and 31,520 villages in Shaanxi, Gansu, Sichuan, Hubei, Henan Province, and Chongqing City, showing in Figure 4-2 and Figure 4-3 [16, 17].

The urbanization level of Qinba mountainous area is low, with the urbanization rate of 32.75 %, which is lower than the national average of 56.10 %. The income level of residents in this area is generally low. In 2015, the per capita disposable income of urban residents was 23,392 CNY, 73.6 % of the national average of 31,790 CNY; the per capita net income of rural residents is 8,758 CNY, which is 81.7 % of the national average [15, 18].



Figure 4-2. The satellite map of Qinba mountainous area



Figure 4-3. The Provincial and county division map of Qinba mountainous area

(2) Geographical location of Qinba mountainous area

The Qinba mountainous area includes three landform units, which are the Qinling Mountain, the Hanjiang River valley basin, and the Daba Mountain, with noticeable terrain fluctuation, showing in Figure 4-4 [19]. The Qinba mountainous area a general term for the Qinling Mountains and the Daba Mountains. It is a huge mountain system that spans the central part of China’s mainland and has the east-west trend. The Qinling Mountains can be further categorized into three sections: the western part, the central part, and the eastern part. Meanwhile, the Daba Mountains consist of the Micang Mountains and the Daba Mountains, forming an integral part of this mountainous region.

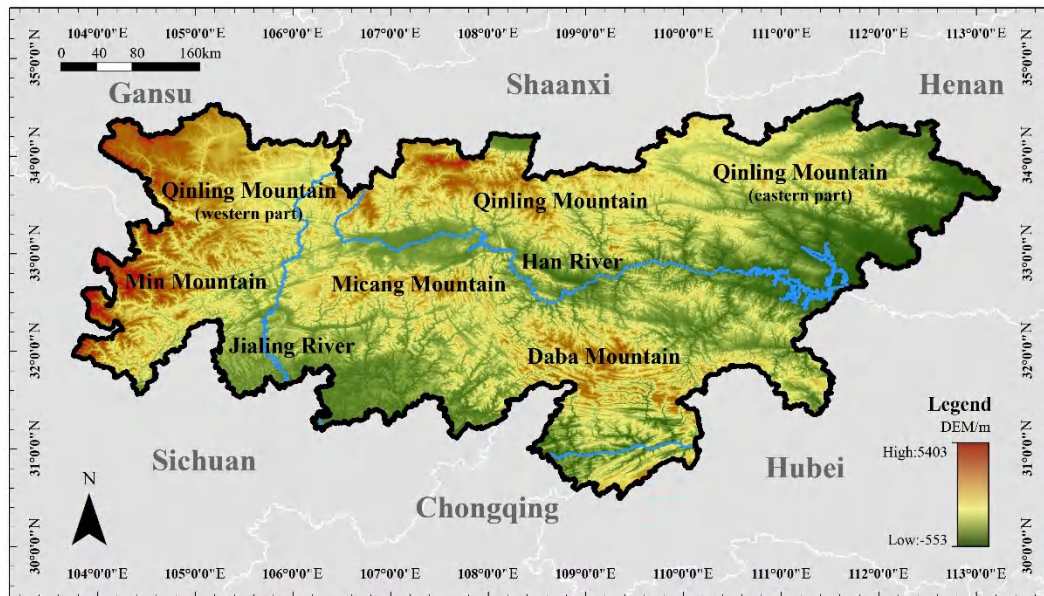


Figure 4-4. The digital elevation model (DEM) map of Qinba mountainous area

The Qinba mountainous area stretches 682 kilometers from east to west, spanning 3 provinces. And mountainous area is divided into geographically undulating transitional areas by many tributaries of the Yellow River and the Yangtze River. It is a complete geographical unit, and has the characteristics of multi-dimensional zonal changes, showing a high degree of complexity, diversity, transition, and sensitivity [20]. Its mountains are steep in the north and gentle in the south, and the mountains are adjacent to each other. There are many small basins and valleys in the study area. The mountain is steep in the north and gentle in the south, and the mountains are adjacent, with many small basins and valleys. The basins in Hanzhong and Ankang City connected by Qinling Mountains and Daba Mountains belong to the typical small basin landforms. And the valley between Shangzhou and Danfeng County is the typical valley landform [21]. According to the altitude, Qinba mountainous area can be divided into high mountain area, with the altitude of more than 1,800m, middle mountain area, with the altitude between 900m to 1,800m, and low mountain area, with the altitude between 500m to 900m.

(3) Climatic characteristics of Qinba mountainous area

Qinba mountainous area lies on China's north-south geography and climate boundary and is covered by mountains and valleys. With the climatic traits of both north and south China, Qinba mountainous area serves as a crucial physical and climatic buffer zone between them. It is belonging to the hot summer and cold winter zone in China's thermal division, characterized by hot summer temperatures with high humidity and low winter temperatures with high humidity, shown in Figure 4-5 [22]. The Qinba mountainous area in the transitional area are diverse and complex in climate. The high mountain area has no summer, and has much precipitation throughout the year, with the annual average air temperature of less than 10°C. The middle mountain area is humid, with the annual average air temperature of 12°C. The low mountain area has sufficient solar radiation, with the annual average air temperature of 14°C

[23].



Figure 4-5. Thermal zoning map in China

(4) The current climate zoning conditions of Qinba mountainous area

As shown in Figure 4-5, China has a vast territory with five thermal regions, such as severe cold region, cold region, hot summer and cold winter region, hot summer, and warm winter region, and mild climate region [24]. However, there are still large differences in meteorological characteristics in the five thermal regions. Under the condition of maintaining the primary thermal zone, the current standard also proposes a secondary zoning scheme, which uses the value of HDD18 and CDD26 to subdivide China into 11 sub-climate zones [13].

However, China, with its extensive landmass spanning 9.6 million square kilometers, encompasses a diverse range of climatic conditions. Figure 4-6 highlights the significant expanse of the hot summer and cold winter region, covering an area of 1,800,000 square kilometers. The Qinba mountainous area, covers an area of 225,000 square kilometers within China's hot summer and cold winter zone, is a geographical area in China, encompassing the Qinling and Daba mountain ranges, as well as the hilly and mountainous areas between them. As shown in Figure 4-2 and 4-4, due to variations in geographical environments, the climate conditions in this region also exhibit significant changes. As a result, it becomes crucial to undertake a climate subdivision within this region.

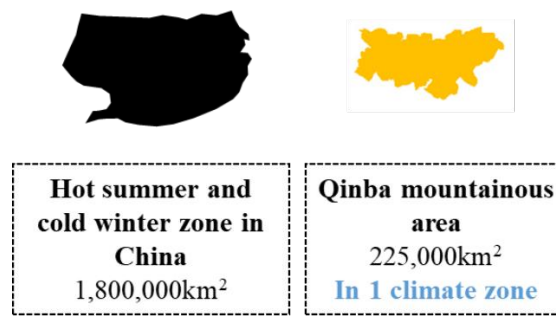


Figure 4-6. The thermal zoning of the Qinba mountainous region

4.2.3. Motivation

Most of the study area is located in the sub-region with the HDD18 of 700~2000°C·d, which is still a broad scope. Moreover, the zoning scheme does not consider the cooling demand, or involve other meteorological factors such as the wind speed, relative humidity, and solar radiation intensity that affect the building’s passive design parameters. The current climate zone in the Qinba mountainous area needs to be subdivided to match the different thermal comfort temperature ranges and passive strategies [25, 26].



Figure 4-7. The meteorological stations distribution map of Qinba mountainous area

As shown in Figure 4-7, in this study, 75 meteorological stations in the study zone were used to collect the meteorological observation factors, such as the air temperature, relative humidity, wind speed, and solar radiation intensity in the past ten years [27]. The Kriging method was used to decide climatic sub-regions [28, 29]. Furthermore, the neutral temperature of each climatic sub-region is calculated. The research uses the above analysis to help the climatic sub-region in the study area match the appropriate passive strategies to improve the indoor thermal

comfort and reduce building energy consumption [30].

4.2.4. Method and data source

(1) Spatial interposition method

The spatial interposition method converts the measured data of discrete points in space into continuous data surfaces [31]. Spatial interpolation is often used in statistical analysis of meteorological data [32, 33]. The commonly used spatial interposition methods based on ArcGIS software include the trend surface method, natural neighbor method, spline function method, etc. However, these methods lack the introduction of covariates, which is not applicable to analyzing temperature changes in mountainous areas. The Co-Kriging method allows the introduction of multiple factors as covariates for the spatial interposition of climate elements, significantly improving the interpolation accuracy [28, 31]. In this study, the Co-Kriging method is used, and the influence of elevation on the estimated point value is considered.

(2) Data sources and processing

1) The daily average temperature, monthly relative humidity, wind speed, and spatial data of Qinba mountainous area are collected from the daily surface climate data set in China (V3.0); the solar radiation intensity data is collected from the Nasa meteorological data set; the spatial distribution of meteorological stations is obtained from the Chinese Academy of Sciences' Resource and Environmental Science and Data Center (<http://www.resdc.cn/>); the digital elevation data (DEM) of the study area is collected from the geospatial data cloud (<http://www.gscloud.cn/>).

2) Meteorological elements have the characteristics of periodic changes and trend changes. An extended period database will reduce the credibility of the average temperature in the region and cannot reflect the actual situation in the context of global warming. The research shows that the 10-year meteorological data have particular statistical significance, and the global temperature rises by 0.3~0.4°C every decade [34]. As a result, meteorological data from January 1, 2011, to December 31, 2020, is employed as the research data foundation.

3) This research used the Co-Kriging method to analyze the continuous spatial and temporal distribution and variation characteristics of air temperature, relative humidity, wind speed, solar radiation intensity in Qinba mountainous area. A total of 75 meteorological stations of the China Meteorological Administration in the study area were chosen, as shown in Figure 4-7. As the distribution of meteorological stations comprehensively considers the factors such as spatial distribution uniformity, topography, and altitude in the location of meteorological stations, the average distribution of meteorological stations and large station density can make the spatial interpolation results to be more accurate.

4.3. Research proposal

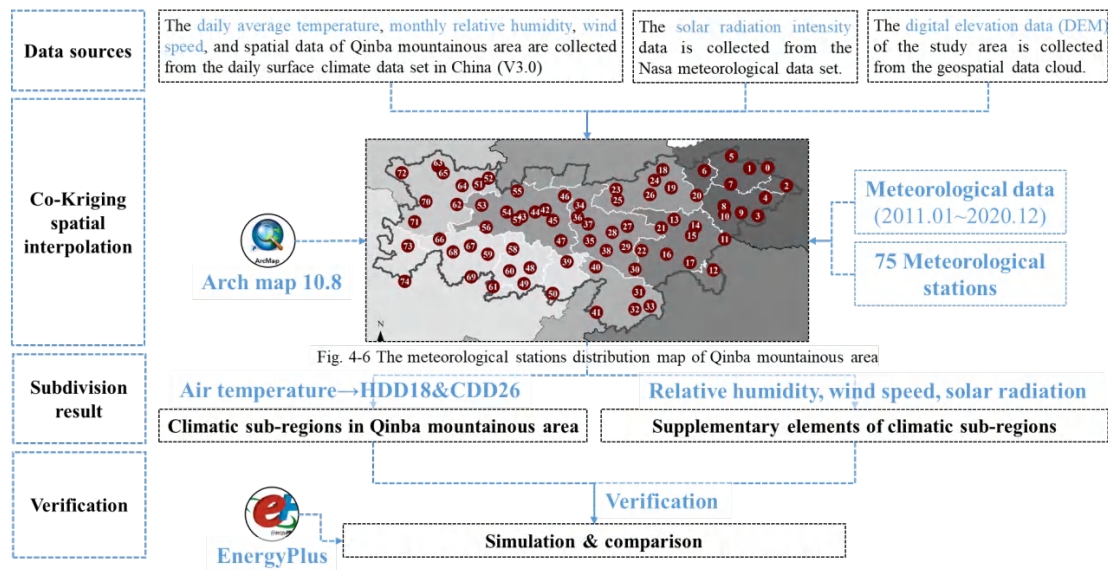


Figure 4-8. The research structure of climatic subdivision in Qinba mountainous area

Figure 4-8 shows the research structure of climatic subdivision in Qinba mountainous area. In this chapter, the research utilized Co-Kriging spatial interpolation and computer simulation methods to subdivide the Qinba mountainous area into 5 climatic sub-regions and classified the supplementary climatic elements to describe the region's climatic characteristics.

4.3.1. Climatic subdivision

As Qinba mountainous area has the climate characteristics of hot in summer and cold in winter, the outdoor temperature in winter and summer will directly affect the thermal loads in winter and summer. Therefore, the outdoor air temperature is used as the main climate index to control the scope of climate zoning. In the current specification [13], the HDD18 and the CDD26 are used as the basis for the secondary climate zoning of China's thermal regions. As a result, based on the spatial interpolation method, the values of HDD18 and CDD26 were used as the zoning indicators to subdivide the Qinba mountainous climate zone.

4.3.2. Supplementary elements of climatic sub-regions

In addition, the mean radiant temperature, affected by relative humidity, air temperature, wind speed, and solar radiation, directly influences people's actual thermal sensation. The passive strategy can improve the indoor thermal environment without consuming energy. Passive design strategies such as shading, ventilation, and additional sunspace are related to meteorological factors such as relative humidity, wind speed, and solar radiation. Understanding the other meteorological elements helps to match the appropriate passive design strategy for the building. Therefore, in addition to using HDD18 and CDD26 to subdivide the climate zone of Qinba mountainous area, we also need to analyze and summarize the

characteristic of the other meteorological elements, such as relative humidity, wind speed, and solar radiation, in each climatic sub-region.

4.3.3. Verification of climatic sub-regions

Finally, we select the typical counties in the climatic sub-regions and compare their various meteorological elements to confirm the rationality of climate subdivision scheme. In addition, we input the meteorological data of each climatic sub-region under the premise of the same benchmark building and simulate the heating and cooling energy consumption of the benchmark building, then compare the annual thermal energy consumption, heating energy consumption, and cooling energy consumption.

4.4. Results of climatic subdivision in Qinba mountainous area

4.4.1. Climatic sub-regions in Qinba mountainous area

(1) Annual average daily temperature

In this region, the daily mean air temperature of 75 meteorological stations in the Qinba mountainous area from January 1, 2011, to December 31, 2020, was accumulated and averaged, and the annual daily average temperature over the past decade was obtained, characterizing the cold and hot conditions of an area.

Due to the monsoon, global warming and many other reasons, the annual temperature in the same location also fluctuates. In order to reflect the temperature changes more objectively in the specific region, the daily temperature of 10 years is averaged to obtain the annual daily average temperature (T_{daily}). As a result, we obtained 27375 (365×75) set of air temperature data from 75 meteorological stations from January 1 to December 31.

(2) Value of HDD18 and CDD 26

stationid	name	Lat	Lon	altitude	Month	Day	T_{daily}	CDD26	stationid	name	Lat	Lon	altitude	Month	Day	T_{daily}	HDD18
57348	Fengjie	31.016667	109.533333	299.8	6	18	26.55	0.55	57348	Fengjie	31.016667	109.533333	299.8	1	1	8.49	9.51
57348	Fengjie	31.016667	109.533333	299.8	6	19	26.89	0.89	57348	Fengjie	31.016667	109.533333	299.8	1	2	8.41	9.59
57348	Fengjie	31.016667	109.533333	299.8	6	20	26.31	0.31	57348	Fengjie	31.016667	109.533333	299.8	1	3	8.04	9.96
57348	Fengjie	31.016667	109.533333	299.8	6	21	26.45	0.45	57348	Fengjie	31.016667	109.533333	299.8	1	4	7.75	10.25
57348	Fengjie	31.016667	109.533333	299.8	6	22	26.87	0.87	57348	Fengjie	31.016667	109.533333	299.8	1	5	8.19	9.81
57348	Fengjie	31.016667	109.533333	299.8	6	23	26.98	0.98	57348	Fengjie	31.016667	109.533333	299.8	1	6	8.47	9.53
57348	Fengjie	31.016667	109.533333	299.8	6	24	26.53	0.53	57348	Fengjie	31.016667	109.533333	299.8	1	7	7.85	10.15
57348	Fengjie	31.016667	109.533333	299.8	6	25	26.09	0.09	57348	Fengjie	31.016667	109.533333	299.8	1	8	7.73	10.27
57348	Fengjie	31.016667	109.533333	299.8	6	26	26.38	0.38	57348	Fengjie	31.016667	109.533333	299.8	1	9	7.88	10.12
57349	Fengjie	31.016667	109.533333	299.8	6	27	27.04	1.04	57348	Fengjie	31.016667	109.533333	299.8	1	10	7.47	10.53
57350	Fengjie	31.016667	109.533333	299.8	6	28	27.58	1.58	57348	Fengjie	31.016667	109.533333	299.8	1	11	7.62	10.38
57351	Fengjie	31.016667	109.533333	299.8	6	29	27.16	1.16	57348	Fengjie	31.016667	109.533333	299.8	1	12	7.69	10.31
57352	Fengjie	31.016667	109.533333	299.8	6	30	26.9	0.9	57348	Fengjie	31.016667	109.533333	299.8	1	13	8.31	9.69
57353	Fengjie	31.016667	109.533333	299.8	7	1	27.52	1.52	57348	Fengjie	31.016667	109.533333	299.8	1	14	8.48	9.52
57354	Fengjie	31.016667	109.533333	299.8	7	2	28.27	2.27	57348	Fengjie	31.016667	109.533333	299.8	1	15	8.54	9.46
57355	Fengjie	31.016667	109.533333	299.8	7	3	28.09	2.09	57348	Fengjie	31.016667	109.533333	299.8	1	16	8.38	9.62
57356	Fengjie	31.016667	109.533333	299.8	7	4	27.06	1.06	57348	Fengjie	31.016667	109.533333	299.8	1	17	8.65	9.35

Figure 4-9. The computational process of HDD18 and CDD26

Then, this research uses the annual daily average temperature (T_{daily}) as the input parameter, the HDD18 and CDD26 of the 75 meteorological stations are calculated. Firstly, we screened out the days with the air temperature under 18°C to calculate the value of HDD18, and the air temperature above 26°C to calculate the value of CDD26. Then, we sum the values of the daily

HDD18 and CDD26 to obtain the annual value of HDD18 and CDD26. The HDD 18 and CDD26 calculation processes are shown in Figure 4-9.

By calculation, we obtained the value of HDD18 and CDD26 of the 75 meteorological stations, shown in Table 4-1.

Table 4-1. The value of HDD18 and CDD26 at the 75 meteorological stations

No.	Name	Altitude	HDD18	CDD26	No.	Name	Altitude	HDD18	CDD26
1	Dangchuan	1753.2	1754.4	2932.77	41	Ningqiang	836.1	837.1	2203.49
2	Wudu	1079.1	1080.3	1676.5	42	Nanzheng	536.5	537.5	1814.44
3	Wenxian	1014.3	1015.5	1598.53	43	Nanjiang	579.3	580.5	1486.74
4	Pingwu	893.2	894.9	1676.5	44	Wangcang	485.7	486.9	1400.23
5	Beichuan	597.2	598.4	1439.01	45	Ziyang	503.8	505	1751.34
6	Lixian	1404.6	1405.8	2810.08	46	Shiquan	484.9	485.9	1862.51
7	Xihe	1579	1580.2	3111.48	47	Hanyin	413.1	414.3	1791.52
8	Luonan	963.4	964.2	2663.36	48	Wanyuan	674	675	1679.77
9	Luoning	408.2	408.7	2080.68	48	Zhenba	693.9	695.1	2007.94
10	Lushi	658.5	659.5	2396.22	50	Xunyang	285.5	286.5	1548.78
11	Luanchuan	742.4	743.4	2402.53	51	Ankang	290.8	291.7	1608.44
12	Ruyang	336.5	334	1990.02	52	Langao	438.5	439.5	1674.81
13	Chengxian	970	971.2	2390.72	53	Pingli	570.3	571.2	1867.06
14	Kangxian	1221.2	1222.4	2667.35	54	Zhuxi	448.2	449.6	1967.34
15	Lueyang	794.2	794.9	2020.96	55	Yunxi	317.3	318.1	1831.27
16	Huixian	930.8	932	2422.4	56	Yunyang	244.8	245.6	1688.32
17	Liangdang	961.4	962.6	2483.21	57	Baihe	322.5	323.6	1743.84
18	Mianxian	548.1	549.5	1779.88	58	Shiyan	286.5	287.3	1715.94
19	Liuba	1032.1	1033.3	2524.32	59	Zhushan	307	308.4	1659.49
20	Yangxian	468.6	470	1851.46	60	Fangxian	426.9	427.9	1898.51
21	Hanzhong	509.5	510.7	1726.96	61	Danjiangkou	133.4	134.8	1612.09
22	Chenggu	486.4	487.8	1846.03	62	Xichuan	233	234.5	1786.39
23	Xixiang	446	447.4	1864.31	63	Cangxi	459.9	460.8	1325.14
24	Foping	827.2	827.9	2203.57	64	Bazhong	417.7	419	1357.49
25	Ningshan	802.4	802	2347.32	65	Yilong	655.7	657.2	1477.41
26	Zhashui	818.2	819.4	2423.97	66	Tongjiang	482.4	483.5	1456.8
27	Shangxian	742.2	743	2260.23	67	Pingchang	364.2	365.1	1381.13
28	Zhenan	693.7	694.9	2042.52	78	Xuanhan	389.4	390.5	1308.82
29	Danfeng	639	639.8	2061.82	69	Chengkou	798.2	800	1978.78
30	Shangnan	523	523.8	2059.06	70	Yunyang	297.2	296.4	1052.53
31	Shanyang	660.2	661	2202.96	71	Zhenping	995.8	996.8	2336.98
32	Xixia	250.3	251.3	1742.35	72	Wuxi	337.8	339.8	1265.89
33	Songxian	440.7	439.7	2089.3	73	Fengjie	299.8	300.3	1014.88
34	Neixiang	221.2	222.3	1861.19	74	Wushan	606.8	607.8	1282.97
35	Lushan	145.7	146.8	2022.29	75	Baokang	327.7	329.1	1745.73
36	Zhenping	234	235	1872.28					
37	Nanzhao	231.1	230.4	1935.15					
38	Qingchuan	782	783	1933.32					
39	Guangyuan	545.4	546.4	1465.71					
40	Jiange	544.5	545.4	1503.34					

(3) Spatial distribution analysis of HDD18 and CDD 26.

By employing the temperature parameters HDD18 and CDD26 as the main variables, and the DEM data (Altitude data) as the co-variable, this study applies the Co-Kriging method to calculate the interpolation of a continuous spatial surface. Figure 4-10 and 4-11 shows the spatial distribution of HDD 18 and CDD 26.

1) Spatial distribution of HDD18

As shown in Figure 4-10, there is a significant difference in the values of HDD18, as the maximum value of HDD18 in the study area is 3111.5 °C·d, and the minimum value of HDD18 is 1014.9°C·d. Due to the influence of latitude, the value of HDD18 in the study area shows a decreasing trend from north to south, that is, the north part of the study area has a longer heating time than the south part. However, the HDD18 isoline is not parallel to the latitude line. Due to the influence of mountains, the HDD18 isoline coincides with the mountain contour lines.

According to the maximum value, minimum value, and interval range of the HDD18 in Qinba mountainous area, based on the principle of equal value distribution, the study area is divided into 3 regions. Since there are only few values of HDD18 greater than 2800°C·d, this area is classified into the area of HDD18 (2200°C·d~2800°C·d). And the three-level division of HDD18 in Qinba mountainous area is obtained, with the value range of HDD18 (1000 °C·d ~1600 °C·d), HDD18 (1600 °C·d ~2200 °C·d), and HDD18 (2200 °C·d ~3200 °C·d).

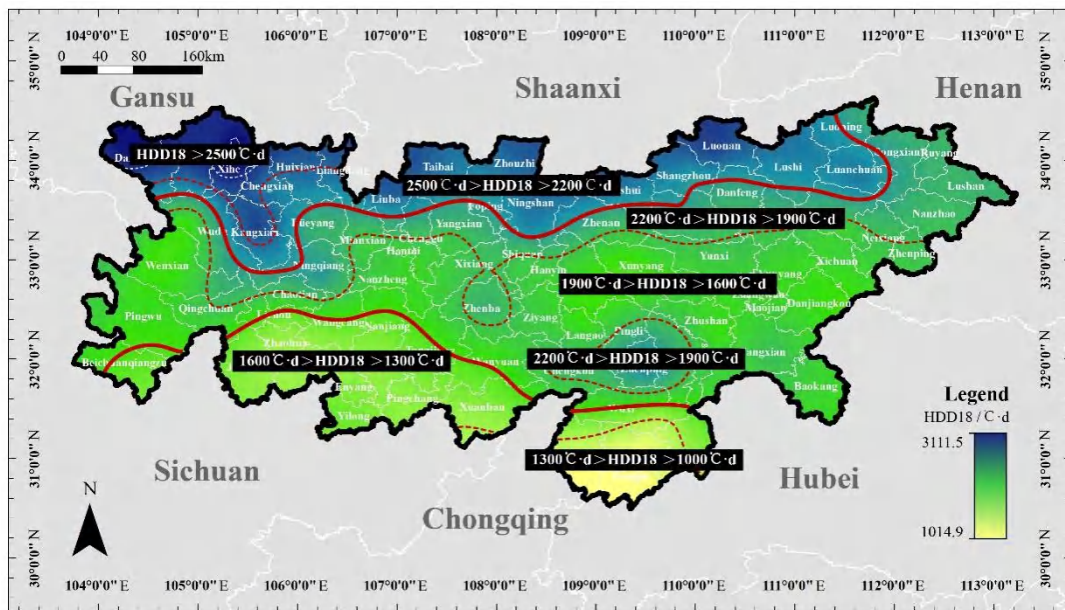


Figure 4-10. Spatial distribution of HDD18 in Qinba mountainous Area

2) Spatial distribution of CDD26

Figure 4-11 shows the spatial distribution of CDD 26. In general, the value of HDD18 in Qinba mountainous area is much larger than that of CDD26, so the energy consumption of heating in winter will be much higher than that of cooling in summer. The maximum value of CDD26 in the study area is 199.5°C·d, and the minimum value is 0°C·d. Due to the influence

of latitude, the value of CDD26 in the study area shows a increasing trend from north to south, that is, the south part of the study area has a longer cooling time than the north part. Moreover, in general, the northwest part is mostly mountainous areas with high mountains and valleys, while the southeast area is less mountainous and has a small range of valley plains. Due to the influence of terrain, the values of CDD26 in the study area show a distribution pattern of low in the northwest and high in the southeast, and the correlation between the CDD26 isoline line and the mountain contour line is not prominent.

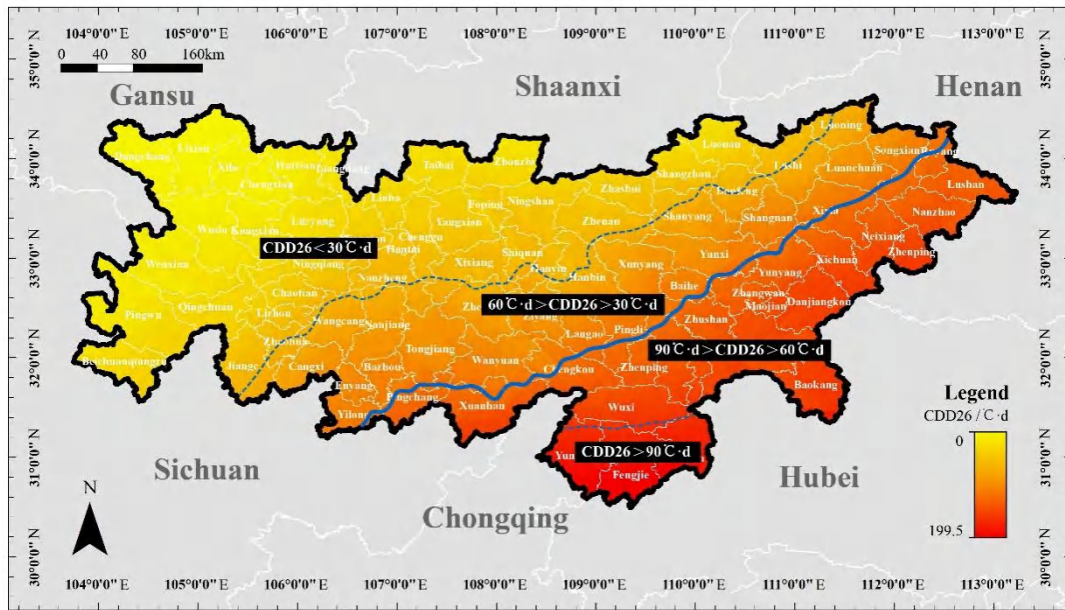


Figure 4-11. Spatial distribution of CDD26 in Qinba mountainous Area

According to the maximum value, minimum value, and interval range of the CDD26 in Qinba mountainous area, based on the principle of equal value distribution, the study area is divided into 2 regions. Since there are only few values of CDD26 greater than $120^{\circ}\text{C}\cdot\text{d}$, this area is classified into the area of HDD18 ($60^{\circ}\text{C}\cdot\text{d}\sim 120^{\circ}\text{C}\cdot\text{d}$). And the two-level division of CDD26 in Qinba mountainous area is obtained, with the value range of CDD26 ($0^{\circ}\text{C}\cdot\text{d}\sim 60^{\circ}\text{C}\cdot\text{d}$), and HDD18 ($60^{\circ}\text{C}\cdot\text{d}\sim 200^{\circ}\text{C}\cdot\text{d}$).

(4) Climate subdivision.

Through field research, we found that the residents in the study area have a much lower score on thermal comfort in winter than in summer, and the value of HDD18 is much higher than the value of CDD26. Therefore, Qinba mountainous area is divided into 3 sub-regions according to the three level of HDD18 values: Region A is the area with the lowest heating demand, and its HDD18 value range is $1000\sim 1600^{\circ}\text{C}\cdot\text{d}$; Region B is the area with moderate heating demand, and its HDD18 value range is $1600\sim 2200^{\circ}\text{C}\cdot\text{d}$; Region C is the area with the highest heating demand, and its HDD18 value range is $2200\sim 3200^{\circ}\text{C}\cdot\text{d}$. On this basis, considering the value of CDD26, the region A, B, C continue to be subdivided into region A1, B1, C with the CDD26 value below $60^{\circ}\text{C}\cdot\text{d}$, and region A2, B2 with the CDD26 value above $60^{\circ}\text{C}\cdot\text{d}$.

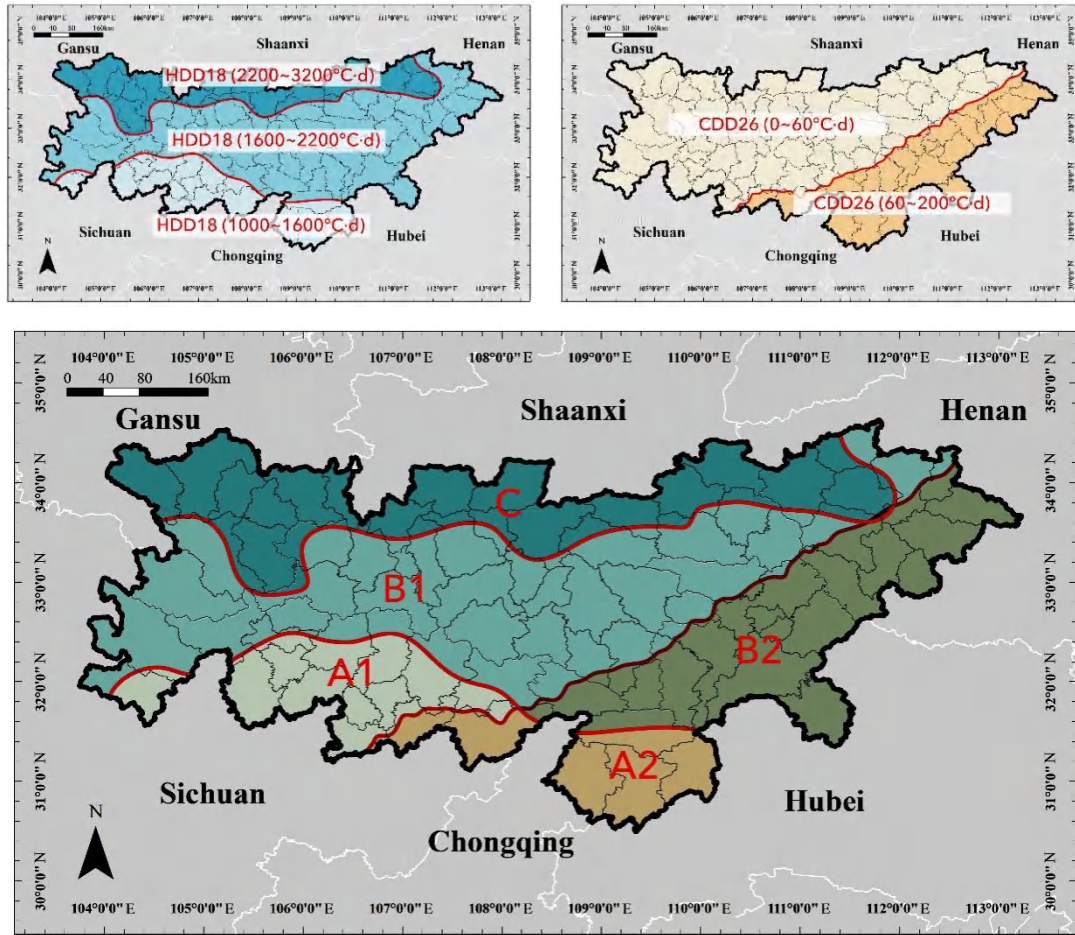


Figure 4-12. The subdivision of HDD18 CDD26

As shown in Figure 4-12, the study could use the isoline of HDD18 and CDD26 as the basis for sub-climatic zoning. Therefore, sorting by annual building thermal loads from low to high, the value ranges of HDD18 and CDD26 in each climatic sub-region are: Climatic sub-region A1 ($1000^{\circ}\text{C}\cdot\text{d} < \text{HDD18} < 1600^{\circ}\text{C}\cdot\text{d}$, $60^{\circ}\text{C}\cdot\text{d} < \text{CDD26} < 200^{\circ}\text{C}\cdot\text{d}$); Climatic sub-region A2 ($1000^{\circ}\text{C}\cdot\text{d} < \text{HDD18} < 1600^{\circ}\text{C}\cdot\text{d}$, $60^{\circ}\text{C}\cdot\text{d} < \text{CDD26} < 200^{\circ}\text{C}\cdot\text{d}$); Climatic sub-region B1 ($1600^{\circ}\text{C}\cdot\text{d} < \text{HDD18} < 2200^{\circ}\text{C}\cdot\text{d}$, $0^{\circ}\text{C}\cdot\text{d} < \text{CDD26} < 60^{\circ}\text{C}\cdot\text{d}$); Climatic sub-region B2 ($1600^{\circ}\text{C}\cdot\text{d} < \text{HDD18} < 2200^{\circ}\text{C}\cdot\text{d}$, $60^{\circ}\text{C}\cdot\text{d} < \text{CDD26} < 200^{\circ}\text{C}\cdot\text{d}$); Climatic sub-region C ($2200^{\circ}\text{C}\cdot\text{d} < \text{HDD18} < 3200^{\circ}\text{C}\cdot\text{d}$, $0^{\circ}\text{C}\cdot\text{d} < \text{CDD26} < 60^{\circ}\text{C}\cdot\text{d}$). The HDD18 and CDD values of each climatic sub-region are summarized in Table 4-2.

Table 4-2. The value ranges of HDD18 and CDD26 in each climatic sub-region

Climatic sub-region	Value of HDD18	Value of CDD26
A1	$1000^{\circ}\text{C}\cdot\text{d} < \text{HDD18} < 1600^{\circ}\text{C}\cdot\text{d}$	$0^{\circ}\text{C}\cdot\text{d} < \text{CDD26} < 60^{\circ}\text{C}\cdot\text{d}$
A2	$1000^{\circ}\text{C}\cdot\text{d} < \text{HDD18} < 1600^{\circ}\text{C}\cdot\text{d}$	$60^{\circ}\text{C}\cdot\text{d} < \text{CDD26} < 200^{\circ}\text{C}\cdot\text{d}$
B1	$1600^{\circ}\text{C}\cdot\text{d} < \text{HDD18} < 2200^{\circ}\text{C}\cdot\text{d}$	$0^{\circ}\text{C}\cdot\text{d} < \text{CDD26} < 60^{\circ}\text{C}\cdot\text{d}$
B2	$1600^{\circ}\text{C}\cdot\text{d} < \text{HDD18} < 2200^{\circ}\text{C}\cdot\text{d}$	$60^{\circ}\text{C}\cdot\text{d} < \text{CDD26} < 200^{\circ}\text{C}\cdot\text{d}$
C	$2200^{\circ}\text{C}\cdot\text{d} < \text{HDD18} < 3200^{\circ}\text{C}\cdot\text{d}$	$0^{\circ}\text{C}\cdot\text{d} < \text{CDD26} < 60^{\circ}\text{C}\cdot\text{d}$

In addition, according to the principle of spatial continuity and county zoning integrity, the zoning is further optimized to obtain the 5 climatic sub-regions of Qinba mountainous area, as shown in Figure. 4-13. Region B1 and C are cold in winter and cool in summer, having high heating demand and low cooling demand. Region B2 has relatively high heating and cooling demand. The winter temperatures of region A1 and A2 are relatively high, so the heating demand is the lowest, but region A2 has higher cooling demand than region A1.

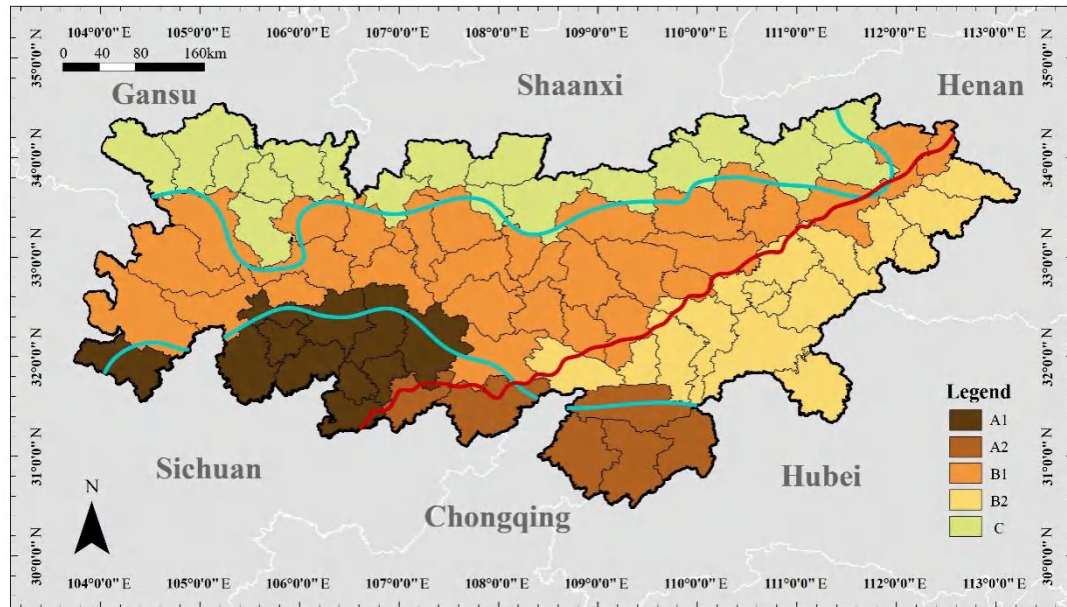


Figure 4-13. The climatic sub-regions in Qinba mountainous area

4.4.2. Supplementary elements of climatic sub-regions in Qinba mountainous area

The mean radiant temperature, affected by relative humidity, air temperature, wind speed, and solar radiation, directly influences people's actual thermal sensation. Therefore, the rational use of passive strategies such as ventilation, shading, sunspace and etc., will help to further increase the indoor thermal comfort level. In the research, the monthly average relative humidity, wind speed and total solar radiation intensity of 75 stations in Qinba mountainous area from January 2011 to December 2020 were used as the complementary elements to Supplementary explanation of climatic sub-regions.

Table 4-3. The annual mean relative humidity, wind speed and solar radiant intensity of the 75 meteorological stations

No.	Name	RH (%)	WS (m/s)	SR (MJ/m ²)	No.	Name	RH (%)	WS (m/s)	SR (MJ/m ²)
1	Dangchuan	65.63	1.25	5632.09	41	Ningqiang	79.91	1.21	4472.06
2	Wudu	54.81	1.49	5386.39	42	Nanzheng	78.79	0.99	4472.06
3	Wenxian	60.25	1.45	4672.66	43	Nanjiang	71.99	1.56	4472.06
4	Pingwu	72.63	1.06	4672.66	44	Wangcang	71.69	0.86	4472.06
5	Beichuan	76.95	1.63	4214.81	45	Ziyang	78.78	1.02	4595.36

6	Lixian	67.43	1.31	5300.71	46	Shiquan	77.27	1.29	4943.30
7	Xihe	71.00	1.50	5300.71	47	Hanyin	75.19	1.53	4595.36
8	Luonan	69.78	1.11	5234.36	48	Wanyuan	70.75	1.57	4595.36
9	Luoning	62.34	1.97	5237.28	48	Zhenba	77.06	1.25	4558.61
10	Lushi	66.18	1.65	5237.28	50	Xunyang	70.38	1.42	4718.02
11	Luanchuan	65.42	2.05	5062.86	51	Ankang	72.08	1.22	4718.02
12	Ruyang	61.25	1.67	5187.20	52	Langao	73.56	1.14	4595.36
13	Chengxian	72.36	1.06	4921.27	53	Pingli	78.39	1.69	4718.02
14	Kangxian	77.98	1.29	4921.27	54	Zhuxi	80.18	1.22	4718.02
15	Lueyang	73.47	1.85	4798.30	55	Yunxi	72.93	1.26	5032.37
16	Huixian	74.81	1.21	4798.30	56	Yunyang	70.68	1.81	5032.37
17	Liangdang	70.98	0.90	4798.30	57	Baihe	74.42	1.03	4747.54
18	Mianxian	73.68	1.26	4798.30	58	Shiyan	71.71	1.56	4747.54
19	Liuba	74.58	1.57	4798.30	59	Zhushan	74.46	0.93	4747.54
20	Yangxian	76.69	1.14	4912.13	60	Fangxian	75.88	1.38	4747.54
21	Hanzhong	75.32	1.07	4912.13	61	Danjiangkou	70.68	1.47	4743.65
22	Chenggu	77.30	1.02	4912.13	62	Xichuan	65.23	1.37	5062.86
23	Xixiang	77.98	1.23	4558.61	63	Cangxi	75.97	1.32	4222.62
24	Foping	72.24	1.29	4912.13	64	Bazhong	75.57	1.28	4263.77
25	Ningshan	80.08	0.97	4943.30	65	Yilong	76.22	1.77	4263.77
26	Zhashui	72.52	1.30	5001.59	66	Tongjiang	77.30	1.22	4268.74
27	Shangxian	66.70	2.05	5001.59	67	Pingchang	78.22	1.11	4268.74
28	Zhenan	73.00	1.37	5001.59	78	Xuanhan	78.65	1.29	4268.74
29	Danfeng	65.38	1.68	5032.37	69	Chengkou	78.23	0.96	4416.26
30	Shangnan	70.18	1.12	5032.37	70	Yunyang	75.96	1.45	4194.54
31	Shanyang	69.70	1.35	5001.59	71	Zhenping	75.58	1.99	4466.20
32	Xixia	65.10	1.77	5062.86	72	Wuxi	72.84	1.03	4466.20
33	Songxian	62.38	2.00	5187.20	73	Fengjie	69.29	1.82	4466.20
34	Neixiang	72.66	1.69	5062.86	74	Wushan	69.10	1.78	4466.20
35	Lushan	67.38	1.61	5001.59	75	Baokang	73.23	0.99	4600.84
36	Zhenping	68.43	2.23	5001.59					
37	Nanzhao	67.08	1.30	5001.59					
38	Qingchuan	76.99	1.06	4505.08					
39	Guangyuan	68.69	1.57	4505.08					
40	Jiange	72.68	1.55	4505.08					

(1) Relative humidity.

The thermal comfort of personnel is considerably influenced by relative humidity. In winter, high humidity will aggravate the cold feeling. The overall relative humidity in the study area is very high, as 93.3% of the area has a value of more than 60%, and 72% of more than 70%. Through data analysis, it can be seen that the annual average air humidity is positively correlated with the monthly average relative humidity, and the linear regression analysis shows that the correlation between the annual average relative humidity and the monthly average humidity is high. Therefore, the annual average relative humidity can be used to describe the

real humidity situation of each county in Qinba mountainous area. In this study, the average monthly relative humidity from 2011 to 2020 was used to calculate the average annual relative humidity for ten years. The annual average relative humidity of a meteorological station was analyzed by space interpolation method, and the average annual relative humidity variation trend of the study region is calculated, shown in Figure 4-14.

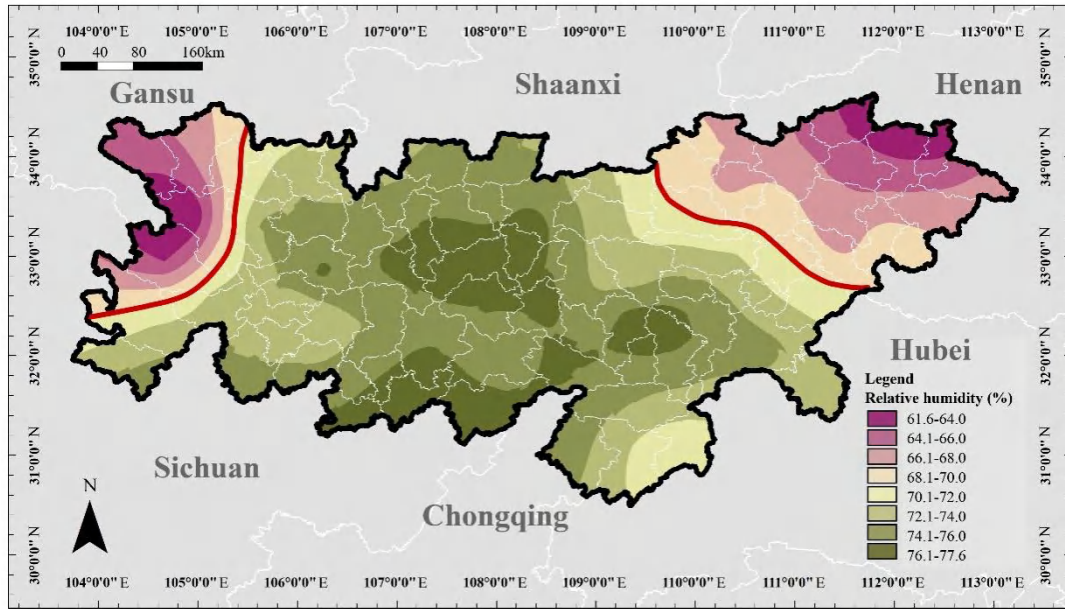


Figure 4-14. Spatial distribution of the relative humidity value in Qinba mountainous Area

According to the average annual relative humidity variation trend, the relative humidity in Qinba mountainous area is divided into two groups, showing in Table 4-4.

Table 4-4. The classification of relative humidity

Classification	H1	H2
Standard deviation	6.4	5.9
Mean relative humidity range (%)	55~70	70~80
Proportion (%)	23.5	76.5

The relative humidity of group H1 fluctuated significantly, with a standard deviation of $\sigma=6.4$, and the average relative humidity was relatively moderate, in the range of 55%~70%, accounting for 23.5% of the total sample size. The relative humidity of group H2 also fluctuated significantly, with the standard deviation $\sigma=5.9$. The average relative humidity of group H2 is high, located in the range of 70%~80%, accounting for 76.5% of the total sample size. The relative humidity partition can guide the building to use ventilation and mechanical dehumidification to improve indoor thermal comfort.

In addition, according to the principle of spatial continuity and county zoning integrity, the relative humidity zoning is further optimized, as shown in Figure 4-15.



Figure 4-15. The relative humidity subdivision in Qinba mountainous area

(2) Wind speed.

Appropriate natural ventilation can not only take away the excess moisture in the room but also enhance the indoor thermal comfort level to a certain extent. The specification defines that 0.0m/s ~ 0.2m/s as windless state; 0.3m/s ~ 1.5m/s is the soft wind state, with the smoke indicating the wind direction, and the wind vane does not rotate; 1.6m/s ~ 3.3m/s is a clear wind state, people could feel wind, and the leaves have a little noise; 3.4m/s ~ 5.4m/s is the breeze state, with branches swinging and flag stretching; 5.5m/s ~ 7.9m/s is the small wind, with the dust and paper blowing [35]. According to the wind speed in Qinba mountainous area, the windless state and soft wind state occupies most of the time, and in extreme cases, the wind speed can reach the small wind state.

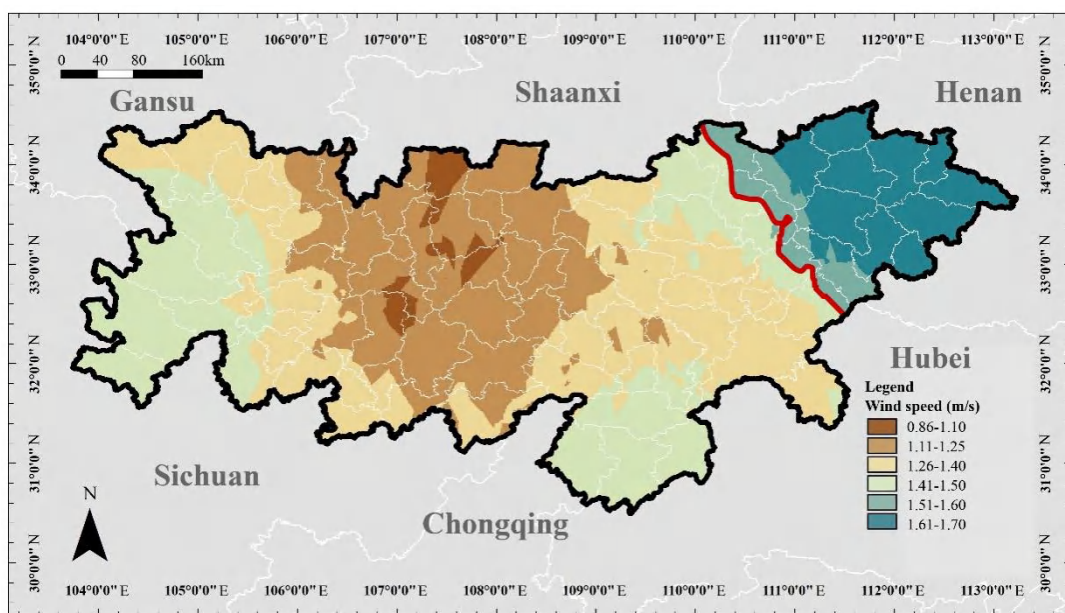


Figure 4-16. Spatial distribution of the wind speed value in Qinba mountainous Area

The wind speed in Qinba mountainous area is relatively low, at 0.8m/s~2.2m/s. Through data analysis, it can be seen that the annual average wind speed is positively correlated with the monthly average wind speed, and the linear regression analysis shows that the correlation between the annual average wind speed and monthly average wind speed is high. Therefore, the annual average wind speed can be used to describe the real wind speed situation of each county in Qinba mountainous area. In this study, the average monthly wind speed from 2011 to 2020 was used to calculate the average annual wind speed for ten years. Then, the annual average wind speed of a meteorological station was analyzed by space interpolation method, and the average annual wind speed variation trend of the study region is calculated, shown in Figure 4-16.

According to the average annual wind speed variation trend, the wind speed in Qinba mountainous area are divided into two groups, showing in Table 4-5.

The wind speed fluctuation of group W1 and W2 was not noticeable, with the standard deviation $\sigma=0.08\sim0.25$. The wind speed of group W1 was small, ranging from 0.86 to 1.49 m/s, and the average wind speed was 1.19 m/s, accounting for 85.2% of the total sample size. The average wind speed of group W2 was 1.50~2.23m/s, and the average wind speed was 1.77m/s, accounting for 14.8% of the total sample size. In general, the wind speed in the study area is low, utilizing both mechanical and natural ventilation can improve the indoor physical environment. In addition, cold air infiltration in winter will increase indoor heating energy consumption, which should be comprehensively improved by enhancing building air tightness.

In addition, according to the principle of spatial continuity and county zoning integrity, the wind speed zoning is further optimized, as shown in Figure 4-17.



Figure 4-17. The relative humidity subdivision in Qinba mountainous area

Table 4-5. The classification of wind velocity

Classification	W1	W2
Standard deviation	0.14	0.18
Mean wind velocity range (m/s)	0.86~1.49	1.53~2.23
Proportion (%)	85.2	14.8

(3) Solar radiation intensity.

Building thermal loads are mostly impacted by solar radiation intensity in the winter and summer. The annual total solar radiation resources in Qinba mountainous area is moderate deviation, with the value of 4198~5579MJ/m², which belongs to the third level of solar radiation (5016~5852 MJ/m²) and the fourth level of solar radiation (4190~5016 MJ/m²).

Through data analysis, it can be seen that the total annual solar radiation is positively correlated with the monthly average solar radiation, and the linear regression analysis shows that the correlation between these two values is high. Therefore, the total annual solar radiation can be used to describe the real solar radiation situation of each county in Qinba mountainous area. In this study, the monthly average solar radiation from 2011 to 2020 was used to calculate the total annual solar radiation for ten years. Then, the total annual solar radiation of a meteorological station was analyzed by space interpolation method, and the total annual solar radiation variation trend of the study region is calculated, shown in Figure 4-18.

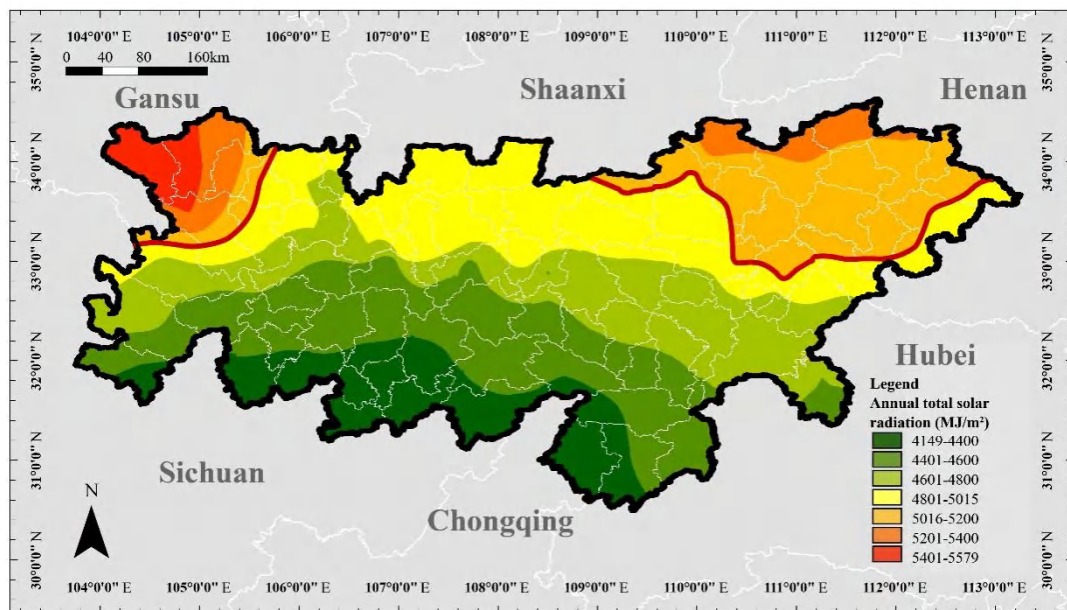


Figure 4-18. Spatial distribution of the total annual solar radiation value in Qinba mountainous Area

According to the total annual solar radiation variation trend, the wind speed in Qinba mountainous area is divided into two groups, showing in Table 4-6.

	H2W1R1	Shanyang, Chaotian, Wanyuan, Pingwu, Qingchuan, Xixiang, Zhenba, Hanyin, Ziyang, Langao, Baihe, Mianxian, Nanzheng, Hantai, Chenggu, Yangxian, Shiquan, Hanbin, Zhenan, Xunyang, Yunxi, Lueyang, Pingli
B2	H1W2R1	Zhenping
	H1W2R2	Lushan, Nanzhao, Neixiang, Xichuan
	H2W1R1	Danjiangkou, Zhuxi, Chengkou, Maojian, Zhangwan, Yunyang, Zhushan, Fangxian, Baokang, Zhenping
C	H1W1R2	Lixian, Xihe, Dangchang, Shangzhou
	H1W2R2	Luonan, Lushi, Luoning, Luanchuan
	H2W1R1	Chengxian, Kangxian, Ningqiang, Huixian, Liangdang, Taibai, Zhouzhi, Foping, Zhashui, Ningshan, Liuba

4.5. Verification of climatic sub-regions

In order to verify the rationality of the climate subdivision scheme, the daily meteorological data of the typical counties in the 5 climatic sub-regions in the Qinba mountainous area were selected to analyze the differences in meteorological characteristics. Based on these meteorological data, EnergyPlus is used to simulate the energy consumptions of the target dwelling, and the correlations between its energy consumption levels and climate zoning scheme is analyzed.

4.5.1. The climate conditions of the 5 climatic sub-regions

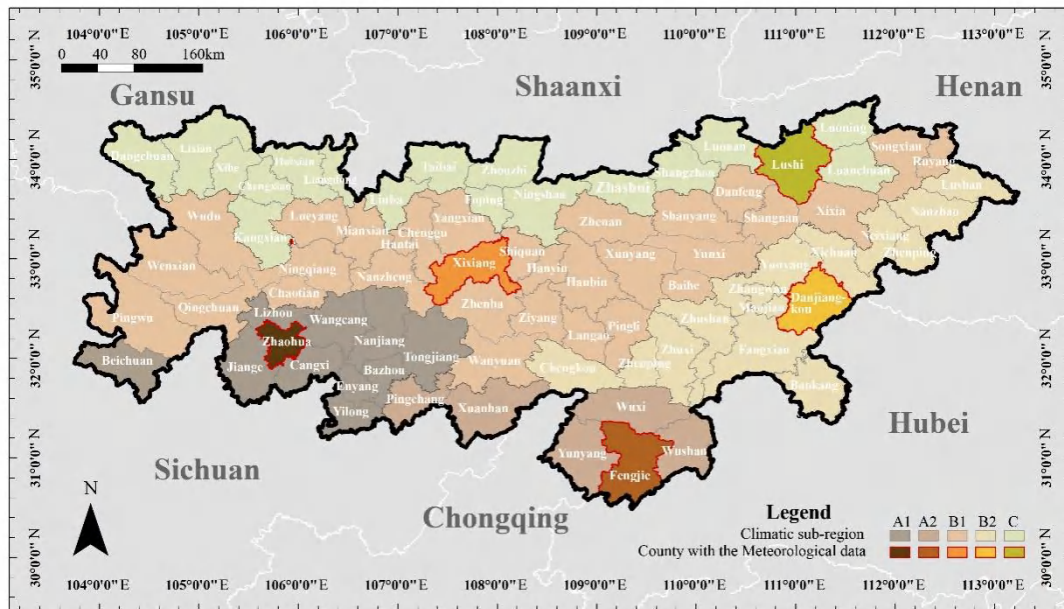


Figure 4-20. The counties with typical meteorological data in Qinba mountainous area

The selected representative counties in Qinba mountainous area include Zhaohua county (sub-region A1) in Guangyuan City, Sichuan Province, Fengjie County (sub-region A2) in Chongqing City, Xixiang County (sub-region B1) in Hanzhong City, Shaanxi Province, Danjiangkou City (sub-region B2) in Shiyan City, Hubei Province, and Lushi County (sub-

region C) in Sanmenxia City, Henan Province. The locations of these 5 counties are shown in Figure 4-20.

Although the Qinba mountainous have similar climatic characteristics, there are still differences. Firstly, the climate characteristics of the 5 typical counties are analyzed.

(1) Climatic sub-region A1 (Zhaohua County).

The daily meteorological data collected in Zhaohua County in the climatic sub-region A1 is shown in Figure 4-21.

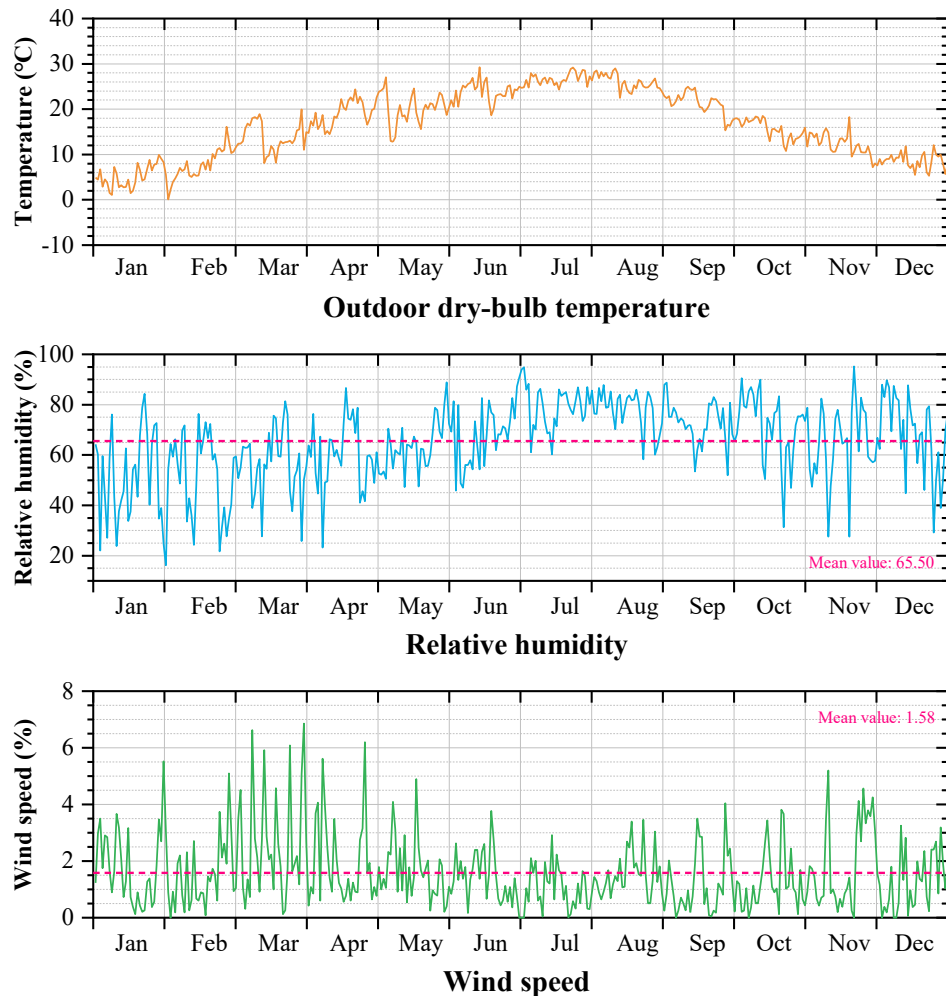


Figure 4-21. The meteorological data in climatic sub-region A1

1) Air temperature. The temperature fluctuates significantly into the 4 seasons. In winter, the mean value of air temperature is 6.76°C, the lowest air temperature is 0.08°C, and the highest air temperature is 16.08°C, which is far lower than the human comfort temperature of 18°C. In summer, the average temperature is 25.45°C, the lowest temperature is 18.62°C, and the highest temperature is 29.23°C, which basically meets the human comfort temperature range of under 26°C. In spring and fall, the mean values of air temperature are 17.47°C and 18.77°C, the minimum values are 8.12°C and 7.20°C, and the maximum values are 27.07°C and 24.96°C, respectively. The temperature fluctuates greatly in spring and fall, which can basically meet the

thermal comfort temperature of human body. But there are still some time that the air temperature is lower than the specification requirements of 18 °C.

2) Relative humidity. The average annual relative humidity in this area is large. And the relative humidity in summer and fall is relatively large, with the values of 75.09% and 69.70%, respectively, and the maximum values are as high as 94.83% and 95.16%. The relative humidity in winter and spring is relatively small, with the average values of 57.09% and 59.98%, but the maximum value is still far beyond the human comfort range, reaching 89.71% and 88.92%.

3) Wind speed. The annual dominant wind direction is northeast wind, the annual wind speed is small, with the average value of 1.58m/s. The maximum wind speed is in spring, with the mean value of 2.05m/s, and the minimum wind speed is in summer, with the value of 1.32m/s. The wind speeds in winter and fall are 1.53m/s and 1.42m/s, respectively.

(2) Climatic sub-region A2 (Fengjie County).

The daily meteorological data collected in Fengjie County in the climatic sub-region A2 is shown in Figure 4-22.

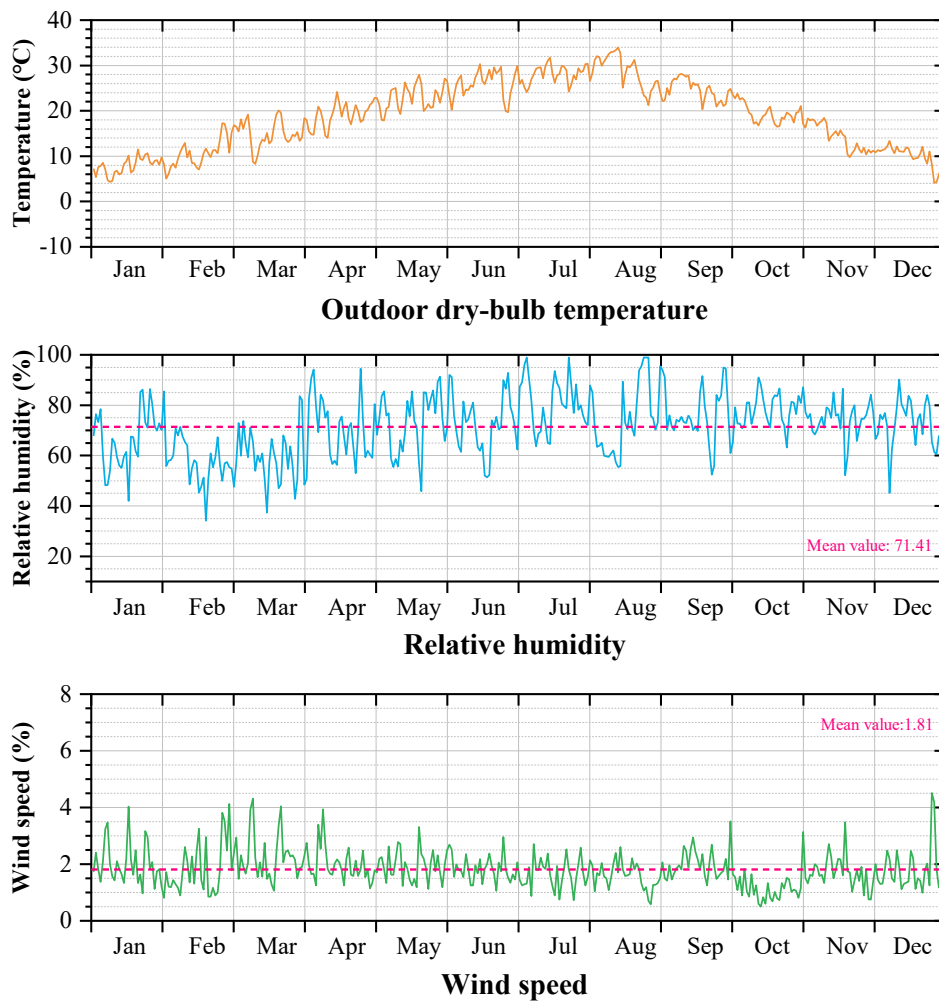


Figure 4-22. The meteorological data in climatic sub-region A2

1) Air temperature. The temperature fluctuates significantly into the 4 seasons. In winter, the mean value of air temperature is 9.36°C, the lowest air temperature is 4.14°C, and the highest air temperature is 17.25°C, which is far lower than the human comfort temperature of 18°C. In summer, the average temperature is 27.58°C, the lowest temperature is 19.72°C, and the highest temperature is 27.97°C, which is higher than the human comfort temperature range of under 26°C. In spring and fall, the mean values of air temperature are 18.87°C and 19.43°C, the minimum values are 8.29°C and 9.79°C, and the maximum values are 27.97°C and 28.12°C, respectively. The temperature fluctuates greatly in spring and fall, which can basically meet the thermal comfort temperature of human body. But there are still some time that the air temperature is lower than the specification requirements of 18 °C.

2) Relative humidity. The average annual relative humidity in this area is large, with the value of 71.41%. And the relative humidity in summer and fall is relatively large, with the values of 75.94% and 76.19%, respectively, and the maximum values are as high as 99.00% and 94.92%. The relative humidity in winter and spring is relatively small, with the average values of 65.98% and 67.48%, but the maximum value is still far beyond the human comfort range, reaching 90.16% and 94.46%.

3) Wind speed. The annual dominant wind direction is northeast wind, the annual wind speed is small, with the average value of 1.81m/s. The maximum wind speed is in spring, with the mean value of 2.05m/s, and the minimum wind speed is in fall, with the value of 1.70m/s. The wind speeds in winter and summer are 1.88m/s and 1.70m/s, respectively.

(3) Climatic sub-region B1 (Xixiang County).

The daily meteorological data collected in Xixiang County in the climatic sub-region B1 is shown in Figure 4-23.

1) Air temperature. The temperature fluctuates significantly into the 4 seasons. In winter, the mean value of air temperature is 3.08°C, the lowest air temperature is -3.86°C, and the highest air temperature is 9.16°C, which is far lower than the human comfort temperature of 18°C. In summer, the average temperature is 24.72°C, the lowest temperature is 19.09°C, and the highest temperature is 30.31°C, which basically meets the human comfort temperature range of under 26°C. In spring and fall, the mean values of air temperature are 13.98°C and 14.54°C, the minimum values are 0.02°C and -1.35°C, and the maximum values are 24.09°C and 24.90°C, respectively. The temperature fluctuates greatly in spring and fall, and there are still days that the temperatures are under the thermal comfort range of 18°C.

2) Relative humidity. The average annual relative humidity in this area is large, with the value of 70.05%. And the relative humidity in summer and fall is relatively large, with the values of 75.88% and 71.89%, respectively, and the maximum values are as high as 98.71% and 97.79%. The relative humidity in winter and spring is relatively small, with the average values of 63.37% and 68.94%, but the maximum value is still far beyond the human comfort range, reaching 97.79% and 95.46%.

3) Wind speed. The annual dominant wind direction is northeast wind, the annual wind speed is relatively large than the other places in Qinba mountainous area, with the average value of 2.54m/s. The maximum wind speed is in spring, with the mean value of 2.98m/s, and the minimum wind speed is in fall, with the value of 2.14m/s. The wind speeds in winter and summer are 2.39m/s and 2.64m/s, respectively.

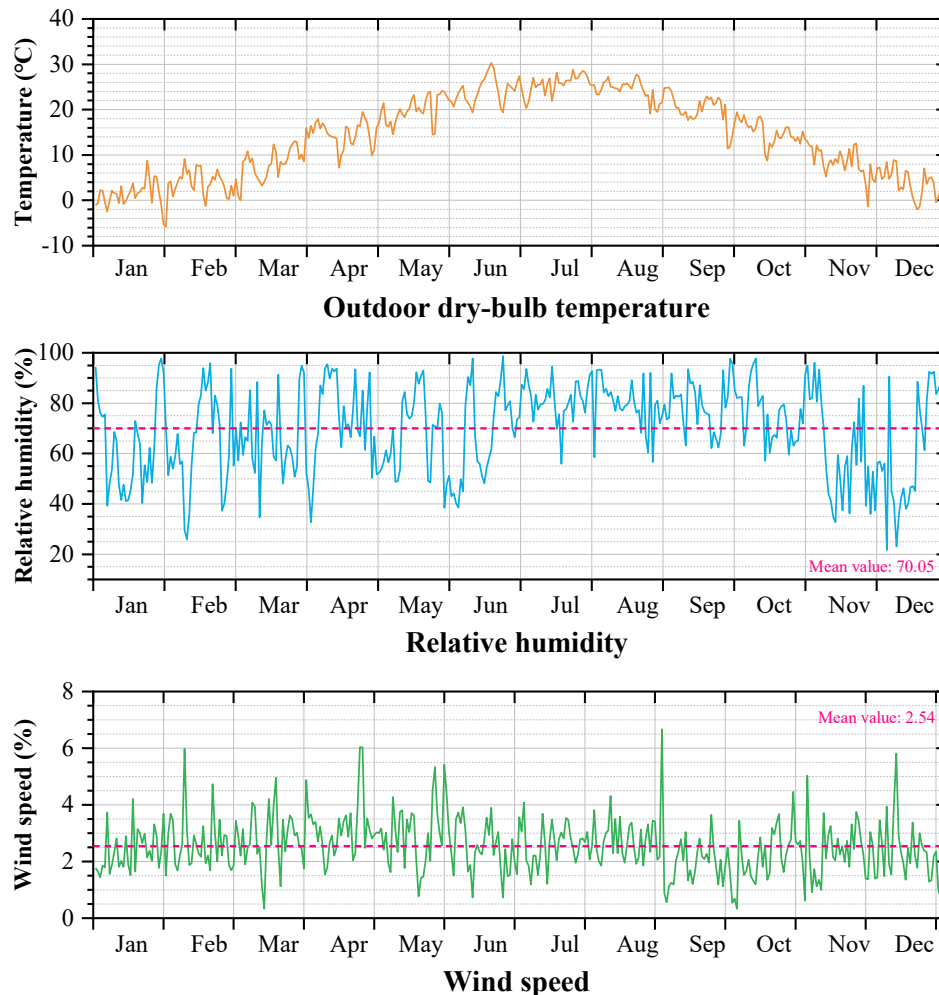


Figure 4-23. The meteorological data in climatic sub-region B1

(4) Climatic sub-region B2 (Dangjiangkou County).

The daily meteorological data collected in Dangjiangkou County in the climatic sub-region B2 is shown in Figure 4-24.

1) Air temperature. The temperature fluctuates significantly into the 4 seasons. In winter, the mean value of air temperature is 4.48°C, the lowest air temperature is -2.05°C, and the highest air temperature is 10.02°C, which is far lower than the human comfort temperature of 18°C. In summer, the average temperature is 26.37°C, the lowest temperature is 19.10°C, and the highest temperature is 31.09°C, which is higher than the human comfort temperature range of under 26°C. In spring and fall, the mean values of air temperature are 15.45°C and 16.44°C, the minimum values are -0.68°C and 2.9°C, and the maximum values are 25.94°C and 31.18°C,

respectively. The temperature fluctuates greatly in spring and fall, and there are still days that the temperatures are beyond the scope of the thermal comfort range.

2) Relative humidity. The average annual relative humidity in this area is large, with the value of 75.41%. The relative humidities in the 4 seasons are relatively average, with the mean value of 73.17%, 74.15%, 79.78%, and 74.48%, and the maximum values are as high as 95.29%, 98.08%, 96.29%, and 94.29 in winter, spring, summer, and fall, respectively.

3) Wind speed. The annual dominant wind direction is northeast wind, the annual wind speed is small, with the average value of 1.76m/s. The maximum wind speed is in spring, with the mean value of 1.93m/s, and the minimum wind speed is in fall, with the value of 1.61m/s. The wind speeds in winter and summer are 1.67m/s and 1.83m/s, respectively.

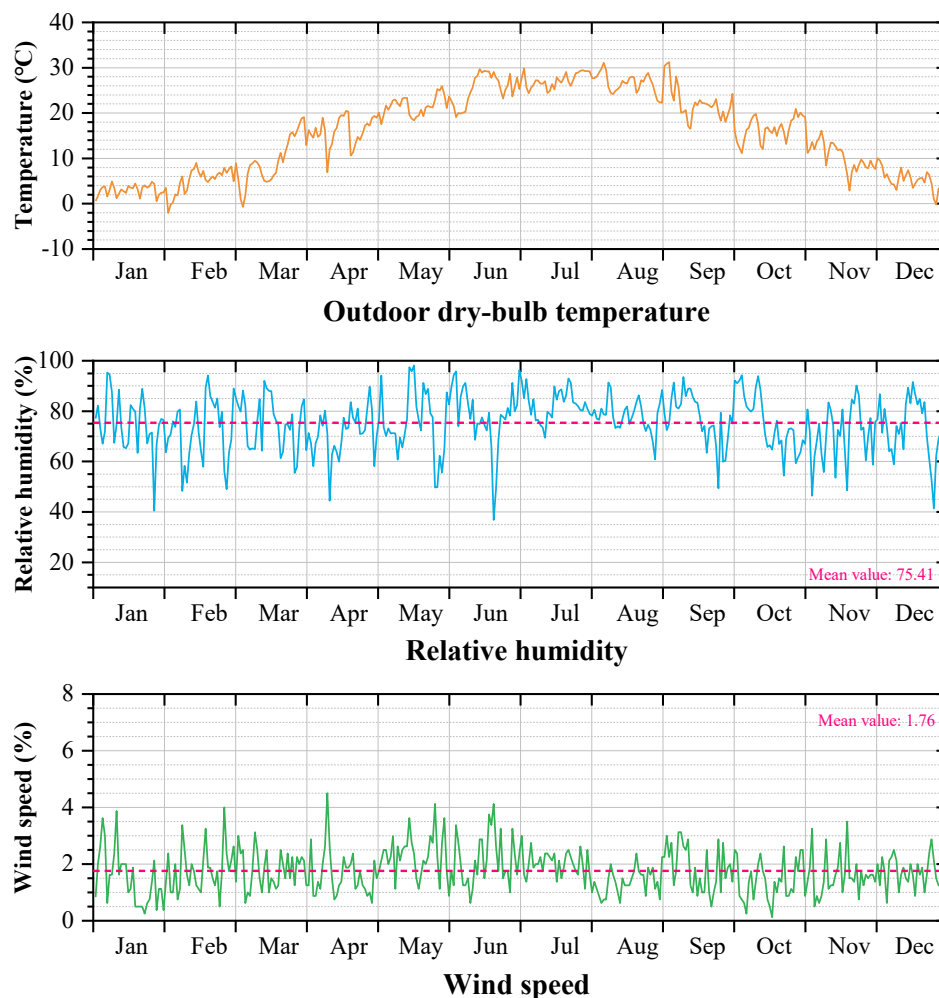


Figure 4-24. The meteorological data in climatic sub-region B2

(5) Climatic sub-region C (Lushi County).

The daily meteorological data collected in Lushi County in the climatic sub-region C is shown in Figure 4-25.

1) Air temperature. The temperature fluctuates significantly into the 4 seasons. In winter, the mean value of air temperature is 1.64°C, the lowest air temperature is -5.76°C, and the highest

air temperature is 9.37°C , which is far lower than the human comfort temperature of 18°C . In summer, the average temperature is 24.06°C , the lowest temperature is 14.61°C , and the highest temperature is 28.86°C , which basically meets the human comfort temperature range of under 26°C . In spring and fall, the mean values of air temperature are 14.15°C and 13.25°C , the minimum values are 0.45°C and 1.87°C , and the maximum values are 24.55°C and 21.88°C , respectively. The temperature fluctuates greatly in spring and fall, and there are still days that the temperatures are under the thermal comfort range of 18°C .

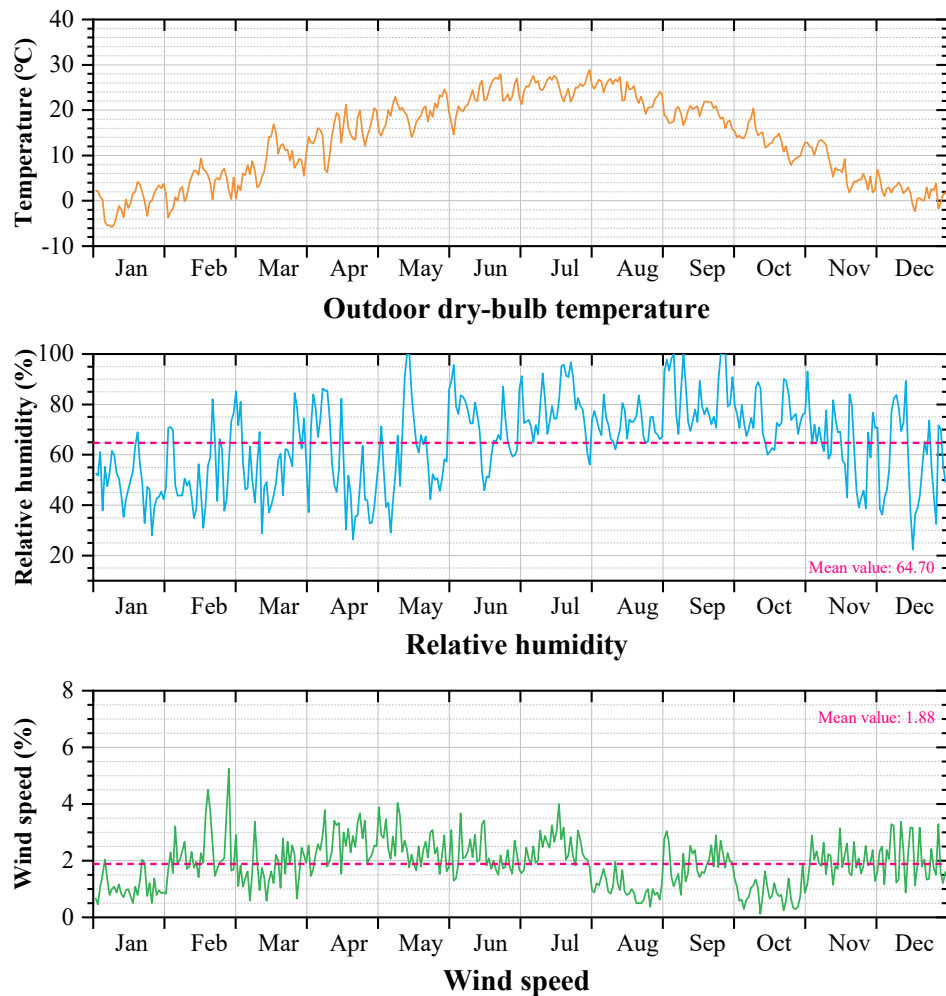


Figure 4-25. The meteorological data in climatic sub-region C

2) Relative humidity. The average annual relative humidity in this area is large, with the value of 64.70%. And the relative humidity in summer and fall is relatively large, with the values of 73.77% and 74.24%, respectively, and the maximum values are as high as 96.67% and 98.89%. The relative humidity in winter and spring is relatively small, with the average values of 55.12% and 57.99%, but the maximum value is still far beyond the human comfort range, reaching 93.13% and 98.32%.

3) Wind speed. The annual dominant wind direction is northeast wind, the annual wind speed is small, with the average value of 1.88m/s. The maximum wind speed is in spring, with

the mean value of 2.27m/s, and the minimum wind speed is in fall, with the value of 1.59m/s. The wind speeds in winter and summer are 1.81m/s and 1.86m/s, respectively.

(6) Comparison of meteorological data

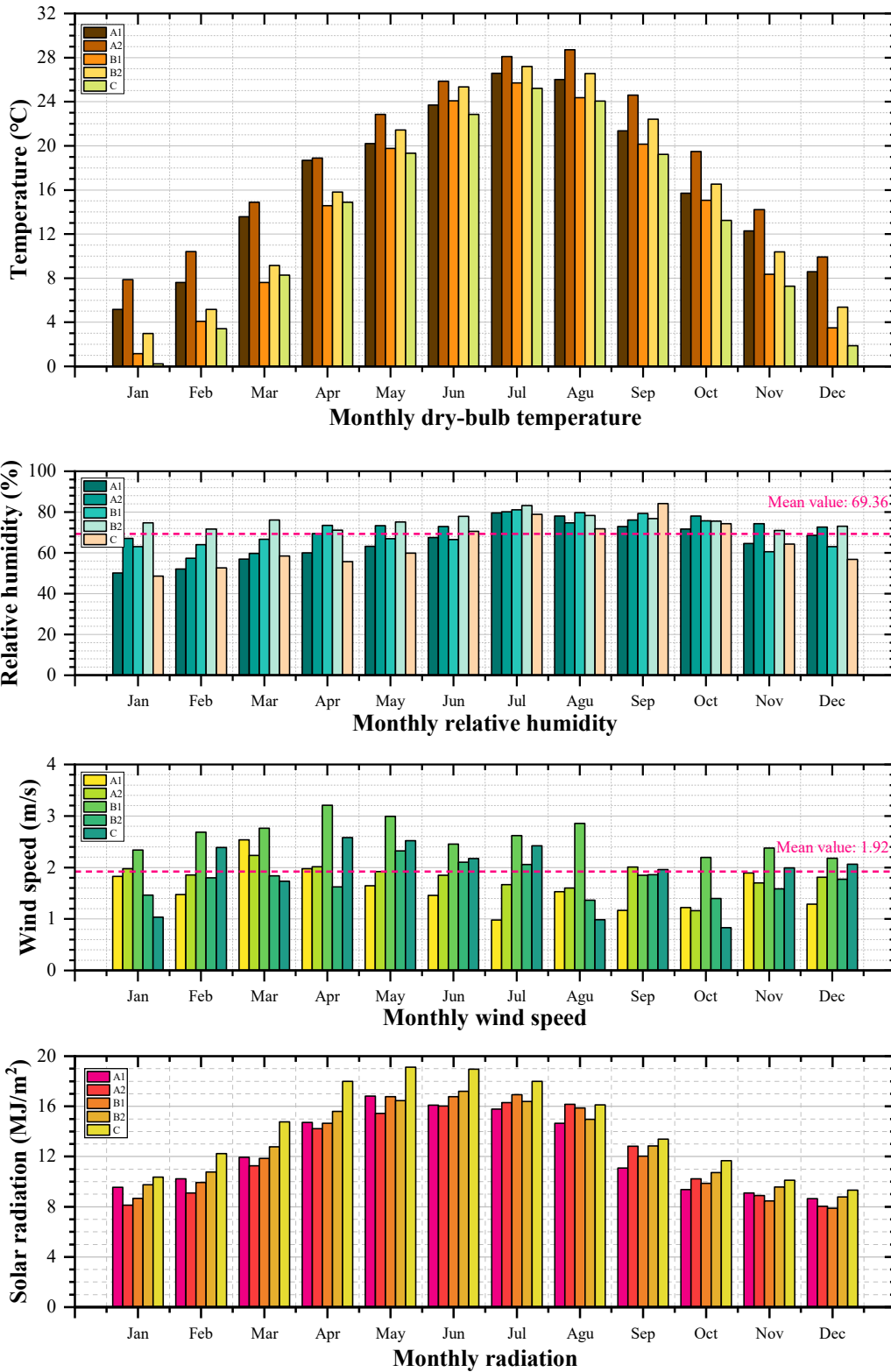


Figure 4-26. The monthly meteorological data in 5 climatic sub-regions

Comparing the monthly meteorological data of the 5 representative counties, the law of meteorological characteristics can be more clearly found. Figure 4-16 shows the monthly air temperature, relative humidity, and wind speed of the 5 representative counties. And Table 4-8, 4-9, 4-10, and 4-11 shows the seasonal analysis of the air temperature, relative humidity, wind speed, and solar radiation of the 5 representative counties.

1) Air temperature. As we can see from meteorological data analysis of each climatic sub-region, the building is mainly heated in the whole winter and part of the spring and fall, and mainly cooled in summer. From Figure 4-26 and Table 4-8, the mean air temperatures are 17.47°C, 18.87°C, 13.98°C, 15.46°C, 14.15°C in spring, 18.77°C, 19.43°C, 14.54°C, 16.44°C, and 13.25°C in fall, 7.67°C, 9.36°C, 3.08°C, 4.48°C, 1.64°C in winter, respectively. In winter, spring and fall, the average temperatures in sub-region A1 and A2 are much higher than that in other regions, and the temperatures in sub-region B1 and B2 is higher than that in sub-region C. This can be inferred that for the value of HDD18, sub-region C is the highest, followed by sub-region B1, B2, and sub-region A1, A2 are the lowest. Moreover, in summer, the air temperatures in A1 and B2 are higher than that in sub-region A1, B1 and C, indicating that the value of CDD26 of sub-region A2 and B2 in summer are higher than that in sub-region A1, B1 and C. As a result, the change law of air temperatures in the 5 representative counties in each climatic sub-regions conform to the climate subdivision logic of Qinba mountainous area.

Table 4-8. The seasonal air temperature analysis

Sub-region	Air temperature (°C)											
	Spring			Summer			Fall			Winter		
	T _{mean}	T _{min}	T _{max}	T _{mean}	T _{min}	T _{max}	T _{mean}	T _{min}	T _{max}	T _{mean}	T _{min}	T _{max}
A1	17.47	8.12	27.07	25.45	18.62	29.23	18.77	7.02	24.96	7.67	0.08	16.08
A2	18.87	8.29	27.97	27.58	19.72	33.94	19.43	9.79	28.12	9.36	4.15	17.25
B1	13.98	0.02	24.09	24.72	19.09	30.31	14.54	-1.35	24.90	3.08	-3.86	9.16
B2	15.46	-0.68	25.94	26.37	19.1	31.09	16.44	2.90	31.18	4.48	-2.05	10.02
C	14.15	0.45	24.55	24.06	14.61	28.86	13.25	1.88	21.88	1.64	-5.76	9.37

Although the climate subdivision of Qinba mountainous area is mainly based on the value of HDD18 and CDD26, which are closely related to air temperature, it is still necessary to study the seasonal variation of relative humidity and wind speed to better match the passive design parameters on residential buildings.

2) Relative humidity. As we can see from Figure 4-26 and Table 4-9, the average annual relative humidity in the study area is large, with the mean value of 69.36%. The relative humidity of each climate zone shows a certain variation with the seasons. The relative humidity summer and fall (from July to October) is relatively large, with the mean value of 75.09%, 75.49%, 75.88%, 79.79%, 73.77% in the 5 sub-regions in summer, and 69.70%, 76.19%, 71.89%, 74.48%, 74.24% in the 5 sub-regions in winter, respectively. And the relative

humidity in winter (in January and February) is relatively small, with the mean value of 57.09, 65.98, 63.37, 73.17, 55.12 in the 5 sub-regions respectively. However, the variation trend of relative humidity in each climatic sub-region is not obvious, which also proves the need for climate supplementary elements to define other meteorological parameters such as relative humidity.

Table 4-9. The seasonal relative humidity analysis

Sub-region	Relative Humidity (%)											
	Spring			Summer			Fall			Winter		
	H _{mean}	H _{min}	H _{max}	H _{mean}	H _{min}	H _{max}	H _{mean}	H _{min}	H _{max}	H _{mean}	H _{min}	H _{max}
A1	59.98	23.25	88.92	75.09	45.83	94.83	69.70	27.54	95.17	57.09	16.25	89.71
A2	67.48	37.89	94.46	75.94	51.38	99.00	76.19	52.17	94.92	65.98	34.08	90.17
B1	68.94	32.75	95.46	75.88	38.58	98.71	71.89	32.79	97.79	63.37	21.71	97.79
B2	74.15	44.5	98.08	79.79	36.88	96.29	74.48	46.46	94.29	73.17	40.5	95.29
C	57.99	26.42	98.32	73.77	45.83	96.67	74.24	38.71	98.89	55.12	28.04	93.13

3) Wind speed. In the study area, the annual dominant wind direction is northeast wind. From Figure 4-26 and Table 4-10, the annual wind speed is small, with the average value of 1.92m/s. The maximum wind speed is in spring (from March to May), with the mean value of 2.05m/s, 2.05m/s, 2.98m/s, 1.93m/s, and 1.81m/s in the 5 sub-region, respectively. There is no obvious seasonal variation of wind speed in other seasons. The summer wind speeds are 1.32 m/s, 1.70 m/s, 2.64 m/s, 1.84 m/s, 2.27m/s in the 5 sub-regions; the fall wind speeds area 1.42 m/s, 1.62 m/s, 2.14 m/s, 1.61 m/s, 1.86m/s in the 5 sub-regions; the winter wind speeds are 1.53 m/s, 1.88 m/s, 2.39 m/s, 1.67 m/s, and 1.59 m/s in the 5 sub-regions, respectively. And the variation trend of wind speed in each climatic sub-region is not obvious, which also proves the need for climate supplementary elements to define other meteorological parameters such as wind speed.

Table 4-10. The seasonal wind speed analysis

Sub-region	Wind speed (m/s)											
	Spring			Summer			Fall			Winter		
	W _{mean}	W _{min}	W _{max}	W _{mean}	W _{min}	W _{max}	W _{mean}	W _{min}	W _{max}	W _{mean}	W _{min}	W _{max}
A1	2.05	0.13	6.86	1.32	0	3.77	1.42	0	5.20	1.53	0	5.51
A2	2.05	1.06	4.31	1.70	0.58	2.96	1.62	0.5	3.51	1.88	0.82	4.51
B1	2.98	0.33	6.04	2.64	0.73	6.66	2.14	0.33	5.03	2.39	0.56	5.98
B2	1.93	0.63	4.50	1.84	0.63	4.13	1.61	0.13	3.50	1.67	0.25	4.00
C	1.81	0.46	5.25	2.27	0.58	4.04	1.86	0.38	4.00	1.59	0.13	3.15

Although the wind speed in the 4 seasons is not much different, the wind in summer takes away the excess temperature and humidity from the room, and the wind in spring, fall and

winter will cause the indoor heat loss due to the infiltration of cold wind. Therefore, in the passive design of residential buildings, the strategy of increasing air tightness and ventilation should be reasonably used to improve indoor thermal comfort.

4) Solar radiation. From Figure 4-26 and Table 4-11, the variation trend of solar radiation is similar to that of air temperature. The maximum solar radiation is in summer (from June to August), with the mean value of 15.50 MJ/m², 16.16 MJ/m², 16.52 MJ/m², 16.19 MJ/m², and 17.70 MJ/m² in the 5 sub-regions, respectively. The minimum solar radiation is in winter (from December to February), with the mean value of 9.47 MJ/m², 8.42 MJ/m², 8.83 MJ/m², 9.77 MJ/m², and 10.64 MJ/m², respectively. The solar radiations are 14.50 MJ/m², 13.64 MJ/m², 14.42 MJ/m², 14.94 MJ/m², and 17.29 MJ/m² in spring, and 9.85 MJ/m², 10.64 MJ/m², 10.12 MJ/m², 11.05 MJ/m², and 11.72 MJ/m² in fall in the 5 climatic sub-regions, respectively.

Although the amount of solar radiation is related to the variation of air temperature, it has no obvious relationship with the subdivision logic of climatic sub-regions in Qinba mountainous area. For example, the sub-region C with the highest HDD18 value and the lowest CDD26 value has the highest solar radiation. And the sub-region A2 with the lowest HDD18 value and highest CDD26 value has a relatively low solar radiation. This shows that the solar radiation is not proportional to the air temperature, and there is a complex coupling relationship between them. As a result, the solar radiation changes obviously with the seasons. We should reasonably use the solar radiation in winter, spring and fall to heat the indoor air temperature, improve the indoor thermal comfort, and adopt appropriate measures to prevent excess heat from entering the room in summer.

Table 4-11. The seasonal solar radiation analysis

Sub-region	Solar radiation (MJ/m ²)			
	Spring R _{mean}	Summer R _{mean}	Fall R _{mean}	Winter R _{mean}
A1	14.50	15.50	9.85	9.47
A2	13.64	16.16	10.64	8.42
B1	14.42	16.52	10.12	8.83
B2	14.94	16.19	11.05	9.77
C	17.29	17.70	11.72	10.64

4.5.2. Building energy simulation in each climatic sub-region

(1) Setting of simulation model.

In order to simulate the annual building thermal loads in each sub-climate region, the research team applies the annual meteorological data of the 5 representative counties and uses EnergyPlus as the engine to simulate the thermal energy consumption of the target dwelling, so as to compare the energy consumption level of the climatic sub-regions.

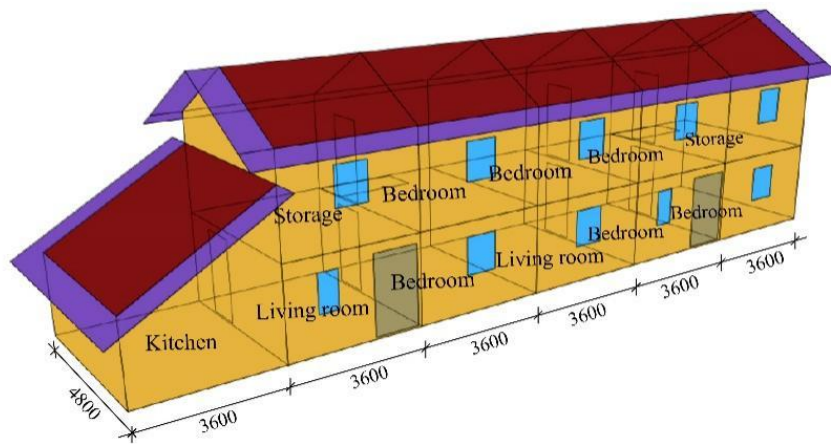


Figure 4-27. The traditional dwelling for simulation

Since the urbanization rate of Qinba mountainous area is only 30.6 %, most of the buildings in this area are still rural residential buildings. Therefore, the “I” shape residential building was chosen as the target object for energy consumption simulation, showed in Figure 4-27.

Table 4-12. The parameters of the simulated model in EnergyPlus

Parameters		Values
Heat transfer coefficient of enclosure structure	Exterior wall heat transfer coefficient	0.8 W/(m ² ·K)
	Roof heat transfer coefficient	0.6 W/(m ² ·K)
	Window heat transfer coefficient	2.2 W/(m ² ·K)
South window-wall ratio	-	0.1
Air change rate	-	1.0 h ⁻¹
Indoor comfort range	Only heat or cool the main use room	Keep the indoor thermal environment at 18~26°C during personnel in the indoor time period
Per capita building area of diverse types of rooms	Main use room	25 m ² /person
	Auxiliary room (Kitchen, toilet, storage)	5 m ² /person
Personnel in the indoor time period	Living room	7:00~22:00
	Bedroom	21:00~8:00
	Auxiliary room	7:00~8:00, 11:00~12:00, 18:00~19: 00
Personnel heat dissipation rate	Living room (sitting posture)	125.60 W/person
	Bedroom (lying posture)	83.74 W/person
	Auxiliary room (moderate labor)	209.34 W/person
Power density of illuminance	-	5 W/m ²

In order to compare the energy consumption differences of the unified reference building in each climatic sub-region, the thermal parameters of the reference building in this study are set according to the General Specification for Building Energy Efficiency and Renewable Energy Utilization[36]. The personnel heat dissipation is set according to the Evaluation Standard for Indoor Thermal and Humid Environment of Civil Buildings[37]. The simulation model parameters are set as shown in Table 4-12.

(2) Simulation result

The total annual thermal, heating, and cooling load of the typical dwelling in each sub-region are illustrated in Table 4-13 and Figure 4-28.

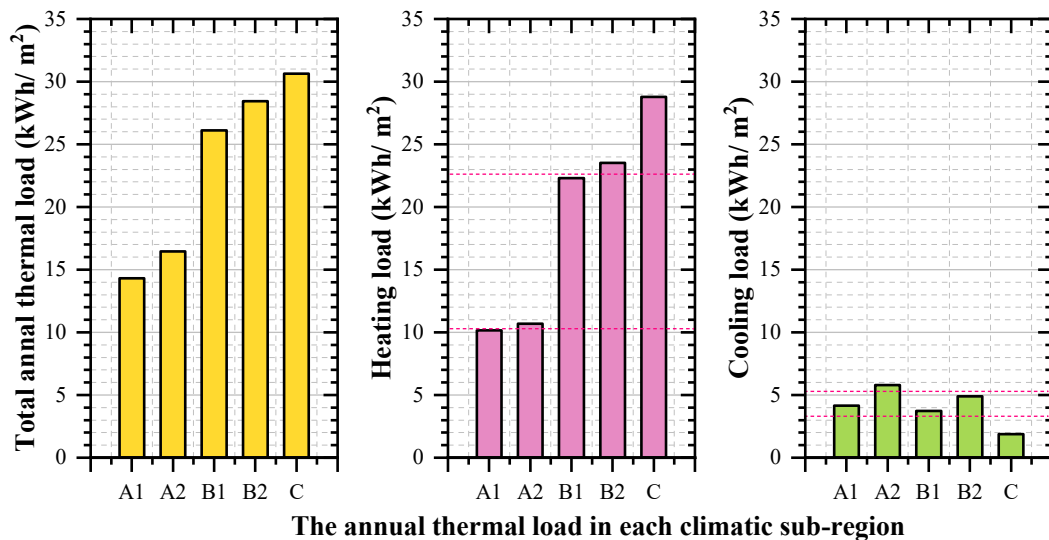


Figure 4-28. The traditional dwelling for simulation

According to the annual heating loads, A1 and A2 were the lowest, at 10.15 kWh/m² and 10.68 kWh/m², followed by B1 and B2 at 22.29 kWh/m² and 23.53 kWh/m², which are 119.9% higher than group A. Region C's annual heating energy consumption is the highest, reaching 28.77 kWh/m², 176.2% higher than group A. The annual heating loads shows a rising trend from sub-region A1, A2, to sub-region B1, B2, finally to sub-region C.

According to the annual cooling energy consumption, the A2 and B2 were 5.79 kWh/m² and 4.90 kWh/m², which were 64.5% higher than that of A1, B1, C of 4.16 kWh/m², 3.74 kWh/m², and 1.87 kWh/m². The annual cooling loads shows a rising trend from sub-region B1, B2, C to sub-region A1, A2.

According to the annual thermal loads, it shows an upward trend from region A1 to C, with the value of 14.31 kWh/m², 16.46 kWh/m², 26.11 kWh/m², 28.43 kWh/m², and 30.64 kWh/m², respectively. The simulation results are consistent with the climatic sub-regions' expected energy consumption level.

The standard deviations of total annual thermal, heating, and cooling loads are 7.34, 8.28, and 1.47, indicating that the total annual thermal load, heating load, and cooling load of the target buildings in climatic sub-regions differ a lot.

Table 4-13. The parameters of the simulated model in EnergyPlus

Sub-region	County	Total annal thermal load kWh/ m ²	Heating load kWh/ m ²	Cooling load kWh/ m ²
A1	Guangyuan	14.31	10.15	4.16
A2	Fengjie	16.46	10.68	5.79
B1	Shangnan	26.11	22.29	3.74
B2	Danjiangkou	28.43	23.53	4.90
C	Lushi	30.64	28.77	1.87
Mean value		23.19	19.08	4.09
Standard deviation		7.34	8.28	1.47

As a result, using the same design standards in the hot summer and cold winter region is not conducive to matching the energy-saving technologies and reducing the building energy consumption.

4.6. Summary

In this section, the Qinba mountainous area are subdivided into 5 climatic sub-regions, and the climatic supplementary elements are also classified to describe the climatic characteristics of the region. The main conclusions of this chapter are as follows:

(1) Qinba mountainous region situated at the center of China, with a total area of about 225,000 km², which is 60% of the land area of Japan. However, the Qinba mountainous area and the area around it both belongs to the hot summer and cold winter zone in Chian. its 18 million square kilometer area are both hot in summer and cold in winter, which are totally 1,800,000 km². Although Qinba mountainous area has very different climatic characteristics, the architecture design code and human thermal comfort standard is the same, the specifications precision are low.

(2) The meteorological data of Qinba mountainous area from 2011 to 2020 were collected to refine climatic sub-regions of this area. By using the Co-Kriging method and statistics method, 5 climatic sub-regions of the Qinba mountainous area were divided based on the value of HDD18 and CDD26. And the value ranges of HDD18 and CDD26 in each climatic sub-region are: Climatic sub-region A1 (1000°C·d < HDD18 < 1600°C·d, 60°C·d < CDD26 < 200°C·d); Climatic sub-region A2 (1000°C·d < HDD18 < 1600°C·d, 60°C·d < CDD26 < 200°C·d); Climatic sub-region B1 (1600°C·d < HDD18 < 2200°C·d, 0°C·d < CDD26 < 60°C·d); Climatic sub-region B2 (1600°C·d < HDD18 < 2200°C·d, 60°C·d < CDD26 < 200°C·d); Climatic sub-region C (2200°C·d < HDD18 < 3200°C·d, 0°C·d < CDD26 < 60°C·d).

(3) In addition, by using Co-Kriging method and statistics method, the 5 climatic sub-regions were added the supplementary meteorological information such as relative humidity, wind speed, and solar radiation. The temperature characteristics affect the energy consumption demand of heating and cooling. Furthermore, the supplementary meteorological elements provide guidance for the passive design strategy in sub-regions. This research could provide a basis for the selection of passive strategies.

(4) In order to evaluate the validity of the climate subdivision scheme, we select 5 representative counties in each of the climatic sub-region in Qinba mountainous area and make comparative analysis of their meteorological data. The result shows that the change law of air temperatures in the 5 representative counties in each climatic sub-regions conform to the climate subdivision logic of Qinba mountainous area.

(5) The total annual thermal, heating, and cooling load of the typical dwelling in each sub-region are illustrated an upward trend from region A1 to C. The annual heating energy consumption shows the largest in sub-region C, followed by sub-region B1, B2, and the smallest in sub-region A1, A2. The annual cooling energy consumptions in sub-region A2 and B2 are higher than that in sub-region A1, B1 and C. The simulation results are consistent with the climatic sub-regions' expected energy consumption level, indicating that using the same design standards in the hot summer and cold winter region is not conducive to matching the energy-saving technologies and reducing the building energy consumption.

Reference

- [1] J. Xi, "Address at the General Debate of the seventy-fifth Session of the United Nations General Assembly," in *People's Daily*, ed. Beijing, China: People's Daily Press, 2020.
- [2] Y. Elaouzy and A. El Fadar, "Energy, economic and environmental benefits of integrating passive design strategies into buildings: A review," *Renewable and Sustainable Energy Reviews* vol. 167, p. 112828, 2022.
- [3] M. Hu, K. Zhang, Q. Nguyen, and T. Tasdizen, "The effects of passive design on indoor thermal comfort and energy savings for residential buildings in hot climates: A systematic review," *Urban Climate*, vol. 49, p. 101466, 2023.
- [4] X. Gong, Y. Akashi, and D. Sumiyoshi, "Optimization of passive design measures for residential buildings in different Chinese areas," *Building and Environment*, vol. 58, pp. 46-57, Dec 2012.
- [5] S. Liu, Y. T. Kwok, K. K.-L. Lau, W. Ouyang, and E. Ng, "Effectiveness of passive design strategies in responding to future climate change for residential buildings in hot and humid Hong Kong," *Energy and Buildings*, vol. 228, p. 110469, 2020.
- [6] L. Bai, L. Yang, B. Song, and N. Liu, "A new approach to develop a climate classification for building energy efficiency addressing Chinese climate characteristics," *Energy*, vol. 195, p. 116982, 2020.
- [7] ASHRAE/IESNA, "ASHRAE/IES Standard 90.1–1989 Energy Efficient Design of New Buildings Except Low-rise Residential Buildings," ed: ASHRAE Atlanta, GA, 1989.
- [8] Thermal Environmental Conditions for Human Occupancy: ANSI/ASHRAE Standard 55-2017 (Supersedes ANSI/ASHRAE Standard 55-2013) Includes ANSI/ASHRAE Addenda Listed in Appendix N, 2017.
- [9] National Construction Code NCC 2016 Building Code of Australia—Volume One (BCA), 2016.
- [10] J. Yuan, C. Farnham, K. Emura, and Buildings, "Optimal combination of thermal resistance of insulation materials and primary fuel sources for six climate zones of Japan," *Energy and Buildings*, vol. 153, pp. 403-411, 2017.
- [11] "Nation House Energy Rating Scheme - Climate Zone Map (accessed March 16, 2017)," ed: Department of the Environment and Energy, 2012.
- [12] C. e. commission, "Building climate zones," in *California energy maps*, ed: California energy commission, 2020.
- [13] Thermal design code for civil building (GB 50176-2016), 2016.
- [14] Design standard for energy efficiency of residential buildings in hot summer and cold winter zone (JGJ 134-2010), 2010.
- [15] B. Jing, "Research on evolution pattern and spatial management and control of man-land system in Qinba mountainous area," Ph.D. Thesis, Northwest University, 2020.

[16] Y. Zhang, Y. He, Y. Li, and L. Jia, "Spatiotemporal variation and driving forces of NDVI from 1982 to 2015 in the Qinba Mountains, China," *Environmental Science and Pollution Research*, vol. 29, no. 34, pp. 52277-52288, 2022.

[17] S. Chen, M. S. Mehmood, S. Liu, and Y. Gao, "Spatial Pattern and Influencing Factors of Rural Settlements in Qinba Mountains, Shaanxi Province, China," *Sustainability*, vol. 14, no. 16, p. 10095, 2022.

[18] D. xu et al., "The green & circular development strategy of the Qinba Mountain Area," *Engineering Sciences*, vol. 18, no. 05, pp. 1-9, 2016.

[19] J. Zhang, J. WU, G. Qin, J. Feng, and W. Zhao, "Spatio-temporal dynamics of surface solar radiation and agroclimatic zoning in the Qinling-Bashan Mountains," *Scientia Geographica Sinica*, vol. 40, no. 10, pp. 1742-1752, 2020.

[20] Y. Gao, "Research on Suitable Ecological Construction Modes of Rural Residence in Hot-humid and Cold-wet Mountain Area in Western of China," Ph.D. Thesis, Xi'an University of Architecture and Technology, 2014.

[21] J. Xu and X. Huo, "Study on strategy of inheritance and development of traditional building in Qinba mountains region," *Industrial Construction*, vol. 44, no. 09, pp. 40-44, 2014.

[22] Y. Zhang and C. Liang, "Analysis of annual and seasonal precipitation variation in the Qinba Mountain area, China," *Scientific Reports*, vol. 10, no. 1, p. 961, 2020.

[23] Y. Gao, M. Wang, and J. Liu, "The preliminary investigation on the green building modes of the traditional residences in Qinba Mountain Area," *Architecture & Culture*, vol. No.115, no. 10, pp. 65-67, 2013.

[24] T. Zhang et al., "Towards Improving Rural Living Environment for Chinese Cold Region Based on Investigation of Thermal Environment and Space Usage Status," *Buildings*, vol. 12, no. 12, p. 2139, 2022.

[25] J. Liu and L. Yang, "Thermal design of a zero energy cave-dwelling solar house," *Acta Energetica Solaris Sinica*, no. 03, pp. 302-310, 1999.

[26] J. Liu, L. Wang, Y. Yoshino, and Y. Liu, "The thermal mechanism of warm in winter and cool in summer in China traditional vernacular dwellings," *Building and Environment*, vol. 46, no. 8, pp. 1709-1715, Aug 2011.

[27] H. Li, Y. Yang, K. Lv, J. Liu, and L. Yang, "Compare several methods of select typical meteorological year for building energy simulation in China," *Energy*, vol. 209, p. 118465, 2020.

[28] A. Sekulić, M. Kilibarda, D. Protić, M. P. Tadić, and B. Bajat, "Spatio-temporal regression kriging model of mean daily temperature for Croatia," *Theoretical Applied Climatology*, vol. 140, pp. 101-114, 2020.

[29] J. Xiong et al., "Subdivision of hot summer and cold winter zone for building thermal performance," *Journal of HV&AC*, vol. 49, no. 04, pp. 12-18, 2019.

[30] G. Zhang, Q. Zhang, F. Wang, Q. Wang, and R. Liang, "Study on Influencing Factors of Energy Consumption in Traditional Rural Dwellings of Kangding Prefecture Based on

DesignBuilder," *Building Science*, vol. 35, no. 06, pp. 108-115, 2019.

[31] S. Samanta, D. K. Pal, D. Lohar, and B. Pal, "Interpolation of climate variables and temperature modeling," *Theoretical Applied Climatology*

vol. 107, pp. 35-45, 2012.

[32] Z. Zhang and Q. Du, "A bayesian kriging regression method to estimate air temperature using remote sensing data," *Remote Sensing*, vol. 11, no. 7, p. 767, 2019.

[33] Z. Han, J. Liao, Q. Qi, H. Sun, J. J. W. C. Wang, and M. Computing, "Radio environment map construction by kriging algorithm based on mobile crowd sensing," vol. 2019, 2019.

[34] P. Shi et al., "Climate change regionalization in China (1961–2010)," *Science China Earth Sciences*, vol. 57, pp. 2676-2689, 2014.

[35] G. T. Meaden et al., "Comparing the theoretical versions of the Beaufort scale, the T-Scale and the Fujita scale," *Atmospheric research*, vol. 83, no. 2-4, pp. 446-449, 2007.

[36] General Specification for Building Energy Efficiency and Renewable Energy Utilization (GB55015-2021), 2021.

[37] Design standard for energy efficiency for rural residential buildings (GB/T50824-2013), 2013.

Chapter 5

FIELD SURVEY AND TRADITIONAL DWELLING' ENVIRONMENTAL MEASUREMENT IN THE CLIMATIC SUB-REGIONS

**CHAPTER FIVE: FIELD SURVEY AND TRADITIONAL DWELLING'
ENVIRONMENTAL MEASUREMENT IN THE CLIMATIC SUB-REGIONS**

FIELD SURVEY AND TRADITIONAL DWELLING' ENVIRONMENTAL MEASUREMENT IN THE CLIMATIC SUB-REGIONS..... 1

5.1. Contents 1

5.2. Materials and methodology 1

 5.2.1. Research background..... 1

 5.2.2. Research scope 2

 5.2.2. Method..... 3

5.3. Research proposal..... 3

5.4. Traditional villages in Qinba mountainous area 4

 5.4.1. Settlements' site selection and characteristics 4

 5.4.2. Case study 5

 5.4.3. The settlement climate suitability strategy in Qinba mountainous area 7

5.5. Traditional dwelling in Qinba mountainous area 8

 5.5.1. Courtyard form 9

 5.5.2. Building function and form 11

 5.5.3. Building structure 15

 5.5.4. Building construction 16

5.6. The physical environment measurement of traditional dwelling 18

 5.6.1. Traditional dwelling in climatic sub-region A1 19

 5.6.2. Traditional dwelling in climatic sub-region A2 23

 5.6.3. Traditional dwelling in climatic sub-region B1 27

 5.6.4. Traditional dwelling in climatic sub-region B2 31

 5.6.5. Traditional dwelling in climatic sub-region C 35

5.7. Summary 40

Reference 42

5.1. Contents

Although the settlements in the Qinba Mountainous Area are restricted by the geomorphic environment, the settlement characteristics and architectural styles with regional features have been formed through the settlements' site selection, spatial morphology, and construction technology. In this chapter, the research team conducted investigations, measurements, and analysis on the traditional dwellings in the Qinba mountainous area from three levels: the settlements, courtyards, and buildings.

This chapter summarized the site selection of 3 types of mountainous settlements, which are settlement in the gully, settlement leaning against the mountain, and settlement on the mountain slope, and their climate suitability characteristics in the Qinba Mountainous Area. In addition, through the field research, it can be seen that the building layout of traditional dwellings in Qinba mountainous area can be divided into 4 types, the "P"-shaped dwelling, the "L"-shaped dwelling, the "U"-shaped dwelling, and the "□"-shaped building. And according to the architectural form, the courtyards are divided into 3 types: open courtyards, semi-open courtyards, and closed courtyards. Finally, the physical environment measurements were conducted on the indoor and outdoor environments of traditional dwellings in the 5 climatic sub-regions in Qinba mountainous area. The results shows that the area is cold and humid in winter, generally humid and some areas are hot in summer. And the traditional dwellings have a certain regulating effect on the indoor physical environment.

5.2. Materials and methodology

5.2.1. Research background

Under the background of the global ecological and environmental crisis brought by the rapid development of human society and the negative impact brought by the large-scale construction of villages and towns, the traditional settlements and the natural environment are basically in a balanced state. In the long-term process of formation, development and evolution, the traditional settlement must have its rationality and inevitability as a response to the natural environment. When the traditional settlement is in a specific area, it needs to be improved to adapt to the local climate and geographical environment. However, since the traditional settlements were constructed spontaneously by villagers, lacking of theoretical guidance, the settlements have limitations such as insufficient light and poor ventilation, inevitably increasing the energy consumption, which lead to the contradiction between the natural elements in the settlement ecosystem [1].

At the same time, traditional dwellings themselves have high historical, cultural, artistic, and ecological values. They witness the development and changes of a place and reflect the

historical and cultural characteristics of the local people's lifestyle, cultural customs, architectural technology, and other aspects. The building materials and structures of traditional dwellings are usually products of the utilization of local natural resources and environmental adaptation, with good ecological performance and environmental adaptability. Protecting traditional dwellings helps to protect the local ecological environment and ecological civilization.

5.2.2. Research scope

The agricultural civilization nurtured by rural settlements is the foundation of human agricultural development [2]. In China, rural settlements are an important cultural and spiritual carrier. The Qinba mountainous area, including the Qinling Mountains, the Daba Mountains, and adjacent regions, has been inhabited and reproduced by humans for hundreds of thousands of years, making it one of the important birthplaces of Chinese civilization.

The superior natural resources have made the Qinba mountainous area a key ecological functional area in China, with many traditional villages of extremely high cultural value distributed throughout the area, including 140 national-level traditional villages. The national-level traditional village core density zoning map of the Qinba mountainous area is shown in Figure 5-1, indicating that the traditional villages in this area exhibit spatial clustering characteristics and are mainly distributed in the northwestern part of Sichuan Province, southern part of Shaanxi Province, southern part of Gansu Province, and the border area of Henan and Hubei provinces [3].

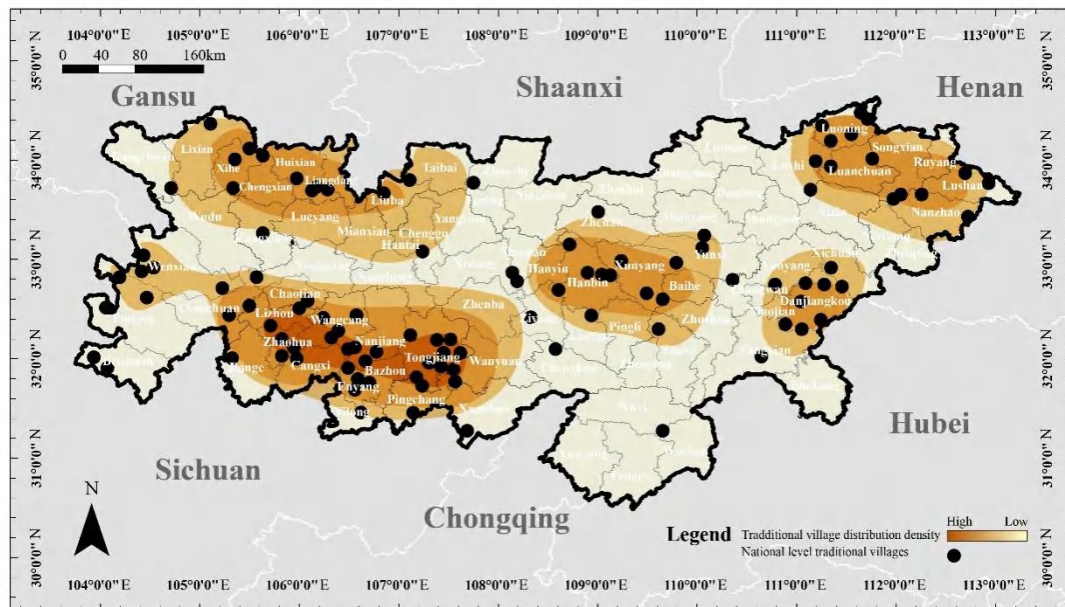


Figure 5-1. Distribution of traditional villages in Qinba Mountainous Area

Based on the climatic sub-division of the Qinba mountainous area and considering the distribution of traditional villages, accessibility to transportation, and other factors, from July 2020 to January 2023, the research team conducted on-site surveys, questionnaire surveys, physical environment tests, and other research work in the selected counties of the 5 sub-climate regions, shown in Figure 5-2. The research team investigated a total of 24 counties and 63 villages in the Qinba mountainous area, with a focus on 21 key villages, including 5 national-level traditional villages and 13 provincial-level traditional villages.

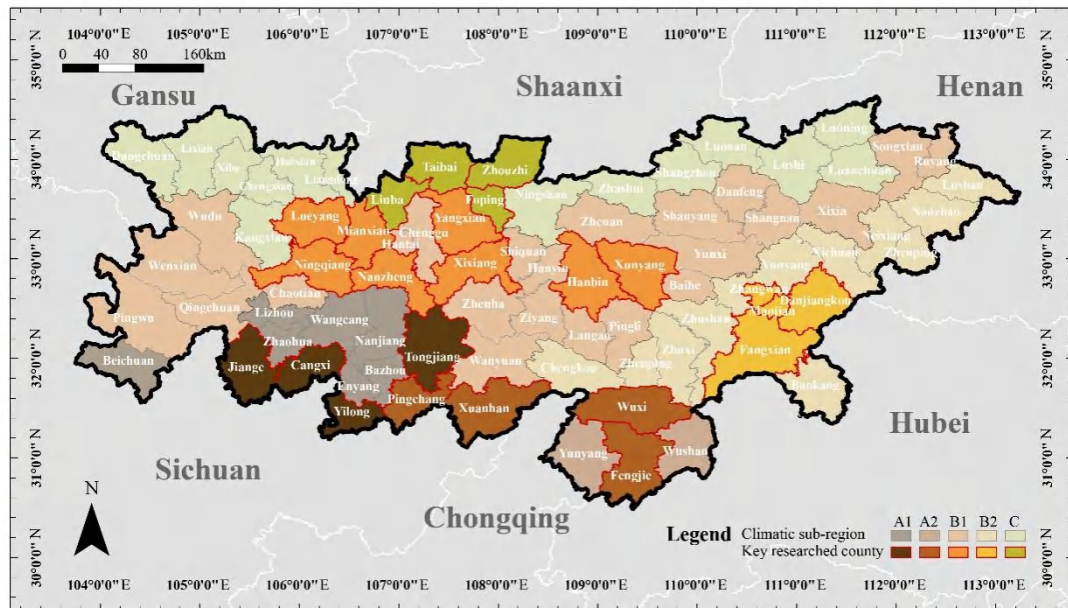


Figure 5-2. The key researched counties

5.2.2. Method

This chapter primarily employs the field survey method to conduct on-site visits and investigations of representative traditional villages and residential dwellings in Qinba mountainous area. Field survey method is a research approach commonly utilized in the fields of social sciences and humanities. It involves researchers personally entering the site to collect data and conduct observations. The advantages of field survey method lie in its ability to provide rich and in-depth data, thereby facilitating a comprehensive understanding of specific social groups or phenomena. It also allows for capturing subtle details of daily life and the underlying cultural and social contexts [4]. Field survey methods typically include participant observation, interviews, questionnaire surveys, recording cultural practices and behaviors, and collecting social network data, among others [5].

5.3. Research proposal

The site investigations are conducted in term of the climatic sub-regions. The field survey

was applied on the selected traditional villages in Qinba mountainous area. The survey included 3 main parts, which are traditional villages, courtyards, traditional dwellings. The main research contents are shown in Table 5-1.

(1) Traditional villages. The research content of the traditional villages includes the villages' geographic environment, settlement planning, and regional culture, etc.

(2) Traditional courtyards. The research content of the traditional courtyards includes the courtyards' site information, plane layout, and landscape environment, etc.

(3) Traditional dwellings. The research content of the traditional dwellings includes the buildings' orientation, plane layout, function, structure, construction, elevation information, outdoor and indoor physical environment measurement, etc.

Table 5-1. Research Content of traditional villages

Category	Research content
Village	Geographic environment, climatic environment, settlement planning, regional culture
Courtyard	Site information, Courtyard form, landscape
Dwelling	Orientation, plane layout, function, structure, construction, elevation information, outdoor and indoor physical environment measurement

5.4. Traditional villages in Qinba mountainous area

5.4.1. Settlements' site selection and characteristics

Qinba Mountainous Area has complex terrains, mountains surrounded, rivers staggered. The main settlements are distributed at the southern foot of Qin Mountains. According to the topographic classification, the settlements can be divided into three types, which are settlement in the gully, settlement leaning against the mountain, and settlement on the mountain slope, shown in Table 5-2 [6-8].

(1) Settlement in the Gully. The settlement in the gully refers that, within the settlement's radiation range of 1000 meters, there are mountains in both relative directions of the settlement, and the mountains' vertical height is greater than 20 meters [9].

The settlements in the gully are usually at the foot of a mountain, with rivers flowing through, having high humidity. For the settlements in the river valley, the mountains block the wind from the outside environment, forming a relatively closed settlement environment. Besides, the mountains block the solar radiation, making the temperature of the settlement more appropriate in the daytime, but moist from the evening to the morning of the second day.

(2) Settlement Leaning against the Mountain. The settlement leaning against the mountain refers that, within the settlement's radiation range of 1000 meters, the settlement only has one

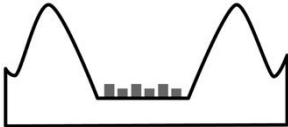
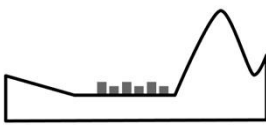
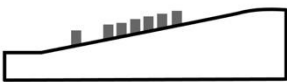
side adjacent to a mountain, and the mountains' vertical height is greater than 20 meters [10].

The microclimate of these settlements is mainly concentrated with only one side of the mountain. The mountains have a shielding effect on solar radiation of the settlements. The year-round sunshine duration of these settlements decreases with increasing slope [11].

(3) Settlement on the Mountain Slope. The settlement on the mountain slope refers that, within the settlement's radiation range of 1000 meters, the settlement is on the slope of the mountain side, and the mountains' vertical height is greater than 20 meters [12].

In general, the low-altitude settlements have high comfort level. The mountain slope direction determines the microclimate of the settlement. The high-altitude settlements have a large amount of solar radiation and the minimum air humidity [13].

Table 5-2. The settlements' site selection

Settlement in the gully	Settlement leaning against the mountain	Settlement on the mountain slope
		

5.4.2. Case study

In this part, three typical settlements are selected in Qinba Mountainous Area, and their internal climate characteristics in winter and summer are investigated. They are Qingmichuan Ancient Town in Hanzhong City, which is the settlement in the gully, Fenghuang Ancient Town in Shangluo City, which is the settlement leaning against the mountain, and Shuhe Ancient Town in Ankang City, which is the settlement on the mountain slope. The details of these three examples are shown in Table 5-3.

(1) The Qingmichuan Ancient Town. The Qingmichuan Ancient Town is located at the junction of three provinces, including Shaanxi Province, Gansu Province, and Sichuan Province. It was an important military and commercial site in ancient times. It is in the valley area between two mountains, facing the water and with hills on the back. However, the mountain is in the south direction of the settlement. The settlement is divided into the south part and north part by the river. The mountain on the south side of Qingmichuan Town blocks the sunshine, reducing the solar radiation time. The layout of the town is in an “s” shape, with the east-west trend, forming a sunward side and shady side. Buildings facing the south receive solar radiation all year round, while buildings facing the north do not.

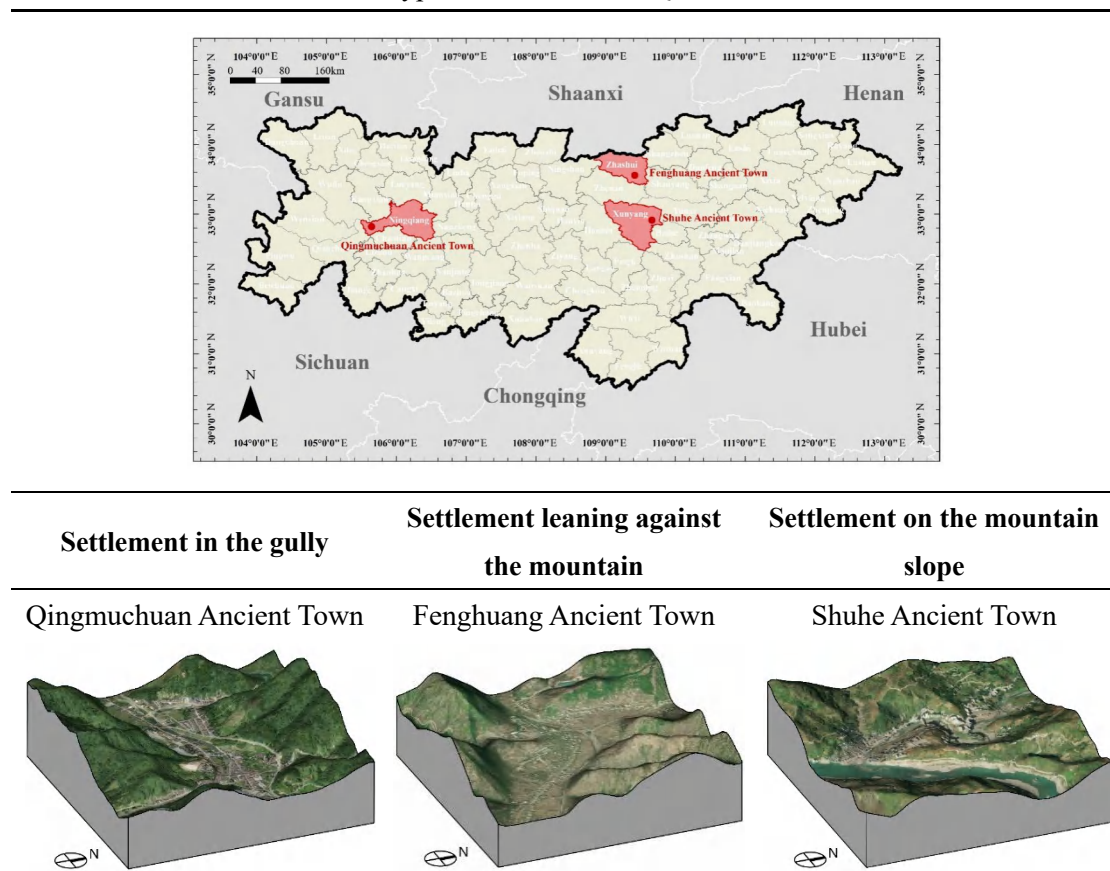
(2) The Fenghuang Ancient Town. The Fenghuang Ancient Town is located at the junction of three rivers. This town, with developed water transportation, was the only way to the south

part of the Qinba Mountainous Area in ancient times, and it was an important commercial site. It is in the open area on the north side of Fenghuang Mountain, adjacent to a river, having limited solar radiation. The settlement is arranged in an “s” shape. The buildings orientated both to the south and to the north.

(3) The Shuhe Ancient Town. The Shuhe Ancient Town is located at both the east and west sides of Shu River. This town was an important ancient waterway and commercial gathering place. The site selection of Shuhe Town has a certain advantage in obtaining solar radiation. As the town is on the east hillside of the north-south mountain, the whole day of solar radiation starts from the sunrise and would not be blocked by the mountain. However, the mountain on the west side of the settlement affects the solar radiation in the afternoon.

Through the investigations, the settlements' site selection in Qinba Mountainous Area is not completely following the principle of facing the water and with hills on the back. The settlements were built based on the terrain, the military and commercial conditions. Some of the settlements' site selection was affected by the historical factors, abandoning the requirements of human comfort. Therefore, the settlements have the problems such as the insufficient solar radiation, the poor ventilation, the poor humidity, etc. Especially during the winter, the settlements' thermal environment is undesirable [14].

Table 5-3. Three typical settlements in Qinba mountainous area



5.4.3. The settlement climate suitability strategy in Qinba mountainous area

Based on the survey and research, according to the site selection, the settlements in Qinba Mountainous Area has the common problems of insufficient sunlight and poor ventilation. Strategies in improving the microclimate around the settlements could be proposed to make up for the adverse factors brought by site selection to cope with the natural environment [5][7].

(1) Settlement in the Gully. For the settlement in the gully, the main strategies to improve the microclimate are to maximize sunlight in winter and strive for natural ventilation in summer. In winter, the settlements could take advantage of the mountains and woodlands in north and west to prevent the cold wind. The settlement in the gully climate suitability strategies and planning guidelines are summarized in Table 5-4 [9].

Table 5-4. The climate suitability strategy of settlement in the gully

	Solar radiation	Ventilation
Existing problems	Different directions of valleys have different shades of sunshine.	The vegetation around the settlement is scattered and does not guide the natural wind well.
Climate suitability strategies	<p>East-west valley: The settlement should move to north to minimize the sunshine blocked by the mountain in the south.</p> <p>North-south valley: The settlement has fixed annual solar radiation time.</p>	Based on the gully's landform and direction, the natural wind could enter settlement along the gully, with the fixed wind direction and homogeneous wind flow. Besides, the organized vegetation could help to guide the wind for cooling in summer and guard against wind for insulation in winter.
Planning guidelines	The solar radiation time of the settlement is significantly affected by the mountain. The planning strategy should minimize the influence of the mountain and forest land on the solar radiation time.	Combined with the surrounding vegetation planting environment, plants could be planted in the downwind of the dominant summer wind. And the air inlet of the settlement could introduce the natural wind into the settlement and reduce the air loss.

(2) Settlement Leaning against the Mountain. For the settlement leaning against the mountain, the main strategy to improve the microclimate is to strive for sunshine in winter and look for natural ventilation in summer. The building should be arranged in the south, southeast or southwest direction as far as possible. The settlement should make full use of solar radiation, plant deciduous trees in the south, which could get shade in summer, and strive for sunshine in

winter. Besides, the settlement could use water to organize ventilation and cooling. The settlement leaning against the mountain climate suitability strategies and planning guidelines are summarized in Table 5-5 [10].

Table 5-5. The climate suitability strategy of settlement leaning against the mountain

	Solar radiation	Ventilation
Existing problems	Solar radiation: Mountains block solar radiation.	Ventilation: Affected by the mountain wind, the settlement site selection determines the local wind direction.
Climate suitability strategies	The solar radiation of settlement leaning against the mountain is affected by the mountains. The sunshine condition gradually weakens from the south slope to the north slope. If the settlement site selection is not good, the sunshine condition could be improved by adjusting the internal environment of the settlement. The horizontal layout of the courtyard could be modified to obtain the solar radiation.	The settlement could get the wind along the slope by utilizing the terrain. The settlements on the north or the west slope need to use vegetation to block the cold wind in winter. The wind passage in summer should be as wide as possible to cooling down the settlement.
Planning guidelines	The south slope could be selected as far as possible for the new construction. On the west and north sides of the mountain, the new construction should be as far away from the mountain as possible to reduce the blocking of solar radiation.	The new built settlement should utilize the local eddy formed by the mountains, organize the vegetation, and reasonably introduce the natural wind into the settlement.

(3) Settlement on the Mountain Slope. For the settlement on the mountain slope, the site shall be in the south slope as far as possible. Vegetation should be planted on the north side of the settlement to prevent wind. Vegetation should also be planted on the west side to prevent the afternoon solar radiation. Pond should be put on the south side to improve the temperature and humidity. The settlement on the mountain slope climate suitability strategies and planning guidelines are summarized in Table 5-6 [12].

5.5. Traditional dwelling in Qinba mountainous area

The traditional dwellings in Qinba mountainous area are generally composed of 3 parts: the courtyard, the main building, and the ancillary building. The traditional dwellings often conform to the mountain, parallel to the mountain contour line. The courtyards are often

arranged in front of the residential buildings, and the ancillary buildings, such as animal husbandry and toilets, are generally set behind the house or the beside the house gable wall, maintaining a certain distance with the main house [15]. Figure 5-3 shows the common layout of the traditional dwelling in Qinba mountainous area.



Figure 5-3. The traditional dwelling and courtyard layout form

Table 5-6. The climate suitability strategy of settlement on the mountain slope

	Solar radiation	Ventilation
Existing problems	Solar radiation is significantly affected by slope direction.	The wind on the slope is blocked by the buildings at the foot of the mountain.
Climate suitability strategies	Slope should be utilized to improve the solar radiation in the settlement. The south slope has the best sunshine condition, followed by the east slope, and the north slope has the worst sunshine condition. In the same slope, the higher latitude means the smaller solar altitude angle, leading to less time to get sunshine. And the smaller slope leads to the settlement with lower density to get lighter.	The settlement should utilize the wind along the slope and the water body outside the settlement to cool and moisten the air in summer. Besides, the slope could prevent the cold wind in winter to improve the thermal condition.
Planning guidelines	The characteristics, including the proportion, density, and direction, of the settlement could be identified according to the different conditions of slopes and their influencing factors.	The slope wind could be formed by rational utilization of the geomorphic characteristics of the slope and the wind leading function of green vegetation.

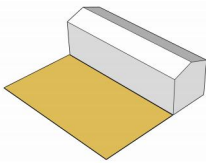
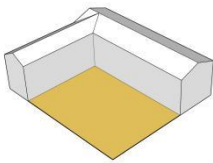
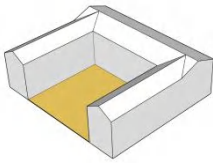
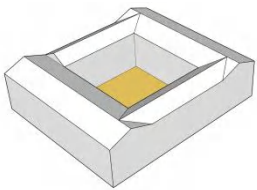
5.5.1. Courtyard form

The typical courtyard is mostly arranged in front of the residential building, generally with the open or semi-open enclosures, without walls. The open and semi-open courtyard layout is not only related to the mountainous terrain, but also to the humid climate of the study area. The

weather in summer is muggy, with the open courtyard, the airflow is easier to enter the building through the courtyard, which can take away the excess heat and moisture inside the building. The open courtyard introduces the natural landscape into the courtyard and provides a wider view. Moreover, this region is rainy, and the open courtyard is also conducive to drainage. The residents use the courtyard as a place for daily living and neighborhood interaction. It not only meets the needs of production and life, but also provides a relatively good outdoor living environment.

Through the field research, it can be seen that the building layout of traditional dwellings in Qinba mountainous area can be divided into 4 types, the “I”-shaped dwelling, the “L”-shaped dwelling, the “U”-shaped dwelling, and the “□”-shaped building [16]. According to the architectural form, the courtyards are divided into 3 types: open courtyards, semi-open courtyards, and closed courtyards, as shown in Table 5-7 [17].

Table 5-7. The courtyard forms in Qinba mountainous area

Open courtyard		Semi-open courtyard	Closed courtyard
			
“I”-shaped dwelling	“L”-shaped dwelling	“U”-shaped dwelling	“□”-shaped dwelling
The open courtyard has good vision and good ventilation. It is an important space for residents’ daily life and neighborhood interaction.		The semi-open courtyard will resist part of the winter wind but affect the summer ventilation. It can also be used as a space for residents’ daily life and neighbor communication.	The enclosed courtyard provides a private outdoor space that blocks the landscape view, ventilation, and neighborhoods.
75.5%		12%	12.5%

(1) Open courtyard

Most of the open courtyards are located in front of the “I”-shaped and “L”-shaped buildings, forming the unilateral or bilateral enclosed courtyard space, accounting for 75.5 % of the total sample size in the Qinba mountainous area. The open courtyard has good vision and good ventilation. It is an important space for residents’ daily life and neighborhood interaction.

(2) Semi-open courtyard

Most of the semi-open courtyards are located in front of “U”-shaped dwellings, forming a courtyard space surrounded by three sides, accounting for 12% of total sample size in the Qinba

mountainous area. The courtyard enclosed by three sides provides a relatively private space, which can provide good landscape and vision. Due to the shelter of the building, it can resist part of the winter wind and provide a more comfortable courtyard environment. However, the ventilation of the courtyard in summer will be affected to a certain extent. The semi-open courtyard can also be used as a space for residents' daily life and neighbor communication.

(3) Closed courtyard

Most of the closed courtyards are enclosed in “□”-shaped dwellings, forming a courtyard space enclosed on all sides, accounting for 12.5% of total sample size in the Qinba mountainous area. The enclosed courtyard provides a private outdoor space that blocks the landscape view, ventilation, and neighborhoods. It can resist part of the cold wind and provide a more comfortable courtyard space in winter and affect the ventilation of the building in summer. The enclosed courtyard is mainly for family services, but not for neighborhood interaction.

5.5.2. Building function and form

Table 5-8. The building forms in Qinba mountainous area

No.	Village	Courtyard form proportion (%)			
		“I”-shaped	“L”-shaped	“U”-shaped	“□”-shaped
1	Baishi Village	52	31	-	17
2	Huilong	44	35	5	16
3	Longtanhe	31	24	18	27
4	Baishisi	46	34	15	5
5	Liyuanba Village	20	22	33	25
6	Xujiaba	68	18	14	-
7	Lianmeng Village	54	33	9	4
8	Qinghe	79	9	4	8
9	Lianhe	56	22	8	14
10	Zhandou	65	24	-	11
11	Xinchun	55	29	10	6
12	Jiangtai	69	18	-	13
13	Zhongjiagou	35	25	20	20
14	Sanguan	50	5	24	21
15	Shuangzhen	55	26	14	5
16	Hongjun	55	32	8	5
17	Zhuyuan	42	25	25	8
18	Chaiping	55	19	22	4
19	Xiadianzi	33	25	20	22
20	Lvjiahe	50	21	9	20
21	Wejiagou	54	34	9	3
22	Nanba	63	18	-	19
23	Tangwan	65	13	10	12
Average Value		52	23.5	12	12.5

The building form of traditional dwelling in Qinba mountainous area is flexible, and the construction processes of some dwellings are not completed in one step. The common evolution process of the traditional dwelling is from “I”-shaped, to “L”-shaped, finally to “U”-shaped and “□”-shaped. The construction of “U”-shaped and “□”-shaped courtyards are initially built in “I”-shaped, then it has experienced several generations of additions, and finally completed a relatively closed courtyard space [8]. During the survey, it was also found that there were various forms of buildings with multiple courtyards such as “H”-shaped and “日”-shaped buildings, which greatly enriched the courtyard space. However, the number of such buildings was very limited and they could be classified as variants of the “□”-shaped dwelling [18].

Among them, the “I”-shaped traditional dwelling has the highest proportion, due to its full utilization of the terrain and satisfaction of people’s basic living needs, as well as the lowest construction cost. The “L”-shaped traditional dwelling is also common, due to its less terrain restriction, satisfaction of people’s normal living needs, and relatively open courtyards. The number of “U”-shaped traditional dwellings is basically the same as that of “□”-shaped ones, having the lowest number, mainly because the construction of them is limited by terrain and the construction cost is higher, requiring a large family population, etc [15]. The statistical results of traditional dwellings’ forms are shown in Table 5-8.

(1) “I”-shaped dwelling

In mountainous areas, due to site restrictions, the “I”-shaped dwelling is the most common architectural layout, accounting for 52% of the total sample size. It has a compact spatial form, flexible orientation, low construction cost, occupies less land, and is particularly flexible and easy to build in rural areas, as shown in Figure 5-4.



Figure 5-4. The “I”-shaped dwelling

As shown in Figure 5-5, the most basic plan layout of the “I”-shaped dwelling is the three units from of “one bright and two dark”, where the middle unit is the living room (bright space) and serves as the public space for external visitors, as well as internal family activities such as

dining. The side units are often used as bedrooms, storage rooms, kitchens, etc. Three-unit dwellings can also be expanded to five or more units on each side.

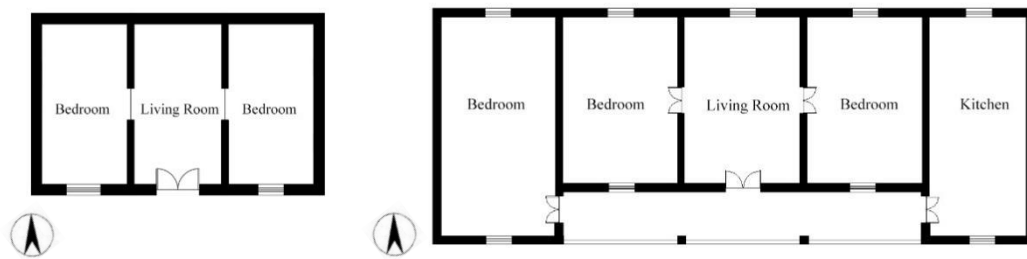


Figure 5-5. The typical plan layout of the “I”-shaped dwelling

The common “I”-shaped traditional dwellings have three, five, or seven units. Additionally, some “I”-shaped dwellings have eaves extended outwards with columns, forming a transitional grey space between the indoor and outdoor areas, called a “porch”. The width of the porch varies in different areas of the Qinba mountainous area, ranging from 1.2m to 2.4 m. The porch not only provides shade and shelter space from rain, but also serves as a space for rest, gathering, dining, and drying. When the porch is not used, the roof will still have a certain degree of overhang on the exterior walls, with an overhang width ranging from 0.6m to 1.0m. The courtyards of “I”-shaped dwellings generally do not have walls and are often open in the front of the house, serving as the spaces for outdoor family and neighborhood activities as well as drying fields for grains [15].

(2) “L”-shaped dwelling



Figure 5-6. The “L”-shaped dwelling

The “L”-shaped traditional dwelling, composed of two perpendicular rectangles, is a common type of residential plan layout in Qinba mountainous area, accounting for 23.5% of the total sample size. The images and plan layout of the “L”-shaped dwelling are shown in Figure 5-6 and 5-7. This layout involves adding a wing perpendicular to one side of the “I”-shaped dwelling (consisting of two to three rooms).

The main living rooms are usually located in the main wing facing the best direction or with an open view, while the kitchen and other utility rooms are placed in the perpendicular wing. The two wings form a relatively open outdoor courtyard. The corner where the two wings meet is often used as a kitchen. Some “L”-shaped dwellings also have a porch, similar to that of the “I”-shaped dwellings. Like the “I”-shaped dwellings, the courtyards of the “L”-shaped dwellings serve as an open outdoor space for family and neighborhood activities [15].

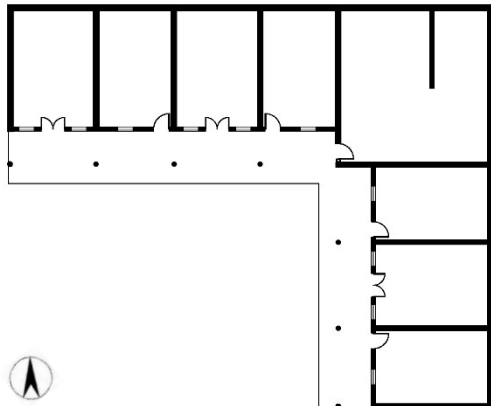


Figure 5-7. The typical plan layout of the “L”-shaped dwelling

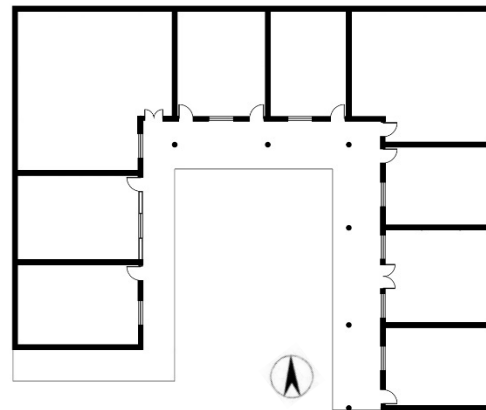


Figure 5-8. The typical plan layout of the “U”-shaped dwelling

(3) “U”-shaped dwelling

On the basis of the “I”-shaped dwelling, the wing is added to each side of the main house, forming a “U”-shaped plan layout. The “U”-shaped dwelling accounts for 12% of the total number of traditional dwellings in the Qinba mountain area. The images and common form of the “U”-shaped dwellings is shown in Figure 5-9 and 5-8. The dwelling already has a clear limitation to the courtyard space, giving a distinct sense of enclosure. Depending on the terrain, the length and number of rooms on both sides may vary, resulting in an asymmetrical building form. The courtyard is lower, forming a sunken courtyard. The “U”-shaped dwellings usually have porches and a more enclosed courtyard.



Figure 5-9. The “U”-shaped dwelling

(4) “□”-shaped dwelling

On the basis of the “I”-shaped dwelling, rooms are added to the two sides and opposite of the main house, forming a symmetrical rectangular plan layout, accounting for 12.5% of the total number of traditional dwellings. The image and common form of the “□”-shaped dwelling is shown in Figure 5-10 and 5-11. The dwelling has a clear definition of the courtyard space, forming an enclosed courtyard with clear boundaries between the inside and outside space. The main wing is usually located on a higher platform, followed by the side wings, and the courtyard is lower, forming a sunken courtyard. The “□”-shaped dwelling usually has eaves and a more enclosed courtyard, which is mainly used for family members.



Figure 5-10. The “□”-shaped dwelling

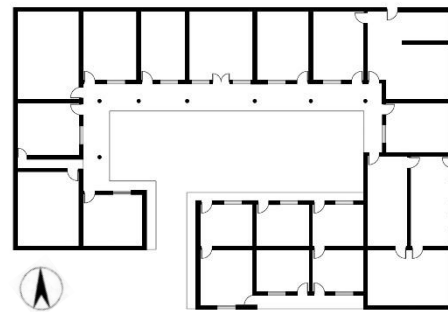
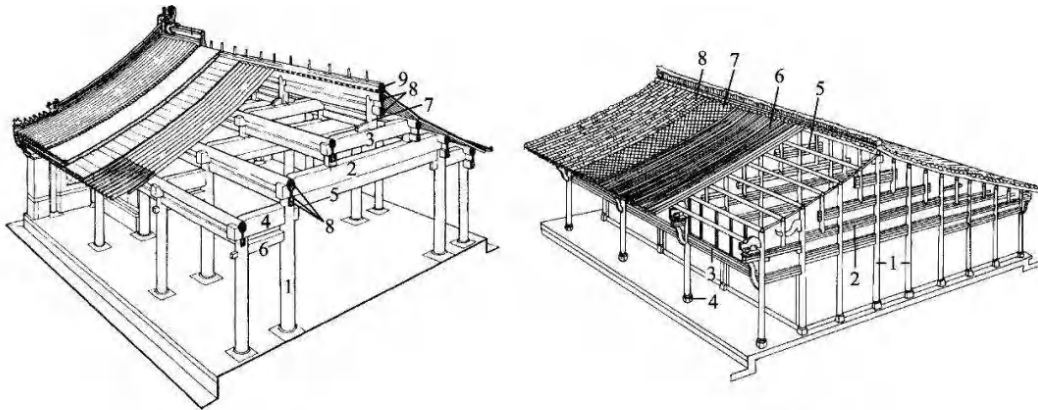


Figure 5-11. The typical plan layout of the “□”-shaped dwelling

5.5.3. Building structure

Due to its unique geographical environment and abundant resources of earth and wood materials, the Qinba mountainous area’s traditional dwellings are mostly constructed using local materials. Therefore, the construction methods of the traditional dwellings mainly consist of earth-wood structures, and the wood frame system is often used [19]. The wood frame system is used to support the weight of the house, while the walls only serve to enclose the space. The common wood frame systems include the “lifting beam type” and the “column and tie type”, whose structure diagrams are shown in Figure 5-12.

The traditional dwellings in the Qinba mountainous area are usually flexibly combined with the room units to form a spatial structure of 3 spans, 5 spans and 7 spans. Among them, the 5 spans building can meet the living functions of 5 ~ 10 people, accounting for the largest proportion. The length and width of the dwellings depend largely on the length and width of the room unit. In the study area, room unit’s length and width are usually between 3m to 5m, and 4m to 7m, respectively. And the traditional dwellings are usually 2 stories building, with the building height of 4.5m to 7m.



(a) Lifting beam structure

(b) Column and tie structure

Figure 5-12. The “Raised beam” and “Through tenon” wood structure diagrams [20]

5.5.4. Building construction

The main climatic features of the Qinba mountainous area are hot and humid in summer, cold and damp in winter, with small diurnal temperature range, large annual precipitation, and little sunshine. Due to the absence of air conditioning equipment in traditional dwellings, the choice of insulation and enclosure materials and construction methods becomes an important consideration in constructing buildings in such climatic conditions [21]. Building structures such as foundations, walls, roofs, doors, and windows are all made according to the local natural environment and climatic factors, and materials are selected based on local conditions, which not only saves construction costs but also gives traditional dwellings a strong regional flavor and demonstrates strong regional adaptability [22, 23].

Based on the traditional construction methods and material characteristics of the traditional dwellings, there are significant differences between the traditional dwellings in the north and south part of Qinba mountain area. The traditional dwellings in Qinba mountainous area showed a trend of decreasing from south to north in the width of the rooms, the south-facing window to wall ratio, the slope of the roof and the degree of architectural decoration.

Changes in the form and building materials of traditional dwellings are related to the climate subdivisions defined in Chapter 4. In the southern part of the research area, with a relatively warm climate, which belongs to the sub-region A1 and A2, traditional dwellings commonly adopt timber walls and bamboo clay walls, with relatively larger window-to-wall ratios of 0.10~0.15. In contrast, in the northern part of the research area, with a relatively cold climate, which belongs to the sub-region B1, B2, and C, traditional dwellings usually use rammed earth walls, and the window-to-wall ratios are smaller, around 0.08~0.12. Figure 5-13 and 5-14 show the building structure in the south and north part of Qinba mountainous area, respectively. The common building structures and construction practices of traditional dwellings in Qinba

mountainous area are as follows:



Figure 5-13. The building structure in climatic sub-region A1 and A2



Figure 5-14. The building structure in climatic sub-region B1, B2 and C

(1) Foundation

In Qinba mountainous area, there are many mountains and rivers, and there are many stones and pebbles, which are convenient to use. However, the weight of stone is large, and mining, processing, and transportation are not easy. Therefore, it is only used for wear-resistant and moisture-proof structural parts, such as foundations, wall foundations, brackets, column bases, and steps. The stones used for foundations are generally regularly shaped and laid layer by layer [24]. The method of masonry is to place larger stones on both sides of the foundation and fill the middle with smaller stones as much as possible to make the surface as flat as possible.

(2) Exterior wall

According to field research, traditional dwellings in Qinba mountainous area have a variety of materials used for the exterior walls. In most traditional dwellings in northern Sichuan and Chongqing, bamboo clay walls are commonly used for exterior walls, while a small number of dwellings use timber walls facing the courtyard for aesthetic purposes, and bamboo clay walls

for the exterior walls facing the mountains. The specific construction for the bamboo clay wall is the bamboo plaited layer in the middle with two grass clay layers on surface. The thickness of the bamboo clay wall is about 50mm, and regular stones with a height of 50cm-60cm are used for the base of the bamboo clay wall to prevent moisture damage [25]. In areas with colder winter climates, such as southern Shaanxi, western Henan, and northern Hubei, the walls are mostly made of rammed earth with good insulation performance, with a thickness of 300~500mm. Some of the dwellings have simple white lime treatment on the surface of the rammed earth wall [26, 27]. And it also uses the stone masonry for the base to prevent moisture damage.

(3) Roof

The traditional dwelling usually has double-sloped overhanging roofs, with clay tiles as the common roofing material. The structure of the clay tile roof is air space in the middle with two clay tile layers on surfaces [28]. And the structure is directly laid or hung on the rafters. This roof structure is commonly used in the hot summer and cold winter region in China due to its simple construction, easy availability of materials, and low cost. However, it has the disadvantage of poor thermal insulation and airtightness. Some dwellings have porches, and the eaves of the sloping roof generally extend 1.0 to 2.4m from the wall. Some dwellings do not have porches, and the depth of the eaves of the sloping roof is about 0.6~0.8m from the wall. The extended eaves can prevent the walls from getting wet by rainwater, protect the walls, and can also be used for daily storage.

(4) Window and door

In general, doors and windows in Qinba mountainous area are made of local wood. Due to the bearing capacity of the rammed earth walls, the openings of doors and windows in the northern part of the area are relatively small, with a window-to-wall ratio of about 0.1. In the southern part of the Qinba mountain area, bamboo clay walls and timber walls are commonly used, and the window-to-wall ratio is about 0.12. The wooden windows are equipped with wooden grids or carvings, without glass [24]. In summer, natural ventilation is achieved through the windows, while in winter, transparent plastic film is added to the windows to prevent wind and provide thermal insulation.

5.6. The physical environment measurement of traditional dwelling

The research team conducted multiple investigations on traditional dwellings in Qinba mountainous area during the coldest month of winter (January) and the hottest month of summer (July) [29]. The research included surveying and mapping of traditional dwellings, physical environment measurements inside and outside the dwellings, and conducting questionnaires. Among them, physical environment testing was conducted on traditional

dwelling in different sub-climatic regions of Qinba mountainous area to understand the real indoor thermal environment of traditional dwellings under extreme climate conditions, and to provide a basis for indoor thermal environment improvement.

Based on the research on the plan layout of traditional dwellings, it was found that in the Qinba mountainous area, 52% of traditional dwellings are the “I” shaped dwelling. And the “L”-shaped, “U”-shaped, and “□”-shaped dwellings are variants of the “I” shaped dwelling, which can be regarded as combinations of the “I” shaped dwelling facing different directions for further exploration in future studies. Therefore, this study only selected the “I” shaped and “L”-shaped dwelling for research.

5.6.1. Traditional dwelling in climatic sub-region A1

(1) Basic information of Liyuanba Village

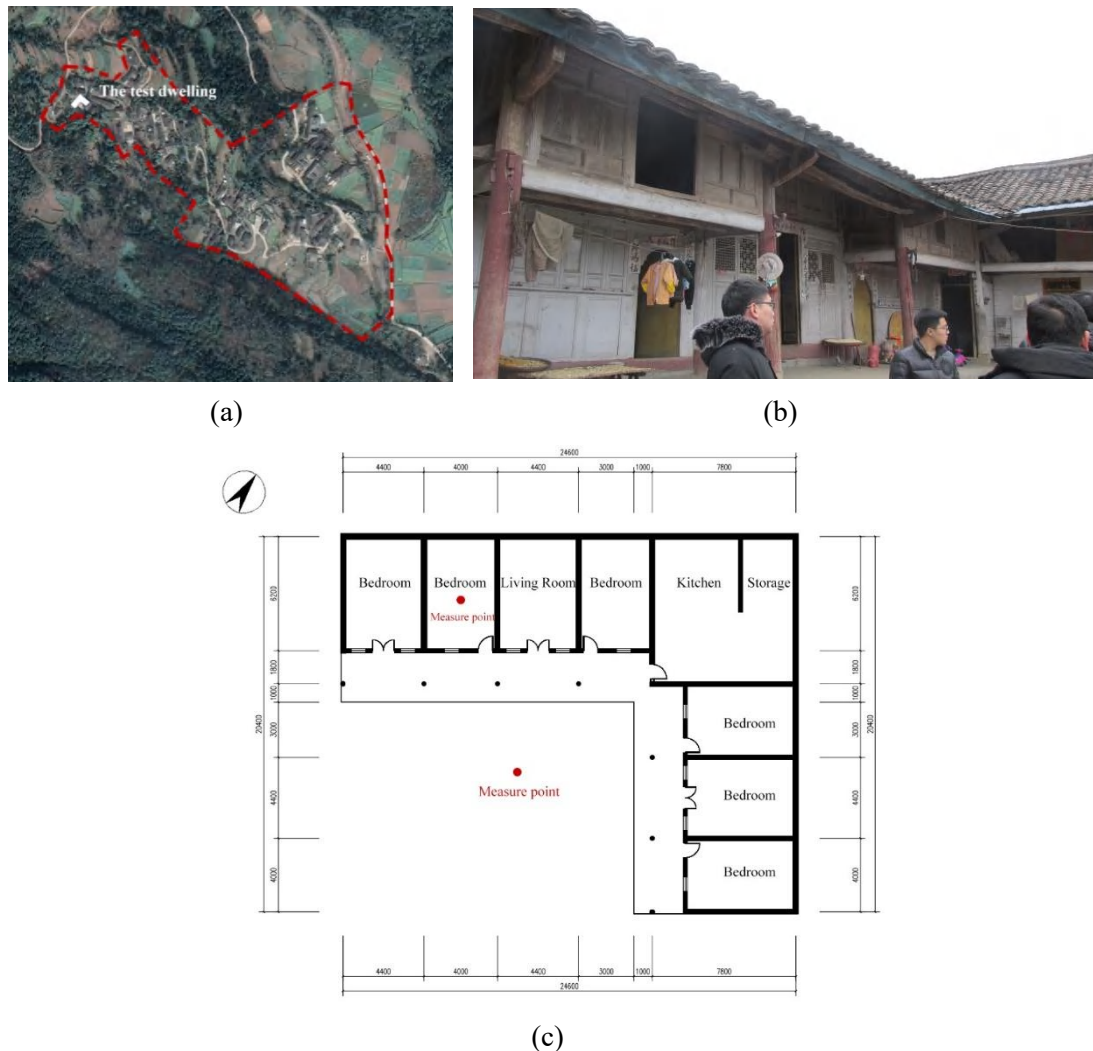


Figure 5-15. The traditional dwelling in Liyuanba Village (a) The location of the traditional village (b) The image of the traditional dwelling (c) The plan of the traditional dwelling

The measured dwelling is located in Liyuanba Village, Tongjiang County, Bazhong City, in climatic sub-region A1. It is listed in the Directory of Chinese Traditional Villages. The village is backed by the Daba Mountains and belongs to the hilly landform with an altitude of 600-750m and an annual rainfall of 1166mm [30]. The village is located in a valley, as shown in Figure 5-15(a), and has a large number of well-preserved traditional dwellings.

(2) The current situation of the test dwelling.

The measured dwelling was built around 1900 and consists of two stories in an “L” shape. The current status and floor plan of the traditional dwelling are shown in Figure 5-15(b) and 5-15(c), respectively. The dwelling faces southeast, with a main span of 5 bays and a secondary span of 4 bays. The width and depth of the room unit are 4m and 6m, respectively. The living room is located in the middle of the main span, while the bedrooms are on both sides of the living room. The kitchen and storage space are located at the corner of the building, and the second floor contains bedrooms and storage space.

The dwelling has wooden frame structure, with bamboo clay walls and timber walls. The building has a stone masonry base at the bottom, which serves as a waterproofing measure. The roof is covered with small clay tiles, and the doors and windows are made of wooden frames with a window-to-wall ratio of 0.14. Currently, the dwelling is inhabited by 7 people spanning 3 generations, with the main rooms accounting for 62.5% of the total number of rooms. The basic information of the traditional dwelling is summarized in Table 5-9.

Table 5-9. The basic information of the measured dwelling in Liyuanba Village

Length	Width	Height	WWR	Orientation	Exterior wall material	Main room ratio
24.6m	20.4m	4.8m	0.14	Southeast	Bamboo clay/ Timber	62.5%

(3) Physical environment measurement

1) The temperature and relative humidity measurement in winter

a. Winter temperature. As shown in Figure 5-16 and Table 5-10, during the 24-hours winter test day in Jiange County, the outdoor maximum air temperature is 6.90°C, the lowest air temperature is 4.70°C and the average air temperature is 5.53°C. The highest indoor air temperature is 8.60°C, the lowest is 6.20°C, and the average air temperature is 7.07°C, which is higher than that of the outdoor, but it is still lower than the thermal comfort temperature range of human body. The fluctuation range of the outdoor and indoor air temperature is relatively gentle, with the value of 2.20°C and 2.40°C, respectively. The average outdoor and indoor mean radiant temperature has the same trend as that of the air temperature. The average outdoor and indoor mean radiant temperature is 5.67°C and 7.20°C, respectively.

In winter, the indoor and outdoor air temperature and mean radian temperature in Jiange County is low, below the thermal comfort temperature range of human body. The traditional

dwelling has certain heat preservation effect and can stabilize the indoor temperature. However, there is a small temperature difference between the indoor and outdoor space due to the poor thermal insulation performance of the house.

Table 5-10. The temperature analysis of the measured dwelling in winter

Measuring point	Air temperature (°C)				Mean radiant temperature (%)			
	Max	Min	Mean	Fluctuation range	Max	Min	Mean	Fluctuation range
Outdoor	6.90	4.70	5.53	2.20	7.30	4.90	5.67	2.40
Indoor	8.60	6.20	7.07	2.40	8.70	6.30	7.20	2.40

b. Winter relative humidity. As we can see from Figure 5-16 and Table 5-11, during the 24-hours winter test day in Jiange County, the maximum value, minimum value, and mean value of the outdoor relative humidity are 83.20%, 69.90%, and 79.50%, respectively. And the maximum, minimum, and mean indoor relative humidity is 76.29%, 66.80%, and 72.01%, respectively. The variation range of outdoor relative humidity was 13.30%, compared with that of the indoor value of 9.49%.

In winter, the indoor and outdoor relative humidity in Jiange County in most of the day is very high. Although the indoor relative humidity and its variation range is smaller than that of the outdoor, it is still far beyond the human comfort requirements.

Table 5-11. The relative humidity analysis of the measured dwelling in winter

Measuring point	Relative humidity (%)			
	Max	Min	Mean	Fluctuation range
Outdoor	83.20	69.90	79.50	13.30
Indoor	76.29	66.80	72.01	9.49

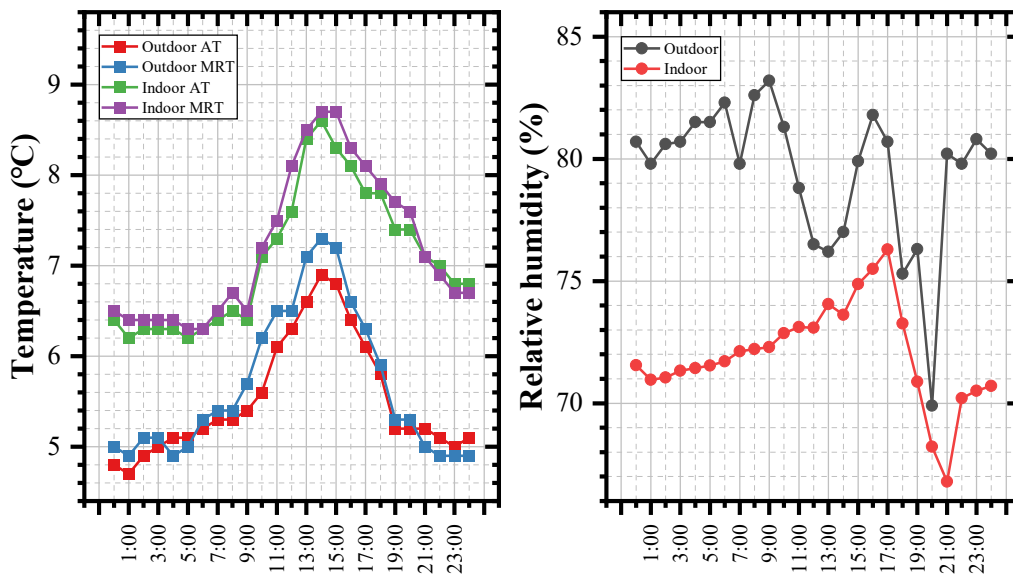


Figure 5-16. The temperature and humidity of the measured dwelling in winter in Liyuanba Village

2) The temperature and relative humidity measurement in summer

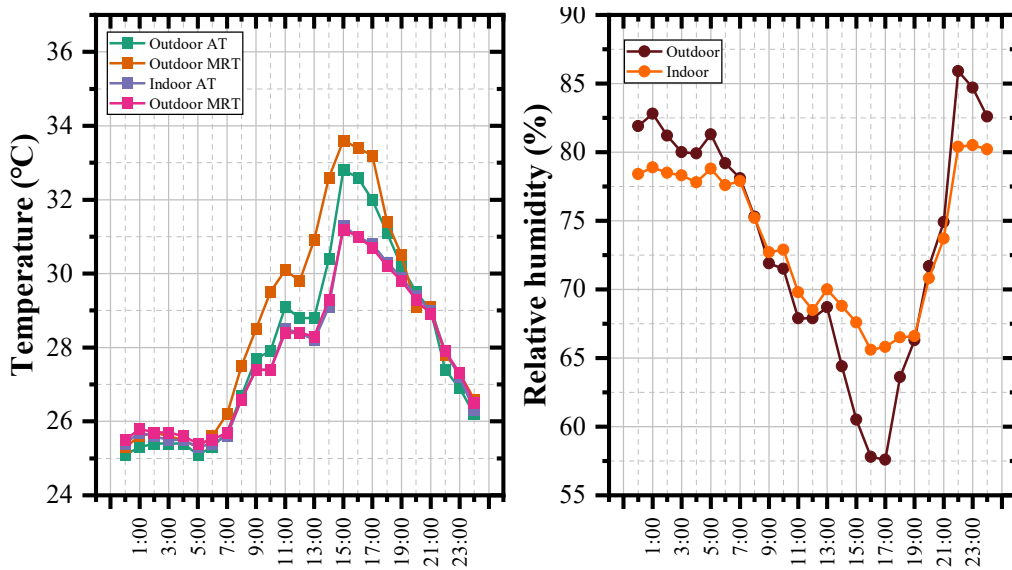


Figure 5-17. The temperature and relative humidity of the measured dwelling in winter in Liyuanba Village

a. Summer temperature. As shown in Figure 5-17 and Table 5-12, during the 24-hours summer test day in Jiange County, the outdoor maximum air temperature is 32.80°C, the lowest air temperature is 25.10°C and the average air temperature is 27.99°C. The highest indoor air temperature is 31.30°C, the lowest is 25.30°C, and the average air temperature is 27.71°C. The fluctuation range of the indoor air temperature is 6.00°C, which is gentler than that of the outdoor air temperature with the value of 7.70°C. The average indoor and outdoor mean radiant temperature has the same trend as that of the air temperature. The average outdoor and indoor mean radiant temperature is 28.63°C and 27.74°C, respectively.

Table 5-12. The temperature analysis of the measured dwelling in summer

Measuring point	Air temperature (°C)				Mean radiant temperature (%)			
	Max	Min	Mean	Fluctuation range	Max	Min	Mean	Fluctuation range
Outdoor	32.80	25.10	27.99	7.70	33.60	25.30	28.63	8.30
Indoor	31.30	25.30	27.71	6.00	31.20	25.40	27.74	5.80

In summer, the indoor and outdoor air temperature and mean radiant temperature is high in part of the time, exceeding the thermal comfort temperature range of human body. The regulating effect of traditional dwelling on the indoor temperature is not obvious.

a. Summer relative humidity. As we can see from Figure 5-17 and Table 5-13, during the 24-hours summer test day in Jiange County, the maximum value, minimum value, and mean value of the outdoor relative humidity are 85.90%, 57.60%, and 73.50%, respectively. And the maximum, minimum, and mean indoor relative humidity is 80.50%, 65.60%, and 73.67%,

respectively. The variation range of outdoor relative humidity was 28.30%, compared with that of the indoor value of 14.90%. The indoor and outdoor humidity in Jiange County in summer has been maintained at a high level, exceeding the requirements of human comfort.

Table 5-13. The relative humidity analysis of the measured dwelling in summer

Measuring point	Relative humidity (%)			
	Max	Min	Mean	Fluctuation range
Outdoor	85.90	57.60	73.50	28.30
Indoor	80.50	65.60	73.67	14.90

5.6.2. Traditional dwelling in climatic sub-region A2

(1) Basic information of Baishi Village

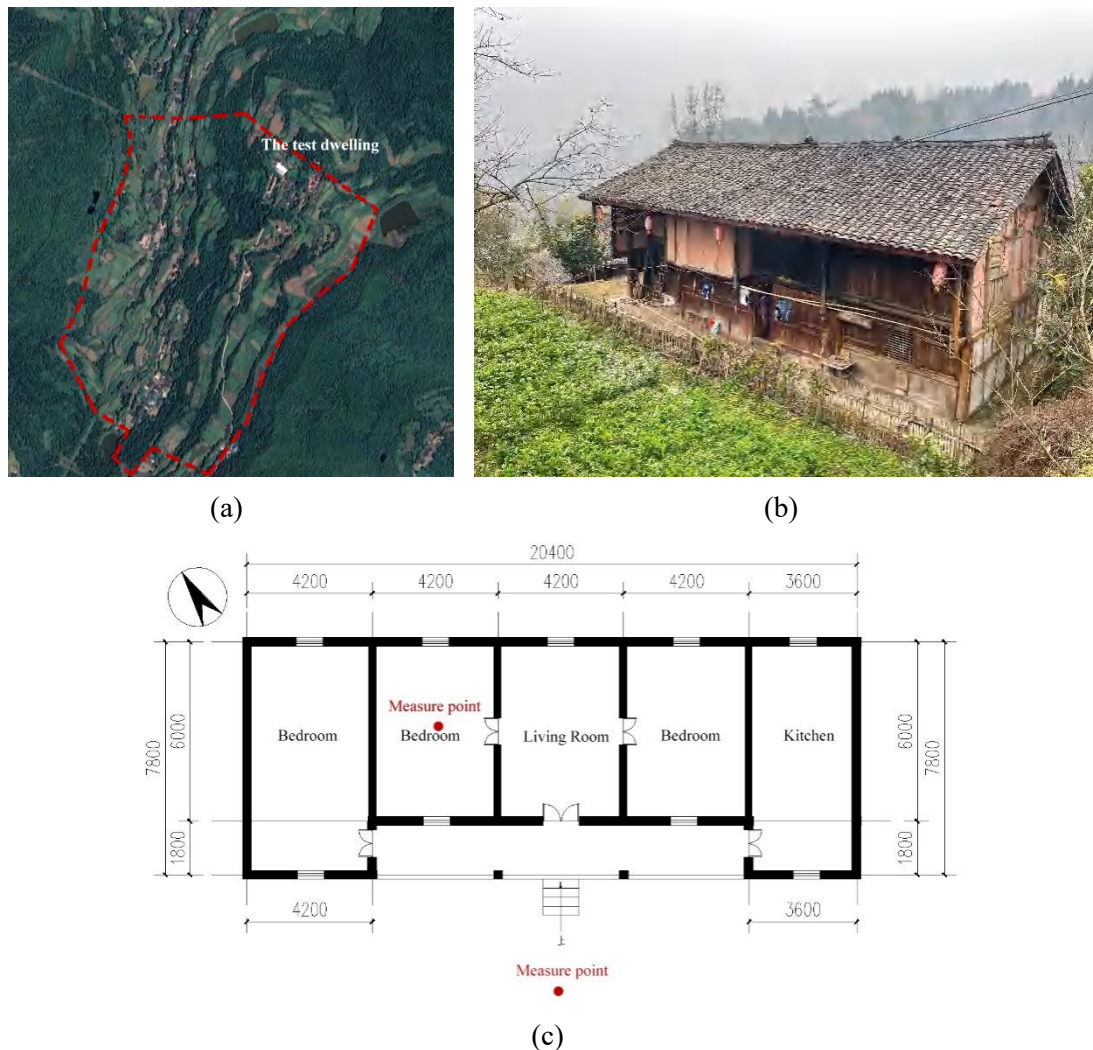


Figure 5-18. The traditional dwelling in Baishi Village (a) The location of the traditional village (b) The image of the traditional dwelling (c) The plan of the traditional dwelling

The tested dwelling is located in Baishi Village, Pingchang County, Bazhong City, in the

calimatic sub-region A2. The village is backed by the Daba Mountains and belongs to a hilly terrain with an altitude of around 850 meters, an annual rainfall of 1000mm, and an average annual temperature of 16.5°C [31]. The village is scattered along the mountain slopes, as shown in Figure 5-18(a), and preserves many traditional dwellings.

(2) The current situation of the test dwelling.

The tested traditional dwelling was built around 1910 and has two floors, forming an “I” shape. As shown in Figure 5-18(b) and 5-18(c), the dwelling faces southeast with a total of 5 bays, and the width and depth of the room unit are 4.2m and 6m, respectively. The living room is located in the middle, and the bedrooms are on both sides of the living room, while the kitchen is on the east side of the building. The second floor is used for bedrooms and storage space. The dwelling has wooden frame structure, with bamboo clay walls and timber walls. The building has a stone masonry base at the bottom, which serves as a waterproofing measure. The roof is covered with small clay tiles, and the doors and windows are made of wooden frames with a window-to-wall ratio of 0.12. Currently, the dwelling is inhabited by 2 generations of 5 people, and the main living area accounts for 70% of the total area. The basic information of the traditional dwelling is shown in Table 5-14.

Table 5-14. The basic information of the measured dwelling in Baishi Village

Length	Width	Height	WWR	Orientation	Exterior wall material	Main room ratio
20.4m	7.8m	5.3m	0.12	Southeast	Bamboo clay/ Timber	70%

(3) Physical environment measurement

1) The temperature and relative humidity measurement in winter.

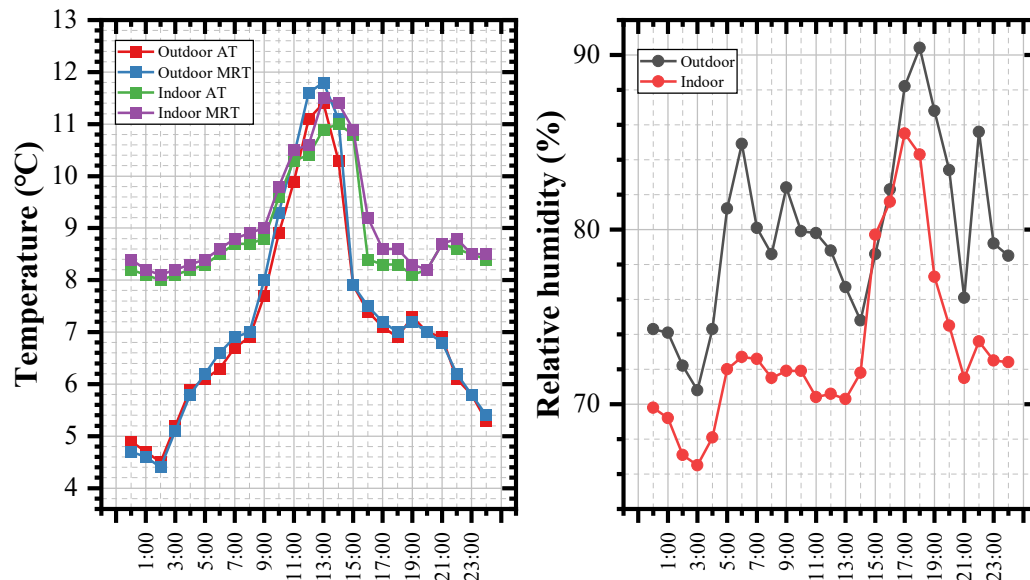


Figure 5-19. The temperature and relative humidity of the measured dwelling in winter in Baishi Village

a. Winter temperature. As shown in Figure 5-19 and Table 5-15, during the 24-hours winter test day in Pingchang County, the outdoor maximum air temperature is 11.40°C, the lowest air temperature is 4.50°C and the average air temperature is 7.13°C. The highest indoor air temperature is 11.01°C, the lowest is 8.10°C, and the average air temperature is 9.08°C, which is higher than that of the outdoor, but it is still lower than the thermal comfort temperature range of human body. The fluctuation range of the indoor air temperature is 2.91°C, which is gentler than that of the outdoor air temperature with the value of 6.90°C. The average indoor and outdoor mean radiant temperature has the same trend as that of the air temperature. The average outdoor and indoor mean radiant temperature is 7.26°C and 9.08°C, respectively. The indoor and outdoor air temperature and mean radian temperature in Pingchang County in winter is too low, far below the thermal comfort temperature range of human body. The traditional dwelling can keep the indoor temperature maintain at a stable level and prevent drastic temperature fluctuations.

Table 5-15. The temperature analysis of the measured dwelling in winter

Measuring point	Air temperature (°C)				Mean radiant temperature (°C)			
	Max	Min	Mean	Fluctuation range	Max	Min	Mean	Fluctuation range
Outdoor	11.40	4.50	7.13	6.90	11.80	4.40	7.26	7.40
Indoor	11.01	8.10	9.08	2.91	11.50	8.10	9.08	3.40

b. Winter relative humidity. As we can see from Figure 5-19 and Table 5-16, during the 24-hours winter test day in Pingchang County, the maximum value, minimum value, and mean value of the outdoor relative humidity are 90.40%, 70.80%, and 79.68%, respectively. And the maximum, minimum, and mean indoor relative humidity is 85.50%, 66.50%, and 73.17%, respectively. The variation range of outdoor relative humidity was 19.60%, compared with that of the indoor value of 19.00%.

In winter, the indoor and outdoor relative humidity in Pingchang County in most of the day is very high. Although the indoor relative humidity and its variation range is smaller than that of the outdoor, it is still far beyond the human comfort requirements. The improvement of indoor humidity in traditional dwellings is not obvious.

Table 5-16. The relative humidity analysis of the measured dwelling in winter

Measuring point	Relative humidity (%)			
	Max	Min	Mean	Fluctuation range
Outdoor	90.40	70.80	79.68	19.60
Indoor	85.50	66.50	73.17	19.00

2) The temperature and relative humidity measurement in summer

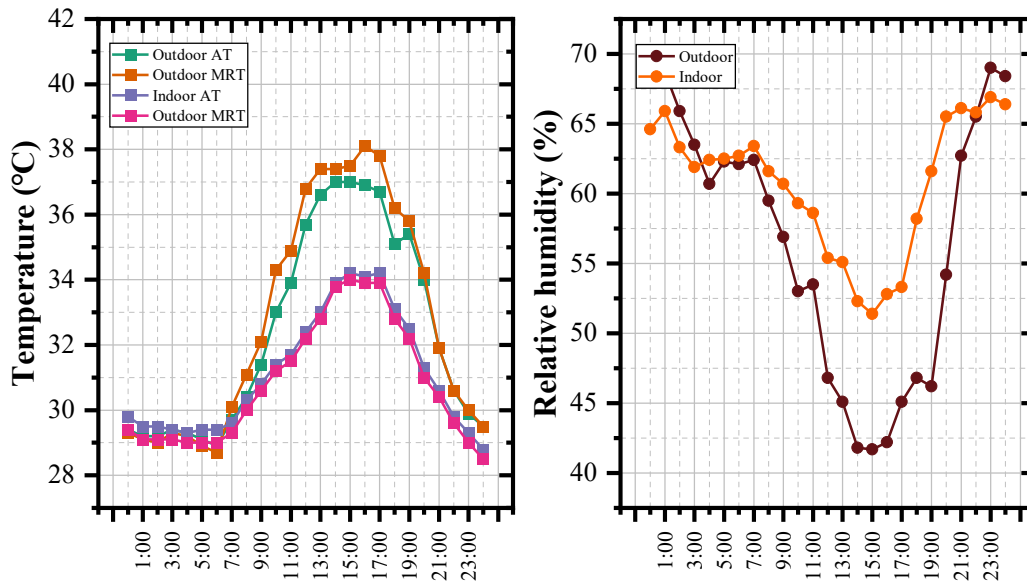


Figure 5-20. The temperature and relative humidity of the measured dwelling in winter in Baishi Village

a. Summer temperature. As shown in Figure 5-20 and Table 5-17, during the 24-hours summer test day in Pingchang County, the outdoor maximum air temperature is 37.00°C, the lowest air temperature is 28.90°C and the average air temperature is 32.37°C. The highest indoor air temperature is 34.20°C, the lowest is 28.80°C, and the average air temperature is 31.09°C. The fluctuation range of the indoor air temperature is 5.40°C, which is gentler than that of the outdoor air temperature with the value of 8.10°C. The average indoor and outdoor mean radiant temperature has the same trend as that of the air temperature. The average outdoor and indoor mean radiant temperature is 32.77°C and 30.82°C, respectively.

In summer, the indoor and outdoor air temperature and mean radiant temperature is high in most of the day, exceeding the thermal comfort temperature range of human body. The regulating effect of traditional dwelling on the indoor temperature is not obvious.

Table 5-17. The temperature analysis of the measured dwelling in summer

Measuring point	Air temperature (°C)				Mean radiant temperature (%)			
	Max	Min	Mean	Fluctuation range	Max	Min	Mean	Fluctuation range
Outdoor	37.00	28.90	32.37	8.10	38.10	28.70	32.77	9.40
Indoor	34.20	28.80	31.09	5.40	34.01	28.50	30.82	5.51

b. Summer relative humidity. As we can see from Figure 5-20 and Table 5-18, during the 24-hours summer test day in Pingchang County, the maximum value, minimum value, and

mean value of the outdoor relative humidity are 69.00%, 41.70%, and 56.51%, respectively. And the maximum, minimum, and mean indoor relative humidity is 66.90%, 51.40%, and 60.71%, respectively. The variation range of outdoor relative humidity was 27.30%, compared with that of the indoor value of 15.50%.

The indoor and outdoor relative humidity in Pingchang County in summer is moderate, basically meets the standard requirements. And the variation range of indoor relative humidity is smaller than that of outdoor, indicating that the traditional dwelling has the function of adjusting humidity.

Table 5-18. The relative humidity analysis of the measured dwelling in summer

Measuring point	Relative humidity (%)			
	Max	Min	Mean	Fluctuation range
Outdoor	69.00	41.70	56.51	27.30
Indoor	66.90	51.40 <td>60.71</td> <td>15.50</td>	60.71	15.50

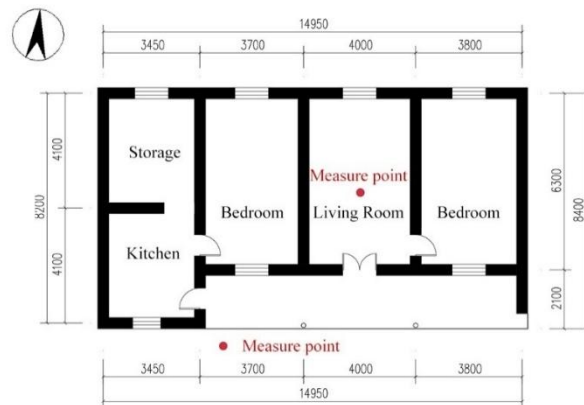
5.6.3. Traditional dwelling in climatic sub-region B1

(1) Basic information of Nanba Village



(a)

(b)



(c)

Figure 5-21. The traditional dwelling in Nanba Village (a) The location of the traditional village (b) The image of the traditional dwelling (c) The plan of the traditional dwelling

The tested dwelling is located in Nanba Village, Qingmuchuan Town, Ningqiang County, Hanzhong City, which belongs to the climatic sub-region B1. Qingmuchuan Town is a famous historical and cultural town in China, with a north high and south low terrain and an elevation of 680 meters. The annual rainfall is 980mm, and the average annual temperature is 13.5°C [32]. The village is located in a valley area, as shown in Figure 5-21(a), and some traditional dwellings are preserved in the village.

(2) The current situation of the test dwelling.

The tested traditional dwelling is located in Nanba village, built around 1920. It is a two-story "I"-shaped dwelling, as shown in Figure 5-21(b) and 5-21(c). The building is oriented to south and has four bays. The west bay was added on the basis of the original three bays. The width and depth of the room unit are 3.8m and 6.3m, respectively. The central room is the living room, and there are bedrooms on both sides. The kitchen and storage room are located on the western side, while the second floor is mainly used for bedrooms and storage. The traditional dwelling adopts rammed earth walls, with a stone masonry foundation at the bottom that provides waterproofing. The roof is covered with small clay tiles, and the windows and doors are made of wooden frames with a window-to-wall ratio of 0.10. Currently, the traditional dwelling is inhabited by two generations of three people, and the main living area accounts for 70% of the total area. The basic information of the traditional dwelling is presented in Table 5-19.

Table 5-19. The basic information of the measured dwelling in Nanba Village

Length	Width	Height	WWR	Orientation	Exterior wall material	Main room ratio
14.95m	8.4m	5.1m	0.10	South	Rammed earth	70%

(3) Physical environment measurement

1) The temperature and relative humidity measurement in winter

a. Winter temperature. As shown in Figure 5-22 and Table 5-20, during the 24-hours winter test day in Ningqiang County, the outdoor maximum air temperature is 6.50°C, the lowest air temperature is 1.10°C and the average air temperature is 3.54°C. The highest indoor air temperature is 8.30°C, the lowest is 5.6°C, and the average air temperature is 6.61°C, which is higher than that of the outdoor, but it is still lower than the thermal comfort temperature range of human body. The fluctuation range of the indoor air temperature is 2.7°C, which is gentler than that of the outdoor air temperature with the value of 5.4°C. The average indoor and outdoor mean radiant temperature has the same trend as that of the air temperature. The average outdoor and indoor mean radiant temperature is 3.90°C and 6.38°C, respectively.

The indoor and outdoor air temperature and mean radian temperature in Ningqiang County in winter is too low, far below the thermal comfort temperature range of human body. And the

traditional dwelling has certain heat preservation effect and can stabilize the indoor temperature.

Table 5-20. The temperature analysis of the measured dwelling in winter

Measuring point	Air temperature (°C)				Mean radiant temperature (%)			
	Max	Min	Mean	Fluctuation range	Max	Min	Mean	Fluctuation range
Outdoor	6.5	1.1	3.54	5.4	7.7	1	3.9	6.7
Indoor	8.3	5.6	6.61	2.7	8.4	5.2	6.38	3.2

b. Winter relative humidity. As we can see from Figure 5-22 and Table 5-21, during the 24-hours winter test day in Ningqiang County, the maximum value, minimum value, and mean value of the outdoor relative humidity are 95.7%, 70.6%, and 86.77%, respectively. And the maximum, minimum, and mean indoor relative humidity is 77.8%, 68.9%, and 74.03%, respectively. The variation range of outdoor relative humidity was 25.1%, compared with that of the indoor value of 8.9%.

The indoor and outdoor relative humidity in Ningqiang County in most of the day is very high. Although the indoor relative humidity and its variation range is smaller than that of the outdoor, it is still far beyond the human comfort requirements.

Table 5-21. The relative humidity analysis of the measured dwelling in winter

Measuring point	Relative humidity (%)			
	Max	Min	Mean	Fluctuation range
Outdoor	95.7	70.6	86.77	25.1
Indoor	77.8	68.9	74.03	8.9

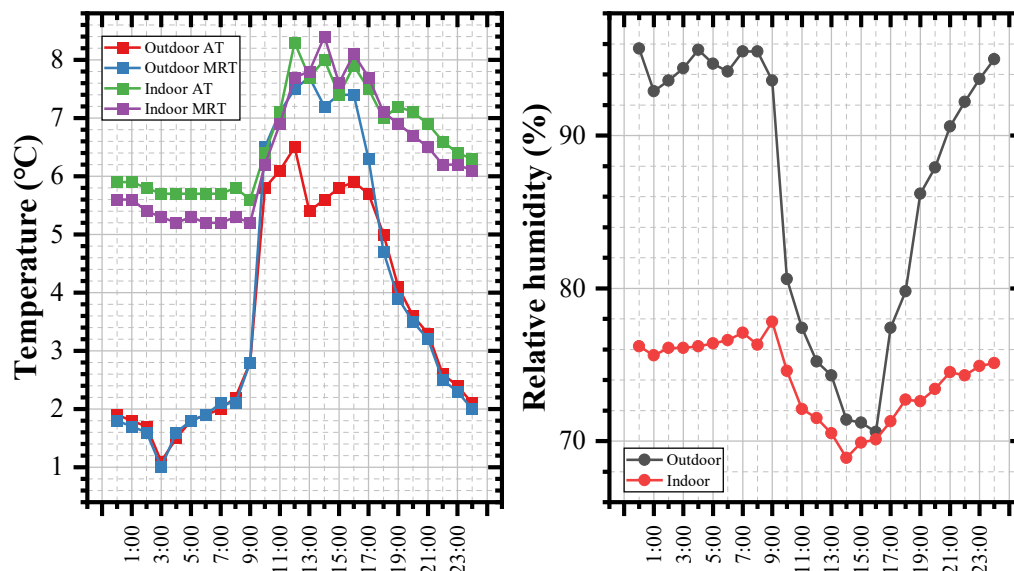


Figure 5-22. The temperature and relative humidity of the measured dwelling in winter in Nanba Village

2) The temperature and relative humidity measurement in summer

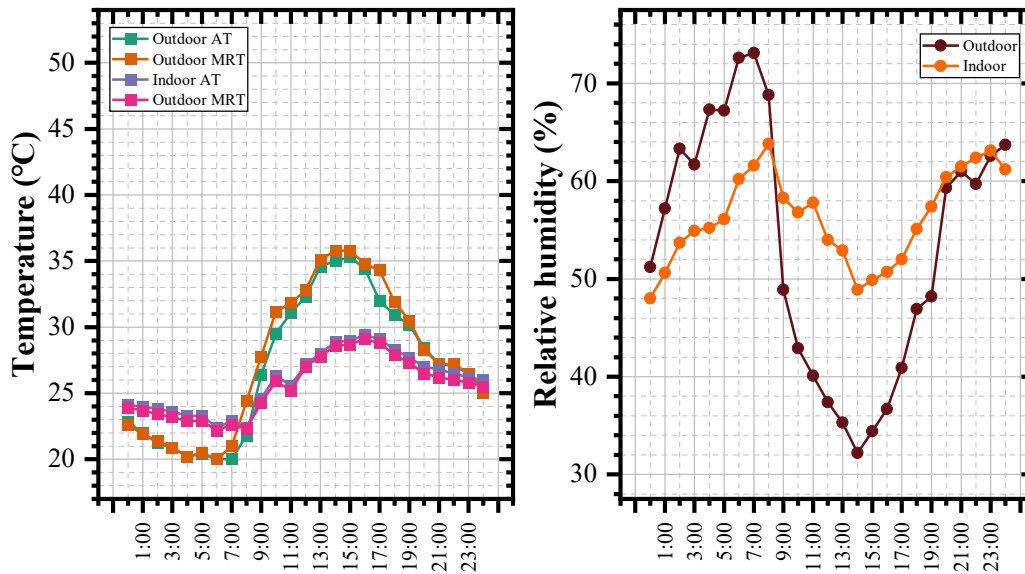


Figure 5-23. The temperature and relative humidity of the measured dwelling in winter in Nanba Village

a. Summer temperature. As shown in Figure 5-23 and Table 5-22, during the 24-hours summer test day in Ningqiang County, the outdoor maximum air temperature is 35.3°C, the lowest air temperature is 20°C and the average air temperature is 27.02°C. The highest indoor air temperature is 29.4°C, the lowest is 22.4°C, and the average air temperature is 25.86°C, which is cooler than the outdoor temperature and meets the thermal comfort requirements of residents most of the time. The fluctuation range of the indoor air temperature is 7°C, which is gentler than that of the outdoor air temperature with the value of 15.3°C. The average indoor and outdoor mean radiant temperature has the same trend as that of the air temperature. The average outdoor and indoor mean radiant temperature is 27.56°C and 25.51°C, respectively.

In summer, although the outdoor air temperature and mean radian temperature in Ningqiang County is high, the indoor air temperature and mean radian temperature basically meet the thermal comfort requirements of residents, indicating that the traditional dwelling can keep the indoor space cool by isolating excess heat in the summer.

Table 5-22. The temperature analysis of the measured dwelling in summer

Measuring point	Air temperature (°C)				Mean radiant temperature (%)			
	Max	Min	Mean	Fluctuation range	Max	Min	Mean	Fluctuation range
Outdoor	35.30	20.00	27.02	15.30	35.80	19.80	27.56	16.00
Indoor	29.40	22.40	25.86	7.00	29.10	22.20	25.51	6.90

b. Summer relative humidity. As we can see from Figure 5-23 and Table 5-23, during the 24-hours summer test day in Ningqiang County, the maximum value, minimum value, and mean value of the outdoor relative humidity are 73.1%, 32.2%, and 53.30%, respectively. And the maximum, minimum, and mean indoor relative humidity is 63.80%, 48.0%, and 56.26%, respectively. The variation range of outdoor relative humidity was 40.9%, compared with that of the indoor value of 15.8%.

Table 5-23. The relative humidity analysis of the measured dwelling in summer

Measuring point	Relative humidity (%)			
	Max	Min	Mean	Fluctuation range
Outdoor	73.10	32.20	53.30	40.90
Indoor	63.80	48.00	56.26	15.80

The indoor and outdoor relative humidity in Ningqiang County in summer is moderate, basically meets the standard requirements. And the variation range of indoor relative humidity is smaller than that of outdoor, indicating that the traditional dwelling has the function of adjusting humidity.

5.6.4. Traditional dwelling in climatic sub-region B2

(1) Basic information of Xiadianzi Village

The tested dwelling is located in Xiadianzi Village, Jundian Town, Fangxian County, Shiyan City, which belongs to the climatic sub-region B2 and has been selected as a traditional Chinese village. The village is mainly located on the foothills and flat terrains, with an altitude of about 726 meters. The annual rainfall is 914 mm and the average annual temperature is 10~15°C, with a population of 15,000 people [33]. The village is distributed along the river and the main roads in a belt shape and is a typical valley-type village, as shown in Figure 5-24(a). Traditional dwellings are well-preserved in the village.

(2) The current situation of the test dwelling.

The tested dwelling was built around 1940 and consists of one floor, in an “L” shape. The current condition and floor plan of the traditional dwelling are shown in Figure 5-24(b) and 5-24(c), respectively. The dwelling is oriented in a north-south direction, with the main orientation spanning 7 bays and the secondary orientation spanning 2 bays. The width and depth of the room unit are 4m and 5.5m, respectively. The living room is located in the middle of the main orientation, and the bedrooms are located on both sides. The kitchen and auxiliary rooms are located at the corners of the building.

The dwelling adopts rammed earth walls, and reinforced with bricks at the lower part, which not only ensures a sturdy structure but also provides partial waterproofing. The walls are

decorated with plaster. The roof is covered with clay tiles, and the doors and windows are wooden frames with a window-wall ratio of 0.08. The traditional dwelling is currently inhabited by two generations of six people, and the main use rooms account for 75% of the total area. The basic information of the traditional dwelling is shown in Table 5-24.

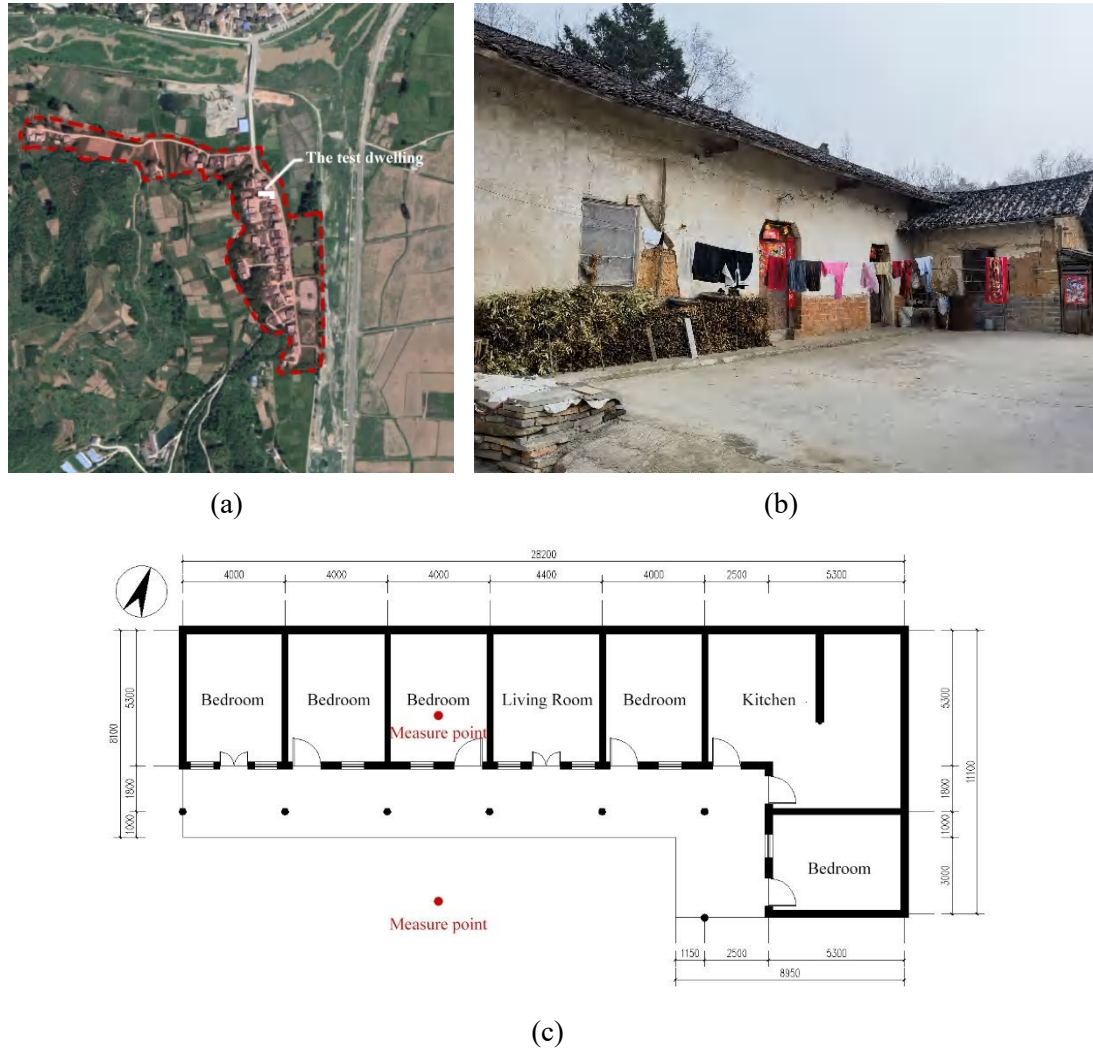


Figure 5-24. The traditional dwelling in Xiadianzi County (a) The location of the traditional village (b) The image of the traditional dwelling (c) The plan of the traditional dwelling

Table 5-24. The basic information of the measured dwelling in Xiadianzi Village

Length	Width	Height	WWR	Orientation	Exterior wall material	Main room ratio
28.2m	11.1m	4.2m	0.08	South	Rammed earth	75%

(3) Physical environment measurement.

1) The temperature and relative humidity measurement in winter.

a. Winter temperature. As shown in Figure 5-25 and Table 5-25, during the 24-hours winter

test day in Fang County, the outdoor maximum air temperature is 8.60°C, the lowest air temperature is 2.60°C and the average air temperature is 4.28°C. The highest indoor air temperature is 9.0°C, the lowest is 6.4°C, and the average air temperature is 6.98°C, which is higher than that of the outdoor, but it is still lower than the thermal comfort temperature range of human body. The fluctuation range of the indoor air temperature is 2.6°C, which is gentler than that of the outdoor air temperature with the value of 6.0°C. The average indoor and outdoor mean radiant temperature has the same trend as that of the air temperature. The average outdoor and indoor mean radiant temperature is 4.49°C and 6.64°C, respectively.

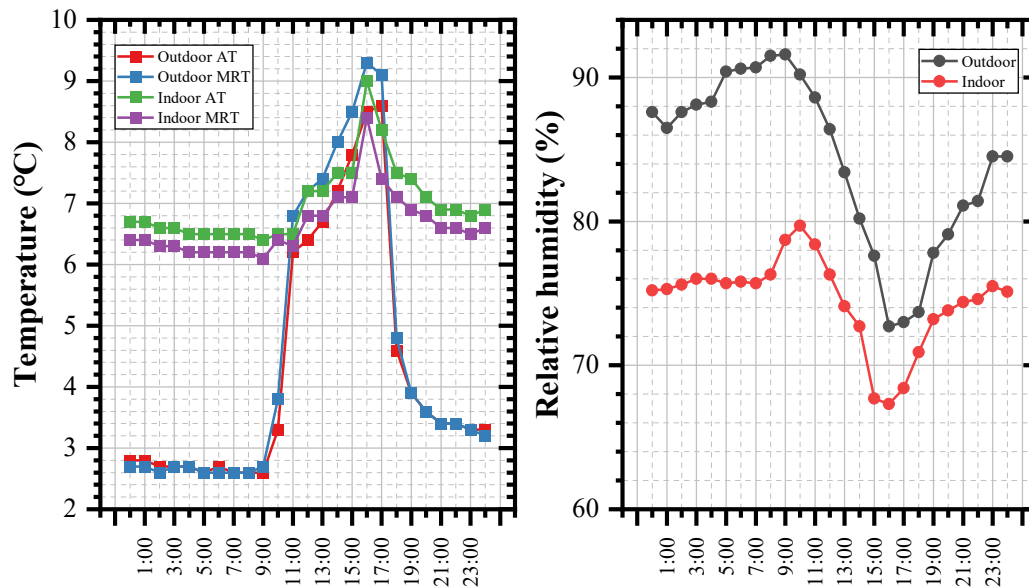


Figure 5-25. The temperature and relative humidity of the measured dwelling in winter in Xiadianzi Village

The indoor and outdoor air temperature and mean radian temperature in Foping County in winter is too low, far below the thermal comfort temperature range of human body. And the traditional dwelling has certain heat preservation effect and can stabilize the indoor temperature.

Table 5-25. The temperature analysis of the measured dwelling in winter

Measuring point	Air temperature (°C)				Mean radiant temperature (%)			
	Max	Min	Mean	Fluctuation range	Max	Min	Mean	Fluctuation range
Outdoor	8.6	2.6	4.28	6	9.3	2.6	4.49	6.7
Indoor	9	6.4	6.98	2.6	8.4	6.1	6.64	2.3

b. Winter relative humidity. As we can see from Figure 5-25 and Table 5-26, during the 24-hours winter test day in Fang County, the maximum value, minimum value, and mean value of the outdoor relative humidity are 91.60%, 72.7%, and 84.28%, respectively. And the

maximum, minimum, and mean indoor relative humidity is 79.7%, 67.3%, and 74.50%, respectively. The variation range of outdoor relative humidity was 18.9%, compared with that of the indoor value of 12.4%.

Table 5-26. The relative humidity analysis of the measured dwelling in winter

Measuring point	Relative humidity (%)			
	Max	Min	Mean	Fluctuation range
Outdoor	91.6	72.7	84.28	18.9
Indoor	79.7	67.3	74.50	12.4

The outdoor relative humidity in Fang County in most of the day is very high. Although the indoor relative humidity and its variation range is smaller than that of the outdoor, it is still far beyond the human comfort requirements.

2) The temperature and relative humidity measurement in summer

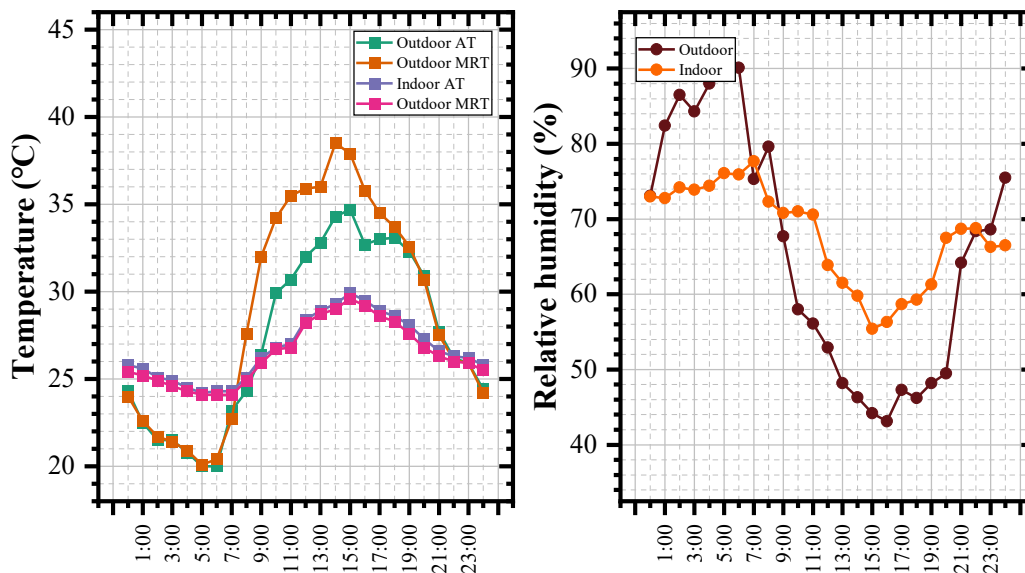


Figure 5-26. The temperature and relative humidity of the measured dwelling in winter in Xiadianzi Village

a. Summer temperature. As shown in Figure 5-26 and Table 5-27, during the 24-hours summer test day in Fang County, the outdoor maximum air temperature is 34.7°C, the lowest air temperature is 20.30°C and the average air temperature is 27.40°C. The highest indoor air temperature is 29.9°C, the lowest is 24.2°C, and the average air temperature is 26.70°C, which is cooler than the outdoor temperature and meets the thermal comfort requirements of residents. The fluctuation range of the indoor air temperature is 5.70°C, which is gentler than that of the outdoor air temperature with the value of 14.70°C. The average indoor and outdoor mean

radiant temperature has the same trend as that of the air temperature. The average outdoor and indoor mean radiant temperature is 28.90°C and 26.43°C, respectively.

Generally speaking, the outdoor air temperature in Fang County is high in most of the daytime, exceeding the thermal comfort temperature range of human body. However, the indoor air temperature is relatively moderate in most of the time, and the traditional dwelling prevents excess heat from entering the house in summer and keeps a moderate indoor thermal environment.

Table 5-27. The temperature analysis of the measured dwelling in summer

Measuring point	Air temperature (°C)				Mean radiant temperature (%)			
	Max	Min	Mean	Fluctuation range	Max	Min	Mean	Fluctuation range
Outdoor	34.7	20.30	27.40	14.7	38.5	20.1	28.90	18.4
Indoor	29.9	24.2	26.70	5.7	29.6	24.1	26.43	5.5

b. Summer relative humidity. As we can see from Figure 5-26 and Table 5-28, during the 24-hours summer test day in Fang County, the maximum value, minimum value, and mean value of the outdoor relative humidity are 92.90%, 43.10%, and 65.46%, respectively. And the maximum, minimum, and mean indoor relative humidity is 77.7%, 55.4%, and 67.87%, respectively. The variation range of outdoor relative humidity was 49.8%, compared with that of the indoor value of 22.3%.

Generally speaking, the indoor and outdoor relative humidity in Fang County in summer is high during nighttime, exceeding 70% of the standard requirements. And the variation range of indoor relative humidity is smaller than that of outdoor, indicating that the traditional dwelling has the function of adjusting humidity.

Table 5-28. The relative humidity analysis of the measured dwelling in summer

Measuring point	Relative humidity (%)			
	Max	Min	Mean	Fluctuation range
Outdoor	92.9	43.1	65.46	49.8
Indoor	77.7	55.4	67.87	22.3

5.6.5. Traditional dwelling in climatic sub-region C

(1) Basic information of Tangwan Village

The tested dwelling is located in Tangwan Village, Yuanjiazhuang Town, Foping County, in climatic sub-region C. The village is situated in a valley at an altitude of approximately 780m, with an annual average rainfall of 937mm and an average temperature of 11.5°C, and a population of about 10,000 [33]. The village is arranged in a strip shape along the valley, with

the main road as the center, forming a typical valley-type village pattern as shown in Figure 5-27(a). Except for the old street in the village, which has retained its original layout, most of the other traditional dwellings have been rebuilt or renovated.

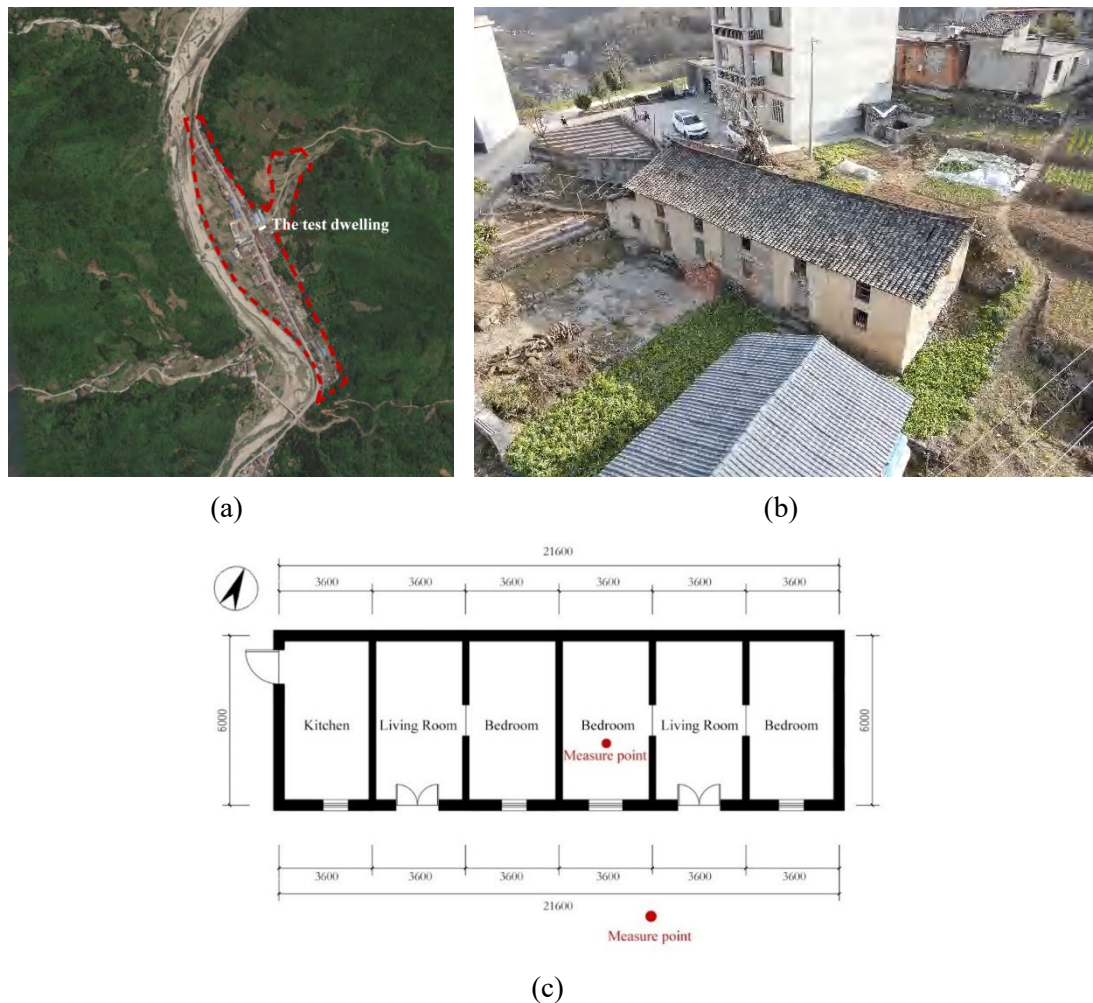


Figure 5-27. The traditional dwelling in Tangwan Village (a) The location of the traditional village (b) The image of the traditional dwelling (c) The plan of the traditional dwelling

(2) The current situation of the test dwelling

The tested dwelling was built around 1920 and is a two-story “I”-shaped dwelling. The images and first floor plan of the traditional dwelling are shown in Figure 5-27 (b) and 5-27(c), respectively. The dwelling faces south, with a total of 6 bays. The width and depth of the room unit are 3.6m and 6.0m, respectively. The living room is located in the middle, with bedrooms on either side, and the kitchen is on the west side of the building. Additionally, some bedrooms and storage rooms are on the second floor. The dwelling is constructed with rammed earth walls, with a stone base for waterproofing and no plaster decoration on the interior and exterior walls. The roof material is clay tiles, and the doors and windows are made of wooden frames, with a

window-to-wall ratio of 0.10. Currently, the house is inhabited by 7 people, and the main living area accounts for 27.2% of the total floor area. The basic information of the traditional dwelling is shown in Table 5-29.

Table 5-29. The basic information of the measured dwelling in Tangwan Village

Length	Width	Height	WWR	Orientation	Exterior wall material	Main room ratio
21.6m	6.0m	4.8m	0.10	South	Rammed earth	72.7%

(3) Physical environment measurement

1) The temperature and relative humidity measurement in winter

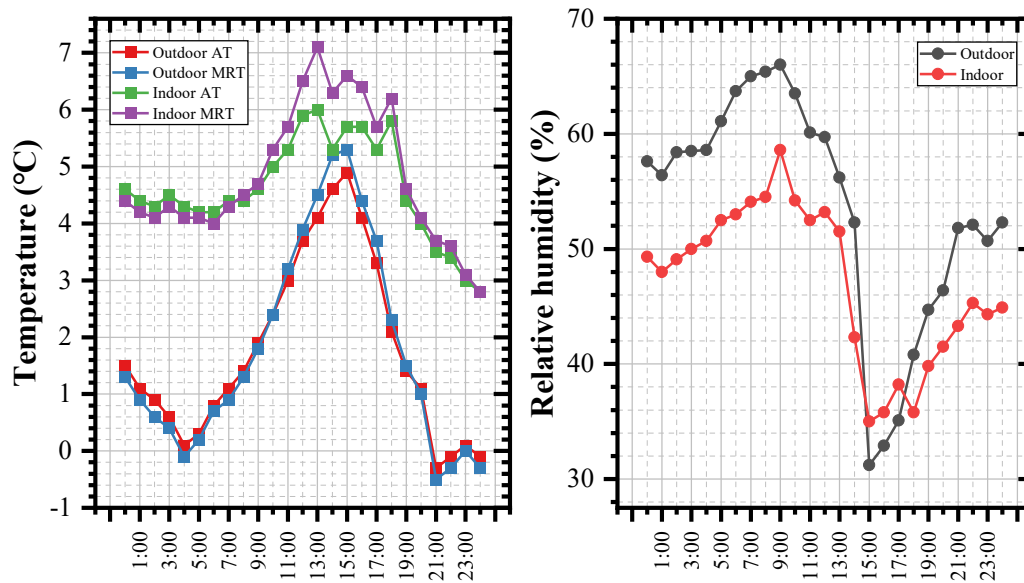


Figure 5-28. The temperature and relative humidity of the measured dwelling in winter in Tangwan Village

a. Winter temperature. As shown in Figure 5-28 and Table 5-30, during the 24-hours winter test day in Foping County, the outdoor maximum air temperature is 4.90°C , the lowest air temperature is -0.30°C and the average air temperature is 1.76°C . The highest indoor air temperature is 6°C , the lowest is 2.8°C , and the average air temperature is 4.60°C , which is higher than that of the outdoor, but it is still lower than the thermal comfort temperature range of human body. The fluctuation range of the indoor air temperature is 3.2°C , which is gentler than that of the outdoor air temperature with the value of 5.2°C . The average indoor and outdoor mean radiant temperature has the same trend as that of the air temperature. The average outdoor and indoor mean radiant temperature is 1.77°C and 4.3°C , respectively.

Generally speaking, the indoor and outdoor air temperature and mean radian temperature in Foping County in winter is too low, far below the thermal comfort temperature range of human

body. And the traditional dwelling has certain heat preservation effect and can stabilize the indoor temperature.

Table 5-30. The temperature analysis of the measured dwelling in winter

Measuring point	Air temperature (°C)				Mean radiant temperature (%)			
	Max	Min	Mean	Fluctuation range	Max	Min	Mean	Fluctuation range
Outdoor	4.90	-0.30	1.76	5.20	5.30	-0.50	1.77	5.80
Indoor	6.00	2.80	4.60	3.20	7.10	2.80	4.82	4.30

b. Winter relative humidity. As we can see from Figure 5-28 and Table 5-31, during the 24-hours winter test day in Foping County, the maximum value, minimum value, and mean value of the outdoor relative humidity are 66.01%, 31.2%, and 53.62%, respectively. And the maximum, minimum, and mean indoor relative humidity is 58.6%, 35%, and 47.1%, respectively. The variation range of outdoor relative humidity was 34.81%, compared with that of the indoor value of 23.6%.

Table 5-31. The relative humidity analysis of the measured dwelling in winter

Measuring point	Relative humidity (%)			
	Max	Min	Mean	Fluctuation range
Outdoor	66.01	31.20	53.62	34.81
Indoor	58.60	35.00	47.10	23.60

Generally speaking, the indoor and outdoor relative humidity in Foping County in winter meets the standard requirements, and the variation range of indoor relative humidity is smaller than that of outdoor, indicating that the traditional dwelling have the function of adjusting humidity.

2) The temperature and relative humidity measurement in summer.

a. Summer temperature. As shown in Figure 5-29 and Table 5-32, during the 24-hours summer test day, the outdoor maximum air temperature is 28.10°C, the lowest air temperature is 17.30°C and the average air temperature is 22.21°C. The highest indoor air temperature is 23.10°C, the lowest is 19.90°C, and the average air temperature is 21.02°C, which is cooler than the outdoor temperature and meets the thermal comfort requirements of residents. The fluctuation range of the indoor air temperature is 3.20°C, which is gentler than that of the outdoor air temperature with the value of 10.8°C. The average indoor and outdoor mean radiant temperature has the same trend as that of the air temperature. The average outdoor and indoor mean radiant temperature is 22.68°C and 20.64°C, respectively.

Generally speaking, the indoor and outdoor air temperature and mean radian temperature in Foping County in summer basically meet the thermal comfort requirements of residents, and

the traditional dwelling can keep the indoor space cool by isolating excess heat in the summer.

Table 5-32. The temperature analysis of the measured dwelling in summer

Measuring point	Air temperature (°C)				Mean radiant temperature (%)			
	Max	Min	Mean	Fluctuation range	Max	Min	Mean	Fluctuation range
Outdoor	28.10	17.30	22.21	10.8	29.20	17.60	22.68	11.60
Indoor	23.10	19.90	21.02	3.20	23.20	19.50	20.64	3.70

b. Summer relative humidity. As we can see from Figure 5-29 and Table 5-33, during the 24-hours summer test day, the maximum value, minimum value, and mean value of the outdoor relative humidity are 89.30%, 40.90%, and 66.16%, respectively. And the maximum, minimum, and mean indoor relative humidity is 80.50%, 46.20%, and 64.3%, respectively. The variation range of outdoor relative humidity was 48.4%, compared with that of the indoor value of 34.3%.

Generally speaking, the indoor and outdoor relative humidity in Foping County in summer is high in part of the time, exceeding 70% of the standard requirements. And the variation range of indoor relative humidity is smaller than that of outdoor, indicating that the traditional dwelling have the function of adjusting humidity.

Table 5-33. The relative humidity analysis of the measured dwelling in winter

Measuring point	Relative humidity (%)			
	Max	Min	Mean	Fluctuation range
Outdoor	89.30	40.90	66.16	48.40
Indoor	80.50	46.20	64.30	34.30

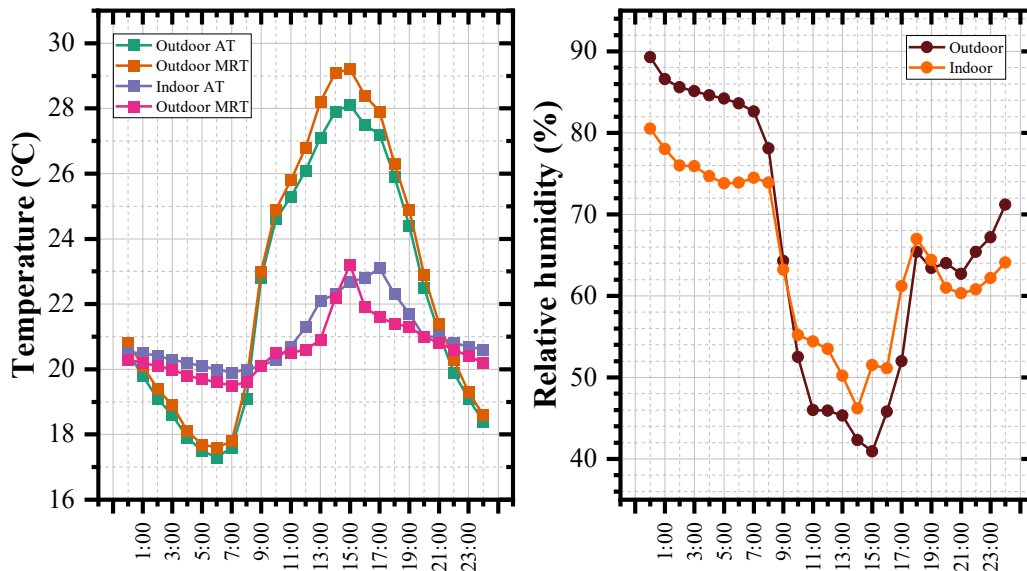


Figure 5-29. The temperature and relative humidity of the measured dwelling in winter in Tangwan Village

5.7. Summary

In this chapter, by using the field survey method, the characteristics of traditional settlements, courtyards, and residential dwellings were summarized, and the environmental parameters measurement of 5 sub-climatic sub-regions were conducted. The main conclusions are as follows:

(1) According to the mountain geomorphic environment and settlement location in Qinba Mountainous Area, the settlements in this area could be divided into three types, which are settlement in the gully, settlement leaning against the mountain, and settlement on the mountain slope. Three typical types of settlements are selected for investigation to summarize the advantages and problems of climate suitability of traditional mountainous settlements' site selection in Qinba Mountainous Area. It could be seen that, in summer, the climate adaptability is good, the surrounding environment of settlement could be used to obtain better microclimate, and the settlement location is conducive to internal ventilation and solar radiation. However, in winter, based on the insufficient solar radiation and poor ventilation, the thermal comfort of the settlement is undesirable. At last, the paper puts forward the climate adaptability strategies and regeneration planning guidelines of the traditional mountainous settlements in Qinba Mountainous Area.

(2) Through the field research, it can be seen that the building layout of traditional dwellings in Qinba mountainous area can be divided into 4 types, the "I"-shaped dwelling, the "L"-shaped dwelling, the "U"-shaped dwelling, and the "□"-shaped building, accounting for 52.0%, 23.5%, 12.0% and 12.5% of the total sample size, respectively. According to the architectural form, the courtyards are divided into 3 types: open courtyards, semi-open courtyards, and closed courtyards, accounting for 75.5%, 12%, and 12.5% of the total sample size, respectively.

(3) The traditional dwellings in Qinba mountainous area showed a trend of decreasing from south to north in the width of the rooms, the south-facing window to wall ratio, the slope of the roof and the degree of architectural decoration. In the southern part of the research area, with a relatively warm climate, which belongs to the sub-region A1 and A2, traditional dwellings commonly adopt timber walls and bamboo clay walls, with relatively larger window-to-wall ratios of 0.10~0.15. In contrast, in the northern part of the research area, with a relatively cold climate, which belongs to the sub-region B1, B2, and C, traditional dwellings usually use rammed earth walls, and the window-to-wall ratios are smaller, around 0.08~0.12.

(4) The research team also conducted multiple investigations on traditional dwellings in Qinba mountainous area during winter and summer. Through the measurement of the physical environment of the traditional dwellings in 5 climatic sub-regions, the Qinba mountainous area is generally cold in winter with high relative humidity, and indoor temperature and relative humidity cannot meet the requirements of human comfort. In summer, except for some areas

where indoor temperature exceeds human comfort requirements at certain times, most of the time the indoor temperature is moderate. However, the overall humidity in the Qinba mountainous area in summer is high and cannot meet human comfort requirements. In general, the variation range of indoor temperature and humidity in traditional dwellings is smaller than that outdoors. The traditional dwellings have a certain regulating effect on the indoor physical environment.

Reference.

- [1] Y. Liu, *Building Climatology*. Beijing, China: China Building Industry Press, 2010.
- [2] B. Jing, "Research on evolution pattern and spatial management and control of man-land system in Qinba mountainous area," Ph.D. Thesis, Northwest University, 2020.
- [3] P. Zhang, J. Li, and Z. Li, "Spatial-temporal distribution characteristics and influencing factors of traditional villages in Qinling-Daba mountains," *Journal of Human Settlement in West China*, vol. 35, no. 03, pp. 116-124, 2020.
- [4] G. Guan, "Investigation Study Spatially Of Dong-Traditional-Village In Qiandongnan Region," Master Thesis, Xi'an University of Architecture and Technology, 2015.
- [5] T. Kane, "Indoor temperatures in UK dwellings: investigating heating practices using field survey data," © Tom Kane, 2013.
- [6] Q. Zhang, "Relevance Study on Settlement Space Characters and Climate Adaptation," Doctoral thesis, Huazhong University of Science and Technology, 2012.
- [7] P. Jia, "Southern Shaanxi Mountain Settlement Climate Adaptation of the Traditional Settlements Environment Space Characteristics," Master Thesis, Xi'an University of Architecture and Technology, 2015.
- [8] S. Chen, M. S. Mehmood, S. Liu, and Y. Gao, "Spatial Pattern and Influencing Factors of Rural Settlements in Qinba Mountains, Shaanxi Province, China," *Sustainability*, vol. 14, no. 16, p. 10095, 2022.
- [9] J. Zhai, "Preliminary studying on the characteristics of Climatic Adaptability of Valley Traditional Settlement environment Space Form," Master Thesis, Xi'an University of Architecture and Technology, 2014.
- [10] M. Cao, "Preliminary studying on the characteristics of Climatic Adaptability of Backer Traditional Settlement environment Space Form," Master Thesis, Xi'an University of Architecture and Technology, 2014.
- [11] J. Zhang, "Study on integral protection and renewal design of traditional villages in southern Shaanxi," Master Thesis, Xi'an University of Architecture and Technology, 2020.
- [12] J. Liang, "Slope type climate adaptation of the traditional settlements environment space characteristics," Master Thesis, Xi'an University of Architecture and Technology, 2014.
- [13] R. Yang, Q. Xu, and H. Long, "Spatial distribution characteristics and optimized reconstruction analysis of China's rural settlements during the process of rapid urbanization," *Journal of rural studies*, vol. 47, pp. 413-424, 2016.
- [14] J. Qiming, *Geography of Rural Settlements*. Beijing, China: Science Press, 1988.
- [15] Y. Gao, M. Wang, and J. Liu, "The preliminary investigation on the green building modes of the traditional residences in Qinba Mountain Area," *Architecture & Culture*, no. 10, pp. 65-67, 2013.

[16] L. Zhao and J. Xu, "Architectural design of Residential Buildings in Qinba Mountains based on knowledge mapping," *Case Studies in Thermal Engineering*, vol. 14, p. 100412, 2019.

[17] S. Yang, "Research on spatial morphology evolution and design strategy of folk dwellings in southern shaanxi province," Master Thesis, Chang'an University, 2019.

[18] X. Juan, L. Ziliang, G. Weijun, Y. Mengsheng, and S. Menglong, "The comparative study on the climate adaptability based on indoor physical environment of traditional dwelling in Qinba mountainous areas, China," *Energy and Buildings*, vol. 197, pp. 140-155, 2019.

[19] Y. Gao, "Research on Suitable Ecological Construction Modes of Rural Residence in Hot-humid and Cold-wet Mountain Area in Western of China," Ph.D. Thesis, Xi'an University of Architecture and Technology, 2014.

[20] D. Liu, *History of Ancient Chinese Architecture*. Beijing, China: China Architecture & Building Press, 1984.

[21] Y. Zhu, J. Zhao, G. Sang, and Q. Zhao, "Thermal performance and energy-saving construction for rural architecture in Qinba Mountain Areas," *Journal of Ningxia University*, vol. 38, no. 04, pp. 426-432, 2017.

[22] J. Xu and X. Huo, "Study on strategy of inheritance and development of traditional building in Qinba mountains region," *Industrial Construction*, vol. 44, no. 09, pp. 40-44, 2014.

[23] J. Xu, "The strategy of planning and construction research on rural settlement in Qinba mountain area," Ph.D. Thesis, Xi'an University of Architecture and Technology, 2011.

[24] F. Tang, "Research on spatial morphology evolution and design strategy of folk dwellings in southern shaanxi province," Master Thesis, Xi'an University of Architecture and Technology, 2011.

[25] Y. Xu and Z. Yang, "Research on indoor thermal environment and enclosure's thermal characteristics of dwellings with muddy wall circled by bamboos," *Journal of Chongqing University*, vol. 44, no. 03, pp. 22-30, 2021.

[26] T. Zhang, "Study on climate adaptability of typical traditional dwellings envelop," Doctoral Thesis, Xi'an University of Architecture and Technology, 2013.

[27] Z. Tao, Z. Qiwei, Z. Yuxuan, and L. Jiaping, "Research on Winter Climate Adaptabilities and Improvement Strategies of Traditional Rammed Earth Dwellings with Slate Roofs in Qinba Mountains, China."

[28] Y. Zhou and L. gong, "Research on energy-saving renovation of residential cold tile roof in traditional village in Zunyi," *Urbanism and Architecture*, vol. 18, no. 17, pp. 68-71, 2021.

[29] T. Zhang, Q. Zhang, and Y. Mai, "Test Study on Summer Thermal Environment of R ammed Earth Dwellings in Qinba Mountainous Area," *Building Science*, vol. 37, no. 08, pp. 104-109, 2021.

[30] Y. Tang, "Landscape morphology analysis and conservation renewal design of Liyuanba Ancient Village in Tongjiang County," Master Thesis, Sichuan Normal University, 2019.

[31] Y. Zeng, "The study on folk architecture in Sichuan and Chongqing area," Master Thesis, Chongqing University, 2006.

[32] Q. Zhang, "Preliminary study on the traditional dwellings of Qingmochuan Ancient Town in Southern Shaanxi," Master Thesis, Chongqing University, 2008.

[33] J. Zhang, "Research on morphological characteristics and optimization of traditional buildings in Hanzhong based on indoor thermal environment," Master Thesis, Chang'an University, 2022.

Chapter 6

THERMAL COMFORT INVESTIGATION OF THE CLIMATIC SUB-REGIONS

CHAPTER SIX: THERMAL COMFORT INVESTIGATION OF THE CLIMATIC SUB-REGIONS

<i>THERMAL COMFORT INVESTIGATION OF THE CLIMATIC SUB-REGIONS</i>	1
6.1. Contents	1
6.2. Materials and methodology	1
6.2.1. Research background	1
6.2.2. Motivation	2
6.2.4. Summary of traditional dwellings	2
6.2.3. Methods	5
6.3. Research proposal	6
6.3.1. Measurement of environmental parameters	6
6.3.2. Questionnaire research	7
6.4. Analysis of the environmental parameters	8
6.4.1. Temperature	8
6.4.2. Relative humidity	10
6.5. Analysis of indoor thermal comfort	11
6.5.1. Thermal environment evaluation index	11
6.5.2. Residents' thermal adaptive behavior analysis	12
6.5.3. Residents' indoor thermal sensation vote	12
6.5.4. Neutral temperature	14
6.5.5. Thermal comfort range	16
6.5.6. The relationship of MTS and PMV	17
6.6. Energy consumption simulation based on neutral temperature in the climatic sub-regions	20
6.6.1. Energy consumption simulation	20
6.6.2. Simulation result analysis	20
6.6.3. Suggestion on improving indoor thermal environment	21
6.7. Summary	22
Reference	24

6.1. Contents

Traditional dwelling has achieved harmony between building and climatic environment, which has the potential for sustainable development in rural residential buildings. However, few studies have concentrated on the thermal comfort and sensation. In this study, traditional dwellings in the 5 climatic sub-regions in Qinba mountainous area were selected as the research object, and a subjective sensation analysis on the indoor thermal environment was conducted.

The result shows that residents are more satisfied with the indoor thermal environment in summer than in winter. The neutral temperatures of residents are 15.8°C, 15.8°C, 14.3°C, 14.3°C, 13.4°C in winter and 26.6°C, 27.3°C, 26.6°C, 27.3°C, and 26.6°C in summer respectively. In winter, the predicted indoor neutral temperature is higher than the measured thermal neutral temperature, and in summer, the predicted indoor neutral temperature is lower than the measured thermal neutral temperature, showing that the residents have certain adaptability to the actual thermal environment.

Then, the annual building thermal loads of typical traditional dwellings in the 5 climatic sub-regions' representative counties based on standard requirements and measured neutral temperature are simulated. The annual building thermal load based on the measured neutral temperature is much lower than that based on the standard required temperature, indicating that making the appropriate heating and cooling setpoint according to the measured neutral temperature in different climate regions could be more conducive to meeting the thermal comfort needs of residents and reduce building energy consumption to a certain extent.

6.2. Materials and methodology

6.2.1. Research background

Thermal comfort field study has recently attracted the attention of researchers from all around the world. A large number of field test results show that there is a significant difference between the measured thermal sensation of the indoor thermal environment and the predicted results using the international thermal comfort standard ASHRAE 55-2017 [1] and ISO 7730 [2]. The neutral temperature and thermal comfort range vary with the annual average temperature in different regions due to human behavioral adaptability and psychological expectation of the climate [3-6]. The primary research areas of academics from across the world in the field study of thermal comfort are concentrated in public buildings like offices [7, 8] and schools [9, 10], while the research on residential structures is primarily concentrated in urban areas [11]. Due to the scattered distribution and free layout of rural houses, scholars' research on rural residential buildings mainly focuses on the overall layout of settlements [12, 13] and the evolution of residential forms [14, 15]. The research on the indoor thermal environment and comfort of rural residential buildings is very limited.

In addition to China's vast territory, there are differences in climatic conditions and lifestyles

in different regions, and there are also great differences in the heat needs of residents in various areas. At present, the existing research on the thermal comfort of rural residential buildings in China is still concentrated in a few specific areas. Yang et al. [16], Zhu et al. [17], Zhang et al. [18] and Sheng et al [19]. calculated the neutral temperature and the thermal comfort range of rural residential buildings in Shaanxi Province, Hebei Province, Shandong Province, and Heilongjiang Province respectively, which belong to the cold region and severe cold region in china, and finally gave the thermal environment improvement strategies for the rural residential buildings. However, the field investigation of thermal comfort in rural areas is centred on the cold region and severe cold regions as these regions have a relatively harsh indoor thermal environment in winter, and the indoor thermal environment has a higher priority to be renovated.

6.2.2. Motivation



The free operation mode of the rural residential buildings in hot summer and cold winter regions is different from the mixed regulation mode of the buildings in cities. In order to study the indoor thermal comfort of rural residential buildings in this region, the research team conducted on-site environmental parameter tests and subjective thermal sensation questionnaire surveys in winter and summer in rural areas of the Qinba mountainous area. This chapter mainly analyzes the thermal sensation of rural residents in the 5 climatic sub-regions in the study area, the factors affecting thermal sensation, as well as the environmental adaptability measures, and establishes the thermal comfort models for rural residents in each sub-climatic region in Qinba mountainous area.

6.2.4. Summary of traditional dwellings

Through a large number of investigations on settlement units and traditional dwellings in Qinba mountainous area in Chapter 5, the author finds that there are certain rules in the spatial distribution of traditional dwellings. The large acreage of the mountainous region of Qinba features diverse residential building exterior structures in various locations. Our research team discovered that in traditional dwellings, the width of rooms, the proportion of south windows to walls, the slope of roofs, and the amount of architectural ornamentation all reduced from south to north. In particular, the climatic conditions of the hilly region of Qinba are intimately related to the building envelope. The building envelope of the traditional dwellings in the north part is generally rammed earth wall, mainly concentrated in Hanzhong, Ankang, Shiyuan, and other northern cities in Qinba mountainous area. However, the building envelope in the south is dominated by bamboo clay envelopes and timber walls, mainly concentrated in Bazhong, Guangyuan, Longnan, and other southern cities in the Qinba mountainous area. Generally, the building structure system is highly uniform in the study area, with the beam-lifted frame, in which the column and tie are wooden structures. In order to meet the functional needs of the plane, the building generally used a “standard room” with certain width as the building unit to

lay out the plane. This structure belongs to the frame structure, which could provide a flexible plane layout. The roof adopts the small blue tile structure; doors and windows are mostly single-layer wooden doors and windows. The images of the researched dwellings in the south and north parts of Qinba mountainous area are shown in Table 6-1.

Table 6-1. The basic information of the traditional dwellings in Qinba mountainous area

	The traditional dwelling in Sub region A1, A2	The traditional dwelling in Sub region B1, B2, C
		
Roof	Air space in the middle with two clay tile layers on surfaces $^1D=25\text{mm}$ $^2R=0.296\text{m}^2\cdot\text{K}/\text{W}$ $^3U=2.242\text{W}/\text{m}^2\cdot\text{K}$	Air space in the middle with two clay tile layers on surfaces $D=25\text{mm}$ $R=0.296\text{m}^2\cdot\text{K}/\text{W}$ $U=2.242\text{W}/\text{m}^2\cdot\text{K}$
External wall	Bamboo plaited layer in the middle with two grass clay layers on surface / Timber wall $D_1=50\text{mm}$ $D_2=30\text{mm}$ $R_1=0.300\text{m}^2\cdot\text{K}/\text{W}$ $R_2=0.216\text{m}^2\cdot\text{K}/\text{W}$	Rammed earth wall $D=390\text{mm}$ $R=0.870\text{m}^2\cdot\text{K}/\text{W}$
Internal wall	Timber wall $D=30\text{mm}$ $R=0.216\text{m}^2\cdot\text{K}/\text{W}$	Clay wall $D=200\text{mm}$ $R=0.215\text{m}^2\cdot\text{K}/\text{W}$
Window	Single layer wooden material $D=20\text{mm}$ $R=0.140\text{m}^2\cdot\text{K}/\text{W}$	Single layer wooden material $D=20\text{mm}$ $R=0.140\text{m}^2\cdot\text{K}/\text{W}$
Door	Single layer wooden material $D=20\text{mm}$ $R=0.140\text{m}^2\cdot\text{K}/\text{W}$	Single layer wooden material $D=20\text{mm}$ $R=0.140\text{m}^2\cdot\text{K}/\text{W}$
Ground	Rammed earth ground $-$ $R=0.293\text{m}^2\cdot\text{K}/\text{W}$	Rammed earth ground $-$ $R=0.293\text{m}^2\cdot\text{K}/\text{W}$

¹T refers to the construction thickness (mm) of building component; ²R refers to the overall thermal resistance ($\text{m}^2\cdot\text{K}/\text{W}$) of building component.

(1) Dwelling form.

The layout of traditional dwellings is flexible. The plane forms of traditional dwellings can be divided into 4 types, such as “I” shape, “L” shape, “U” shape, and “□” shape, accounting for 52.0%, 23.5%, 12.0%, and 12.5% of the total samples, respectively.

However, the construction process of some dwellings is not completed in one step. The usual evolution process is from “I” shape to “L” shape, and finally to the “U” shape and “□” shape. And the “U” shape and “□” shape courtyards are based on the “I” shape building, which has experienced several generations of construction and finally completed a relatively closed courtyard space.

The majority of the traditional dwellings in Qinba mountainous region are situated on hillsides. The location of the dwellings must be leveled due to the terrain’s limitations. Local residents constructed the “I” shape structure to minimize the amount of earthwork. In terms of function, the living room is centered, and the bedrooms are on both sides. Then, with the increase in family population, more bedrooms are added on one side or both sides of the “I” shape building to meet the functional requirements. The enclosed courtyard space can build a safer, quieter, and more comfortable living environment.

(2) Structures and Materials.

The traditional dwellings were constructed with local materials that are inexpensive and easy to construct. The main building has the beam-lifted frame, in which the column and tie are wooden structures. In order to meet the functional needs of the plane, the building generally used a “standard room” with certain width as the building unit to lay out the plane. This structure belongs to the frame structure, which could provide a flexible plane layout.

Walls are generally non-bearing structures, using materials of bamboo, rammed earth, stone, wood, etc. The roof adopts the small blue tile structure, doors and windows are mostly single-layer wooden doors and windows. The materials of the main components of the traditional dwellings are shown in Table 6-1.

(3) Space Usage Frequency

According to space usage frequency analysis, shown in Figure 6-1, the residents spend 74.0% and 60.5% of the daytime in the living room and bedroom in winter and summer, respectively. And the average time spent outside is 14.2% and 25.4% during winter and summer, respectively. During the daytime in winter, the residents spend more time indoors than that in summer because the building has a certain degree of adjustment to the climate, and the indoor temperature fluctuates less than the outdoor temperature. In addition, the residents spend most of their indoor time in the living room and bedroom during the day. As a result, the consideration of residents’ indoor thermal comfort and the transformation of the residential thermal environment could only focus on the mainly used rooms such as the living room and bedroom.

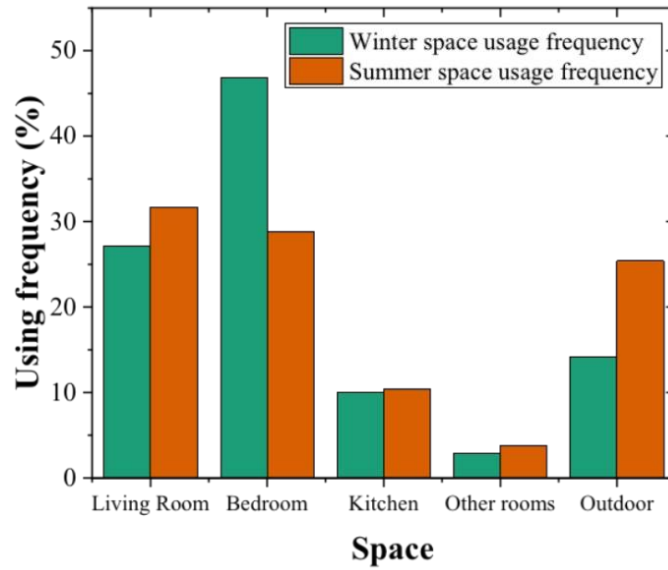


Figure 6-1. The space usage frequency analysis

6.2.3. Methods

(1) Field survey method

The field survey method refers to the method of conducting on-site observations and collecting data in research [20]. The field survey method usually includes participant observation, in-depth interviews, questionnaires, etc., to obtain comprehensive information. This study applied the field survey method, including architectural surveying, questionnaires, and physical measurement [21]. Architectural surveying is the basis of traditional residential research. Through a large number of actual surveys, this study summarized a series of basic information on the spatial distribution, plan layout, and architectural details of traditional residential buildings in the Qinba Mountain area, providing a foundation for further analysis and simulation. The survey questionnaire is the basic data for summarizing and analyzing problems, including subjective and objective aspects. The questionnaire can take the form of inquiry or actual recording. The subjective questionnaire includes residents' subjective heat perception, frequency of spatial use, and measures for local climatic environments. The objective questionnaire includes the weather on the day of the survey, residents' clothing conditions, heating and cooling measures, etc. Physical testing mainly refers to the physical testing of the indoor and outdoor thermal environment of traditional residential buildings, including outdoor temperature and relative humidity, wind speed, and indoor temperature and relative humidity testing. By sorting out the survey data, common problems of residential buildings and the inherent connections between multiple variables can be obtained.

(2) Statistical method

Data statistics method refers to the method of collecting data and analyzing it to understand the relationships, trends, differences, and other characteristics between data [22]. Among them,

linear regression equation is a common data statistical method used to describe the linear relationship between two variables [23]. It describes the relationship between the dependent variable and the independent variable by finding the best fitting line and can be used to predict the value of the dependent variable based on the value of the independent variable [24]. Linear regression analysis was applied in this chapter to fit the relationship between residents' thermal sensation votes and indoor operative temperature, and then to determine the neutral temperature and thermal comfort temperature range for residents.

6.3. Research proposal

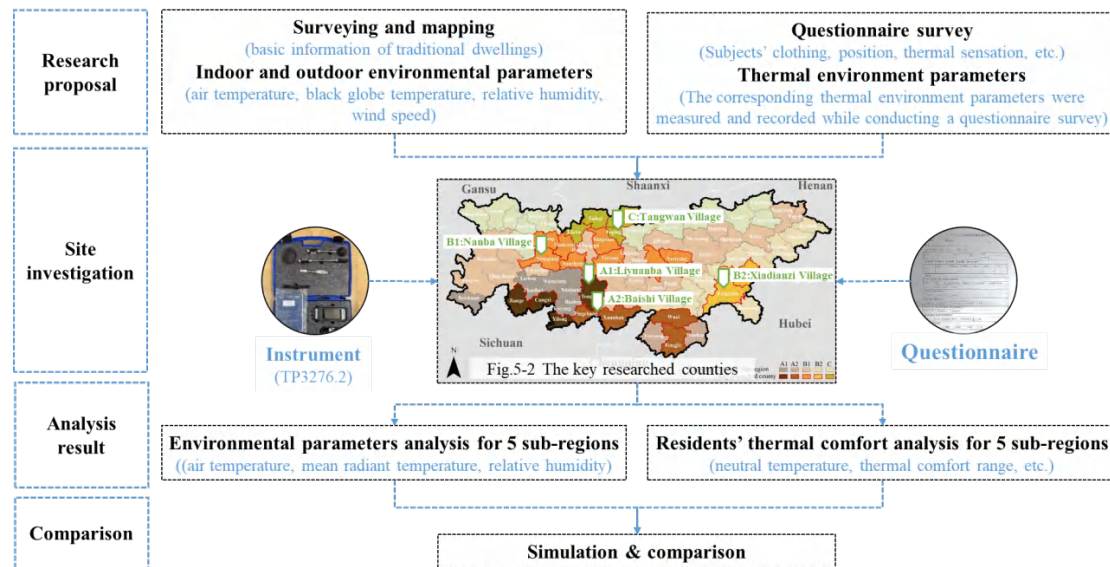


Figure 6-2. The research structure of climatic subdivision in Qinba mountainous area

Figure 6-2 shows the research structure of thermal comfort investigation in the climatic sub-regions in Qinba mountainous area. In this chapter, by using field survey, statistical analysis, and computer simulation method, the indoor thermal environment of traditional dwellings in the 5 climatic sub-regions in Qinba mountain area was compared, the thermal sensation of residents was investigated.


The thermal environment measurement of the traditional dwellings was arranged in January, the coldest month in winter, and July, the hottest month in summer, between July 2020 and January 2023.

6.3.1. Measurement of environmental parameters

The continuous 48h thermal environment measurement of the rural dwellings in the 5 climatic sub-regions, including Tongjiang (sub-region A1), Pingchang (sub-region A2), Ningqiang (sub-region B1), Fangxian (sub-region B2), and Foping (sub-region C), in winter were arranged from January 26, 2021, to January 31, 2022, and January 14, 2023, to January 20, 2023. And the summer measurements were arranged from July 15, 2021, to July 21, 2021, and July 4, 2022, to July 14, 2022. The data were recorded every 30 minutes, so every group of

data has a total of 96 sets. To ensure the accuracy, a set of 24 hours data was selected for analysis. The main parameters of the measurement include the outdoor air temperature, the outdoor relative humidity, the indoor air temperature, the indoor air relative humidity and the indoor black ball temperature. The indoor measuring point is set in the center of the room and is 1.4 m above the ground. The main information about the instrument is displayed in Table 6-2.

Table 6-2. The instruments' parameters

Meteorological Parameters	Instrument	Images	Measuring range	Precision
Air temperature	TP3207.2		-40~100°C	1/3DIN
Relative humidity	TP3207.2R		0~100%	±2%
Wind velocity	AP3203.2		0.05~5 m/s	± (0.05+0.5%)
Black globe temperature	TP3276.2		-30~120°C	1/3DIN

6.3.2. Questionnaire research

The research team distributed 816 questionnaires and collected 801 valid questionnaires, including 456 questionnaires in winter and 345 questionnaires in summer. Table 6-3 displays the subjects' general situation.

Table 6-3. The basic situation of the subjects

Factor	classification	Proportion
Age	21~40	13.2%
	41~60	38.5%
	61~80	48.3%
Gender	Male	56.8%
	Female	43.2%

The questionnaire survey includes subjects' clothing, thermal sensation, and other subjective evaluation, the thermal sensation voting questionnaire is shown in Table 6-4. The corresponding thermal environment parameters were measured and recorded while conducting a questionnaire survey, which allowed for the construction of a scatterplot figure for the indoor temperature and thermal sensation.

Table 6-4. Thermal sensation voting questionnaire

+3	+2	+1	0	-1	-2	-3
Hot	Warm	Slightly warm	Neutral	Slightly cool	Cool	Cold

6.4. Analysis of the environmental parameters

The measurement of the environmental parameters includes the measurement of physical quantities such as indoor and outdoor air temperature, relative humidity, black globe temperature, and wind speed in the traditional dwellings. By analyzing the measured results, it is found that there are differences in outdoor and indoor meteorological elements in each climatic sub-region. In Chapter 5, detailed explanations regarding the specific measurements of the traditional dwellings in each climatic sub-regions can be found. In this chapter, the measurement data of traditional dwellings from 5 sub-regions will be consolidated into a single graph, enabling analysis of their differences.

6.4.1. Temperature

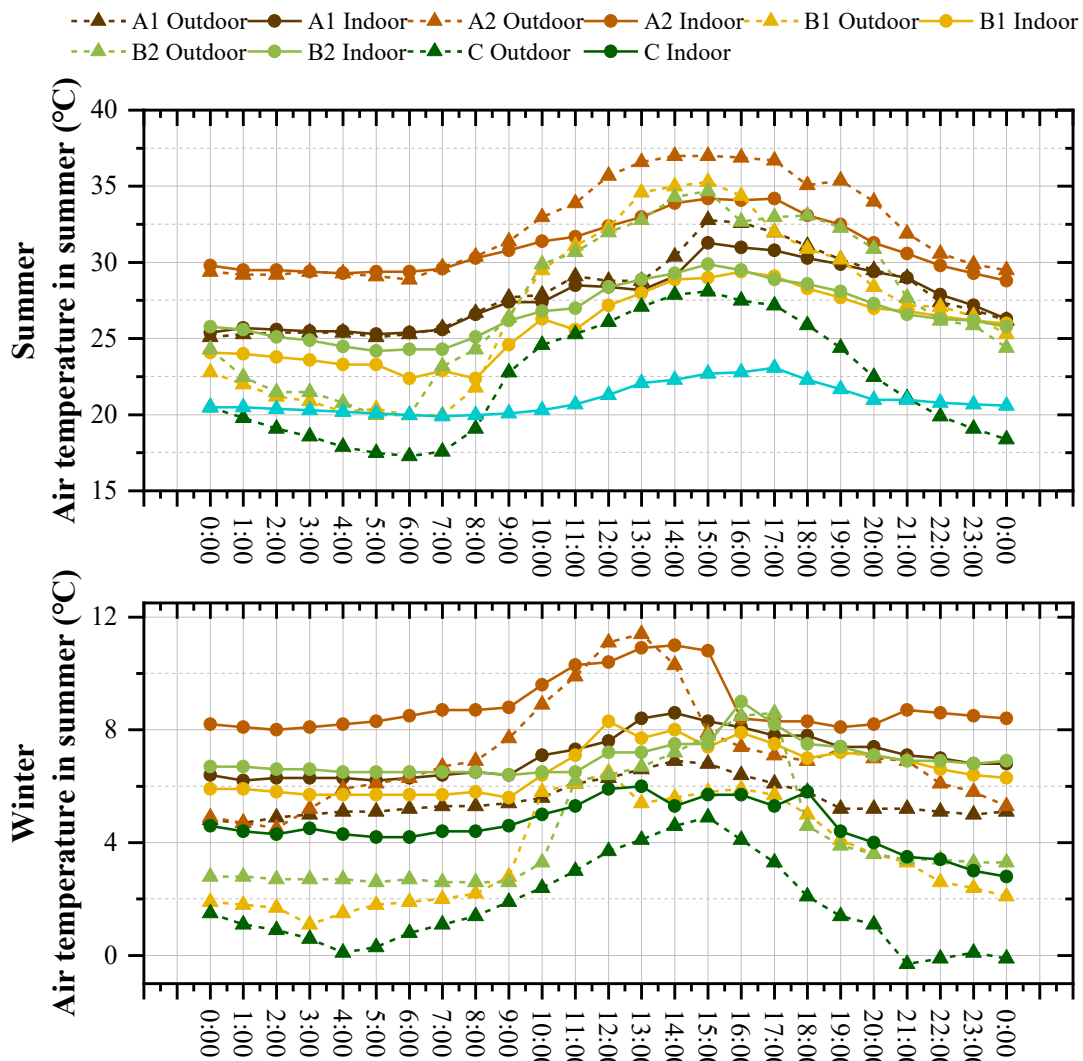


Figure 6-3 The measured air temperature in winter and summer in the 5 climatic sub-regions

The measured air temperature in winter and summer are shown in Figure 6-3. The outdoor air temperature on the winter survey day varied from 4.5°C to 11.4°C, 1.1°C to 8.6°C, and -

0.3°C to 4.9°C in sub-region A (A1, A2), B (B1, B2) and C, respectively. The indoor temperature ranged from 6.2°C to 11.4°C, 5.6°C to 9.0°C, and 4.2°C to 6.0°C in sub-region A, B, and C, respectively. The test results show that, in winter, most of the indoor temperature in the 5 sub-regions was below the winter rural residential building temperature limitation of 8°C [25]. The outdoor air temperature on the summer survey day varied from 17.3°C to 35.3°C, and 20.0°C to 36.9°C in the sub-region 1 (A1, B1, and C) and sub-region 2 (A2 and B2). The indoor temperature ranged from 19.9°C to 31.3°C, and 24.2°C to 34.2°C in sub-region 1 and 2. On most of the summer days, the indoor air temperature satisfied the criteria of under 30°C [25]. In summer, compared to sub-region 2, sub-region 1 is cooler and has a greater change in temperature between day and night.

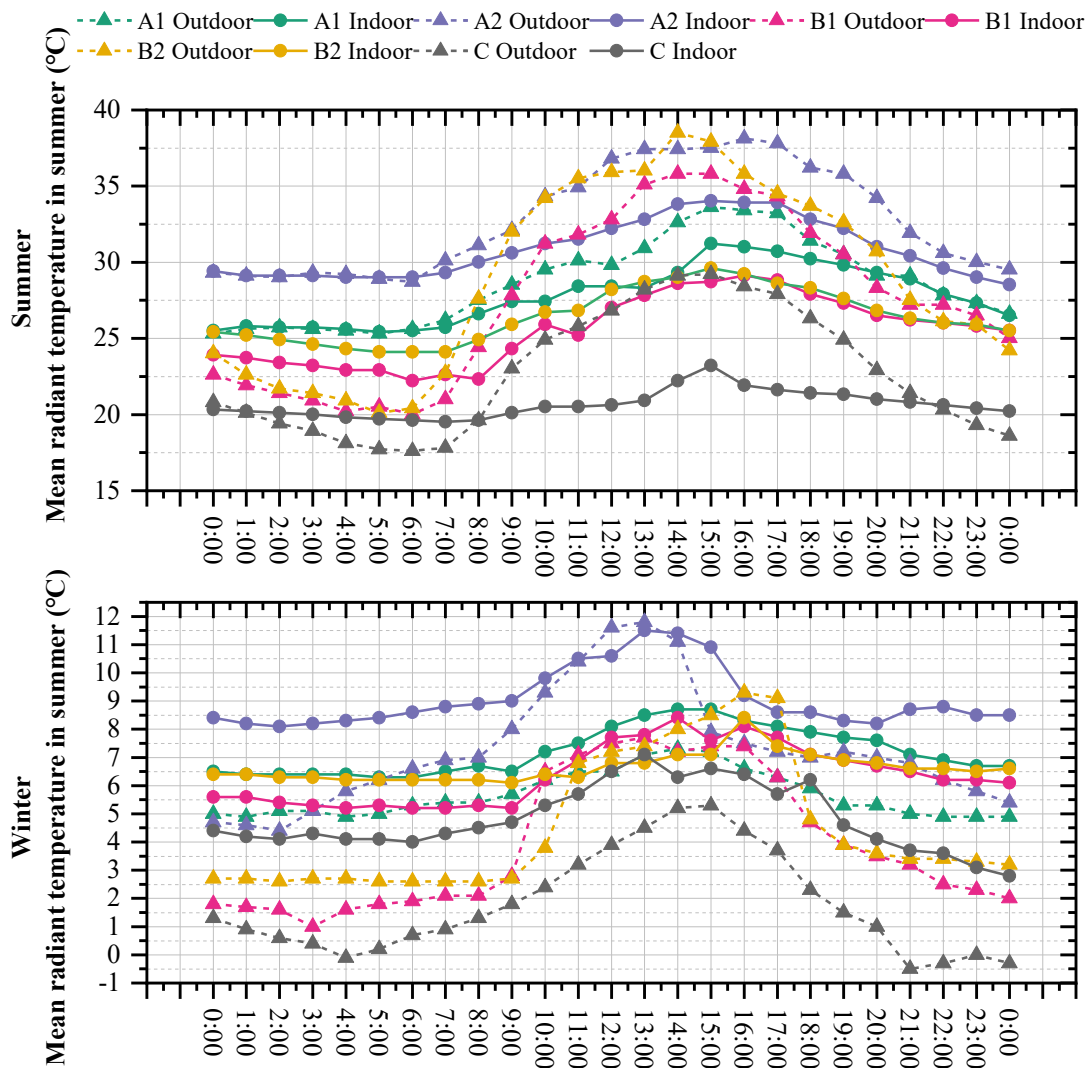


Figure 6-4 The measured mean radiant temperature in winter and summer in the 5 climatic sub-regions

The measured mean radiant temperature in winter and summer are shown in Figure 6-4. The variation trends of mean radiant temperature and air temperature in traditional dwellings within

the 5 climatic sub-regions are similar, indicating that traditional dwellings have a certain regulating effect on indoor mean radiant temperature.

6.4.2. Relative humidity

The measured relative humidity in winter and summer are in Figure 6-5. The outdoor relative humidity ranged from 28.8% to 98.9%, and 32.4% to 92.9% in winter and summer. the indoor humidity ranged from 64.2% to 80.4%, and 64.2% to 80.4% in the two seasons too. In addition, the indoor relative humidity was frequently more than 60% both in summer and winter, and only 21.7% and 32.5% of the year the indoor relative humidity satisfied the criteria of under 60% [25].

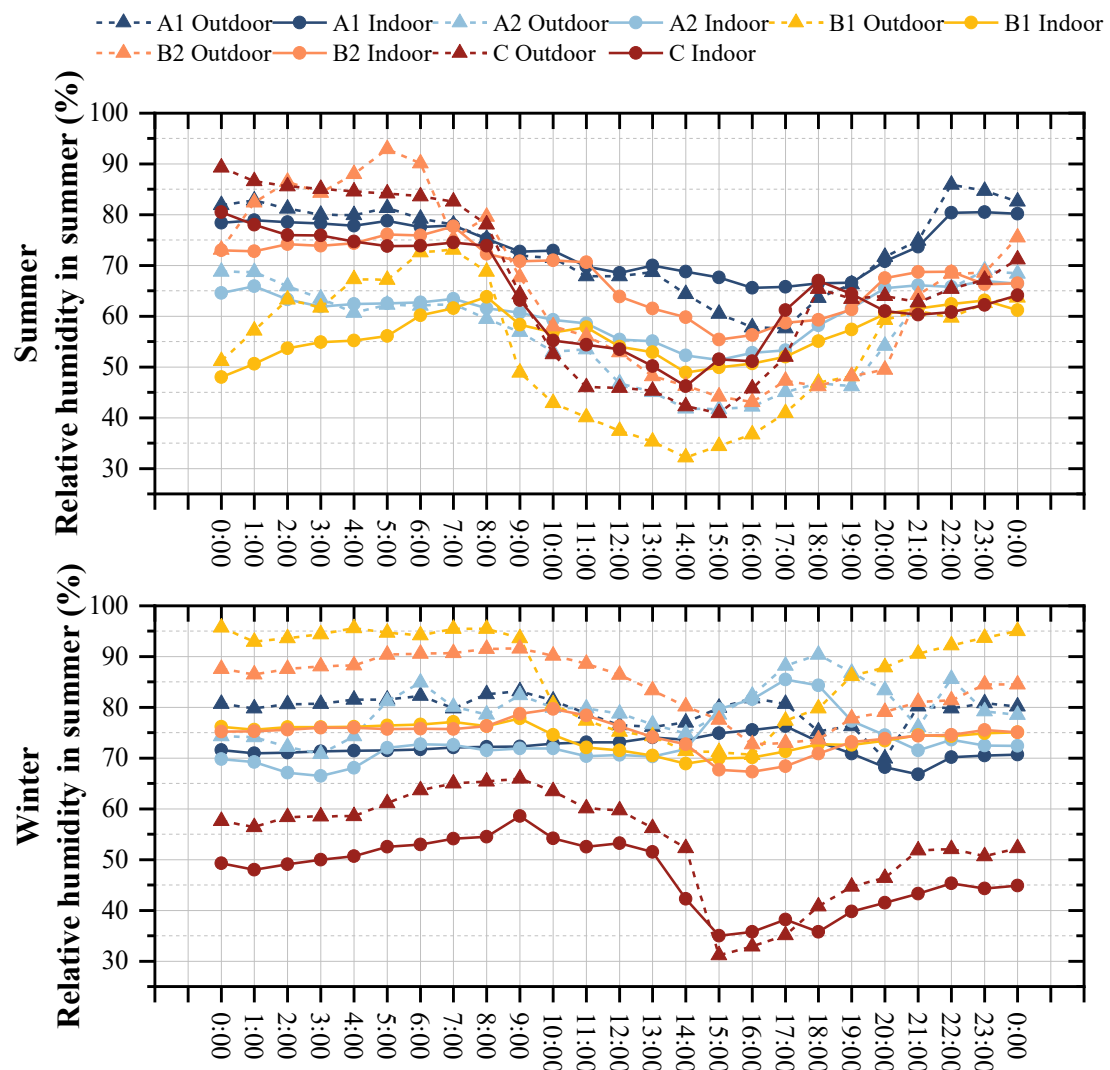


Figure 6-5. The measured relative humidity in winter and summer in the 5 climatic sub-regions

6.5. Analysis of indoor thermal comfort

6.5.1. Thermal environment evaluation index

It is commonly accepted that operative temperature (T_{op}) is generally used as the thermal comfort evaluation criteria to describe the area of human thermal sensation. T_{op} comprehensively considers the influence of the air temperature (T_a) and the mean radiant temperature (T_{mr}), and can accurately describe the thermal sensation of residents [1, 2]. The calculation process of T_{op} is shown in the Formula (6-1):

$$T_{op} = \frac{h_r T_{mr} + h_c T_a}{h_r + h_c} \quad (6-1)$$

Where h_r is the linear radiative heat transfer coefficient, $W/(m^2 \cdot K)$; h_c is the convective heat transfer coefficient, $W/(m^2 \cdot K)$ [1]; T_a is the air temperature, $^{\circ}C$; T_{mr} is the mean radiant temperature, $^{\circ}C$.

Or the T_{op} can also be calculated as Formula (6-2) [2]:

$$T_{op} = \frac{[T_{mr} + (T_a \cdot \sqrt{10v_a})]}{1 + \sqrt{10v_a}} \quad (6-2)$$

Where v_a is the indoor air velocity, m/s; T_a is the air temperature, $^{\circ}C$; T_{mr} is the mean radiant temperature, $^{\circ}C$.

It is also acceptable to approximate this relationship, shown in Formula (6-3), for occupants engaged in near sedentary physical activity (with metabolic rates between 1.0 met and 1.3 met), not in direct sunlight, and not exposed to air velocities greater than 0.10 m/s [1].

$$T_{op} = \frac{T_a + T_{mr}}{2} \quad (6-3)$$

Where T_a is the air temperature, $^{\circ}C$; T_{mr} is the mean radiant temperature, $^{\circ}C$.

The mean radiant temperature can be estimated using a black-globe thermometer. According to ISO 7730 Standard, the calculation process of mean radiant temperature is shown in the Formula (6-4) [2]:

$$T_{mr} = \left[(T_g + 273.15)^4 + \frac{1.1 \cdot 10^8 v_a^{0.6}}{\varepsilon \cdot D_g^{0.4}} \cdot (T_g - T_a) \right]^{0.25} - 273.15 \quad (6-4)$$

Where T_g is the black globe temperature, $^{\circ}C$; v_a is the indoor air velocity, m/s; D_g is the diameter of the globe, mm; ε is the emissivity of the globe, no dimension.

With the operative temperature as the independent variable, the corresponding relation could be obtained by linear regression analysis. When the average thermal sensation voting value is 0, the value of operative temperature equals the thermal neutral temperature.

6.5.2. Residents' thermal adaptive behavior analysis

The previous studies shows that the common thermal adaptation behaviors include changing the thermal resistance of clothing, changing the amount of activity, adjusting doors and windows or equipment, etc [26].

(1) Clothing Thermal Resistance

The subjects' clothing was recorded during the investigation, and according to ASHRAE 55-2007 [1], the subjects' clothing thermal resistance was calculated through linear regression analysis, expressed in unit clo ($1\text{ clo} = 0.155\text{ m}^2 \cdot \text{K}/\text{W}$). By the coefficient of determination R^2 , it can be seen that there is a high correlation between clothing thermal resistance and indoor temperature. According to the calculation, in winter, the average clothing thermal resistance of the subjects was 1.43 clo, 1.73clo, and 1.82 clo in sub-region A (A1, A2), B (B1, B2), and C, respectively. In winter, the clo value above 1.5 does not comply with ASHRAE Standard 55-2017. In summer, due to the high air temperature in the Qinba mountainous area, the residents' clothing is mainly short sleeves, and the clothing characteristics are not much different in the sub-climate zones. Therefore, according to the ASHRAE Standard 55-2017, the clothing thermal resistance of each sub-climate region in the study area is set to 0.5 clo. Further analysis shows that the thermal resistance of clothing is inversely proportional to the indoor air temperature. When the indoor temperature decreases, the thermal resistance of residents' clothing increases.

(2) Metabolic Rate

As the subjects were in a state of slight activity in sitting position during the questionnaire survey, and the state was maintained for more than 30 minutes, according to the statistical analysis of the metabolic rate in ASHRAE Standard 55-2017, the metabolic rate of the subjects was set to 1.2 et, which represents the metabolic level of those who have slight activity in sitting posture.

As a result, in the study area, the main way for residents to regulate the cold response in winter is to increase the thermal resistance of clothing and enhance the activity intensity to change the metabolism.

6.5.3. Residents' indoor thermal sensation vote

The analysis of human thermal sensation is based on the statistical summary of the thermal sensation vote of the questionnaire survey. The voting options are ASHRAE general seven-level indexing indicators, and the corresponding indicators are -3 (Cold), -2 (Cool), -1 (Slightly cool), 0 (Neutral), 1 (Slightly warm), 2 (Warm), 3 (Hot), shown in Table 6-4 [1].

The results of residents’ thermal sensation voting in the 5 climatic sub-regions in Qinba mountainous area are analyzed, and the statistics of thermal sensation votes of the climatic sub-regions are shown in Figure 6-6.

During winter, in the sub-region A (A1, A2), B (B1, B2), and C, without heating measures, there are 36.3%, 28.6%, and 17.8% of the residents have thermal sensation within the acceptable range (-1, 0, +1), 36.7%, 35.7%, and 42.2% of the residents feel cool (-2), and 27.0%, 35.7%, and 40.0% of the residents feel cold (-3), respectively. Residents’ satisfaction with the indoor thermal environment in winter showed a downward trend in areas A (A1, A2), B (B1, B2) and C. This is due to the fact that in Chapter 4, the value of HDD18 is used as the basis for the winter sub-climate division. The winter temperature in sub-region A (A1, A2), B (B1, B2) and C showed a significant downward trend, which affected the subjective thermal sensation vote of residents.

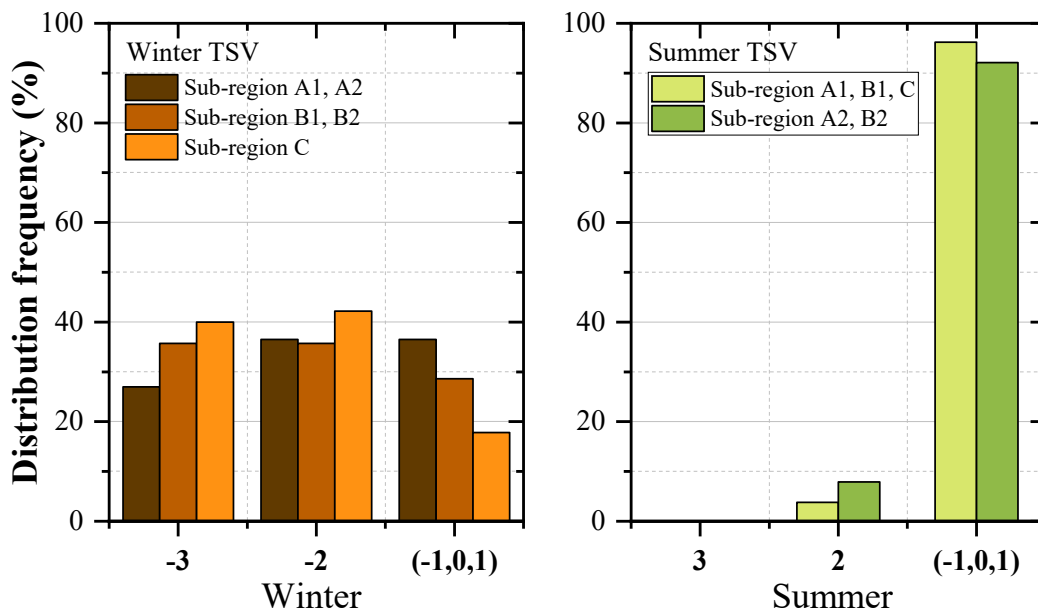


Figure 6-6. The thermal sensation votes (TSV) analysis

During summer, in sub-region 1(A1, B1, C) and 2(A2, B2), without cooling measures, 96.2%, and 92.1% of residents have thermal sensation within the acceptable range (-1, 0, +1), 3.8%, and 7.9% of the residents feel warm (+2), and no residents feel hot (+3). Residents ‘ satisfaction with the indoor thermal environment in summer is higher in sub-region 1(A1, B1, C) than in sub-region 2(A2, B2). This is because the value of CDD26 in sub-region 1(A1, B1, C) is lower than that in sub-region 2(A2, B2), and the temperature in sub-region 1(A1, B1, C) is lower and thermal environment is more comfortable in summer.

The distribution frequency of each climatic sub region is summarized in Table 6-5. In general, the indoor thermal environment in the study area during winter is poor. There is 70.5% of the residents in the study area feel uncomfortable, and the indoor thermal environment is failing to meet residents’ expectations for thermal comfort. And most of the time in summer, the indoor

thermal environment is comfortable, as 94.6% of the residents have thermal sensation within the acceptable range. The indoor thermal environment in the study area could meet residents' requirements for thermal comfort in summer.

Table 6-5. Thermal sensation voting analysis

Sub-regions	Winter TSV (%)			Summer TSV (%)		
	Cold	Cool	Acceptable range	Hot	Warm	Acceptable range
	-3	-2	-1, 0, 1	+3	+2	-1, 0, 1
A1	27	36.7	36.3	0	3.8	96.2
A2	27	36.7	36.3	0	7.9	92.1
B1	35.7	35.7	28.6	0	3.8	96.2
B2	35.7	35.7	28.6	0	7.9	92.1
C	40	42.2	17.8	0	3.8	96.2
Average value	33.1	37.4	29.5	0	5.4	94.6

6.5.4. Neutral temperature

Neutral temperature refers to the temperature when people can neither feel hot nor cold, and it can maintain normal body temperature of the most comfortable ambient temperature. At this temperature, the body's oxygen consumption, metabolic rate is the lowest, the amount of evaporative heat dissipation is also very small [27]. As residents have certain adaptability to the climate environment, the uniform neutral temperature cannot meet the thermal comfort requirements of residents in different regions. Therefore, understanding the neutral temperatures of different climate zones is helpful to determine the cooling and heating setpoints in these areas, so as to save building energy consumption while meeting the thermal comfort of residents [28].

There are some differences in the indoor thermal and humid environment of traditional residential buildings in the climatic sub-regions of the study area, which encourages residents to adapt to the indoor thermal environment actively and ultimately form diversified thermal demands. We plot the thermal sensation votes and operative temperatures recorded during voting in different climate zones into scatter plots to fit the thermal comfort equation. In order to improve the accuracy of the analysis, the bin method is used to take the average values of the operative temperatures and the thermal sensation votes with 0.5°C interval. Then, the linear regression analysis of the mean thermal sensation voting (MTS) and the indoor operating temperature (T_{op}) of the traditional dwellings in the climatic sub-regions was performed. The analysis is used to explore the actual thermal comfort level of residents in different climate zones, and finally the thermal sensation prediction equation of residents in different climate zones is obtained.

(1) Neutral temperature in winter.

The linear fitting result of the MTS and T_{op} in sub-region A (A1, A2), B (B1, B2), and C during winter are shown in Figure 6-7. The actual thermal sensation prediction equation in sub-

region A (A1, A2), B (B1, B2), and C are shown in equation (6-5), (6-6), and (6-7). The correlation coefficients R^2 are 0.76975, 0.79189, and 0.80001 in equation (6-5), (6-6), and (6-7), respectively, indicating that MTS has a high correlation with T_{op} in winter.

$$MTS_{A1, A2} = 0.26501 \cdot T_{op} - 4.17516, R^2 = 0.79189 \quad (6-5)$$

$$MTS_{B1, B2} = 0.29828 \cdot T_{op} - 4.25931, R^2 = 0.76975 \quad (6-6)$$

$$MTS_C = 0.25219 \cdot T_{op} - 3.37236, R^2 = 0.80001 \quad (6-7)$$

When the MTS value is 0, T_{op} is the neutral temperature according to the PMV-PPD equation. Based on the calculated data, in winter, the neutral temperatures of the indoor space are 15.8°C, 14.3°C, and 13.4°C in the sub-region A (A1, A2), B (B1, B2), and C, respectively. The neutral temperature shows a gradual downward trend in climatic sub-region A (A1, A2), B (B1, B2), and C, which is due to the gradual decrease of the outdoor air temperature in these three regions. Residents have stronger adaptability to lower temperatures in sub-region C, followed by sub-region B (B1, B2) and A (A1, A2).

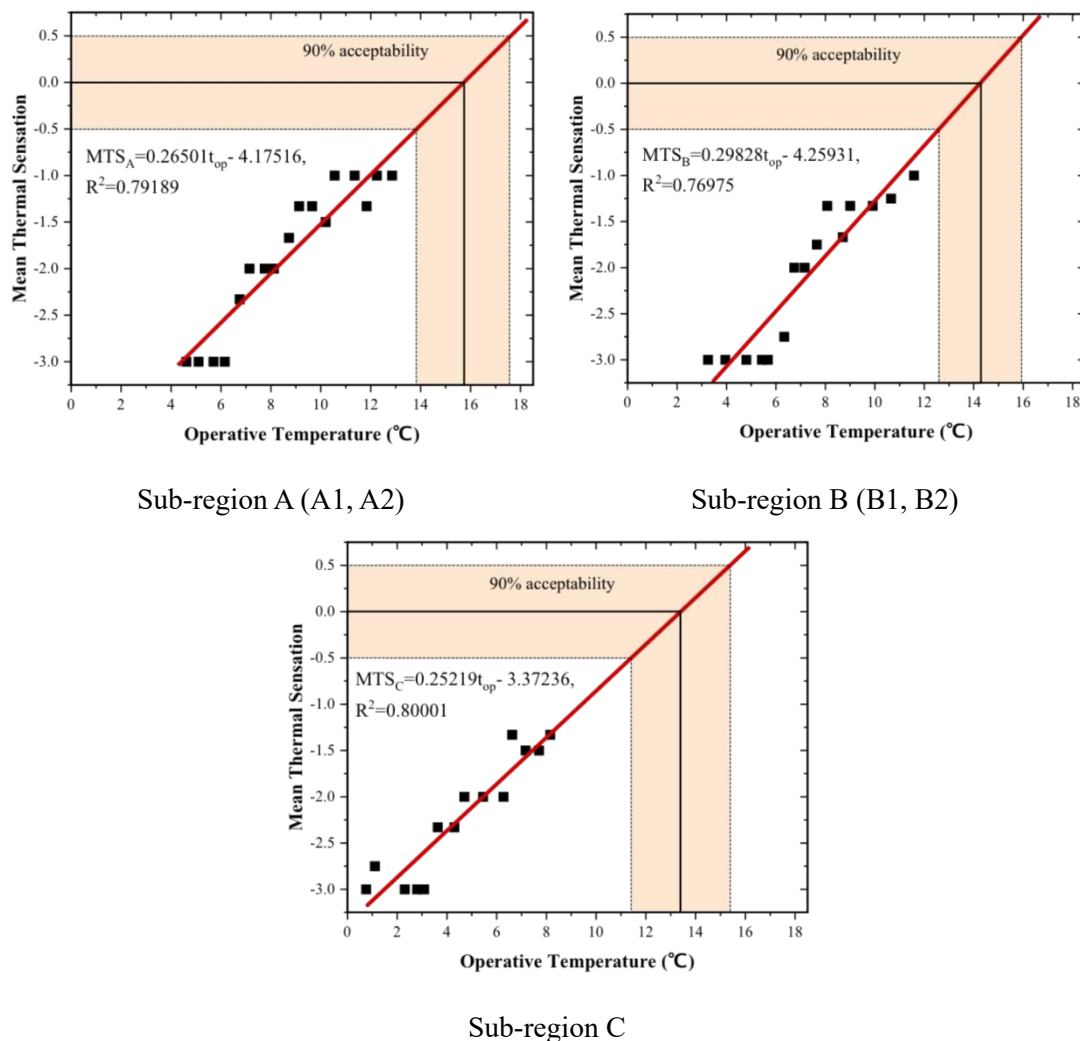


Figure 6-7. The relationship between MTS and the operative temperature in winter

(2) Neutral temperature in summer.

Similarly, the analysis in summer could be obtained. The linear fitting result of the MTS and T_{op} in sub-region 1(A1, B1, C) and 2(A2, B2) during summer are shown in Figure 6-8. The actual thermal sensation prediction equation in sub-region 1(A1, B1, C) and 2(A2, B2) are shown in equation (6-8), and (6-9). The correlation coefficients R^2 are 0.75033, and 0.60629 in equation (6-8), and (6-9), respectively, indicating that MTS has a high correlation with T_{op} in summer.

$$MTS_{A1, B1, C} = 0.09692 \cdot t_{op} - 2.57373, R^2 = 0.75033 \quad (6-8)$$

$$MTS_{A2, B2} = 0.08471 \cdot t_{op} - 2.31248, R^2 = 0.60629 \quad (6-9)$$

Based on the calculated data, in summer, the neutral temperatures of the indoor space are 26.6°C, 27.3°C in the sub-region 1(A1, B1, C) and 2(A2, B2), respectively. The hotter sub-region A2, and B2 has a higher thermal neutral temperature than that in the cooler sub-region A1, B1, and C, which indicates that residents have stronger adaptability to high temperature in sub-region A2 and B2.

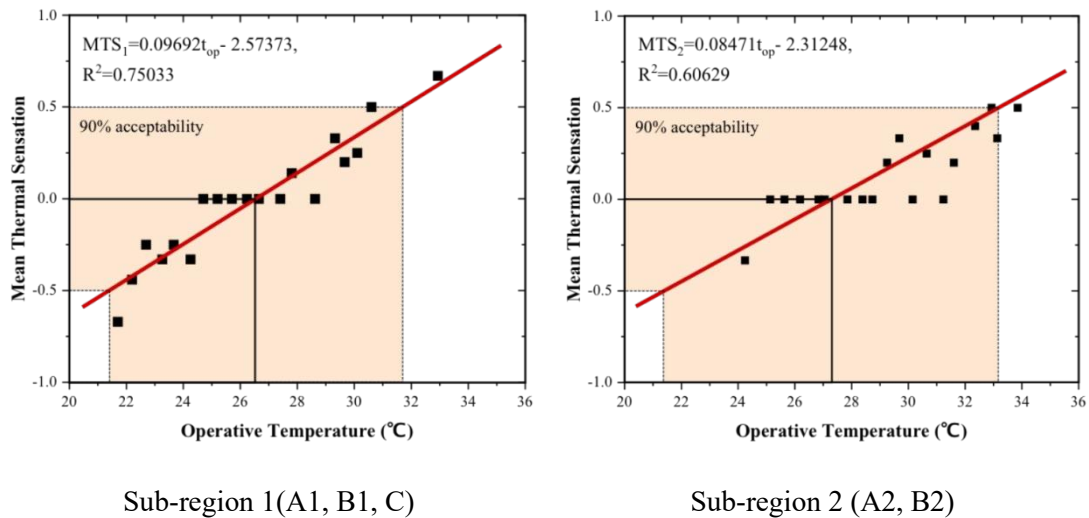


Figure 6-8. The relationship between MTS and the operative temperature in summer

6.5.5. Thermal comfort range

According to the ASHRAE standard 55-2017, 90% of the occupants will feel comfortable when the value of MTS is between -0.5 and 0.5 [1].

(1) Thermal comfort range in winter.

During winter, according to equation (6-5), (6-6), and (6-7), when the $MTS=0.5$ and -0.5 , the thermal comfortable range are 13.9 to 17.6°C, 12.6 to 16.0°C, and 11.4 to 15.4°C in subregion A (A1, A2), B (B1, B2), and C, respectively. The thermal comfort range and the neutral temperature show the same trends in in the sub-region A (A1, A2), B (B1, B2), and C.

(2) Thermal comfort range in summer.

During summer, according to equation (6-8), and (6-9), when the MTS=0.5 and -0.5, the thermal comfortable range are 21.4 to 31.7°C, and 21.4 to 33.2°C in subregion 1(A1, B1, C) and 2(A2, B2). Respectively. The thermal comfort range and the neutral temperature show the same trends in in the sub-region 1(A1, B1, C) and 2(A2, B2).

6.5.6. The relationship of MTS and PMV

Predicted Mean Vote (PMV) is a thermal comfort evaluation index based on the Fanger thermal comfort equation. It is the average voting value of the residents' prediction of the thermal environment based on the thermal comfort equation. However, mean thermal sensation voting (MTS) refers the thermal sensation voting value of the residents to the actual thermal environment [29].

The research team also compared the mean thermal sensation votes (MTS) and predicted mean vote (PMV) to see the difference between the theoretical value and the actual value. The measured relative humidity, air temperature, wind speed, metabolic rate, and clothing thermal resistance are substituted into the PMV calculation program (CBE Thermal Comfort Tool, <https://comfort.cbe.berkeley.edu/>) to obtain the PMV value. Then, the linear regression analysis of T_{op} with PMV, and MTS of the traditional dwellings in the climatic sub-regions was performed, respectively.

(1) The relationship of MTS and PMV in winter.

The linear fitting result of the T_{op} with PMV, and MTS in sub-region A (A1, A2), B (B1, B2), and C during winter are shown in Figure 6-9. And the PMV sensation prediction equation in sub-region A (A1, A2), B (B1, B2), and C in winter are shown in equation (6-10), (6-11), and (6-12).

$$PMV_{A1, A2} = 0.15077 \cdot t_{op} - 2.4683, R^2 = 0.99902 \quad (6-10)$$

$$PMV_{B1, B2} = 0.1453 \cdot t_{op} - 2.43641, R^2 = 0.99109 \quad (6-11)$$

$$PMV_C = 0.15439 \cdot t_{op} - 2.50663, R^2 = 0.99706 \quad (6-12)$$

When the PMV value is 0, T_{op} is the predicted neutral temperature according to the PMV-PPD equation. Based on the calculated data, in winter, the predicted indoor neutral temperature is 16.4 °C, 16.8 °C, and 16.2 °C, which is warmer than the surveyed thermal neutral temperature of 15.8°C, 14.3 °C, and 13.4 °C, respectively. It shows that residents have stronger adaptability to cold environment than predicted value in winter. Moreover, the predicted neutral temperature has no obvious change trend in different climatic sub-regions in Qinba mountainous area, showing that the adaptability of residents to the local climate environment is not fully considered.

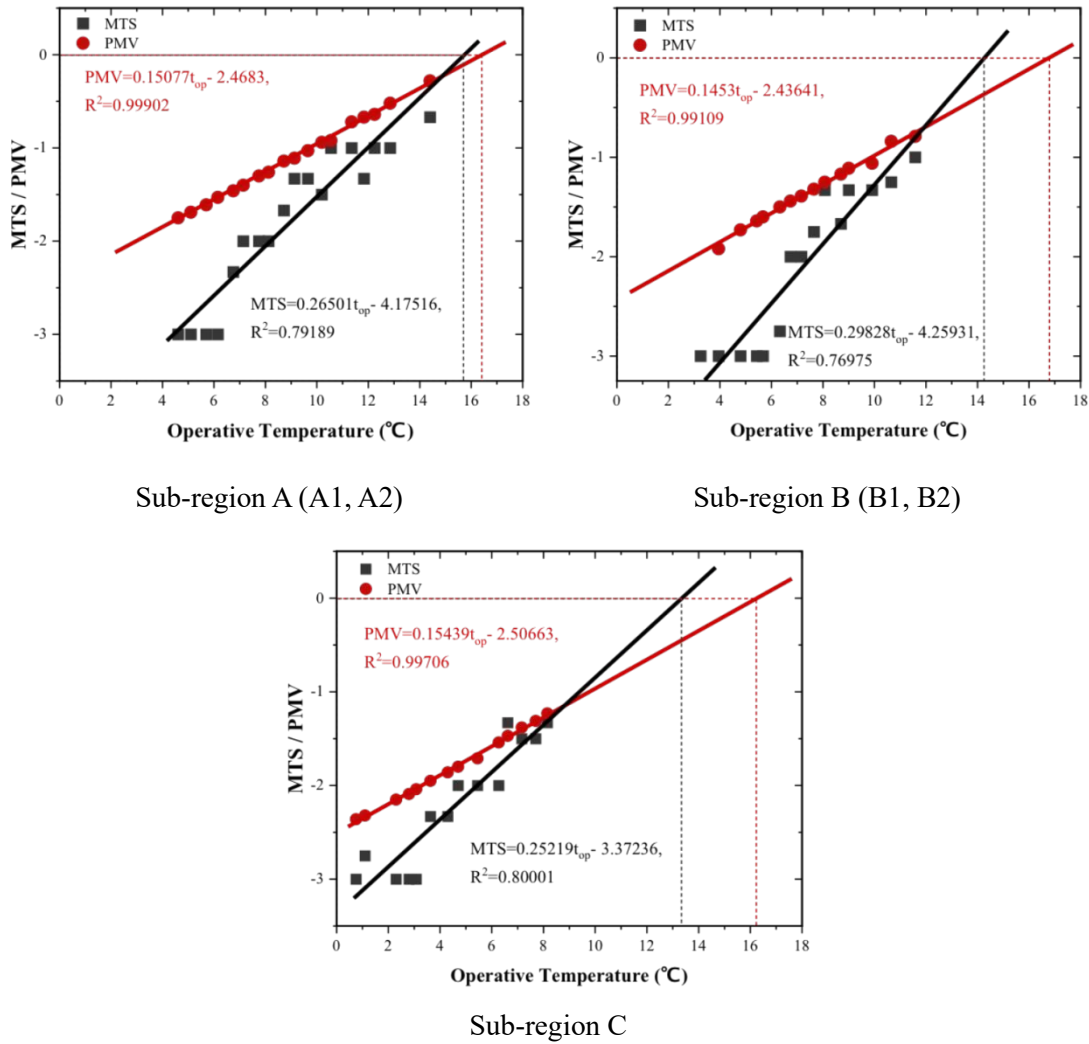


Figure 6-9. The relationship between MTS and PMV in winter

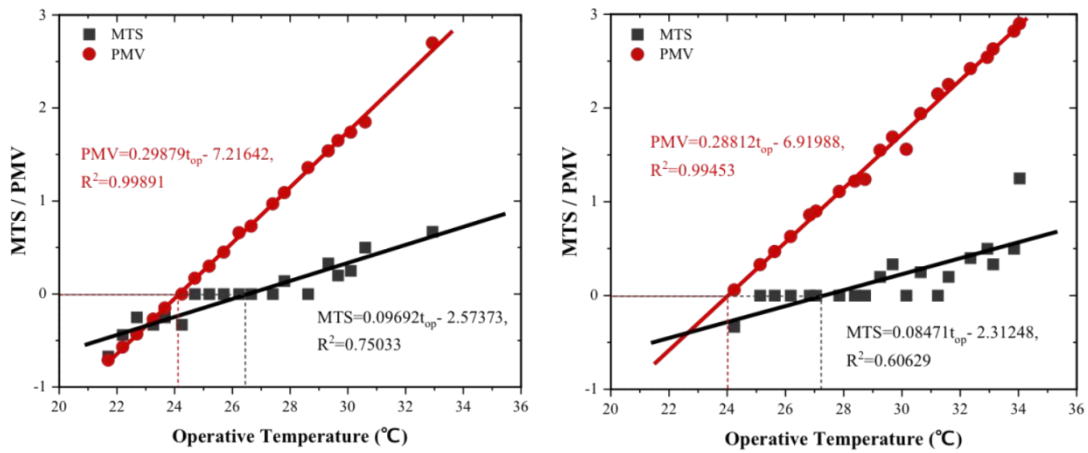
(2) The relationship of MTS and PMV in summer.

Similarly, the analysis in summer could be obtained. The linear fitting result of the T_{op} with PMV, and MTS in sub-region 1(A1, B1, C) and 2(A2, B2) during summer are shown in Figure 6-10. And the PMV sensation prediction equation in sub-region 1(A1, B1, C) and 2(A2, B2) in summer are shown in equation (6-13), and (6-14).

$$PMV_{A1, B1, C} = 0.29879 \cdot t_{op} - 7.21642, R^2 = 0.99891 \quad (6-13)$$

$$PMV_{A2, B2} = 0.28812 \cdot t_{op} - 6.91988, R^2 = 0.99453 \quad (6-14)$$

In summer, in the sub-region 1(A1, B1, C), and 2(A2, B2), the predicted indoor neutral temperature is 24.2 °C, and 24.0 °C, which is lower than the surveyed thermal neutral temperature of 26.6°C, and 27.3 °C. In summer, residents have stronger adaptability to the hot environment than the prediction model.



Sub-region 1(A1, B1, C)

Sub-region 2 (A2, B2)

Figure 6-10. The relationship between MTS and PMV in summer

The measured and predicted neutral temperature and thermal comfortable range in each climatic sub-region in Qinba mountainous area are shown in Table 6-6.

Table 6-6. The main values of indoor thermal comfort in the climatic sub-regions

	Neutral Temperature		Predicted Neutral Temperature		Thermal Comfort Range	
	(°C)		(°C)		(°C)	
	Winter	Summer	Winter	Summer	Winter	Summer
A1	15.8	26.6	16.4	24.2	13.9~17.6	21.4~31.7
A2	15.8	27.3	16.4	24.0	13.9~17.6	21.4~33.2
B1	14.3	26.6	16.8	24.2	12.6~16.0	21.4~31.7
B2	14.3	27.3	16.8	24.0	12.6~16.0	21.4~33.2
C	13.4	26.6	16.2	24.2	11.4~15.4	21.4~31.7

The analysis above indicates that during summer, in the relatively high temperature sub-region 2 (A2, B2), the residents have better adaptation to hot weather than sub-region 1(A1, B1, C). And in winter, the occupants’ tolerance for cold weather is sub-region C, B (B1, B2), and A (A1, A2) from high to low. Moreover, in winter, the measured neutral temperature is lower than the predicted neutral temperature, and in summer, the actual measured neutral temperature is higher than the predicted neutral temperature. This showed that residents have certain adaptability to the actual thermal environment, and the thermal comfort range of the human body is more comprehensive than the theoretical prediction.

In summary, the thermal comfort of residents is affected by their long-term living environment to a certain extent, and the indoor temperature of the living environment is proportional to the heat demand of residents. It shows that the indoor thermal environment limits the heat demand of residents to a certain extent through long-term adaptation.

6.6. Energy consumption simulation based on neutral temperature in the climatic sub-regions

6.6.1. Energy consumption simulation

According to the sub-climatic zoning of Qinba mountainous area, the annual meteorological data of the representative county in each climatic sub-region, A1 (Guangyuan), A2 (Fengjie), B1(Shangnan), B2 (Danjiangkou), C (Lushi), are used as the energy consumption simulation meteorological file, and EnergyPlus is used as the simulation engine to simulate the annual building thermal loads of the target building. To reflect the actual situation of building energy consumption in climatic sub-regions, the building thermal performance parameters in climatic sub-regions are set according to Table 6-1, and the heating and cooling setpoints of the simulated building are determined according to the neutral temperature in winter and summer showing in Table 6-6. Meanwhile, to compare the numerical difference between the thermal loads of the target building based on the measured neutral temperature and standard requirements, the heating and cooling setpoints of the comparison group are set to 18°C and 26°C, respectively.

6.6.2. Simulation result analysis

The annual building thermal loads of typical traditional dwellings in the 5 climatic sub-regions' representative counties based on standard requirements and measured neutral temperature are shown in Figure 6-11. The annual thermal loads based on the measured neutral temperature are 37.86 kWh/m², 33.33 kWh/m², 45.42 kWh/m², 44.61 kWh/m², and 50.44 kWh/m² from climatic sub-region A1 to C, respectively, which is 31.32 %, 35.28 %, 37.86 %, 39.37 %, and 41.82 % lower than that based on the standard requirements of 54.87 kWh/m², 50.50 kWh/m², 73.09 kWh/m², 73.58 kWh/m², and 86.69 kWh/m².

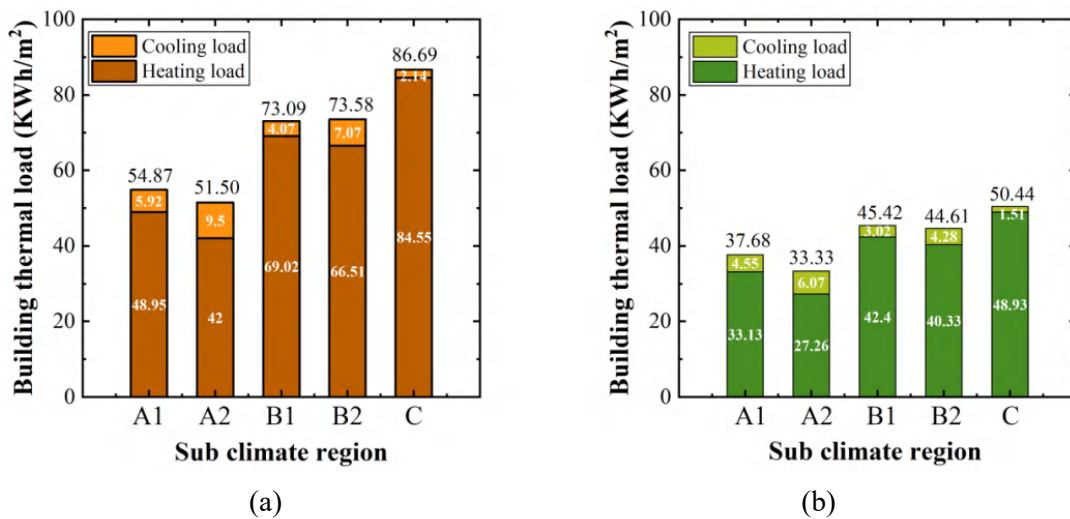


Figure 6-11. The annual thermal loads in sub-regions (a) The annual thermal loads based on design standard (b) The annual thermal loads based on measured neutral temperature

Compared with the annual heating loads based on the standard requirements, sub-regions A1 and A2 are the lowest, followed by sub-regions B1 and B2, and sub-regions C are the highest. In climatic sub-regions A1 to C, the annual heating loads based on the measured neutral temperature are 33.13kWh/m², 27.26kWh/m², 42.40kWh/m², 40.33kWh/m², and 48.93kWh/m², respectively, which is 32.32 %, 35.10 %, 38.57 %, 39.36 % and 42.13 % lower than that based on the standard requirements of 48.95 kWh/m², 42.00 kWh/m², 69.02 kWh/m², 66.51 kWh/m², and 84.55 kWh/m², respectively. The energy saving rate of heating energy consumption also shows the lowest trend in sub-regions A1 and A2, followed by B1 and B2 region, and the highest trend in C region, which is in accord with the residents' adaptability to the climate in each climatic sub-region.

Compared with the annual cooling loads based on the standard requirements, sub-region C is the lowest, followed by sub-regions A1 and B1, and sub-regions A2 and B2 are the highest, basically in line with the expected energy consumption level of climatic sub-regions. The cooling energy consumption based on the measured neutral temperature shows the lowest in B1 and C regions, followed by A1 and B1 regions. The largest in A2 region, as the exterior envelope' heat transfer coefficient of sub-region A1, A2 is much larger than that of sub-region B1, B2, and C, resulting in the relatively high cooling energy consumption in sub-region A1 and A2. In climatic sub-regions A1 to C, the annual cooling loads based on the measured neutral temperature are 4.55kWh/m², 6.07kWh/m², 3.02kWh/m², 4.28kWh/m², and 1.51kWh/m², respectively, which is 23.14%, 36.11%, 25.80%, 39.46%, and 29.44% lower than that based on the standard requirements of 5.92 kWh/m², 9.50 kWh/m², 4.07 kWh/m², 7.07 kWh/m², and 2.14 kWh/m², respectively. The energy saving rate of cooling energy consumption are lower in sub-region A1, B1, and C, followed by sub-region A2, B2, which is also in accord with the residents' adaptability to the climate in each climatic sub-region.

Through analysis, making the appropriate heating and cooling setpoint according to the measured neutral temperature in different climate regions could be more conducive to meeting the thermal comfort needs of residents and reduce building energy consumption to a certain extent.

6.6.3. Suggestion on improving indoor thermal environment

According to the analysis of the investigation of traditional dwellings in Qinba mountainous area, the main reasons for the low thermal comfort of the traditional dwellings are summarized as follows: 1) Due to the long construction age and backward construction technology, the thermal performance of the envelope structure of traditional dwellings is poor, and the indoor heat loss is serious. 2) The living and production methods of residents lead to the living room bedroom and other residents' s main activity areas can not be well sealed, resulting in a continuous exchange of indoor and outdoor air, unable to heat storage. 3) old coal-fired furnaces and other heating equipment heating efficiency are low, serious environmental pollution.

(1) Only optimizing the mainly used space by using passive design parameters

As the residents spent 74.0% and 60.5% of the daytime in the mainly used room of the traditional dwelling, it is a good time to only renovate the mainly used room with the passive design parameters such as adding a sunspace, using shading control strategy, and improving the window to wall ratio, which will yield more economical results. Many studies have proved that a passive strategy can significantly improve the indoor environment [30-32]. The use of the passive design strategy is sustainable for the environment and could save post-use costs.

(2) Improving thermal performance of building envelope

According to the analysis, there is still a certain gap between the measured indoor air temperature and the calculated neutral temperature. In order to meet the indoor thermal comfort needs of the residents, methods can be taken to improve the thermal performance of residential building envelopes as a good thermal insulation and heat storage effect on the building envelope might ensure a steady interior thermal environment and thermal comfort [33, 34]. For the thermal comfort transformation of traditional dwellings, on the basis of maintaining their original aesthetic, the measures such as increasing the thermal insulation of exterior walls and roofs, hanging thermal insulation curtains, and replacing exterior windows and doors with good thermal insulation performance can be taken to reduce indoor heat loss.

(3) Promotion of efficient new energy heating equipment

As in summer, 91.8 % of residents think that the indoor thermal environment is comfortable, it is not necessary to adopt refrigeration equipment for traditional dwellings, only heating equipment should be considered. Traditional dwellings could abandon the traditional coal stoves, fire ponds, and other heating equipment with low thermal efficiency and environmental pollution. Combined with their actual situation, new energy can be used for heating, and the heating equipment which is installed on the ground or lighter to avoid damage to the house itself could be selected, such as biogas, geothermal energy, etc.

6.7. Summary

In this chapter, by using field investigation and statistical analysis method, the indoor thermal environment of traditional dwellings in the 5 climatic sub-regions in Qinba mountain area was compared, the thermal sensation of residents was investigated, and the reasons for the poor indoor thermal environment in this area were analyzed. Based on the calculation of neutral temperature and thermal comfort range in this area, strategies to improve the indoor thermal environment are suggested. The main conclusions of this chapter are as follows:

(1) According to the calculation, in winter, the average clothing thermal resistance of the subjects was 1.43 clo, 1.73clo, and 1.82 clo in sub-region A (A1, A2), B (B1, B2), and C, respectively. In winter, the clo value above 1.5 does not comply with ASHRAE Standard 55-2017. In summer, the clothing thermal resistance of each sub-climate region in the study area is 0.5 clo. The main way for residents to regulate the cold response in winter is to increase the

thermal resistance of clothing and enhance the activity intensity to change the metabolism.

(2) Through the questionnaire analysis, without heating measures in winter, 72.5% of the residents think that the indoor thermal environment is cool or cold. In summer, 91.8 % of residents think that the indoor thermal environment is comfortable. In general, the indoor thermal comfort of the mainly used room in winter is failing to meet residents' expectations for thermal comfort, and most of the summertime, the indoor thermal environment could meet residents' requirements for thermal comfort.

(3) According to the human thermal comfort analysis, the residents can adapt to the local climate. The neutral temperatures of residents are 15.8°C, 15.8°C, 14.3°C, 14.3°C, 13.4°C in winter and 26.6°C, 27.3°C, 26.6°C, 27.3°C, and 26.6°C in summer respectively. And the thermal comfort ranges are 13.9~17.6°C, 13.9~17.6°C, 12.6~16.0°C, 12.6~16.0°C, and 11.4~15.4°C in winter and 21.4~31.7°C, 21.4~33.2°C, 21.4~31.7°C, 21.4~33.2°C, 21.4~31.7°C in summer, respectively.

(4) In winter, the predicted indoor neutral temperature is 16.4°C, 16.4°C, 16.8°C, 16.8°C, and 16.2°C in sub-region A1 to C, which is higher than the measured thermal neutral temperature. In summer, the predicted indoor neutral temperature is 24.2°C, 24.0°C, 24.2°C, 24.0°C, 24.2°C in sub-region A1 to C, which is lower than the measured thermal neutral temperature. It indicates that the residents have certain adaptability to the actual thermal environment.

(5) The annual building thermal loads of typical traditional dwellings in the 5 climatic sub-regions' representative counties based on standard requirements and measured neutral temperature are simulated. The annual thermal loads based on the measured neutral temperature are 37.86 kWh/m², 33.33 kWh/m², 45.42 kWh/m², 44.61 kWh/m², and 50.44 kWh/m² from climatic sub-region A1 to C, respectively, which is 31.32 %, 35.28 %, 37.86 %, 39.37 %, and 41.82 % lower than that based on the standard requirements of 54.87 kWh/m², 50.50 kWh/m², 73.09 kWh/m², 73.58 kWh/m², and 86.69 kWh/m². Through analysis, making the appropriate heating and cooling set points according to the measured neutral temperature in different climate regions could be more conducive to meeting the thermal comfort needs of residents and reduce building energy consumption to a certain extent.

(6) According to the analysis, there is still a certain gap between the measured indoor air temperature and the calculated neutral temperature. In order to accommodate occupants' needs for thermal comfort and the unique features of traditional dwellings, strategies such as only optimizing the mainly used space by using passive design parameters, improving the thermal performance of the building envelope, and promoting efficient new energy heating equipment could be taken.

Reference

- [1] Thermal Environmental Conditions for Human Occupancy: ANSI/ASHRAE Standard 55-2017 (Supersedes ANSI/ASHRAE Standard 55-2013) Includes ANSI/ASHRAE Addenda Listed in Appendix N, 2017.
- [2] International standard 7730: Moderate thermal environments-determination of the PMV and PPD indices and specification of the conditions for thermal comfort, 1994.
- [3] S. H. Cao, X. Li, B. Yang, and F. Li, "A review of research on dynamic thermal comfort," *Building Services Engineering Research & Technology*, vol. 42, no. 4, pp. 435-448, Jul 2021, Art. no. 01436244211003028.
- [4] D. Y. Lai et al., "Thermal comfort diversity in Chinese urban residential buildings across various climates," *Energy and Buildings*, vol. 231, Jan 2021, Art. no. 110632.
- [5] H. Y. Yan, "Study on adaptive thermal comfort on the basis of regions and climates of China," Ph.D. Thesis, Xi'an University of Architecture and Technology, 2013.
- [6] Z. Jin, "Thermal adaptation behavior and thermal comfort zone for Chinese resident," Ph.D. Thesis, Chongqing University, 2011.
- [7] S. H. Kwon, Y. Lee, and C. Chun, "Thermal comfort in offices based on office workers' awareness of discomfort," *Building and Environment*, vol. 213, Apr 2022, Art. no. 108851.
- [8] Y.-S. Tsay, R. Chen, and C.-C. Fan, "Study on thermal comfort and energy conservation potential of office buildings in subtropical Taiwan," *Building Environment*, vol. 208, p. 108625, 2022.
- [9] B. Lala, S. Murtyas, and A. Hagishima, "Indoor Thermal Comfort and Adaptive Thermal Behaviors of Students in Primary Schools Located in the Humid Subtropical Climate of India," (in English), *Sustainability*, Article vol. 14, no. 12, p. 19, Jun 2022, Art. no. 7072.
- [10] P. K. Verma and N. Netam, "A case study on thermal comfort analysis of school building," (in English), *Materials Today: Proceedings*, vol. 28, pp. 2501-2504, 2020 2020.
- [11] H. Y. Yan, Z. Sun, F. N. Shi, G. D. Yuan, M. R. Dong, and M. L. Wang, "Thermal response and thermal comfort evaluation of the split air conditioned residential buildings," *Building and Environment*, vol. 221, Aug 2022, Art. no. 109326.
- [12] Q. Huang, W. Song, and C. Song, "Consolidating the layout of rural settlements using system dynamics and the multi-agent system," *Journal of Cleaner Production*, vol. 274, Nov 2020, Art. no. 123150.
- [13] J. Zhang, X. Zhao, X. Guo, W. Xie, and S. Chen, "Study on the spatial layout of hilly area rural settlements of Gannan based on quantification," *Journal of China Agricultural University*, vol. 21, no. 6, pp. 152-163, 2016, Art. no. 1007-4333(2016)21:6<152:Slhznd>2.0.Tx;2-#.
- [14] N. Wei and Y. Liu, "The spatial pattern evolution of dwellings in semi-tableland and semi-mountain area of Guanzhong region," *Journal of Xi'an University of Architecture &*

Technology. Natural Science Edition, vol. 47, no. 4, pp. 575-580, 2015, Art. no. 1006-7930(2015)47:4<575:Gzbsby>2.0.Tx;2-s.

[15] Y. Huang and W. M. Guo, "Evolution of Research on Chinese Vernacular Dwellings," in International Conference on Structures and Building Materials (ICSBM 2013), Guizhou, PEOPLES R CHINA, 2013, vol. 671-674, pp. 2189+, 2013.

[16] L. Yang, Q. Yang, H. Yan, and J. Liu, "Field study on the thermal comfort of rural houses in winter in the Guanzhong region, Shaanxi Province," Journal of Xi'an University of Architecture and Technology (Natural science edition), vol. 43, no. 04, pp. 551-556, 2011.

[17] S. zhu, G. Wang, and S. Yao, "Analysis of winter indoor thermal comfort in rural houses in Qinhuangdao," Journal of Building Energy Efficiency, vol. 50, no. 05, pp. 91-98, 2022.

[18] T. Zhang et al., "Towards Improving Rural Living Environment for Chinese Cold Region Based on Investigation of Thermal Environment and Space Usage Status," Buildings, vol. 12, no. 12, p. 2139, 2022.

[19] X. Sheng, "Field test and analysis of thermal comfort at rural houses and urban residential buildings in severe cold region," Master Thesis, Harbin Institute of Technology, 2013.

[20] T. Kane, "Indoor temperatures in UK dwellings: investigating heating practices using field survey data," © Tom Kane, 2013.

[21] G. Guan, "Investigation Study Spatially Of Dong-Traditional-Village In Qiandongnan Region," Master Thesis, Xi'an University of Architecture and Technology, 2015.

[22] R. L. Ott and M. T. Longnecker, An introduction to statistical methods and data analysis. Cengage Learning, 2015.

[23] D. C. Montgomery, E. A. Peck, and G. G. Vining, Introduction to linear regression analysis. John Wiley & Sons, 2021.

[24] G. A. Seber and A. J. Lee, Linear regression analysis. John Wiley & Sons, 2003.

[25] Design standard for energy efficiency for rural residential buildings (GB/T50824-2013), 2013.

[26] P. Zheng et al., "Thermal adaptive behavior and thermal comfort for occupants in multi-person offices with air-conditioning systems," Building and Environment, vol. 207, p. 108432, 2022.

[27] R. Yao et al., "Evolution and performance analysis of adaptive thermal comfort models—a comprehensive literature review," Building and Environment, p. 109020, 2022.

[28] L. A. Martins, V. Soebarto, and T. Williamson, "A systematic review of personal thermal comfort models," Building and Environment, vol. 207, p. 108502, 2022.

[29] Y. Wang et al., "Indoor Thermal Comfort Evaluation of Traditional Dwellings in Cold Region of China: A Case Study in Guangfu Ancient City," Energy and Buildings, p. 113028, 2023.

[30] Y. Lin, L. Zhao, W. Yang, X. Hao, and C.-Q. Li, "A review on research and development of passive building in China," *Journal of Building Engineering*, vol. 42, Oct 2021, Art. no. 102509.

[31] J. Gainza-Barrencia, M. Odriozola-Maritorena, R. Hernandez-Minguillon, and I. Gomez-Arriaran, "Energy savings using sunspaces to preheat ventilation intake air: Experimental and simulation study," *Journal of Building Engineering*, vol. 40, Aug 2021, Art. no. 102343.

[32] A. Dudzinska, "Efficiency of Solar Shading Devices to Improve Thermal Comfort in a Sports Hall," *Energies*, vol. 14, no. 12, Jun 2021, Art. no. 3535.

[33] N. Li, Z. C. Peng, J. Dai, and Z. W. Li, "Performance-Oriented Passive Design Strategies for Shape and Envelope Structure of Independent Residential Buildings in Yangtze River Delta Suburbs," *Sustainability*, vol. 14, no. 8, Apr 2022, Art. no. 4571.

[34] M. Peng, "Application of key technology and materials in the building envelop of passive house and low energy buildings," *New Building Materials*, vol. 42, no. 01, pp. 77-82, 2015.

Chapter 7

EFFECTIVENESS STUDY OF PASSIVE DESIGN PARAMETERS FOR TRADITIONAL DWELLING

CHAPTER SEVEN: EFFECTIVENESS STUDY OF PASSIVE DESIGN PARAMETERS FOR TRADITIONAL DWELLING

EFFECTIVENESS STUDY OF PASSIVE DESIGN PARAMETERS FOR TRADITIONAL DWELLING..... 1

7.1. Contents 1

7.2. Materials and methodology..... 1

 7.2.1. Research background 1

 7.2.2. Methods..... 3

7.3. Research proposal 3

7.4. Effectiveness of the single control variable 4

 7.4.1. Passive design parameters..... 4

 7.4.2. Single control variable Analysis..... 4

 7.4.3. Effectiveness identification of single control variable 22

7.5. Single-objective optimization combination of multi controlled variables 29

 7.5.1. Single-objective optimization 29

 7.5.2. Evaluation of the optimal combination of the multi controlled variables by orthogonal method..... 30

 7.5.3. Simulation of the optimization model of traditional dwellings..... 32

 7.5.4. Temperature and humidity simulation of the traditional dwelling before and after optimization 33

7.6. Summary 35

Reference 37

7.1. Contents

Traditional dwelling has achieved harmony between building and climatic environment, which is one of the most significant prerequisites for sustainability. In this study, the “I” shape traditional dwelling were selected as the representative traditional dwellings in Qinba mountainous area, and 11 passive design parameters extracted from traditional dwellings were utilized to improve its indoor thermal comfort. This research presents an approach in which the energy simulation, and statistical method were integrated to analyze the single control variable to determine the effectiveness of passive design parameters for the 5 climatic sub-regions in Qinba mountainous area by using sensitivity analysis and relative sensitivity analysis. According to the result, the 4 effective passive design parameters are the attached sunroom, the heat transfer coefficient of the external wall, roof, and window.

Meanwhile, the research determined the ranges of the 4 passive design parameters through field investigations and regulatory research and applied the meteorological data from climatic sub-region A1 and a “□” shape residential building to validate the effectiveness of the passive strategy combination by using orthogonal method. Then, the research used the single-objective optimization model focused on reducing building energy consumption to simulate the energy consumption and indoor thermal environment of the test building. The single-objective optimization model for building energy consumption could reduce the annual energy consumption of the simulated dwelling by 65.1% compared with that of the original one and increase the indoor air temperature and mean radiation temperature by 4.31°C and 4.35°C in winter respectively. At the same time, the payback period of the single-objective optimization model for building energy consumption was calculated to verify the effectiveness and economic feasibility of the passive design parameters.

7.2. Materials and methodology

7.2.1. Research background

Since 2020, China is responsible for 26.1% of world greenhouse gas emissions, and has been the world’s greatest energy consumer and carbon emitter [1]. In China, the building sector accounts for approximately 40% of energy consumption and this could be a real challenge to the Chinese construction industry to increase energy efficiency and reduce energy consumption, while it is an opportunity for research academics [2]. Furthermore, China has a considerable number of rural regions, which consumes 24% of the total building energy consumption up to 2018 [3]. The traditional dwellings in the rural area employed passive strategies, by continuous trial and error, to adapt to the local climate, improve the indoor thermal environment and reduce energy consumption to some extent [4]. Since passive buildings could lead to over 80%–90% energy savings, most traditional buildings still have the potential for optimization as they were built based on traditional experience without scientific guidance, therefore, it is urgent to

systematic optimize the passive design strategy of traditional dwellings to lower building energy consumption, minimize carbon emissions and improve their indoor thermal comfort [4, 5].

Typically, the building energy consumption could be significantly reduced by active or passive technologies [6]. The active strategy focused on the electrical equipment, such as refining heating, ventilation, HVAC systems, hot water producing, lighting and any other building services applications. However, the logic of passive strategies is different as it seeks to supply more energy-efficient architectural elements, such as building envelope, shape and layout. Passive technologies often had modest additional capital investment costs compared to the potential benefit in energy savings [7]. Numerous studies looked into actual retrofitting projects that used diverse passive and active technologies in different climates [7-10]. A passive design strategy is crucial for reducing energy use and improving human comfort as it has many advantages over active technologies, such as: 1) passive structures' effective thermal insulation can maintain a comparatively constant internal temperature and humidity; 2) Passive buildings' good air tightness can efficiently minimize indoor dust and ensure the indoor sound insulation requirements; 3) Passive buildings' high efficiency heat recovery can greatly reduce the consumption of primary energy, which could be crucial in lowering energy stress, carbon dioxide emissions and air pollution [6, 9-13]. In Europe, the ultra-low energy consumption passive houses are increasing at an annual rate of 8%, which demonstrates that the development of green low-carbon passive buildings is sustainable path to the development of building energy conservation while providing good thermal comfort performance [14].

As a result, as each region has its own climatic features, living behaviors, local materials, heating and ventilation preference, there is no universal design solution for passive buildings across all climate zones. In addition, despite some researchers' work on rural housing, the majority of academic study is still concentrated on structures in metropolitan settings. Furthermore, researchers who focused on rural residential buildings have not optimized comprehensive passive design methodologies for rural residential structures, which may overlook potentially significant inter-parameter interactions.

Based on the problems we discovered about the indoor thermal environment of traditional dwellings in the Qinba mountainous area and the passive strategies we investigated, the purpose of this study is to analyze the effectiveness of the common passive design parameters for the overall energy saving performance, then determine how energy consumption could be minimized by the optimal combination of the effective passive design parameters. This research would contribute to the optimal combination of passive design strategy for the renovation of the traditional dwellings in the Qinba mountainous area to improve the building energy performance while satisfying the indoor thermal comfort.

7.2.2. Methods

(1) Computer simulation

In this study, EnergyPlus software were utilized for energy simulation. EnergyPlus is a computer program that provides a comprehensive simulation platform for analyzing the energy performance of buildings. Employing advanced modeling techniques, it enables accurate prediction of a building's energy consumption, as well as the thermal and visual comfort of its occupants. With the ability to evaluate a broad range of building designs and systems, such as HVAC equipment, lighting, and building envelope components. EnergyPlus is a valuable tool for architects, engineers, and building energy consultants to optimize building design and system performance while complying with energy codes and standards [15].

The study utilized the most prevalent traditional dwelling in the Qinba mountainous area, which is the "I"-shaped building, as the model for energy consumption simulation, shown in Figure 4-27. The meteorological data from the 5 climatic sub-regions used in Chapter 4 was also applied to the simulation. The building envelope structure and energy simulation software settings were consistent with those in Chapter 6.

(2) Statistical method

Statistical analysis is a process of acquiring knowledge and supporting decision-making by collecting, organizing, and interpreting data. The primary objective of data analysis methods is to identify patterns, associations, and trends existing within the data to generate useful information. In this chapter, the statistical method used is the linear regression method. The basic idea of linear regression is to analyze a set of data and establish a linear equation that describes the relationship between the independent and dependent variables. Linear regression assumes that there is a linear relationship between the independent and dependent variables, enabling predictions of unknown data [16]. In this chapter, we employed the linear regression analysis method to investigate the relationship between individual passive design strategies and building thermal loads.

7.3. Research proposal

In this chapter, we utilized computer simulations, statistical analysis, and the orthogonal arrays method to assess the effectiveness of passive design parameters in each sub-region. The aim was to optimize the building energy efficiency through passive design strategies in climatic sub-region A1. Initially, we conducted a single controlled variable study, simulating the energy consumption analysis and calculating the relative sensitivity coefficients of 11 passive design parameters across 5 climatic sub-regions in the Qinba mountainous area. Based on the results, we could identify the effective parameters for passive renovation of traditional dwellings. Subsequently, a multi controlled variable study was conducted using orthogonal arrays analysis to determine the optimal combination of effective passive design parameters. Finally, we simulated the building annual thermal loads of the optimized renovated dwelling in the climatic

sub-region A1 using energy simulation software. The research framework is shown in Figure 7-1.

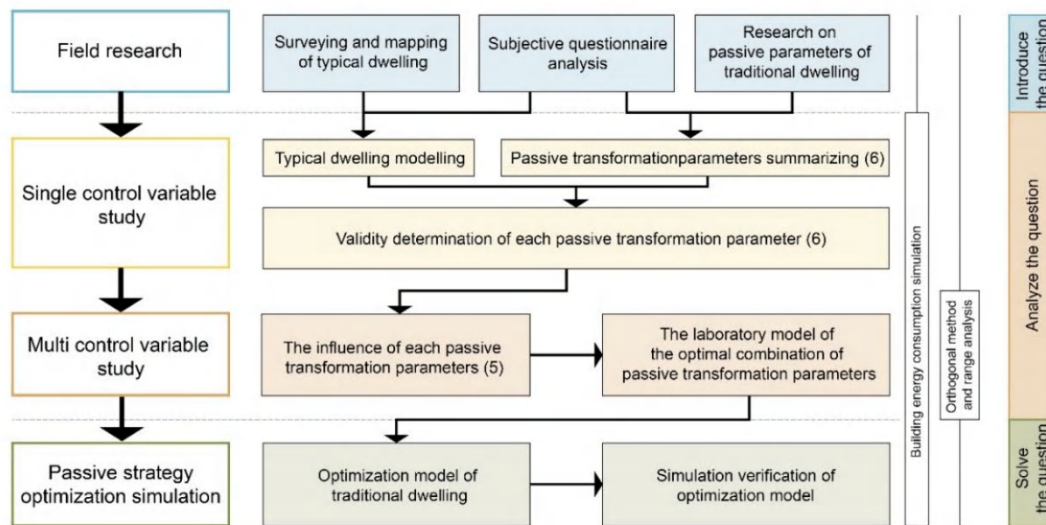


Figure 7-1. Research framework

7.4. Effectiveness of the single control variable

7.4.1. Passive design parameters

According to the site survey, the traditional dwellings in the Qinba mountainous area used low-cost construction technologies and passive strategies with environmental adaptability that could improve its indoor thermal environment to a certain extent. Based on the literature review and extraction of passive strategies commonly used in hot summer and cold winter area, our research team screened the passive design parameters that are relatively important to building energy consumption, including the window-wall ratio, sunroom depth, overhang depth, building orientation, building shape coefficient, heat transfer coefficient of the exterior wall, roof, and exterior window.

7.4.2. Single control variable Analysis

A: SD (Attached sunroom depth)

A sunroom is a common passive design strategy that attaching a glazed space to the building elevation to provide a buffer zone which could impact the thermal and ventilation losses [17]. The sunroom serves as a barrier that prevents excessive heat release from the indoor space in winter. However, it also absorbs more solar radiation in the summer and heats up the indoor temperature [18]. In this study, the attached sunroom aims to maximize the use of solar heating while preserving adequate lighting and comfortable thermal conditions for indoor spaces.

In the Northern Hemisphere, the southward sunroom has the greatest influence on building energy consumption in winter and summer as it could store the maximum heat for the building

[19, 20]. Moreover, as most of our research areas are in hot summer and cold winter zone, and residents' satisfaction with the thermal environment in winter is much lower than that in summer, it is necessary to attach the sunroom to improve the indoor thermal environment in winter. Therefore, this study only evaluated the sunroom added to the south.

In order to obtain the optimal sunroom depth in each climatic sub-region, this study takes the sunroom depth as the simulation input variable, and other building elements are set according to the actual parameters of target model to simulate the impact of sunroom depth on building annual thermal loads. As a solar collector space, the depth of attached sunroom could be designed to be relatively small, generally equal to 0.6m, and if it is utilized as a functional space, the 0.6 m~1.5 m deep sunroom is appropriate [21]. Moreover, the depth of the overhanging eaves of the traditional dwellings in Qinba mountainous area is 0.8 m~2.4m, so the maximum depth of the sunroom can be set to 2.4m. Therefore, in this study, 0.6m~2.4m sunroom depth with the interval of 0.3m was set to simulate the building annual thermal loads. The simulation results of building annual thermal loads based on attached sunroom depth in each climatic sub-region are shown in Table 7-1.

Table 7-1. Building annual thermal loads based on attached sunroom depth

Attached sunroom depth (m)		-	0.6	0.9	1.2	1.5	1.8	2.1	2.4
A1	Thermal loads (kWh/m ²)	37.68	28.95	28.30	27.81	27.45	27.27	27.07	26.89
	Energy saving rate	-	-23.17%	-24.89%	-26.19%	-27.15%	-27.63%	-28.16%	-28.64%
A2	Thermal loads (kWh/m ²)	33.33	26.28	25.61	25.08	24.69	24.42	24.20	24.00
	Energy saving rate	-	-21.15%	-23.16%	-24.75%	-25.92%	-26.73%	-27.39%	-27.99%
B1	Thermal loads (kWh/m ²)	45.42	33.76	32.86	32.10	31.42	30.89	30.43	30.14
	Energy saving rate	-	-25.67%	-27.65%	-29.33%	-30.82%	-31.99%	-33.00%	-33.64%
B2	Thermal loads (kWh/m ²)	44.63	36.16	35.46	34.80	34.18	33.60	33.01	32.44
	Energy saving rate	-	-18.98%	-20.55%	-22.03%	-23.41%	-24.71%	-26.04%	-27.31%
C	Thermal loads (kWh/m ²)	50.44	37.82	37.20	36.62	36.08	35.55	35.01	34.61
	Energy saving rate	-	-25.02%	-26.25%	-27.40%	-28.47%	-29.52%	-30.59%	-31.38%

As shown in Table 7-1, the attached sunroom has a great influence on the building heating and cooling energy consumption. Using the statistical data in Table 7-1, the linear regression analysis of the sunroom depth and building annual thermal loads are carried out. The analysis of the scatter plot shows that when the sunroom depth is 0m, the building annual thermal load deviates far from the regression line. Therefore, when analyzing the linear regression relationship, it is necessary to screen out the situation without sunroom. Figure 7-2 shows the linear regression analysis, it could be seen that the sunroom depth was negatively correlated with the annual building energy consumption of the simulated dwelling.

Without the sunroom, the annual thermal loads were 37.68kWh/m², 33.33 kWh/m², 45.42 kWh/m², 44.63 kWh/m², 50.44kWh/m² in climatic sub-region A1, A2, B1, B2, and C, respectively. When the depth of sunroom was extended from 0.6 m to 2.4 m, the building annual

thermal loads were reduced from 28.95 kWh/m², 26.28 kWh/m², 33.76 kWh/m², 36.16 kWh/m², and 37.82 kWh/m² to 26.89 kWh/m², 24.00 kWh/m², 30.14 kWh/m², 32.44 kWh/m², and 34.61 kWh/m² in climatic sub-region A1, A2, B1, B2, and C, respectively. Adding the sunroom or not has a great influence on the heating and cooling energy consumption of buildings, as the energy saving rate could reach 23.71%, 21.15%, 25.67%, 18.98%, and 25.02% in climatic sub-region A1, A2, B1, B2, and C, respectively. However, the change of building energy consumption caused by increasing the sunroom depth is not so obvious, as the energy saving rate only increase 5% with the sunroom depth increased from 0.6m to 2.4m in each climatic sub-region.

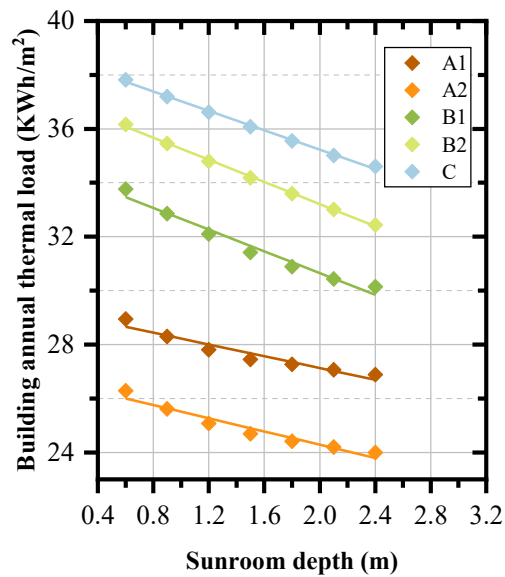


Figure 7-2. Relationship between sunroom depth and building annual thermal load

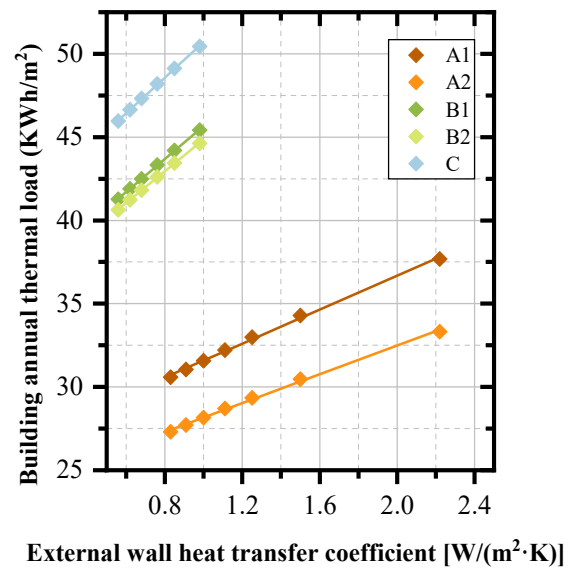


Figure 7-3. Relationship between external wall heat transfer coefficient and building annual thermal load

B: EWHTC (external wall heat transfer coefficient)

A good thermal insulation and heat storage effect on the exterior wall might ensure a steady interior thermal environment and thermal comfort [22, 23]. As an important part of the building envelope, the exterior wall is the most important factor affecting building energy conservation. Relevant literature shows that the building energy consumption of the exterior wall in winter and summer accounts for about 44 % and 37 % of the total building energy consumption [24].

The building energy consumption loss caused by the external wall is determined by the heat transfer coefficient of it. The heat transfer coefficient and thermal inertia of the external wall should meet the standard requirements, so that the external wall of the building has a good thermal insulation and heat storage effect, which can maintain a stable indoor thermal environment, and will not change sharply due to the excessive temperature difference between indoor and outdoor, so as to achieve indoor thermal comfort and necessary energy saving requirements [25]. In hot summer and cold winter region, the exterior wall heat transfer

coefficient should not exceed $1.50 \text{ W}/(\text{m}^2\cdot\text{K})$ [21]. The insulation layer added to the exterior wall is recommended to use the EPS insulation board with a thickness of 20~30 mm in rural area in the hot summer and cold winter region [21].

Through field research, we learned that the external wall structures in each climatic sub-region in the study area are mainly timber wall, bamboo clay wall, and rammed earth wall. The timber wall and bamboo clay wall are mainly distributed in sub-region A1 and A2, and the rammed earth wall is mainly distributed in sub-region B1, B2 and C. The thermal performance indexes of the exterior walls before and after renovation in each climatic sub-region are shown in Table 7-2 and Table 7-3.

Table 7-2. The modified structure of the exterior wall in climatic sub-region A1, A2

No.	Construction layers			U-value ($\text{W}/\text{m}^2\cdot\text{K}$)
	Original structure(mm) Bamboo plaited layer in the middle with two grass clay layers on surface	Eps board (mm)	Cement mortar(mm)	
1	50	0	-	2.22
2	50	9	3	1.5
3	50	14	3	1.25
4	50	18	3	1.11
5	50	22	3	1.00
6	50	26	3	0.91
7	50	30	3	0.83

In climatic sub-region A1 and A2, with exterior of bamboo clay wall, when 30 mm thick EPS insulation board was utilized for building renovation, the exterior wall heat transfer coefficient of the simulated dwelling was reduced from $2.22 \text{ W}/(\text{m}^2\cdot\text{K})$ to $0.83 \text{ W}/(\text{m}^2\cdot\text{K})$. Moreover, the exterior wall heat transfer coefficient should not exceed $1.50 \text{ W}/(\text{m}^2\cdot\text{K})$ according to the standard requirements [21]. Therefore, in sub-region A1 and A2, the exterior wall heat transfer coefficient was set as $0.83 \text{ W}/(\text{m}^2\cdot\text{K}) \sim 1.50 \text{ W}/(\text{m}^2\cdot\text{K})$ to simulate the building annual thermal loads.

Table 7-3. The modified structure of the exterior wall in climatic sub-region B1, B2, C

No.	Construction layers			U-value ($\text{W}/\text{m}^2\cdot\text{K}$)
	Original structure(mm) Rammed earth wall	Eps board (mm)	Cement mortar(mm)	
1	390	0	-	0.98
2	390	6	3	0.85
3	390	12	3	0.76
4	390	18	3	0.68
5	390	24	3	0.62
6	390	30	3	0.56

In climatic sub-region B1, B2 and C with exterior of rammed earth wall, when 30 mm thick EPS insulation board was utilized for building renovation, the exterior wall heat transfer coefficient of the simulated dwelling was reduced from 0.98 W/(m²·K) to 0.56 W/(m²·K). Therefore, in sub-region B1, B2 and C, the exterior wall heat transfer coefficient was set as 0.56 W/(m²·K) ~0.98 W/(m²·K) to simulate the building annual thermal loads.

The simulation results of building annual thermal loads based on external wall heat transfer coefficient in each climatic sub-region are shown in Table 7-4.

Table 7-4. Building annual thermal loads based on external wall heat transfer coefficient

A1	External wall heat transfer coefficient (W/ m ² ·K)	2.22	1.50	1.25	1.11	1.00	0.91	0.83
	Thermal loads (kWh/m ²)	37.68	34.29	32.98	32.21	31.58	31.06	30.58
	Energy saving rate	-	-9.00%	-12.47%	-14.52%	-16.19%	-17.57%	-18.84%
A2	External wall heat transfer coefficient (W/ m ² ·K)	2.22	1.50	1.25	1.11	1.00	0.91	0.83
	Thermal loads (kWh/m ²)	33.33	30.47	29.35	28.71	28.17	27.71	27.30
	Energy saving rate	-	-8.58%	-11.94%	-13.86%	-15.48%	-16.86%	-18.09%
B1	External wall heat transfer coefficient (W/ m ² ·K)	0.98	0.98	0.85	0.76	0.68	0.62	0.56
	Thermal loads (kWh/m ²)	45.42	45.42	44.20	43.32	42.49	41.90	41.27
	Energy saving rate	-	0.00%	-2.69%	-4.62%	-6.45%	-7.75%	-9.14%
B2	External wall heat transfer coefficient (W/ m ² ·K)	0.98	0.98	0.85	0.76	0.68	0.62	0.56
	Thermal loads (kWh/m ²)	44.63	44.63	43.45	42.60	41.82	41.24	40.63
	Energy saving rate	-	0.00%	-2.64%	-4.55%	-6.30%	-7.60%	-8.96%
C	External wall heat transfer coefficient (W/ m ² ·K)	0.98	0.98	0.85	0.76	0.68	0.62	0.56
	Thermal loads (kWh/m ²)	50.44	50.44	49.12	48.19	47.32	46.65	45.96
	Energy saving rate	-	0.00%	-2.62%	-4.46%	-6.19%	-7.51%	-8.88%

And the linear regression analysis of the external wall heat transfer coefficient and building annual thermal loads are carried out according to Table 7-7. The linear regression analysis is shown in Figure 7-3, the external wall heat transfer coefficient is positively correlated with the building annual thermal loads of the simulated dwelling. In sub-region A1 and A2, the external wall heat transfer coefficient has a great influence on the building heating and cooling energy consumption due to the obvious change of the heat transfer coefficient of the external wall after renovation. When the external wall heat transfer coefficient is reduced from 2.22W/(m²·K) to 0.83W/(m²·K) in sub-region A1 and A2, the building annual thermal loads would be decreased from 37.68kWh/m² to 30.58kWh/m², and 33.33 kWh/m² to 27.30 kWh/m², respectively. The building energy saving efficiency can reach 18.84% and 18.09% in sub-region A1 and A2. In sub-region B1, B2, and C, as the heat transfer coefficient of the original rammed earth wall is small and could meet the specification requirements, the change of the heat transfer coefficient of the external wall after the renovation is relatively insignificant. When the external wall heat transfer coefficient is reduced from 0.98W/(m²·K) to 0.56W/(m²·K) in sub-region B1, B2 and

C, the building annual thermal loads would be decreased from 45.42kWh/m² to 41.27kWh/m², 44.63kWh/m² to 40.63kWh/m², and 50.44kWh/m² to 45.96kWh/m², respectively. The building energy saving rate is still high, which is 9.14%, 8.96%, and 8.88%, respectively.

C: RHTC (roof heat transfer coefficient)

The roof is the most intense part of the building envelope by solar radiation [26]. The traditional dwellings in rural areas are mainly one-story buildings, and a small number of two-story buildings. In this case, the roof accounts for 30% ~ 40% of the surface area of the enclosure structure, which has a great impact on indoor thermal comfort and building energy consumption [27]. The building roofs with adequate insulation and heat storage could also help to minimize the building energy consumption [28].

Through field research, we learned that the roof of the traditional dwellings in Qinba mountainous area is double layers tile roof, which has the air space in the middle with two clay tile layers on surfaces. The heat transfer coefficient of the original tile roof is 2.24 W/(m²·K). In hot summer and cold winter region, the roof heat transfer coefficient should not exceed 0.80 W/(m²·K) [21]. And the insulation layer added to the roof is recommended to use the EPS insulation board with the thickness of less than 50 mm. The thermal performance indexes of the exterior walls before and after renovation in each climatic sub-region are shown in Table 7-5.

Table 7-5. The modified structure of the roof

No.	Construction layers			U-value (W/m ² ·K)
	Original structure(mm) tile	Eps board (mm)	Cement mortar(mm)	
1	25	0	-	2.24
2	25	32	3	0.8
3	25	34	3	0.77
4	25	38	3	0.72
5	25	42	3	0.67
6	25	46	3	0.63
7	25	50	3	0.59

When 50 mm thick EPS insulation board was added for building roof, the roof heat transfer coefficient of the simulated dwelling would be reduced from 2.24 W/(m²·K) to 0.59 W/(m²·K). Therefore, in this study, the roof heat transfer coefficient was set as 0.59 W/(m²·K) ~ 0.80 W/(m²·K) to simulate the annual energy consumption. The simulation results of building annual thermal loads based on external wall heat transfer coefficient in each climatic sub-region are shown in Table 7-6.

Table 7-6. Building annual thermal loads based on roof heat transfer coefficient

Roof heat transfer coefficient (W/ m ² ·K)	2.24	0.8	0.77	0.72	0.67	0.63	0.59
A1 Thermal loads (kWh/m ²)	37.68	31.34	31.19	30.94	30.67	30.46	30.25
A1 Energy saving rate	-	-16.83%	-17.22%	-17.89%	-18.60%	-19.16%	-19.72%
A2 Thermal loads (kWh/m ²)	33.33	27.06	26.94	26.68	26.44	26.24	26.03
A2 Energy saving rate	-	-18.81%	-19.17%	-19.95%	-20.67%	-21.27%	-21.90%
B1 Thermal loads (kWh/m ²)	45.42	36.78	36.57	36.23	35.89	35.60	35.30
B1 Energy saving rate	-	-19.02%	-19.48%	-20.23%	-20.98%	-21.62%	-22.28%
B2 Thermal loads (kWh/m ²)	44.63	36.27	36.07	35.72	35.36	35.08	34.78
B2 Energy saving rate	-	-18.73%	-19.18%	-19.96%	-20.77%	-21.40%	-22.07%
C Thermal loads (kWh/m ²)	50.44	39.43	39.06	38.59	38.13	37.75	37.38
C Energy saving rate	-	-21.83%	-22.56%	-23.49%	-24.41%	-25.16%	-25.89%

And the linear regression analysis of the roof heat transfer coefficient and building annual thermal loads are shown in Figure 7-4, the roof heat transfer coefficient is positively correlated with the building annual thermal loads of the simulated dwelling. And it has a great influence on the building heating and cooling energy consumption. When the roof heat transfer coefficient is reduced from 2.24W/(m²·K) to 0.59W/ (m²·K), the building annual thermal loads would be decreased from 37.68kWh/m² to 30.25kWh/m², 33.33 kWh/m² to 26.03 kWh/m², 45.42 kWh/m² to 35.30 kWh/m², 44.63 kWh/m² to 34.78 kWh/m², and 50.44 kWh/m² to 37.38 kWh/m² in climatic sub-region A1, A2, B1, B2, and C, respectively. The energy consumption of the renovated dwelling can be reduced by 19.72%, 21.90%, 22.28%, 22.07%, and 25.89% in each sub-region.

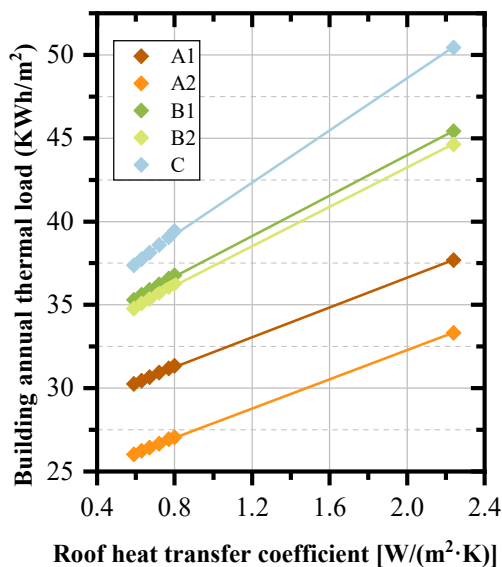


Figure 7-4. Relationship between roof heat transfer coefficient and building annual thermal load

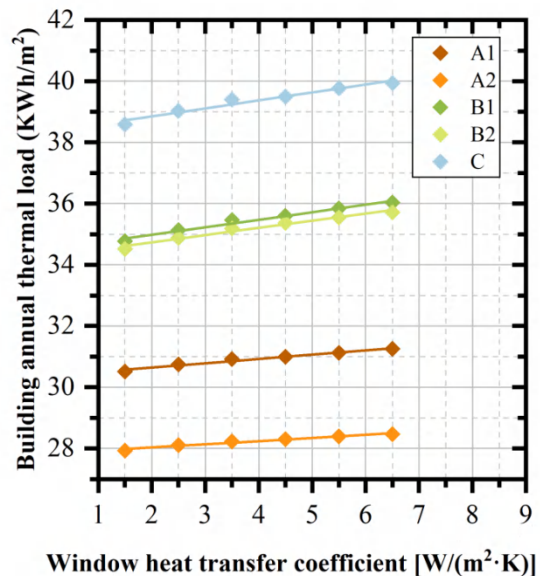


Figure 7-5. Relationship between window heat transfer coefficient and building annual thermal load

D: WHTC (window heat transfer coefficient)

The window with low heat transfer coefficient could limit the heat transfer between indoor and outdoor temperature differences and manage the indoor solar heat gain [29]. In the traditional dwellings in Qinba mountainous area, the main heat gain and heat dissipation of the exterior window are not only related to the window heat transfer coefficient, but also to a large extent due to the poor air tightness of the window, and the cold wind penetration in winter seriously affects the indoor thermal comfort and increases heating and cooling energy consumption [30].

According to ASHRAE 55-2007, the building air tightness could be evaluated by infiltration rate (flow per exterior surface area). At typical building pressures of 4 Pa, the typical values for this property are 0.0001(m³/s per m² facade) for tight building, 0.0003(m³/s per m² facade) for average building, and 0.0006 (m³/s per m² facade) for leaky building. Due to the poor air tightness of the windows of the traditional dwellings in the study area, the infiltration rate of the traditional dwellings before renovation could be set to 0.0006 (m³/s per m² facade). And after renovation, the air tightness of the traditional dwellings is improved, but it still cannot reach the standard for tight building. Therefore, the infiltration rate of the renovated dwelling could be set to 0.0003(m³/s per m² facade). Moreover, in hot summer and cold winter region, the window heat transfer coefficient should be between 1.50 W/(m²·K) and 3.20 W/(m²·K) [21]. In the actual transformation process, the heat transfer coefficient of the commonly used aluminum alloy windows is 6.5 W/(m²·K), while reducing the heat transfer coefficient of the window, the cost of the window increases significantly. And regardless of the heat transfer coefficient of the window, the improvement of air tightness can greatly improve indoor thermal comfort. As a result, from the perspective of economy, the window heat transfer coefficient was set as 1.50 W/(m²·K) ~ 6.50 W/(m²·K) to simulate the annual energy consumption.

The simulation results of building annual thermal loads based on window heat transfer coefficient and building infiltration rate in each climatic sub-region are shown in Table 7-7.

Table 7-7. Building annual thermal loads based on window heat transfer coefficient

Window heat transfer coefficient (W/m ² ·K)		3.24	6.5	5.5	4.5	3.5	2.5	1.5
A1	Thermal loads (kWh/m²)	37.68	31.25	31.13	31.00	30.92	30.74	30.52
	Energy saving rate	-	-17.06%	-17.38%	-17.73%	-17.94%	-18.42%	-19.00%
A2	Thermal loads (kWh/m²)	33.33	28.47	28.39	28.30	28.23	28.11	27.93
	Energy saving rate	-	-14.58%	-14.82%	-15.09%	-15.30%	-15.66%	-16.20%
B1	Thermal loads (kWh/m²)	45.42	36.03	35.84	35.60	35.46	35.13	34.77
	Energy saving rate	-	-20.67%	-21.09%	-21.62%	-21.93%	-22.66%	-23.45%
B2	Thermal loads (kWh/m²)	44.63	35.72	35.55	35.37	35.19	34.88	34.52
	Energy saving rate	-	-19.96%	-20.35%	-20.75%	-21.15%	-21.85%	-22.65%
C	Thermal loads (kWh/m²)	50.44	39.94	39.77	39.49	39.40	39.03	38.58
	Energy saving rate	-	-20.82%	-21.15%	-21.71%	-21.89%	-22.62%	-23.51%

And the linear regression analysis of the window heat transfer coefficient and building annual thermal loads are shown in Figure 7-5. The analysis of the scatter plot shows that when the window heat transfer coefficient is $3.24 \text{ W}/(\text{m}^2 \cdot \text{K})$ with the infiltration rate of $0.0006 \text{ (m}^3/\text{s per m}^2 \text{ facade)}$, the building annual thermal load deviates far from the regression line. Therefore, when analyzing the linear regression relationship, it is necessary to screen out the situation before renovation. The linear regression analysis shows that, when the infiltration rate is $0.0003 \text{ (m}^3/\text{s per m}^2 \text{ facade)}$, and the window heat transfer coefficient is reduced from $6.50 \text{ W}/(\text{m}^2 \cdot \text{K})$ to $1.50 \text{ W}/(\text{m}^2 \cdot \text{K})$, the window heat transfer coefficient is positively correlated with the building annual thermal loads of the simulated dwelling.

And the after renovation, both of the window heat transfer coefficient and building infiltration rate have been improved, the building annual thermal loads would be decreased from $37.68 \text{ kWh}/\text{m}^2$ to $30.52 \text{ kWh}/\text{m}^2$, $33.33 \text{ kWh}/\text{m}^2$ to $27.93 \text{ kWh}/\text{m}^2$, $45.42 \text{ kWh}/\text{m}^2$ to $34.77 \text{ kWh}/\text{m}^2$, $44.63 \text{ kWh}/\text{m}^2$ to $34.52 \text{ kWh}/\text{m}^2$, and $50.44 \text{ kWh}/\text{m}^2$ to $38.58 \text{ kWh}/\text{m}^2$ in climatic sub-region A1, A2, B1, B2, and C, respectively. The energy consumption of the renovated dwelling can be reduced by 19.00%, 16.20%, 23.45%, 22.65%, and 23.51% in each sub-region, respectively.

E: SWWR (south window-wall ratio)

The size of the exterior window will directly affect the heat gain of solar radiation or the heat loss of the building, which will affect the indoor thermal comfort and ultimately affect the building thermal load [31]. The previous studies show that the influence of window-wall ratio on building energy consumption varies in different climate zones [32, 33]. And the building with proper window-wall ratio contributes to a reduction in the building energy consumption by 5%~25% [34].

In the study area, according to the building style, the exterior window normally has a 1.0m sill height, 0.8m window height, and 1.0m window width. And generally, there is one window in each room. Through a lot of research and calculation, the window-wall ratio of the traditional dwellings in Qinba mountainous Area is $0.1 \sim 0.18$. Moreover, in order to ensure the consistency of the facade of traditional dwellings, with a 0.8 m window height of the dwelling, the window-wall ratio was modified by altering the window width, obtaining the result with the maximum allowable window-wall ratio of 0.4. As the result, this study set the window-wall ratio to be $0.1 \sim 0.4$ to simulate the building annual energy consumption. At the same time, we need to study the influence of window-wall ratio on building energy consumption in four directions of south, north, east, and west. Therefore, the study of building window-wall ratio is divided into the analysis of south window-wall ratio, north window-wall ratio, east window-wall ratio, and west window-wall ratio. In this part, the south window-wall ratio will be discussed.

The simulation results of building annual thermal loads based on south window-wall ratio in each climatic sub-region are shown in Table 7-8.

Table 7-8. Building annual thermal loads based on south window-wall ratio

South window-wall ratio	0.10	0.15	0.20	0.25	0.30	0.35	0.40
A1 Thermal loads (kWh/m ²)	37.68	37.41	37.16	36.89	36.65	36.41	36.18
A1 Energy saving rate	-	-0.72%	-1.38%	-2.10%	-2.73%	-3.37%	-3.98%
A2 Thermal loads (kWh/m ²)	33.33	33.21	33.07	32.97	32.85	32.74	32.64
A2 Energy saving rate	-	-0.36%	-0.78%	-1.08%	-1.44%	-1.77%	-2.07%
B1 Thermal loads (kWh/m ²)	45.42	45.25	45.08	44.93	44.81	44.70	44.57
B1 Energy saving rate	-	-0.37%	-0.75%	-1.08%	-1.34%	-1.59%	-1.87%
B2 Thermal loads (kWh/m ²)	44.63	44.71	44.78	44.88	44.98	45.09	45.19
B2 Energy saving rate	-	0.18%	0.34%	0.56%	0.78%	1.03%	1.25%
C Thermal loads (kWh/m ²)	50.44	49.96	49.48	49.05	48.64	48.25	47.98
C Energy saving rate	-	-0.95%	-1.90%	-2.76%	-3.57%	-4.34%	-4.88%

And the linear regression analysis of the south window-wall ratio and building annual thermal loads are shown in Figure 7-6, the south window-wall ratio is negatively correlated with the building annual thermal loads of the simulated dwelling. And it doesn't have a great influence on the building heating and cooling energy consumption. When the south window-wall ratio is increased from 0.1 to 0.4, the building annual thermal loads would be decreased from 37.68kWh/m² to 36.18kWh/m², 33.33 kWh/m² to 32.64 kWh/m², 45.42 kWh/m² to 44.57 kWh/m², 44.63 kWh/m² to 45.19 kWh/m², and 50.44 kWh/m² to 47.98 kWh/m² in climatic sub-region A1, A2, B1, B2, and C, respectively. The energy consumption of the renovated dwelling can be reduced by 3.98%, 2.07%, 1.87%, 1.25%, and 4.88% in each sub-region.

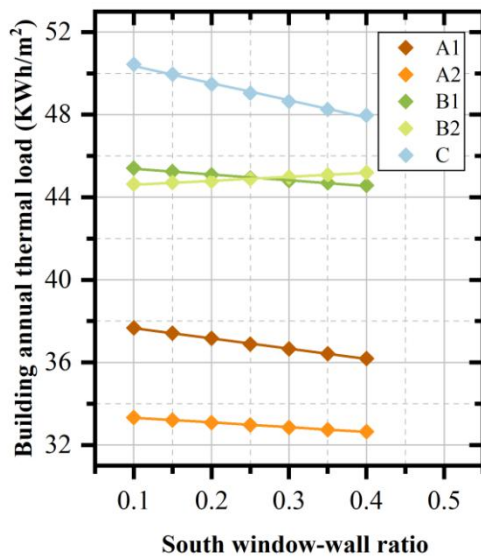


Figure 7-6. Relationship between south window-wall ratio and building annual thermal load

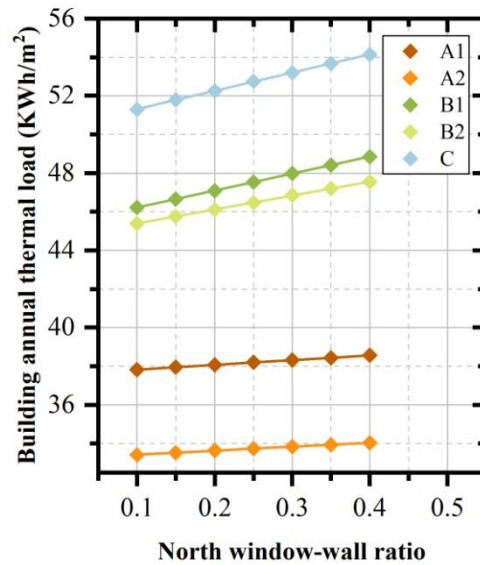


Figure 7-7. Relationship between north window-wall ratio and building annual thermal load

F: NWWR (north window-wall ratio)

The relationships of building annual thermal loads and north window-wall ratio in each climatic sub-region also need to be discussed, shown in Table 7-9.

Table 7-9. Building annual thermal loads based on north window-wall ratio

North window-wall ratio	-	0.10	0.15	0.20	0.25	0.30	0.35	0.40
A1								
Thermal loads (kWh/m ²)	37.68	37.83	37.95	38.07	38.2	38.32	38.44	38.56
Energy saving rate	-	0.40%	0.72%	1.04%	1.38%	1.70%	2.02%	2.34%
A2								
Thermal loads (kWh/m ²)	33.33	33.42	33.53	33.64	33.74	33.84	33.94	34.05
Energy saving rate	-	0.27%	0.60%	0.93%	1.23%	1.53%	1.83%	2.16%
B1								
Thermal loads (kWh/m ²)	45.42	46.22	46.65	47.08	47.53	47.98	48.41	48.85
Energy saving rate	-	1.76%	2.71%	3.65%	4.65%	5.64%	6.58%	7.55%
B2								
Thermal loads (kWh/m ²)	44.63	45.40	45.76	46.11	46.48	46.85	47.19	47.55
Energy saving rate	-	1.73%	2.53%	3.32%	4.15%	4.97%	5.74%	6.54%
C								
Thermal loads (kWh/m ²)	50.44	51.30	51.79	52.26	52.75	53.21	53.68	54.14
Energy saving rate	-	1.70%	2.68%	3.61%	4.58%	5.49%	6.42%	7.34%

The linear regression analysis of the north window-wall ratio and building annual thermal loads are shown in Figure 7-7, the north window-wall ratio is positively correlated with the building annual thermal loads of the simulated dwelling. When the north window-wall ratio is increased from 0.1 to 0.4, the building annual thermal loads would be increased from 37.83kWh/m² to 38.56kWh/m², 33.42 kWh/m² to 34.05 kWh/m², 46.22 kWh/m² to 48.85 kWh/m², 45.40 kWh/m² to 47.55 kWh/m², and 51.30 kWh/m² to 54.14 kWh/m² in climatic sub-region A1, A2, B1, B2, and C, respectively. There is no window on the north side of traditional dwelling, and increasing the window on the north side will increase the building energy consumption, and with the increase of north window-wall ratio, the energy consumption will increase. Adding the north window will increase the annual building thermal loads by 2.34%, 2.16%, 7.55%, 6.54%, and 7.34% in each sub-region.

G: EWWR (east window-wall ratio)

As there is no window on the gable walls of traditional dwellings in Qinba mountainous area, when studying the window-wall ratio in the east and west elevation, the building model should be rotated to east-west direction for energy consumption simulation. The relationships of building annual thermal loads and east window-wall ratio in each climatic sub-region also need to be discussed, shown in Table 7-10.

Table 7-10. Building annual thermal loads based on east window-wall ratio

North window-wall ratio	-	0.10	0.15	0.20	0.25	0.30	0.35	0.40	
A1	Thermal loads (kWh/m ²)	40.16	40.33	40.39	40.45	40.54	40.61	40.69	40.79
	Energy saving rate	-	0.41%	0.57%	0.71%	0.95%	1.12%	1.32%	1.56%
A2	Thermal loads (kWh/m ²)	35.70	35.96	36.08	36.20	36.33	36.45	36.59	36.72
	Energy saving rate	-	0.73%	1.06%	1.40%	1.78%	2.11%	2.49%	2.87%
B1	Thermal loads (kWh/m ²)	46.85	47.38	47.62	47.85	48.12	48.36	48.63	48.91
	Energy saving rate	-	1.13%	1.64%	2.12%	2.71%	3.21%	3.80%	4.39%
B2	Thermal loads (kWh/m ²)	45.15	45.86	46.68	47.59	47.72	48.31	48.70	49.04
	Energy saving rate	-	1.58%	3.40%	5.42%	5.70%	7.01%	7.87%	8.63%
C	Thermal loads (kWh/m ²)	52.61	53.13	53.32	53.54	53.85	54.04	54.33	54.62
	Energy saving rate	-	0.98%	1.35%	1.77%	2.36%	2.71%	3.27%	3.82%

The linear regression analysis of the east window-wall ratio and building annual thermal loads are shown in Figure 7-8, the east window-wall ratio is positively correlated with the building annual thermal loads of the simulated dwelling. When the east window-wall ratio is increased from 0.1 to 0.4, the building annual thermal loads would be increased from 40.33kWh/m² to 40.79kWh/m², 35.96 kWh/m² to 36.72 kWh/m², 47.38 kWh/m² to 48.91 kWh/m², 45.86 kWh/m² to 49.04 kWh/m², and 53.13 kWh/m² to 54.62 kWh/m² in climatic sub-region A1, A2, B1, B2, and C, respectively. Increasing the east window with the window-wall ratio of 0.4 will increase the annual building thermal loads by 1.56%, 2.87%, 4.39%, 8.63%, and 3.82% in each sub-region.

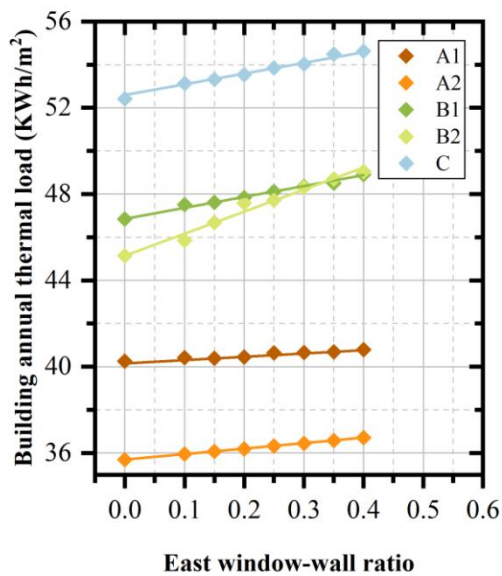


Figure 7-8. Relationship between east window-wall ratio and building annual thermal load

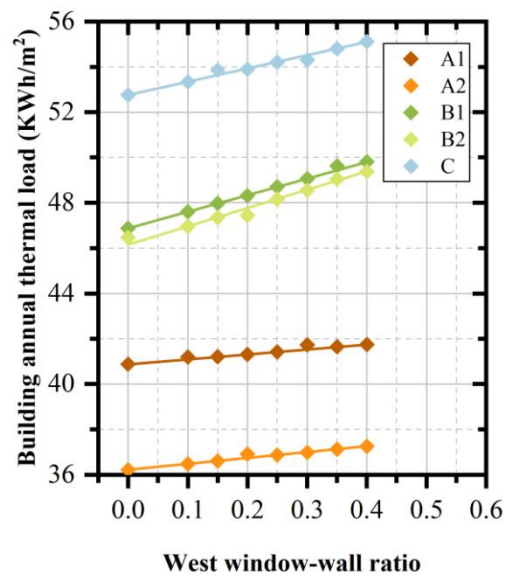


Figure 7-9. Relationship between west window-wall ratio and building annual thermal load

H: WWR (west window-wall ratio)

The relationships of building annual thermal loads and west window-wall ratio in each climatic sub-region also need to be discussed, shown in Table 7-11.

Table 7-11. Building annual thermal loads based on west window-wall ratio

North window-wall ratio	-	0.10	0.15	0.20	0.25	0.30	0.35	0.40	
A1	Thermal loads (kWh/m²)	40.88	41.09	41.20	41.30	41.42	41.52	41.64	41.75
	Energy saving rate	-	0.51%	0.78%	1.03%	1.31%	1.58%	1.87%	2.12%
A2	Thermal loads (kWh/m²)	36.21	36.48	36.61	36.74	36.87	36.99	37.13	37.26
	Energy saving rate	-	0.74%	1.09%	1.44%	1.81%	2.15%	2.52%	2.89%
B1	Thermal loads (kWh/m²)	46.87	47.61	47.97	48.33	48.71	49.06	49.42	49.81
	Energy saving rate	-	1.58%	2.35%	3.11%	3.93%	4.67%	5.45%	6.27%
B2	Thermal loads (kWh/m²)	46.17	46.97	47.36	47.74	48.16	48.55	49.05	49.37
	Energy saving rate	-	1.72%	2.57%	3.40%	4.30%	5.15%	6.24%	6.93%
C	Thermal loads (kWh/m²)	52.76	53.33	53.67	53.90	54.21	54.50	54.81	55.11
	Energy saving rate	-	1.09%	1.72%	2.16%	2.75%	3.30%	3.88%	4.46%

The linear regression analysis of the west window-wall ratio and building annual thermal loads are shown in Figure 7-9, the west window-wall ratio is positively correlated with the building annual thermal loads of the simulated dwelling. When the west window-wall ratio is increased from 0.1 to 0.4, the building annual thermal loads would be increased from 41.09kWh/m² to 41.75kWh/m², 36.48 kWh/m² to 37.26 kWh/m², 47.61 kWh/m² to 49.81 kWh/m², 46.97 kWh/m² to 49.37 kWh/m², and 53.33 kWh/m² to 55.11 kWh/m² in climatic sub-region A1, A2, B1, B2, and C, respectively. Increasing the west window with the window-wall ratio of 0.4 will increase the annual building thermal loads by 2.12%, 2.89%, 6.27%, 6.93%, and 4.46% in each sub-region.

I: OD (overhang depth)

Traditional dwellings adapt to different climatic environments through different eave widths and forms. The eave width directly affects the amount of solar radiation that the building needs to accept and reject [35]. The proper overhang depth and well-designed shade devices can greatly reduce building heating and cooling energy demand, while also improving natural lighting quality and residents' thermal comfort [36].

The climatic sub-region A1 and A2 have relatively mild environment in winter and high temperature in summer, mainly having the traditional dwellings with bamboo clay wall and timber wall. The depth of the eaves is large, which is about 1.5m ~ 1.8m, which can block the solar radiation to a certain extent and provide the shadow space under the cornice corridor. In sub-region B1, due to the influence of people's lifestyle, the cornice corridor is often used as a storage space for crops, so the overhang depth is large, which is about 2.1m ~ 2.4 m. In sub-region B2, and C, the temperature in winter is low, and the heat of solar radiation is needed to

increase the indoor temperature. So, the overhang width is small, which is about 0.6m ~ 0.9 meters. The standard regulation defined that, for the sloped roofs without an organized drainage system, the depth of the building overhang should not be less than 0.5m [37]. Therefore, in this study, the depth of the overhang was set from 0.5 m to 2.4 m to simulate the building energy consumption.

The simulation results of building annual thermal loads based on overhang depth in each climatic sub-region are shown in Table 7-12.

Table 7-12. Building annual thermal loads based on overhang depth

	Overhang depth (m)	1.6	0.5	0.9	1.3	1.7	2.1	2.4
A1	Thermal loads (kWh/m²)	37.68	38.01	37.84	37.72	37.71	37.98	38.43
	Energy saving rate	-	0.88%	0.42%	0.11%	0.08%	0.80%	1.99%
A2	Thermal loads (kWh/m²)	33.33	34.31	33.87	33.54	33.30	33.27	33.42
	Energy saving rate	-	2.94%	1.62%	0.63%	-0.09%	-0.18%	0.27%
B1	Thermal loads (kWh/m²)	45.42	44.50	44.72	44.93	45.10	45.42	45.84
	Energy saving rate	-	-2.03%	-1.54%	-1.08%	-0.70%	0.00%	0.92%
B2	Thermal loads (kWh/m²)	44.63	44.58	44.62	44.54	44.50	44.56	44.72
	Energy saving rate	-	0.18%	-0.02%	-0.20%	-0.29%	-0.16%	0.20%
C	Thermal loads (kWh/m²)	50.44	50.33	50.49	50.67	50.77	50.99	51.57
	Energy saving rate	-	-0.22%	0.10%	0.46%	0.65%	1.09%	2.24%

And the linear regression analysis of the overhang depth and building annual thermal loads are shown in Figure 7-10. In sub-region A1, B1, and C, the overhang depth is positively correlated with the building annual thermal loads of the simulated dwelling. When the overhang depth is decreased from 2.4 to 0.5, the building annual thermal loads would be decreased from 38.43kWh/m² to 38.01kWh/m², 45.84 kWh/m² to 44.50 kWh/m², and 51.57 kWh/m² to 50.33 kWh/m², respectively. In sub-region A2 and B2, the overhang depth is negatively correlated with the building annual thermal loads of the simulated dwelling. When the overhang depth is decreased from 2.4 to 0.5, the building annual thermal loads would be increased from 33.42kWh/m² to 34.31kWh/m², and 44.72 kWh/m² to 44.58 kWh/m². The energy consumption of the renovated dwelling can be reduced by -0.08%, 0.18%, 2.03%, 0.29%, and 0.22% in each sub-region.

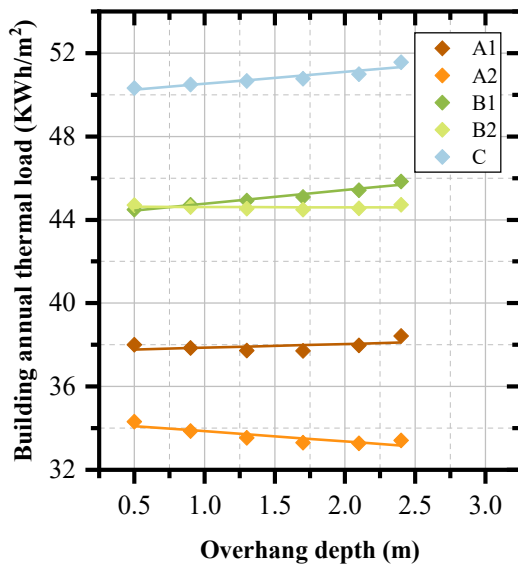


Figure 7-10. Relationship between north window-wall ratio and building annual thermal load

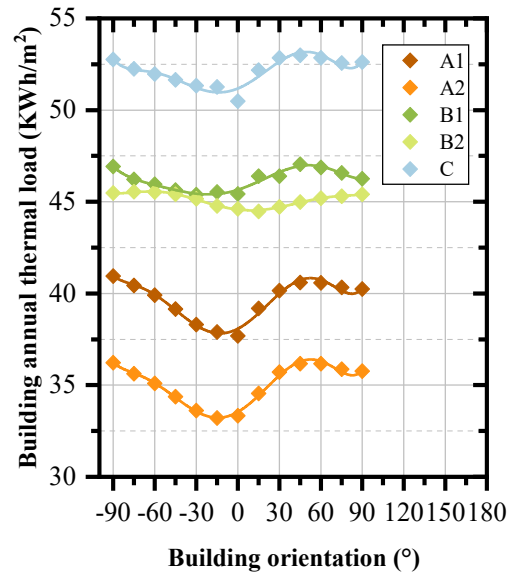


Figure 7-11. Relationship between building orientation and building annual thermal load

J: BO (building orientation)

There are some differences in solar radiation intensity in different orientations. Reasonable use of solar radiation can greatly improve the indoor thermal comfort and reduce building thermal load [38]. In order to obtain the best orientation of each climatic sub-region, this study takes the building orientation as the simulation input variable, and the thermal performance of the envelope structure, the window-wall ratio, the overhang depth and other auxiliary variables are set according to the actual parameters of target model to simulate the impact of building orientations on building annual thermal loads. In this study, the south direction of the building is defined as 0° , the clockwise rotation is defined to be positive, and the counterclockwise rotation is defined to be negative. As China is located in the northern hemisphere, the main solar radiation surface is south, east and west, so the building orientation variation range is set from -90° to 90° , and input variables are simulated with 15° increments. A total of 13 sets of data were simulated for each climate region. The simulation results of building annual thermal loads based on building orientation in each climatic sub-region are shown in Table 7-13.

Table 7-13. Building annual thermal loads based on building orientation

Orientations (°)	-90	-75	-60	-45	-30	-15	0	15	30	45	60	75	90
Thermal loads													
A1	40.95	40.45	39.91	39.14	38.31	37.90	37.68	39.18	40.16	40.60	40.58	40.33	40.24
	(kWh/m ²)												
Energy saving rate													
	8.68%	7.35%	5.92%	3.87%	1.67%	0.58%	-	3.98%	6.58%	7.75%	7.70%	7.03%	6.79%
Thermal loads													
A2	36.23	35.63	35.10	34.38	33.61	33.21	33.33	34.55	35.71	36.17	36.17	35.87	35.77
	(kWh/m ²)												
Energy saving rate													
	9.09%	7.29%	5.69%	3.52%	1.20%	-	0.36%	4.03%	7.53%	8.91%	8.91%	8.01%	7.71%
Thermal loads													
B1	46.93	46.22	45.96	45.63	45.58	45.53	45.42	46.40	46.95	47.05	46.87	46.58	46.26
	(kWh/m ²)												
Energy saving rate													
	3.32%	1.76%	1.19%	0.46%	0.35%	0.24%	-	2.16%	3.37%	3.59%	3.19%	2.55%	1.85%
Thermal loads													
B2	45.48	45.54	45.53	45.41	45.16	44.78	44.62	44.48	44.72	44.98	45.19	45.31	45.41
	(kWh/m ²)												
Energy saving rate													
	2.25%	2.38%	2.36%	2.09%	1.53%	0.67%	0.31%	-	0.54%	1.12%	1.60%	1.87%	2.09%
Thermal loads													
C	52.77	52.26	51.96	51.64	51.33	51.26	50.48	52.18	52.86	52.99	52.86	52.57	52.62
	(kWh/m ²)												
Energy saving rate													
	4.54%	3.53%	2.93%	2.30%	1.68%	1.55%	-	3.37%	4.71%	4.97%	4.71%	4.14%	4.24%

In the climatic sub-region A1 to C, the minimum value of building annual thermal loads appears in the south orientation (0°), 15° west-south orientation (-15°), south orientation (0°), 15° east-south orientation (15°), and south orientation (0°), respectively. The minimum values of building annual thermal loads are 37.68 kWh/m², 33.21 kWh/m², 45.42 kWh/m², 44.48 kWh/m², 50.48 kWh/m² in the climatic sub-region A1, A2, B1, B2, and C, respectively. The optimal building orientation is determined on the basis that the variation of building annual thermal load does not exceed 1% of the minimum value.

It can be seen from Figure 7-11 that there is no obvious linear relationship between building annual thermal loads and building orientation. Building energy consumption decreases and then increases with the building orientation from east to south and then to west. And when the building is oriented southward or southward nearby, the building annual thermal loads reach the lowest value. This is because the south of the building can obtain a large amount of solar radiation heat in winter to reduce the heating energy consumption in winter, and the solar radiation heat in summer is not too high, which has reduced the cooling energy consumption in summer.

Through data analysis, it can be seen that the optimal building orientation in climatic sub-region A1 and A2 is south to 15° west-south (-15°~0°); the optimal building orientation in climatic sub-region B1 is south to 45° west-south (-45°~0°); the optimal building orientation in climatic sub-region B2 is west-south 15° to east-south 30°; the optimal building orientation in climatic sub-region C is south (0°). In this orientation range, the traditional dwellings in each sub-climate zone could make full use of the heat gain of solar radiation to reduce the indoor heat load in winter and reduce the indoor cooling load caused by excessive solar radiation in some directions in summer, and finally achieve the minimum building thermal load.

K: SC (shape coefficient)

In the building energy consumption analysis, the building shape coefficient is a factor that

cannot be ignored. When the building height is determined, the building energy consumption is proportional to the building shape coefficient, that is, the smaller the building shape coefficient, the smaller the building energy consumption [39]. The building shape coefficient is defined as the ratio of the exterior surface area of the building to the building volume [40]. The formula is:

$$C = \frac{F}{V} = \frac{2ah + 2bh + ab}{abh} = \frac{2a + 2b}{ab} + \frac{1}{h} \quad (7-1)$$

Where, C is the building shape coefficient (m^{-1}); F is the building surface area (m^2); V is the building volume (m^3); a is the building plane x-axis side length (m); b is the building plane y-axis side length (m); h is the building height (m).

It can be seen from the formula that the building shape coefficient is related to the building length, width and height. In order to explore the optimal solution of the traditional dwelling's shape in Qinba mountainous area, this research studies the relationship between building shape coefficient and energy consumption under the influence of building length, width and height.

Table 7-14. Building annual thermal loads based on building shape coefficient

	Room unit length (m)	3.3	3.6	3.9	4.2	4.5	4.8
Building length	Shape coefficient	0.746	0.736	0.728	0.720	0.714	0.708
	Thermal loads (kWh/m²)	49.084	48.338	47.706	47.151	46.695	46.260
	Energy saving rate	-	-1.52%	-2.81%	-3.94%	-4.87%	-5.75%
	Room unit width (m)	4.2	4.8	5.4	6.0	6.6	7.2
Building width	Shape coefficient	0.796	0.736	0.690	0.653	0.622	0.597
	Thermal loads (kWh/m²)	51.661	48.338	45.768	43.711	42.041	40.648
	Energy saving rate	-	-6.43%	-11.41%	-15.39%	-18.62%	-21.32%
	Building height (m)	4.5	5.0	5.5	6.0	6.5	7.0
Building height	Shape coefficient	0.750	0.728	0.710	0.694	0.682	0.671
	Thermal loads (kWh/m²)	46.377	49.672	52.984	56.311	59.671	63.030
	Energy saving rate	-	7.10%	14.25%	21.42%	28.67%	35.91%

The traditional dwellings in the Qinba mountainous area are usually flexibly combined with the room units to form a spatial structure of 3 spans, 5 spans and 7 spans. Among them, the 5 spans building can meet the living functions of 5 ~ 10 people, accounting for the largest proportion. The length and width of the dwellings depend largely on the length and width of the room unit. In the study area, room unit's length and width are usually between 3m to 5m, and 4m to 7m, respectively. And the traditional dwellings are usually 2 stories building, with the building height of 4.5m to 7m. Therefore, the simulated model can be set to 5 spans, with the room unit length between 3m to 5m, the room width between 4m to 7m, and building height

between 4.5m to 7m to analysis the annual building thermal loads. When we discuss the shape coefficient of the building, we analyze it by changing the length, width and height of the building, which is a complicated process. Therefore, the climate sub-region B1, which occupied the largest area in Qinba mountainous area, is selected as a representative area for simulation.

The simulation results of building annual thermal loads based on external wall heat transfer coefficient in each climatic sub-region are shown in Table 7-14.

From Table 7-14, it can be seen that when the width and height of the building are unchanged, when the building shape coefficient decreases, the annual building thermal load decreases; in the case of constant building length and height, when the building shape coefficient decreases, the annual building thermal load decreases. However, when the length and width of the building remain unchanged, when the building shape coefficient decreases, the annual building thermal load increases. Therefore, the building shape coefficient cannot be directly used for linear regression analysis with annual building thermal load, so linear regression analysis needs to be performed between the annual building thermal load and the building length, width and height, respectively, shown in Figure 7-12.

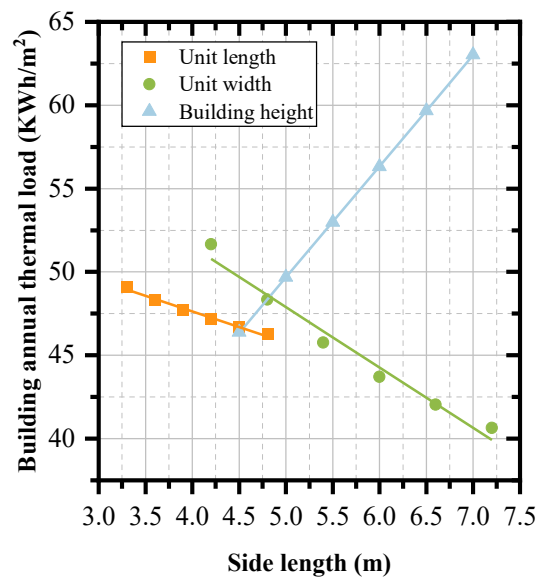


Figure7-12. Relationship between building length/width/height and building annual thermal load

The building length, and building width are negatively correlated with the building annual thermal loads, and the building height is positively correlated with the building annual thermal loads. When the building length is increased from 3.3m to 4.8m, the building annual thermal loads would be decreased from 49.08kWh/m² to 46.26kWh/m², the energy saving rate is 5.75%. When the building width is increased from 4.8m to 7.2m, the building annual thermal loads would be decreased from 51.66kWh/m² to 40.65kWh/m², the energy saving rate is 21.32%. And when the building height is increased from 4.5m to 7.5m, the building annual thermal loads

would be increased from 46.38kWh/m² to 63.03kWh/m²the energy saving rate is -35.91%. It can be seen that increasing the length and width of the building can reduce building energy consumption, but it also needs to be combined with the actual functional requirements. Moreover, the slope of the relationship between the energy consumption and room unit width is greater than the slope of the relationship between the energy consumption and the room unit length, indicating that it is preferred to increase the room width to enlarge the room area. In addition, lower building height can help reduce energy consumption, but it also needs to meet the actual functional requirements. Therefore, in the process of building new construction, lower building height, larger building width and appropriate building length can be applied.

7.4.3. Effectiveness identification of single control variable

(1) Sensitivity analysis of each passive parameter

Through the above analysis, we understand the impact of a single passive design parameter on building energy consumption. To evaluate the effectiveness of each passive parameter in each climatic sub-region, this research introduces the sensitivity coefficient (I_C) to comprehensively evaluate the impact of each passive parameter on building thermal loads [10]. However, there is no obvious linear relationship between building orientation and building energy consumption, and the sensitive coefficient cannot be obtained. Therefore, the analysis of sensitivity coefficient does not include building orientation. Meanwhile, we only simulated the relationship between the building shape coefficient and the building energy consumption in the sub-region B1, and the building shape coefficient cannot be applied to the transformation process of traditional dwellings. Therefore, the sensitivity analysis of sub-region A1, A2, B2, and C does not include the building shape coefficient. The sensitivity coefficient calculation formula is [41]:

$$I_C = \frac{O_P - O_{P'}}{O_{P'}} \bigg/ \frac{I_P - I_{P'}}{I_{P'}} \quad (7-2)$$

Where O_P is the annual building thermal load after renovation (kWh/m²); $O_{P'}$ is the annual building thermal load before renovation (kWh/m²); I_P is the input value of the passive parameter after renovation; $I_{P'}$ is the input value of the passive parameter before renovation.

According to the Formula (7-2), the annual building thermal load's changing rate and the input value of the passive parameter's changing rate based on the neutral temperature of each climatic sub-region were calculated. Then the calculation results were linearly fitted, the slope of the fitting curve of each passive parameter is its sensitivity coefficient (I_C) [42]. The sensitivity coefficients of the passive design parameters are summarized in Table 7-15.

Figure 7-13 to 7-17 shows linear regression analysis of the sensitivity coefficient of the

annual thermal loads to each passive parameter in the 5 climatic sub-regions. Statistically, the positive sensitivity coefficient indicates that the input value of passive parameters is positively correlated with the output value of annual building thermal load; the negative sensitivity coefficient indicates that the input value of passive parameters is negatively correlated with the output value of annual building thermal load [43].

Table 7-15. The sensitivity coefficient of the passive design parameters in each climatic sub-region

Sensitivity coefficient	Passive design parameter	Climatic sub-region				
		A1	A2	B1	B2	C
I _C	¹ SD	0.22191	0.19765	0.23645	0.16799	0.23033
	² EWHTC	0.32617	0.31516	0.21802	0.21326	0.21168
	³ RHTC	0.30999	0.33236	0.34537	0.35603	0.42703
	⁴ WHTC	0.19411	0.16508	0.24059	0.23215	0.24024
	⁵ SWWR	-0.01306	-0.00677	-0.00586	0.00439	-0.01586
	⁶ NWWR	0.00648	0.00610	0.01906	0.01578	0.01833
	⁷ EWWR	0.00397	0.00717	0.01089	0.01960	0.00973
	⁸ WWWR	0.00539	0.00712	0.01538	0.01750	0.01094
	⁹ OD	-0.01123	-0.03193	0.03164	-0.00367	0.00884

¹SD refers to sunroom depth; ²EWHTC refers to the exterior wall heat transfer coefficient; ³RHTC refers to the roof heat transfer coefficient; ⁴WHTC refers to the window heat transfer coefficient; ⁵SWWR refers to the south window-wall ratio; ⁶NWWR refers to the north window-wall ratio; ⁷EWWR refers to the east window-wall ratio; ⁸WWWR refers to the west window-wall ratio; ⁹OD refers to the overhang depth.

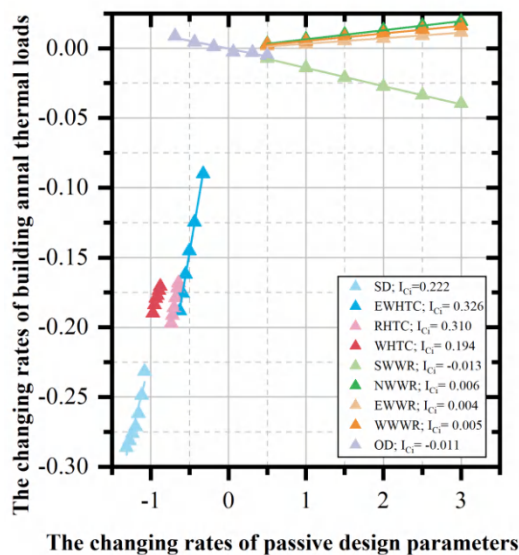


Figure 7-13 The sensitivity analysis of passive design parameters in sub-region A1

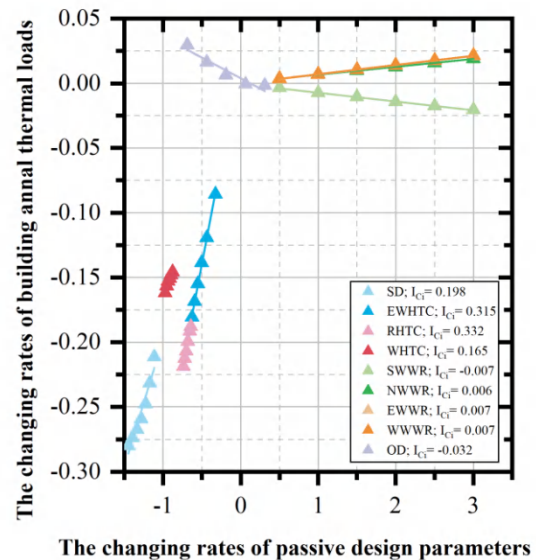


Figure 7-14 The sensitivity analysis of passive design parameters in sub-region A2

As shown in Figure 7-13 and Table 7-15, in sub-region A1, the exterior wall heat transfer coefficient, roof heat transfer coefficient, sunroom depth, window heat transfer coefficient, north window-to-wall ratio, west window-to-wall ratio, east window-to-wall ratio are positively correlated with the annual building thermal load, and the sensitivity coefficients of them showed decreasing trend with the value of 0.32617, 0.30999, 0.22191, 0.19411, 0.00648, 0.00539, and 0.00397, respectively. The overhang depth, and south window-to-wall ratio are negatively correlated with the annual building thermal load, with the value of -0.01123 and -0.01306.

As shown in Figure 7-14 and Table 7-15, in sub-region A2, the roof heat transfer coefficient, exterior wall heat transfer coefficient, sunroom depth, window heat transfer coefficient, east window-to-wall ratio, west window-to-wall ratio, north window-to-wall ratio are positively correlated with the annual building thermal load, and the sensitivity coefficients of them showed decreasing trend with the value of 0.33236, 0.31516, 0.19765, 0.16508, 0.00717, 0.00712 and 0.00610, respectively. The south window-to-wall ratio and overhang depth are negatively correlated with the annual building thermal load, with the value of -0.00677 and -0.03193.

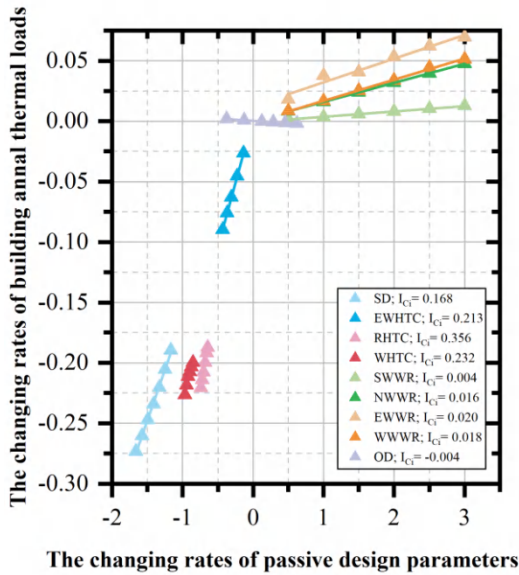


Figure 7-15 The sensitivity analysis of passive design parameters in sub-region B1

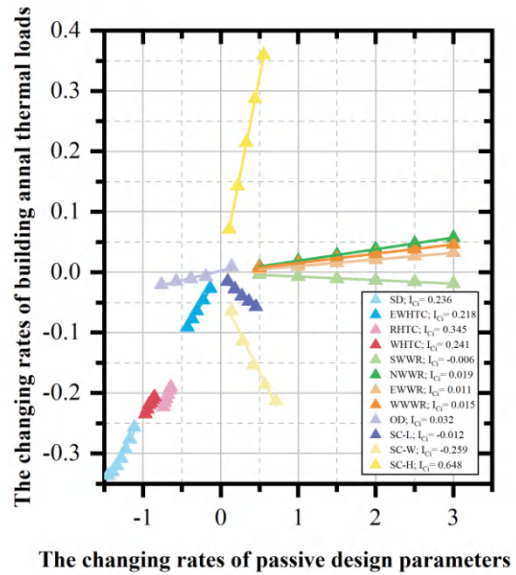


Figure 7-16 The sensitivity analysis of passive design parameters in sub-region B2

As shown in Figure 7-15 and Table 7-15, in sub-region B1, the roof heat transfer coefficient, exterior wall heat transfer coefficient, sunroom depth, window heat transfer coefficient, overhang depth, north window-to-wall ratio, west window-to-wall ratio, and east window-to-wall ratio are positively correlated with the annual building thermal load, and the sensitivity coefficients of them showed decreasing trend with the value of 0.34537, 0.24059, 0.23645, 0.21802, 0.03164, 0.01906, 0.01538, and 0.01089, respectively. The south window-to-wall ratio is negatively correlated with the annual building thermal load, with the value of -0.00586. And in sub-region B1, we also simulated the relationship between building annual thermal loads and

the building length, width and height, respectively. The sensitivity coefficients of them are -0.11580, -0.25890, and 0.64822.

As shown in Figure 7-16 and Table 7-15, in sub-region B2, the roof heat transfer coefficient, exterior wall heat transfer coefficient, window heat transfer coefficient, sunroom depth, east window-to-wall ratio, west window-to-wall ratio, north window-to-wall ratio, and south window-to-wall ratio are positively correlated with the annual building thermal load, and the sensitivity coefficients of them showed decreasing trend with the value of 0.35603, 0.23215, 0.21326, 0.16799, 0.01960, 0.01750, 0.01578, and 0.00439, respectively. The overhang depth is negatively correlated with the annual building thermal load, with the value of -0.00367.

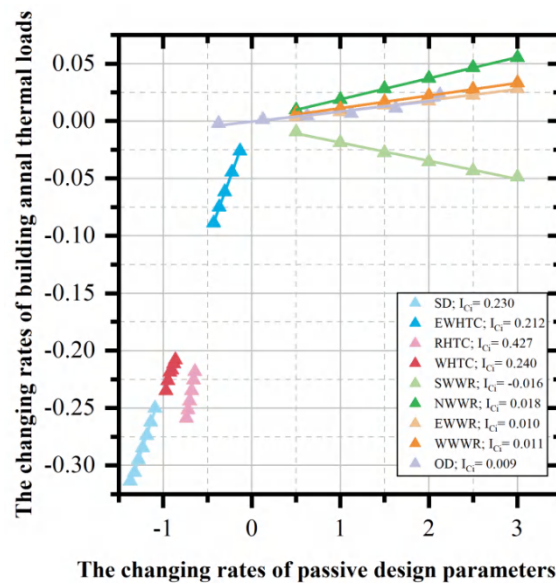


Figure 7-17 The sensitivity analysis of passive design parameters in sub-region C

As shown in Figure 7-17 and Table 7-15, in sub-region C, the roof heat transfer coefficient, window heat transfer coefficient, sunroom depth, exterior wall heat transfer coefficient, north window-to-wall ratio, west window-to-wall ratio, east window-to-wall ratio, and overhang depth are positively correlated with the annual building thermal load, and the sensitivity coefficients of them showed decreasing trend with the value of 0.42703, 0.24024, 0.23033, 0.21168, 0.01833, 0.01094, 0.00973, and 0.00884, respectively. The south window-to-wall ratio is negatively correlated with the annual building thermal load, with the value of -0.01586.

(2) Relative sensitivity analysis of each passive parameter

Meanwhile, in order to investigate the relative sensitivity of each passive parameter to the impact of the annual building thermal load, the relative sensitivity coefficient (ω_i) is defined. The calculation formula is [44]:

$$\omega_i = \frac{|I_{Ci}|}{\sum_{i=1}^n |I_{Ci}|} \quad (7-3)$$

Where ω_i is the relative sensitivity coefficient; I_{Ci} the sensitivity coefficient of each passive parameter; n is the number of passive parameters.

The sensitivity coefficient's absolute value reflects the parameter's influence on the corresponding output results. The larger the absolute value of the sensitivity coefficient is, the bigger the impact of the passive parameter on the annual building thermal load is.

Table 7-16 shows the energy saving efficiency, the sensitivity coefficient, and the relative sensitivity coefficient of the passive parameter for the single passive design parameter in each climatic sub-region.

Table 7-16. The effectiveness of passive design parameters in the climatic sub-regions

Passive parameter	Evaluation index	Climatic sub-region				
		Dwellings with bamboo clay wall		Dwellings with rammed earth wall		
		A1	A2	B1	B2	C
¹ SD	I_{Ci}	0.22191	0.19765	0.23645	0.16799	0.23033
	ω_i	20.32%	18.48%	21.05%	16.30%	19.64%
	Energy efficient rate	23.16%~	21.14%~	22.67%~	19.98%~	25.02%~
		28.62%	28.00%	33.64%	27.32%	31.388%
² EWHTC	I_{Ci}	0.32617	0.31516	0.21802	0.21326	0.21168
	ω_i	29.86%	29.47%	19.41%	20.70%	18.05%
	Energy efficient rate	9.01%~	8.57%~	0~9.14%	0~8.96%	0~8.88%
		18.85%	18.08%			
³ RHTC	I_{Ci}	0.30999	0.33236	0.34537	0.35603	0.42703
	ω_i	28.38%	31.08%	30.75%	34.55%	36.41%
	Energy efficient rate	16.83%~	18.80%~	19.02%~	18.73%~	21.83%~
		19.72%	21.89%	22.28%	22.07%	25.89%
⁴ WHTC	I_{Ci}	0.19411	0.16508	0.24059	0.23215	0.24024
	ω_i	17.77%	15.44%	21.42%	22.53%	20.48%
	Energy efficient rate	17.06%~	14.58%~	20.67%~	19.96%~	20.82%~
		19.01%	16.19%	23.45%	22.65%	23.51%
⁵ SWWR	I_{Ci}	-0.01306	-0.00677	-0.00586	0.00439	-0.01586
	ω_i	1.20%	0.63%	0.52%	0.43%	1.35%
	Energy efficient rate	0.71%~	0.36%~	0.37%~	-0.18%~	0.95%~
		3.97%	2.06%	1.87%	-1.25%	4.88%
⁶ NWWR	I_{Ci}	0.00648	0.0061	0.01906	0.01578	0.01833
	ω_i	0.59%	0.57%	1.70%	1.53%	1.56%
	Energy efficient rate	-0.40%~	-0.27%~	-1.75%~	-1.71%~	-1.70%~

	efficient rate	-2.34%	-2.15%	-7.55%	-6.54%	-7.34%
⁷ EWWR	I _{Ci}	0.00397	0.00717	0.01089	0.0196	0.00973
	ω _i	0.36%	0.67%	0.97%	1.90%	0.83%
	Energy	-0.41%~	-0.73%~	-1.13%~	-1.58%~	-0.98%~
	efficient rate	-1.56%	-2.87%	-4.39%	-8.63%	-3.82%
⁸ WWWR	I _{Ci}	0.00539	0.00712	0.01538	0.0175	0.01094
	ω _i	0.49%	0.67%	1.37%	1.70%	0.93%
	Energy	-0.51%~	-0.74%~	-1.58%~	-1.72%~	-1.09%~
	efficient rate	-2.12%	-2.89%	-6.27%	-6.93%	-4.46%
⁹ OD	I _{Ci}	-0.01123	-0.03193	0.03164	-0.00367	0.00884
	ω _i	1.03%	2.99%	2.82%	0.36%	0.75%
	Energy	-0.08%~	-2.96%~	-1.37%~	-0.21%~	-2.24%~
	efficient rate	-1.99%	0.18%	1.63%	0.30%	0.22%

¹SD refers to sunroom depth; ²EWHTC refers to the exterior wall heat transfer coefficient; ³RHTC refers to the roof heat transfer coefficient; ⁴WHTC refers to the window heat transfer coefficient; ⁵SWWR refers to the south window-wall ratio; ⁶NWWR refers to the north window-wall ratio; ⁷EWWR refers to the east window-wall ratio; ⁸WWWR refers to the west window-wall ratio; ⁹OD refers to the overhang depth.

Figure 7-18 shows the relative sensitivity and relative sensitivity ranks of the passive design parameters in the 5 climatic sub-regions. The values shows that the attached sunroom, the exterior wall heat transfer coefficient, roof heat transfer coefficient, and exterior window heat transfer coefficient has much higher effect on building annual thermal loads than other passive design parameters.

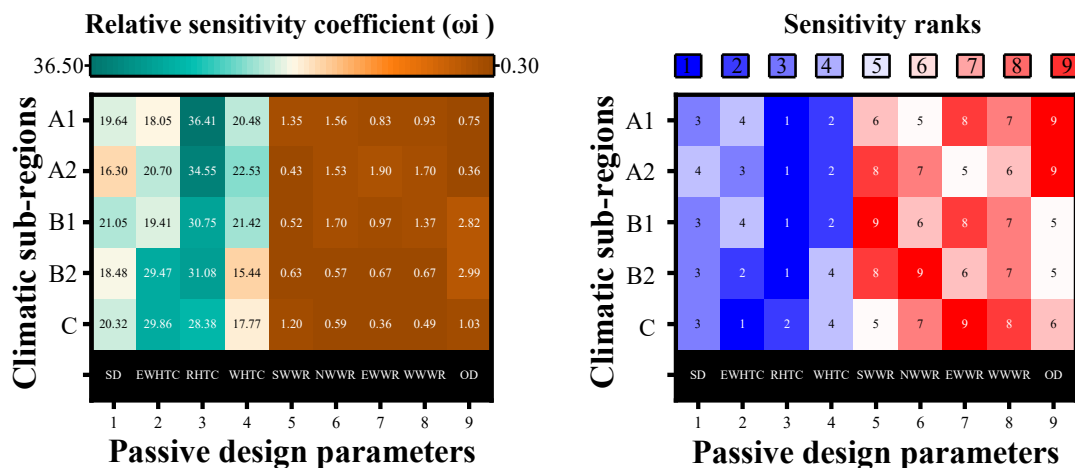


Figure 7-18. The relative sensitivity and sensitivity rank of the passive design parameters

The average values of the relative sensitivity for each passive design parameter are shown in Table 7-17 to evaluate the effectiveness of each passive strategy. The larger the value of relative sensitivity, the more obvious its impact on energy consumption.

Table 7-17. The effectiveness of passive design parameters in the climatic sub-regions

Passive design parameter	Unit	Value range		Average value of ω_i	Effectiveness
		Lower limit	Upper limit		
SD	m	0.6	2.4	19.16%	Efficient
EWHTC	W/(m ² ·K)	0.44	1.50	23.50%	Efficient
RHTC	W/(m ² ·K)	0.59	0.80	32.23%	Efficient
WHTC	W/(m ² ·K)	1.50	6.50	19.53%	Efficient
SWWR	-	0.10	0.40	0.83%	Inefficient
NWWR	-	0.10	0.40	1.19%	Inefficient
EWWR	-	0.10	0.40	0.95%	Inefficient
WWWR	-	0.10	0.40	1.03%	Inefficient
OD	m	0.50	2.40	1.59%	Inefficient

The average values of the relative sensitivity of the annual building thermal loads to the attached sunroom, the exterior wall heat transfer coefficient, roof heat transfer coefficient, and exterior window heat transfer coefficient, which are 19.16 %, 23.50 %, 32.23 %, and 19.53 %, are relatively high, much larger than the relative sensitivity of the south window-wall ratio, north window-wall ratio, east window-wall ratio, west window wall ratio, and the overhang depth of 0.83 %, 1.19%, 0.95%, 1.03%, and 1.59%. The passive parameters, such as the south window-wall ratio, north window-wall ratio, east window-wall ratio, west window-wall ratio, and overhang depth, are considered ineffective as the values of the relative sensitivity coefficient of annual building thermal loads to these parameters are too low. Furthermore, the other passive parameters, attached sunroom, the exterior wall heat transfer coefficient, roof heat transfer coefficient, and exterior window heat transfer coefficient, are judged to be effective.

The relative sensitivity of annual building thermal load to the roof heat transfer coefficient is the highest, which is 28.69 %, 31.68 %, 32.04 %, 36.44 %, and 37.66 %, respectively, from climatic sub-region A1 to C. The energy saving rates of attaching sunroom are 23.16%~28.62%, 21.14%~28.00%, 22.67%~33.64%, 19.98%~27.32%, and 25.02%~31.388% in sub-region A1 to C, respectively. It indicates that the renovation of the roof can save building energy consumption most effectively.

The effectiveness of exterior wall reformation to reduce energy consumption comes in second. The relative sensitivity coefficient of annual building thermal load to the external wall heat transfer coefficient is relatively high. The relative sensitivity coefficient value of 30.19 % and 30.04 % in sub-regions A1 and A2 is much higher than that of 20.23 %, 21.83 %, and 18.67 % in sub-region B1, B2, and C. As the exterior wall materials of traditional dwellings in A1 and A2 regions are mainly bamboo plaited layer in the middle with two grass clay layers on the surface, with the heat transfer coefficient value of 2.222 W / m²·K, which is much higher than that of the rammed earth wall in B1, B2 and C regions of 0.98 W / m² · K. As a result, the heat transfer coefficient value of the renovated exterior wall changes significantly in A1 and A2 regions, which greater impacts the annual building thermal loads. The energy saving rates of

reducing the external wall heat transfer coefficient are 9.01%~18.85%, 8.57%~18.08%, 0~9.14%, 0~8.96%, and 0~8.88% in sub-region A1 to C, respectively.

The effectiveness of attached sunroom comes in third. The relative sensitivity coefficient of annual building thermal load to attached sunroom is relatively high, which is 20.54 %, 18.84 %, 21.94 %, 17.20 %, and 20.31 % from sub-regions A1 to C, respectively. The value is relatively average, indicating that adding the attached sunroom in the south of the dwelling may significantly cut the energy use of buildings. And the energy saving rates of attaching sunroom are 23.16%~28.62%, 21.14%~28.00%, 22.67%~33.64%, 19.98%~27.32%, and 25.02%~31.388% in sub-region A1 to C, respectively.

The last effective passive parameter to reducing building energy consumption is the changing the exterior window. The relative sensitivity coefficient of annual building thermal load to the window heat transfer coefficient is 17.97 %, 15.74 %, 22.32 %, 23.76 %, and 21.19 % from sub-region A1 to C, which arises from the combined impact of the heat transfer coefficient and air tightness of the exterior windows, and the air tightness has a more significant impact. In addition, the sensitivity coefficients of sub-region B1, B2, and C are slightly higher than that of sub-region A1 and A2, indicating that the colder areas are more sensitive to air tightness than the warmer areas. And the energy saving rates of attaching sunroom are 17.06%~19.01%, 14.58%~16.19%, 20.67%~23.45%, 19.96%~22.65%, and 20.82%~23.51% in sub-region A1 to C, respectively.

7.5. Single-objective optimization combination of multi controlled variables

7.5.1. Single-objective optimization

There are many passive design parameters that affect building energy consumption. Section 7.4 has discussed the impact of the 11 common passive parameters on building energy consumption and determined their effectiveness. The 4 passive parameters that have a greater impact on building energy consumption are the attached sunroom, the heat transfer coefficient of external wall, roof, and window. As these factors can be valued within a certain range, there are many building schemes corresponding to the arrangement and combination of different factors and values, resulting in a complex coupling relationship between various factors and building energy consumption.

This research studies the single-objective optimization & multi-variable strategy, that is, only considering the relationship between energy consumption and the various passive design parameters; and the multi-objective optimization & multi-variable strategy, that is, considering the relationships between the objectives such as energy consumption, residents' thermal comfort and economy and the various passive design parameters. In this study, the single-objective optimization and multi-objective optimization were carried out on thousands of schemes with different passive design parameters in each climatic sub-region, and finally, the optimal solution set of passive strategies on traditional dwellings in each sub-region was

obtained.

In this chapter, the single-objective optimization combination of passive design parameters used in the traditional dwelling will be discussed.

7.5.2. Evaluation of the optimal combination of the multi controlled variables by orthogonal method

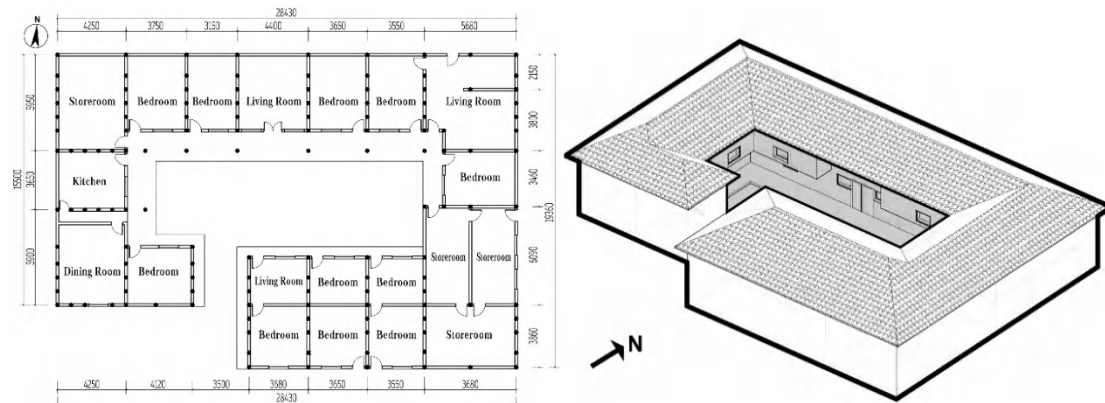


Figure 7-19. The “U”-shaped dwelling in Liyuanba Village for single-objective optimization

As shown in Figure 7-19, this research selected an “U”-shaped traditional dwelling located in Liyuanba Village, Tongjiang County, Bazhong City, in sub-region A1 of Qinba mountainous area, for a single-objective optimization simulation with the primary goal of reducing energy consumption. The simulation involved 4 independent variables, namely the depth of the attached sunroom and the heat transfer coefficients of the external wall, roof, and windows.

The multi controlled variables study employs the orthogonal array and range analysis to evaluate the influence of 4 selected passive design parameters and their interactive effects and evaluated the preferable level between each parameter to obtain the optimal combination of them.

(1) Orthogonal method

To discover the relative importance of each parameter on building energy consumption, all other parameters should be maintained constant while one variable was adjusted to examine how the results would change. Even if 4 variables in Table 7-18 were altered on only 4 levels, as many as $4^4 (= 256)$ simulations would be required, making the analysis nearly unfeasible. The orthogonal arrays involved the selection of a subset of the entire simulation to obtain the same experimental results, which would reduce the number of simulations in this research to 16 times.

(2) Single-objective optimization of the multi controlled variables

In the single-objective optimization of multi controlled variables, the highest level and the lowest level of 4 passive design parameters were evaluated based on the energy saving effect, local architectural culture and building energy saving design standards in sub-region A1. The 4 levels, including the highest level and lowest level, were chosen for each parameter, as shown

in Table 7-18.

Table 7-18. Passive design parameters and their values for optimization

Parameters	Levels for each parameter			
	Level 1	Level 2	Level 3	Level 4
A: SD, m	1.30	1.10	0.90	0.60
B: EWHTC, W/(m ² ·K)	1.50	1.23	1.00	0.86
C: RHTC, W/(m ² ·K)	0.80	0.78	0.74	0.70
D: WHTC, W/(m ² ·K)	3.20	2.70	2.10	1.50

The orthogonal array was used to set simulations with 4 influencing parameters and 4 level values, giving a total of 16 combinations. L16(4⁴) orthogonal array was generated by SPSS software for statistics and calculation, as shown in Table 7-19.

(3) Optimal combination of multi controlled variables

As shown in Table 7-19, the optimal combination of passive design parameters with the energy consumption of traditional dwellings in this area is A1-B1-C1-D1, which is the dwelling with a 1.3 m deep sunroom and has 0.86 W/(m²·K), 0.70 W/(m²·K) and 1.5 W/(m²·K) heat transfer coefficients of exterior walls, roof and window respectively. The building annual thermal loads of the renovated dwelling is 15.82 kWh/m².

Table 7-19. L16(4⁴) orthogonal array for the traditional dwelling in the Qinba mountainous

Case No.	SD	EWHTC	RHTC	WHTC	Annual thermal load (kWh/m ²)	Energy efficiency rate (%)
1	A1 (1.30)	B1 (0.86)	C1 (0.70)	D1 (1.50)	15.82	65.10%
2	A1 (1.30)	B2 (1.00)	C2 (0.74)	D2 (2.10)	17.31	61.80%
3	A1 (1.30)	B3 (1.23)	C3 (0.78)	D3 (2.70)	19.52	56.90%
4	A1 (1.30)	B4 (1.50)	C4 (0.80)	D4 (3.20)	22.31	50.80%
5	A2 (1.10)	B1 (0.86)	C2 (0.74)	D3 (2.70)	16.34	63.90%
6	A2 (1.10)	B2 (1.00)	C1 (0.70)	D4 (3.20)	17.47	61.50%
7	A2 (1.10)	B3 (1.23)	C4 (0.80)	D1 (1.50)	19.63	56.70%
8	A2 (1.10)	B4 (1.50)	C3 (0.78)	D2 (2.10)	22.15	51.10%
9	A3 (0.90)	B1 (0.86)	C3 (0.78)	D4 (3.20)	16.81	62.90%
10	A3 (0.90)	B2 (1.00)	C4 (0.80)	D3 (2.70)	18.19	59.80%
11	A3 (0.90)	B3 (1.23)	C1 (0.70)	D2 (2.10)	19.40	57.20%
12	A3 (0.90)	B4 (1.50)	C2 (0.74)	D1 (1.50)	22.03	51.40%
13	A4 (0.60)	B1 (0.86)	C4 (0.80)	D2 (2.10)	17.15	62.20%
14	A4 (0.60)	B2 (1.00)	C3 (0.78)	D1 (1.50)	18.19	59.90%
15	A4 (0.60)	B3 (1.23)	C2 (0.74)	D4 (3.20)	20.29	55.20%
16	A4 (0.60)	B4 (1.50)	C1 (0.70)	D3 (2.70)	22.59	50.20%

7.5.3. Simulation of the optimization model of traditional dwellings

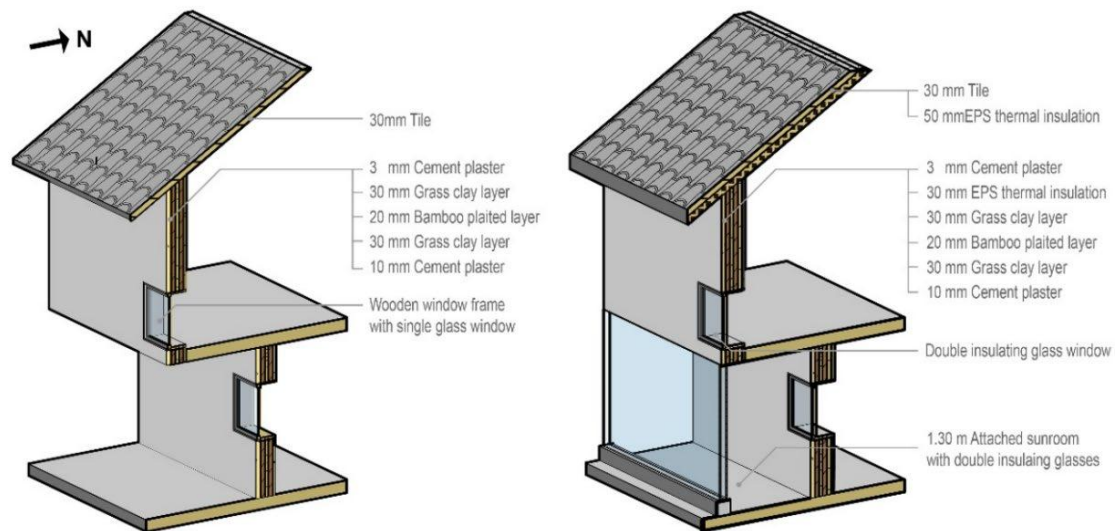


Figure 7-20 Structural diagram of the typical traditional dwelling before and after renovation

Based on orthogonal array and range analysis, the optimal passive strategy combination of traditional dwellings in the Qinba Mountainous area was obtained. No.1 scheme showed the combination of A1-B1-C1-D1 has the lowest annual building thermal load of 15.82 kWh/m² compared with the original one of 45.32 kWh/m², with an energy efficient rate of 65.1%.

The construct details and main technical specifications of the passive design parameters before and after renovation are shown in Figure 7-20 and Table 7-20. In this research, the No.1 scheme was chosen as the optimization model to further investigate its thermal performance.

Table 7-20. Main parameters of the traditional dwelling before and after passive strategy renovation

Passive design parameters	Before renovation		After renovation	
	Building construction	Value	Renovated construction	Optimal value
A:SD	-	-	Attached sunroom	1.3m
B: EWHTC	Bamboo clay wall	2.22 W/(m ² ·K)	Adding EPS thermal insulation	0.86 W/(m ² ·K)
C: RHTC	Tile	2.24 W/(m ² ·K)	EPS thermal insulation	0.70W/(m ² ·K)
D: WHTC	Wooden window	3.24 W/(m ² ·K)	Double insulating glass window	1.50W/(m ² ·K)
Annual building thermal load		45.32 KWh/m ²	-	15.82 KWh/m ²
Energy efficient rate			65.1%	

7.5.4. Temperature and humidity simulation of the traditional dwelling before and after optimization

In order to verify the influence of the passive optimization strategy on the indoor temperature and humidity of traditional dwellings, this study simulated the indoor air temperature, the mean radiant temperature and the relative humidity of the research model before and after renovation in winter and summer. The simulation period in winter and summer was set at the winter design week from 15 January to 21 January and summer design week from 9 July to 15 July respectively. Without using heating and cooling equipment, the variation curves of the indoor air temperature, the mean radiation temperature and the indoor relative humidity of the simulated traditional dwelling before and after renovation in the winter and summer design week are shown in Figures 7-21 and 7-22.

(1) Simulation of the indoor temperature and humidity in winter

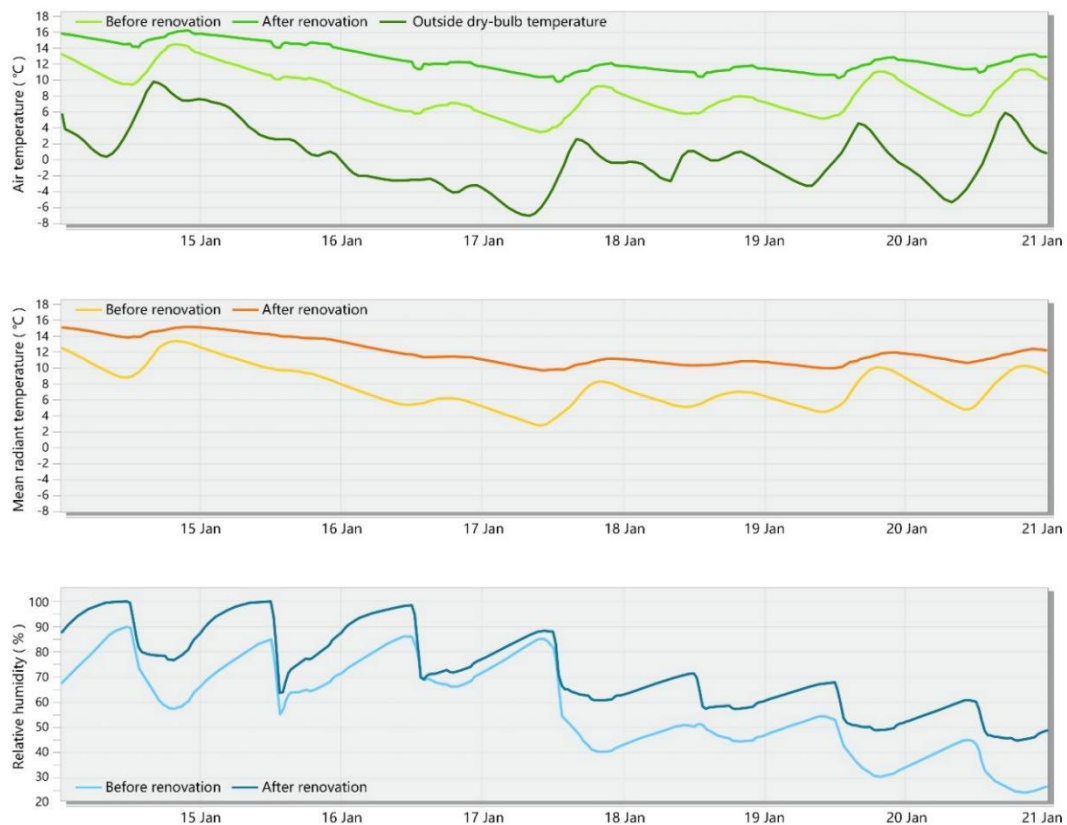


Figure 7-21. The payback period of capital of the traditional dwelling' renovation

1) The indoor temperature simulation in winter. As shown in Figures 7-21, in winter, the outdoor temperature swings rapidly from -6.2°C to 10.2°C . Before the renovation, the fluctuation ranges of the indoor air temperature and mean radiation temperature were $4.3^{\circ}\text{C}\sim 15.2^{\circ}\text{C}$ and $4.3^{\circ}\text{C}\sim 13.7^{\circ}\text{C}$, respectively. After renovation, the wave range of the indoor air temperature and mean radiation temperature was $10.3^{\circ}\text{C}\sim 16.5^{\circ}\text{C}$ and $10.1^{\circ}\text{C}\sim 16.1^{\circ}\text{C}$, respectively. Through data analysis, the overall indoor air temperature and mean radiation

temperature of the simulated dwelling were 4.31°C and 4.35°C higher than those before the renovation in winter. After the renovation, the all-day indoor temperature of the traditional dwelling could reach more than 10°C, meeting the requirements of the design standard, GB/T50824-2013, for energy efficiency for rural residential buildings that the indoor design temperature would not be less than 8°C without heating in winter in the hot summer and cold winter region.

2) The indoor humidity simulation in winter. As shown in Figure 7-21, in winter, the outdoor relative humidity swings from 58% to 97%. The fluctuation ranges of the indoor relative humidity before and after renovation were 24.1%~90.2% and 44.8%~99.6%, respectively. After renovation, the indoor relative humidity of the simulated dwelling was increased by 14.46%, substantially greater than the comfortable range of relative humidity of 30%~70%. As the local outdoor humidity is high in winter, the indoor relative humidity could not be reduced to the comfort range through the passive design strategy but could be adjusted through the dehumidification or heating equipment.

(2) Simulation of the indoor temperature and humidity in summer

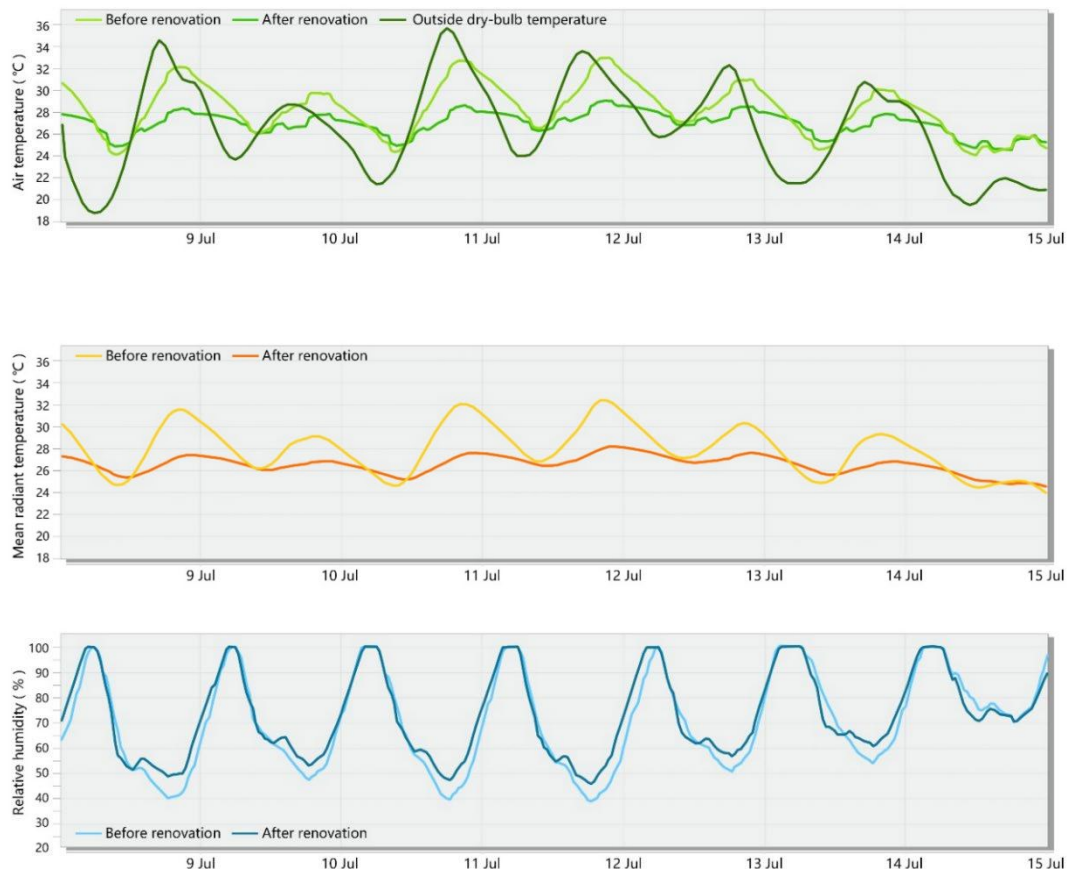


Figure 7-22 The payback period of capital of the traditional dwelling' renovation

1) The indoor temperature simulation in summer. As shown in Figure 7-22, in summer, the outdoor temperature ranges from 18.8°C to 35.6°C. Before the renovation, the fluctuation

ranges of the indoor air temperature and mean radiation temperature were 24.1~32.9°C and 24.0°C~32.4°C, respectively. After renovation, the fluctuation range of the indoor air temperature and mean radiation temperature were 24.5°C~29.2°C and 24.4°C~28.1°C, respectively. The overall indoor air temperature and mean radiation temperature of the simulated dwelling were 1.25°C and 1.34°C lower than those before the renovation in summer. After the renovation, the all-day indoor temperature of the traditional dwelling could meet the requirements of the design standard, GB/T50824-2013, for the energy efficiency of rural residential buildings that the indoor design temperature should not be more than 30°C without cooling measures in summer in hot summer and cold winter region.

2) The indoor humidity simulation in summer. As shown in Figure 7-22, in summer, the outdoor relative humidity swings from 50% to 96%. The fluctuation ranges of the indoor relative humidity before and after renovation were 39.0%~99.2% and 45.0%~99.3%, respectively. After renovation, the indoor relative humidity of the simulated dwelling was increased by 2.30%, higher than the comfortable range of relative humidity of 30%~70%. The indoor humidity environment may be improved by increasing the ventilation rate.

7.6. Summary

Based on the physical model of the traditional dwelling in the Qinba mountainous area, this research utilized computer simulation, statistical analysis, and orthogonal arrays to estimate the effectiveness of passive design parameters, evaluated and validated the single-objective optimization. The conclusions are as follows:

(1) Through a single controlled variable study, the energy consumption analysis of 11 selected passive design parameters were simulated in 5 climatic sub-regions in Qinba mountainous area, and the efficiency of each passive technology on building energy consumption was obtained. The window-wall ratio, overhang depth, building orientation, and building shape coefficient were judged to be inefficient as their impact on building energy consumption is relatively small, with the value of the average relative sensitivity coefficient (ω_i) less than 5%. The 4 effective passive renovation parameters for traditional dwellings were sunroom depth, exterior wall heat transfer coefficient, roof heat transfer coefficient and window heat transfer coefficient as the average relative sensitivity coefficient (ω_i) of these 4 parameters 19.16%, 23.50%, 32.23%, and 19.53%, respectively.

(2) Through a multi controlled variable study, this research applied the orthogonal arrays analysis to evaluate 4 effective parameters to obtain the optimal combination. The optimal combination could reduce the annual energy consumption of the simulated dwelling by 65.1% compared with that of the original one.

(3) Through energy consumption simulation, this research further investigated the thermal performance of the single-objective optimization model. In winter, the indoor air temperature and mean radiant temperature of the traditional dwelling after renovation were increased by

4.31°C and 4.35°C, respectively. In summer, the indoor air temperature and mean radiant temperature of the traditional dwelling after renovation were 1.25°C and 1.34°C lower than that before the renovation. Besides, due to the high humidity in the Qinba mountainous area, the indoor relative humidity of the renovated model has not been significantly improved. Combined with local living habits, the indoor relative humidity could be adjusted to a comfortable range of 30%~ 70% by using the dehumidification or heating equipment in winter and increasing the ventilation time in summer.

Reference

- [1] “China Building Energy Consumption Annual Report 2020,” *Building Energy Efficiency*, vol. 49, no. 02, pp. 1-6, 2021.
- [2] X. Li and C. W. J. I. Yu, “China’s building energy efficiency targets: challenges or opportunities?,” *Indoor and Built Environment*, vol. 21, no. 5, pp. 609-613, 2012.
- [3] C. S. Council, “2019 China Building Energy Consumption Annual Report,” *Construction and Architecture*, no. 07, pp. 30-39, 2020.
- [4] H. Sun, M. Leng, and Buildings, “Analysis on building energy performance of Tibetan traditional dwelling in cold rural area of Gannan,” *Energy and Buildings*, vol. 96, pp. 251-260, 2015.
- [5] J. Su, J. Li, X. Luo, C. W. Yu, and Z. Gu, “Experimental evaluation of a capillary heating bed driven by an air source heat pump and solar energy,” *Indoor and Built Environment*, vol. 29, no. 10, pp. 1399-1411, 2020.
- [6] X. Li, C. Shen, and C. W. Yu, “Building energy efficiency: Passive technology or active technology?,” *Indoor and Built Environment*, vol. 26, no. 6, pp. 729-732, 2017.
- [7] X. Sun, Z. Gou, and S. S.-Y. Lau, “Cost-effectiveness of active and passive design strategies for existing building retrofits in tropical climate: Case study of a zero energy building,” *Journal of Cleaner Production*, vol. 183, pp. 35-45, 2018.
- [8] S. Chang, H. Park, and G. R. Setyantho, “Performance Optimization of a Simplified Passive Design Space in Diversified Climatic Contexts,” *Proceedings of the Korean Society of Ecological and Environmental Architecture*, vol. 20, pp. 31-40, 2020.
- [9] N. A. Fereidani, E. Rodrigues, and A. R. Gaspar, “A review of the energy implications of passive building design and active measures under climate change in the Middle East,” *Journal of Cleaner Production*, vol. 305, p. 127152, 2021.
- [10] W. A. Mahar, G. Verbeeck, S. Reiter, and S. Attia, “Sensitivity analysis of passive design strategies for residential buildings in cold semi-arid climates,” *Sustainability*, vol. 12, no. 3, p. 1091, 2020.
- [11] I. A. Gondal, M. Syed Athar, and M. Khurram, “Role of passive design and alternative energy in building energy optimization,” *Indoor and Built Environment*, vol. 30, no. 2, pp. 278-289, 2021.
- [12] S. Ahady, N. Dev, and A. Mandal, “Solar radiation control passive strategy for reduction of heating and cooling energy use in arid climate: Case of Afghanistan,” *Indoor and Built Environment*, vol. 31, no. 4, pp. 955-971, 2022.
- [13] R. Yao, V. Costanzo, X. Li, Q. Zhang, and B. Li, “The effect of passive measures on thermal comfort and energy conservation. A case study of the hot summer and cold winter climate in the Yangtze River region,” *Journal of Building Engineering*, vol. 15, pp. 298-310, 2018.
- [14] C. Brunsgaard, P. Heiselberg, M.-A. Knudstrup, and T. S. Larsen, “Evaluation of the

indoor environment of comfort houses: Qualitative and quantitative approaches,” *Indoor and Built Environment*, vol. 21, no. 3, pp. 432-451, 2012.

[15] S. El Ahmar, F. Battista, and A. Fioravanti, “Simulation of the thermal performance of a geometrically complex Double-Skin Facade for hot climates: EnergyPlus vs. OpenFOAM,” in *Building Simulation*, 2019, vol. 12, pp. 781-795: Springer.

[16] G. A. Seber and A. J. Lee, *Linear regression analysis*. John Wiley & Sons, 2003.

[17] J. Amoako-Attah and A. B-Jahromi, “Impact of conservatory as a passive solar design of UK dwellings,” in *Proceedings of the Institution of Civil Engineers-Engineering Sustainability*, 2015, vol. 169, no. 5, pp. 198-213: Thomas Telford Ltd.

[18] A. Vukadinović, J. Radosavljević, A. Đorđević, M. Protić, and N. J. S. E. Petrović, “Multi-objective optimization of energy performance for a detached residential building with a sunroom using the NSGA-II genetic algorithm,” vol. 224, pp. 1426-1444, 2021.

[19] M. J. Suarez Lopez, S. Soutullo Castro, A. Navarro Manso, and E. Blanco Marigorta, “Heat collection in an attached sunroom,” *Renewable Energy*, vol. 145, pp. 2144-2150, Jan 2020.

[20] L. Ma et al., “Influence of sunroom on energy consumption of rural residential buildings,” *Solar Energy*, vol. 211, pp. 336-344, 2020.

[21] Design standard for energy efficiency for rural residential buildings (GB/T50824-2013), 2013.

[22] M. Peng, “Application of key technology and materials in the building envelop of passive house and low energy buildings,” *New Building Materials*, vol. 42, no. 01, pp. 77-82, 2015.

[23] Y. Zhao, Y. Chen, and X. Liu, “Optimization of insulation thickness for building external walls in hot summer and cold winter zone,” *BUILDING SCIENCE*, vol. 33, no. 04, pp. 77-84, 2017.

[24] B. Rosti, A. Omidvar, and N. Monghasemi, “Optimal insulation thickness of common classic and modern exterior walls in different climate zones of Iran,” *Journal of Building Engineering*, vol. 27, p. 100954, 2020.

[25] L. Zhang, C. Hou, J. Hou, D. Wei, and Y. J. C. S. i. T. E. Hou, “Optimization analysis of thermal insulation layer attributes of building envelope exterior wall based on DeST and life cycle economic evaluation,” vol. 14, p. 100410, 2019.

[26] W. Jiang et al., “Energy-saving retrofits of prefabricated house roof in severe cold area,” *Energy*, vol. 254, p. 124455, 2022.

[27] Y. Zhou and L. gong, “Research on energy-saving renovation of residential cold tile roof in traditional village in Zunyi,” *Urbanism and Architecture*, vol. 18, no. 17, pp. 68-71, 2021.

[28] P. Bevilacqua, “The effectiveness of green roofs in reducing building energy consumptions across different climates. A summary of literature results,” *Renewable*

Sustainable Energy Reviews, vol. 151, p. 111523, 2021.

[29] S. Zhang, "Research on Energy Saving Reconstruction of Exterior Windows of Existing Residential Buildings in Qingdao Area," Master Thesis, Qingdao University of Technology, 2020.

[30] Y. Zhong and M. Li, "Influence of external window on building energy efficiency in hot-summer & warm-winter climate zone," *Energy Saving in Building*, vol. 10, no. 02, pp. 36-38, 2018.

[31] F. a. Chi, Y. Wang, R. Wang, G. Li, and C. Peng, "An investigation of optimal window-to-wall ratio based on changes in building orientations for traditional dwellings," *Solar Energy*, vol. 195, pp. 64-81, Jan 1 2020.

[32] T. P. Obrecht, M. Premrov, and V. Ž. Leskovar, "Influence of the orientation on the optimal glazing size for passive houses in different European climates (for non-cardinal directions)," *Solar Energy*, vol. 189, pp. 15-25, 2019.

[33] T. Ashrafiyan and N. Moazzen, "The impact of glazing ratio and window configuration on occupants' comfort and energy demand: The case study of a school building in Eskisehir, Turkey," *Sustainable Cities Society*, vol. 47, p. 101483, 2019.

[34] F. Goia, "Search for the optimal window-to-wall ratio in office buildings in different European climates and the implications on total energy saving potential," *Solar Energy*, vol. 132, pp. 467-492, 2016.

[35] M. Krarti, "Evaluation of energy performance of dynamic overhang systems for US residential buildings," *Energy and Buildings*, vol. 234, p. 110699, 2021.

[36] S. M. Al-Masrani and K. M. Al-Obaidi, "Dynamic shading systems: A review of design parameters, platforms and evaluation strategies," *Automation in construction*, vol. 102, pp. 195-216, 2019.

[37] S. Wei and F. Mao, *Building construction*. Tsinghua University Press: Beijing, 2013.

[38] R. Fallahtafti and M. Mahdavinejad, "Optimisation of building shape and orientation for better energy efficient architecture," *International Journal of Energy Sector Management*, vol. 9, no. 4, pp. 593-618, 2015.

[39] M. Duan, Z. Wang, X. LI, and R. Wang, "The determination of community building shape and analysis of influence to public building envelope cooling load," *Journal of Civil, Architecture & Environmental Engineering*, vol. 33, no. S1, pp. 1-5, 2011.

[40] Design standard for energy efficiency of residential buildings in hot summer and cold winter zone (JGJ 134-2010), 2010.

[41] L. Yang, L. Hou, H. Li, X. Xu, and J. Liu, "Regression models for energy consumption prediction in air-conditioned office building," *Journal of Xi'an University of Architecture and Technology (Natural science edition)*, vol. 47, no. 05, pp. 707-711, 2015.

[42] J. C. Lam and S. C. Hui, "Sensitivity analysis of energy performance of office buildings," *Building and Environment*, vol. 31, no. 1, pp. 27-39, 1996.

[43] J. Terés-Zubiaga, A. Campos-Celador, I. González-Pino, and C. Escudero-Revilla, “Energy and economic assessment of the envelope retrofitting in residential buildings in Northern Spain,” *Energy and Buildings*, vol. 86, pp. 194-202, 2015.

[44] X. Song, C. Ye, Q. Xu, H. Li, and W. Ma, “Energy and economy analysis of building envelope retrofitting in the hot summer and warm winter zone of China,” *Advances in New and Renewable Energy*, vol. 4, no. 06, pp. 499-504, 2016.

Chapter 8

MULTI-OBJECTIVE OPTIMIZATION OF COST-EFFECTIVE PASSIVE STRATEGIES FOR TRADITIONAL DWELLING

**CHAPTER EIGHT: MULTI-OBJECTIVE OPTIMIZATION OF COST-EFFECTIVE
PASSIVE STRATEGIES FOR TRADITIONAL DWELLING**

MULTI-OBJECTIVE OPTIMIZATION OF COST-EFFECTIVE PASSIVE STRATEGIES FOR TRADITIONAL DWELLING..... 1

8.1. Contents 1

8.2. Materials and methodology..... 1

 8.2.1. Method 1

 8.2.2. Model setting..... 2

8.3. Research proposal 3

 8.3.1. Multi-Objective optimization model..... 3

 8.3.2. The multi-objectives..... 4

 8.3.3. Multiple regression model..... 6

 8.3.4. NSGA-2 genetic algorithm 6

 8.3.5. The TOPSIS decision-making method..... 6

8.4. Multi-Objective optimization result..... 7

 8.4.1. The fitting of multiple regression equations..... 7

 8.4.2. Decision-making of the passive design strategy 8

 8.4.3. Thermal loads simulation of the optimized dwelling 16

 8.4.4. Thermal comfort improvement of the optimized dwelling 17

8.5. Summary 24

References..... 26

8.1. Contents

Based on the investigation of the effectiveness of passive design parameters in traditional dwellings in Qinba mountainous area presented in Chapter 7, we determined that additional sunrooms, external wall heat transfer coefficient, roof heat transfer coefficient, and external window heat transfer coefficient are effective passive design parameters. In this chapter, we established a multi-objective optimization model based on the targets of “building energy consumption”, “human comfort”, and “economy”, combining the TOPSIS method, NSGA2 genetic algorithm, and multiple regression analysis. The model can obtain the optimal solution for the renovation of traditional dwellings’ by using passive strategies considering the three objectives.

Firstly, the multiple regression equations based on the 4 effective passive design parameters (including sunroom depth, external wall heat transfer coefficient, roof heat transfer coefficient, and window heat transfer coefficient) were fitted to obtain the building annual thermal load, proportion of uncomfortable hours, and renovation investment for each climatic sub-region. In addition, the NSGA-2 genetic algorithm has been used to find the Pareto optimal solution set based on a multi-regression equation with the three objectives (energy efficiency, thermal comfort, and cost-effectiveness). Then, based on the Euclidean distance of the TOPSIS method, 20 optimal solutions for the three-objective optimization in the Pareto set in the 5 climatic sub-regions of the Qinba mountainous area have been obtained. Finally, the building annual thermal loads and indoor comfort values of the optimal renovated dwelling in each climatic sub-region were simulated through energy simulation software.

The optimized renovation scheme for traditional dwellings can reduce energy consumption by 60.43%, 58.02%, 62.30%, 65.12%, and 62.59% in the climatic sub-region A1, A2, B1, B2, and C, respectively. After the renovation, the indoor temperature increases by approximately 3.3°C in winter and decreases by approximately 1.3°C in summer. The passive design strategies can significantly improve the indoor thermal environment of traditional dwellings in each climatic sub-region in Qinba mountainous area.

8.2. Materials and methodology

8.2.1. Method

(1) Computer simulation

In this study, EnergyPlus software were utilized for energy simulation. It is a computer program that provides a comprehensive simulation platform for analyzing the energy performance of buildings. Employing advanced modeling techniques, it enables accurate prediction of a building’s energy consumption, as well as the thermal and visual comfort of its occupants [1].

(2) Statistical method

Statistical analysis involves the acquisition of knowledge and the facilitation of decision-making through the collection, organization, and interpretation of data. Its purpose is to extract valuable information by identifying patterns, associations, and trends within the data [2, 3]. In this chapter, the multiple linear regression is used to fit a mathematical relationship between the three objectives and four passive design parameters. The specific calculation methods will be elaborated in the following section.

(3) Multi-objective optimization

Multi-objective optimization is a technique used to address optimization problems with multiple conflicting objectives. Unlike traditional single-objective optimization that focuses on optimizing a single objective, multi-objective optimization aims to find a set of solutions that strike a balance and trade-off among multiple objectives [4]. In this chapter, the research uses the NSGA-2 (Nondominated Sorting Genetic Algorithm 2) to assist decision-makers in making rational choices (Pareto set) among multiple objectives and identifying optimal solutions for complex problems. NSGA-2 uses a genetic algorithm approach, which involves the use of selection, crossover, and mutation operators to evolve a population of candidate solutions. Then the research conducts multi-objective decision-making with the aim of selecting the top 20 optimal solutions from the Pareto solution set [5]. These solutions will be used for energy consumption and thermal comfort simulations before and after the renovation of traditional residential buildings. Topsis (Technique for Order of Preference by Similarity to Ideal Solution) is a commonly used method for multi-objective decision-making, which determines the optimal solution by comparing the similarity between the candidate solutions and the ideal solution [4] [6]. The detailed introduction to the specific methods can be found in Chapter 3.

8.2.2. Model setting

(1) Energy simulation model

The study utilized the most prevalent traditional dwelling in the Qinba mountainous area, which is the “I”-shaped building, as the model for energy consumption simulation, shown in Figure 4-27. The meteorological data from the 5 climatic sub-regions used in Chapter 4 was also applied to the simulation. The building envelope structure and energy simulation software settings were consistent with those in Chapter 6 and Chapter 7.

(2) NSGA-2 genetic algorithm model

By putting the equations of passive design parameters and multi-objectives in each sub-region into the NSGA-2 system to perform multi-objective optimization, we can set the number of iterations to 2000 and the population size to 50. This algorithm will iteratively optimize the objectives and search for Pareto optimal solutions. However, The Pareto solution set in multi-objective optimization often contains hundreds or even thousands of non-dominated and non-ranked optimal solutions. So based on the Euclidean distance of the TOPSIS method, 20 optimal

solutions for the 3-objective optimization in the Pareto set have been obtained.

8.3. Research proposal

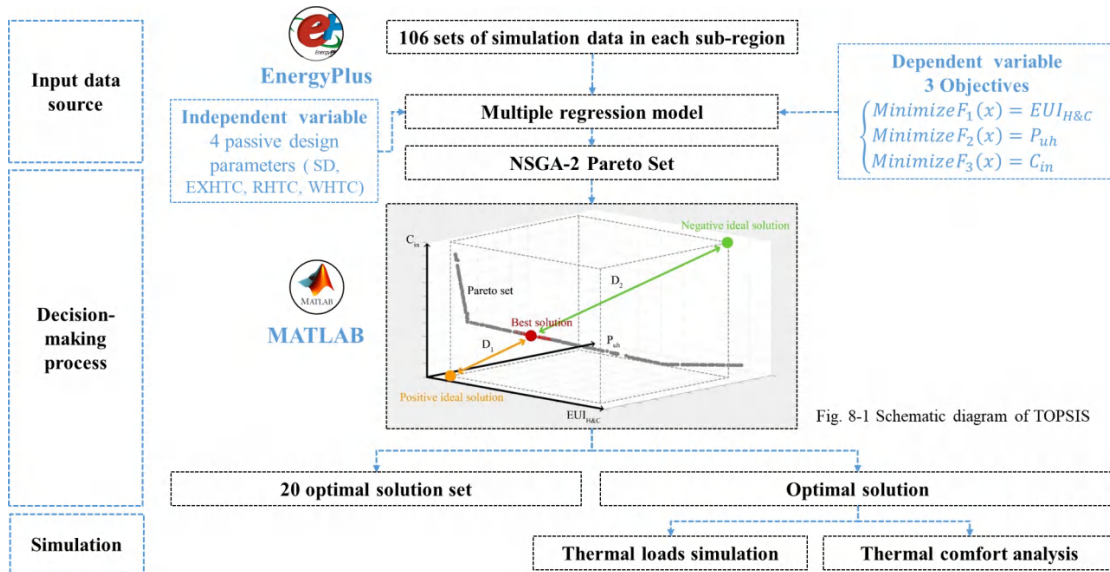


Figure 8-1. The research structure of multi-objective optimization

Figure 8-1 shows the research structure of multi-objective optimization of the traditional dwellings in Qinba mountainous area. In this chapter, by using the computer simulation, statistical analysis, NSGA-2, and TOPSIS method, the multi-objective optimization approaches to enhance the building energy efficiency, thermal comfort, and cost-effectiveness of passive design strategies for traditional dwellings in the 5 climatic sub-regions of Qinba mountainous area were obtained.

8.3.1. Multi-Objective optimization model

Previous studies on energy consumption simulation generally considered the optimal solution of energy consumption simulation and deduce the economic benefits of the optimal solution backward, lacking horizontal comparison of other simulation schemes, so the selection of the optimal scheme has certain limitations. This research intends to address a research vacuum by developing a multi-objective decision making model to achieve cost-effective design solutions for traditional dwellings in Qinba mountainous area. The findings of the study will serve as a reliable reference for building designers, as well as for the modification of energy efficiency design guidelines for the selection of building energy saving schemes.

The main steps of the multi-objective optimization process are as follows: 1) Three objectives, i.e., minimizing building energy consumption, minimizing discomfort hours, and minimizing renovation costs, are selected as dependent variables. Based on the effectiveness analysis conducted in Chapter 7, four passive strategies, including the attached sunroom depth, the exterior wall heat transfer coefficient, the roof heat transfer coefficient, and the window heat transfer coefficient, are chosen as independent variables that affect the 3 objectives. 2) A

multivariate regression mathematical model is established by simulating a large amount of data on 3 dependent variables (building annual thermal load, proportion of uncomfortable hours, and renovation costs) and 4 independent variables (the attached sunroom depth, the heat transfer coefficient of external wall, roof, and window). 3) The three regression models and the range of independent variables are input into the NSGA2 genetic algorithm for iterative optimization to calculate the solution set with the minimum values of building annual thermal load, proportion of uncomfortable hours, and renovation costs. 4) The Topsis decision-making method is used to calculate the three-dimensional Euclidean distance of each solution in the NSGA2 genetic algorithm solution set. The solution with the shortest distance to the positive ideal solution among all schemes is considered the best solution for the climate zone. The top 20 optimal solutions are selected as the optimal solution set.

8.3.2. The multi-objectives

For the improvement of indoor thermal environment and reduction of building energy consumption, it is not comprehensive to only consider one of them. For this study, the purpose of the building renovation is to seek the optimal solution to reduce the energy consumption, improve the indoor thermal comfort and reduce the renovation costs. As a result, the multi-objectives in this study are the building annual thermal load ($EUI_{H\&C}$), the percentage of uncomfortable hours (P_{uh}), and the initial investment of the passive design strategy (C_{in}). The constraint equation of the objective function can be described as:

$$\begin{cases} \text{Minimize } F_1(x) = EUI_{H\&C} \\ \text{Minimize } F_2(x) = P_{uh} \\ \text{Minimize } F_3(x) = C_{in} \end{cases} \quad (8-1)$$

(1) Building annual thermal load ($EUI_{H\&C}$)

Based on background research, in this study, the building annual thermal load are the annual heating and cooling energy calculated by EnergyPlus. The $EUI_{H\&C}$ can be expressed by the annual electricity consumption per unit air-conditioning area. The annual building thermal load calculation formula is [7]:

$$EUI_{H\&C} = \frac{1}{A} \cdot (E_H + E_C) \quad (8-2)$$

Where the $EUI_{H\&C}$ is the building annual thermal load, kWh/m²; A is the total building area, m²; E_H is the annual electricity consumption of heating, kWh; E_C is the annual electricity consumption of cooling, kWh.

(2) Percentage of uncomfortable hours (P_{uh})

By conducting energy consumption simulation on the renovated model without the use of air conditioning systems, the number of uncomfortable hours for 90% of the residents can be obtained as an indicator for evaluating the thermal comfort of the traditional dwelling after renovation. The ratio of the total number of uncomfortable hours to the total number of hours in a year is defined as the ratio of uncomfortable hours, which reflects the actual improvement of the thermal environment in traditional residential buildings. During the time period when residents feel uncomfortable, they can choose various heating and cooling measures to improve thermal comfort. The proportion of uncomfortable hours is also an auxiliary index that reflects the efficiency of passive strategies for building renovation. The formula for calculating the proportion of uncomfortable hours is as follows:

$$P_{uh} = \frac{UH}{AH} \cdot 100\% \quad (8-3)$$

Where the P_{uh} is the percentage of uncomfortable hours, %; the UH is the annual uncomfortable hours, h; the AH is the annual total hours, h.

(3) Initial investment of the passive design strategy (C_{in})

The investment of the renovation of traditional dwelling can measure the effectiveness of renovation strategies, and it could identify the passive strategy combinations that are energy-saving and cost-saving. The total renovation investment includes the sum of investments in various renovation strategies, which involves many factors such as the renovation area, renovation parts, and unit price of renovation strategies. The formula for calculating renovation investment is as follows:

$$C_{in} = \frac{C_{SC} + C_{EWHTC} + C_{RHTC} + C_{WHTC}}{A} \quad (8-4)$$

Where the C_{in} is the net present value of the initial investment of the passive design strategy, CNY/m²; the C_{SC} , C_{EWHTC} , and C_{RHTC} , C_{WHTC} are the total renovation investment of the attachment sunroom, the exterior wall, the roof, and the window, CNY.

Information on the costs of construction materials was obtained from an investigation of manufacturers in different cities. The price of the insulation material EPS is 566 CNY/m³. The price of ordinary insulating glass is 116.51 CNY /m², the price of triple glazing is 266 CNY /m², and the price of LOW-E insulating glass is 163.39 CNY /m², and the installation labour cost is 30 CNY /m².

8.3.3. Multiple regression model

The energy consumption simulation schemes cannot cover all cases of the variable range, so we can use multiple regression analysis to fit the changing pattern between independent and dependent variables. 106 sets of random samples were selected for building energy consumption simulation in each climatic sub-region. Based on the input parameters and output results of the 106 sets of simulations, multiple linear regression method can be used to establish the building annual thermal load prediction model, proportion of discomfort hour prediction model, and renovation investment prediction model for traditional dwelling in each climatic sub-region.[8, 9] The comprehensive expression is shown as Equation 8-5.

$$Y = \beta_0 + X_1\beta_1 + X_2\beta_2 + X_3\beta_3 + X_4\beta_4 \quad (8-5)$$

Where Y is the annual building thermal load, kWh/m²; X_1 is the attached sunroom depth, m; X_2 is the window heat transfer coefficient, W/(m²·K); X_3 is the exterior wall heat transfer coefficient, W/(m²·K); X_4 is the roof heat transfer coefficient, W/(m²·K); $\beta_0 \sim \beta_4$ are the regression coefficient.

8.3.4. NSGA-2 genetic algorithm

The NSGA2 genetic algorithm is a method used for multi-objective optimization problems. It can effectively handle problems with multiple conflicting objectives.[10] During the decision-making process, compromises need to be made between multiple objectives, and NSGA2 can help identify an approximate set of optimal solutions. The NSGA2 algorithm evolves candidate solutions through a genetic algorithm to obtain a Pareto set, which contains all the non-dominated solutions that cannot be dominated by other solutions. In the Pareto set, each solution is an approximation of the optimal solution, but there is a trade-off relationship between them.[11]

8.3.5. The TOPSIS decision-making method

The TOPSIS decision method is a mathematical model used for multi-attribute decision making, with the full name of Technique for Order of Preference by Similarity to Ideal Solution. This method ranks and evaluates different decision alternatives based on their similarity to the positive ideal solution, which has the best attribute values, and negative ideal solution, which has the worst attribute values[12].

In this study, effective passive design parameters such as attached sunroom depth, external wall heat transfer coefficient, roof heat transfer coefficient, and external window heat transfer coefficient are considered as independent variables. The building annual thermal loads, proportion of discomfort hours, and initial renovation investment vary with the independent variables. During the variation of the independent variables, there will be countless solutions,

and this study needs to find the optimal solution that simultaneously satisfies the lowest building annual thermal loads, proportion of discomfort hours, and initial renovation investment.

The TOPSIS decision-making method is used in this study to calculate the three-dimensional Euclidean distance of each scheme in the NSGA2 algorithm solution set for the 5 climatic sub-regions in Qinba mountainous area. The solution with the shortest Euclidean distance to the positive ideal solution is the best solution for that climatic sub-region. D_1 represents the Euclidean distance between each solution and the ideal solution, and D_2 represents the Euclidean distance between each solution and the negative ideal solution. [12-14]

The green point represents the negative ideal solution, the orange point represents the positive ideal solution, and the grey points indicate all other alternatives in the Pareto solution set, as illustrated in Figure 8-2. The best option, represented by the red point, is the one closest to the green point. Cao et al.[15] and Delgarm et al.[16] provide further details on the computation procedure.

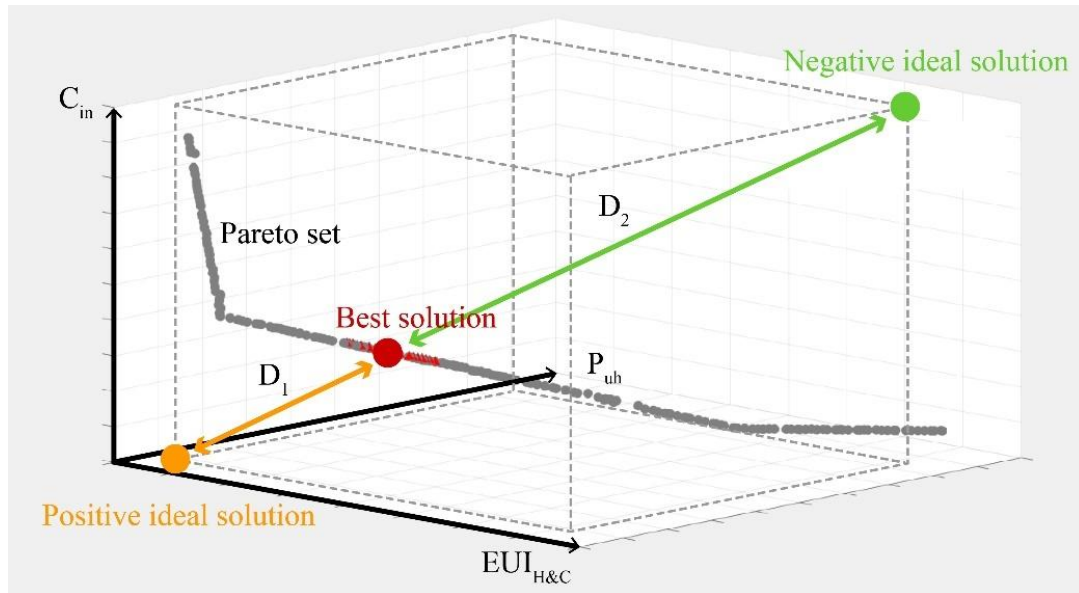


Figure 8-2. Schematic diagram of TOPSIS

8.4. Multi-Objective optimization result

8.4.1. The fitting of multiple regression equations

Through the data analysis software Origin, the multiple regression model fitting was carried out on 106 simulated data sets in each climatic sub-region, and the following results were obtained. The multiple regression equations in climatic sub-region A1 are:

$$\begin{cases} EUI_{H\&C} = 4.73928 + 0.52004X_1 + 3.53596X_2 + 5.24262X_3 + 0.07618X_4 \\ P_{uh} = 0.11145 + 0.00299X_1 + 0.05520X_2 + 0.08097X_3 + 0.00023X_4 \\ C_{in} = 307.16762 + 53.25198X_1 - 29.31962X_2 - 27.85430X_3 - 1.08955X_4 \end{cases} \quad (8-6)$$

The multiple regression equations in climatic sub-region A2 are:

$$\begin{cases} EUI_{H\&C} = 4.99031 + 0.15432X_1 + 3.30264X_2 + 4.65052X_3 + 0.04202X_4 \\ P_{uh} = 0.14502 + 0.00243X_1 + 0.03730X_2 + 0.06852X_3 + 0.00020X_4 \\ C_{in} = 309.83088 + 53.86410X_1 - 31.87479X_2 - 28.37404X_3 - 1.12131X_4 \end{cases} \quad (8-7)$$

The multiple regression equations in climatic sub-region B1 are:

$$\begin{cases} EUI_{H\&C} = 5.70571 - 0.37750X_1 + 6.89811X_2 + 6.78907X_3 + 0.09723X_4 \\ P_{uh} = 0.21295 + 0.00046X_1 + 0.05497X_2 + 0.06485X_3 + 0.00026X_4 \\ C_{in} = 350.71435 + 53.2443X_1 - 119.94037X_2 - 29.30264X_3 - 0.96835X_4 \end{cases} \quad (8-8)$$

The multiple regression equations in climatic sub-region B2 are:

$$\begin{cases} EUI_{H\&C} = 9.0014 - 0.46598X_1 + 6.86878X_2 + 6.63735X_3 + 0.08958X_4 \\ P_{uh} = 0.25291 + 0.00096X_1 + 0.03510X_2 + 0.04394X_3 + 0.00012X_4 \\ C_{in} = 353.08137 + 53.53036X_1 - 121.27247X_2 - 31.84190X_3 - 1.05041X_4 \end{cases} \quad (8-9)$$

The multiple regression equations in climatic sub-region C are:

$$\begin{cases} EUI_{H\&C} = 5.61018 + 0.04187X_1 + 6.99710X_2 + 8.35788X_3 + 0.10480X_4 \\ P_{uh} = 0.21602 + 0.00201X_1 + 0.04813X_2 + 0.05351X_3 + 0.00019X_4 \\ C_{in} = 353.08137 + 53.53036X_1 - 121.27247X_2 - 31.84190X_3 - 1.05041X_4 \end{cases} \quad (8-10)$$

8.4.2. Decision-making of the passive design strategy

In this section, we apply the TOPSIS decision-making method to rank all the solutions in the Pareto solution set, choose the top 20 solutions as the best solutions for each climatic sub-region. At the same time, the values of independent variables and dependent variables corresponding to the optimal solutions can also be obtained.

(1) Optimal solution set in climatic sub-region A1.

Figure 8-3 shows the passive design parameters of the top 20 solutions in climatic sub-region A1. The grey points in the figure represent the numerical distribution of the building annual thermal loads, the percentage of uncomfortable hours, and the discomfort hours and the initial investment of the passive design strategy in the simulation scheme, and the red triangles represent the distribution positions of the 20 optimal solutions in all solution sets.

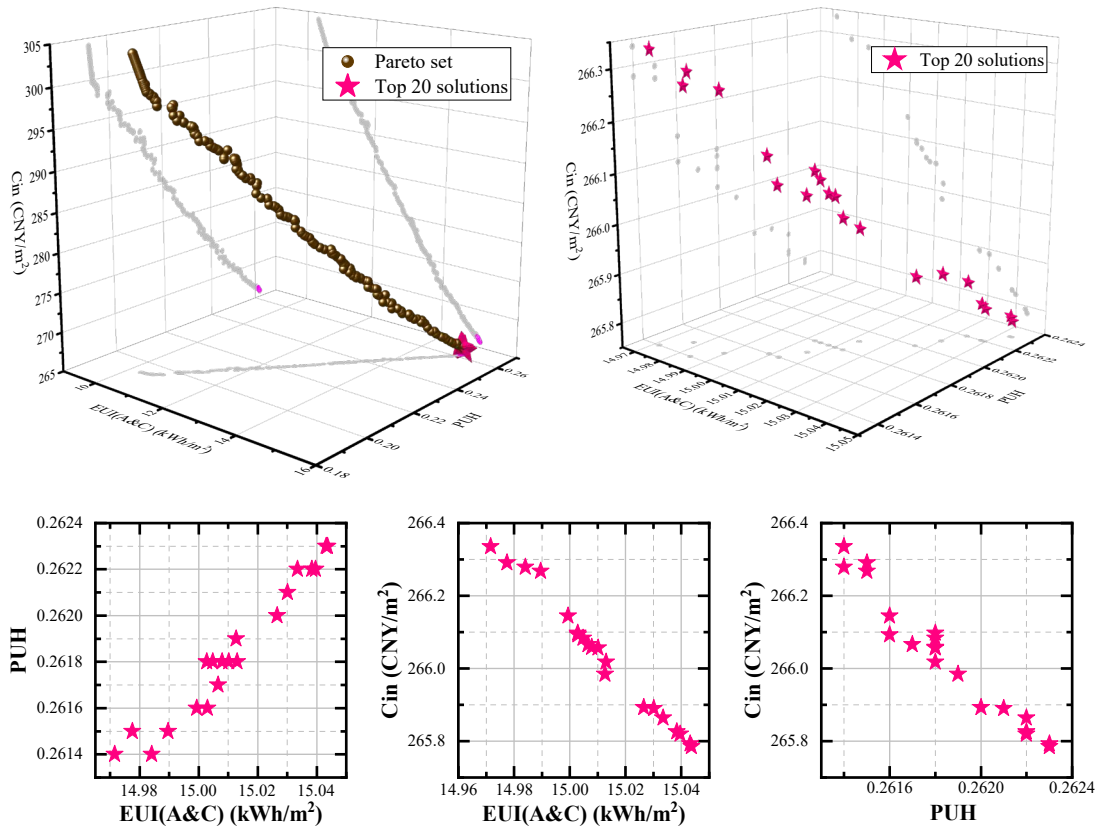


Figure 8-3. Distribution of TOPSIS decision results in Pareto for the climatic sub-region A1

Table 8-1. The top 20 optimal renovation plans in climatic sub-region A1

Rank	EUI _{H&C} kWh/m ²	P _{uh} %	C _{in} CNY/m ²	SD m	EWHTC W/(m ² ·K)	RHTC W/(m ² ·K)	WHTC W/(m ² ·K)
1	14.9896	26.15	266.2672	0.6001	1.4862	0.7999	6.4252
2	15.0432	26.23	265.7924	0.6001	1.4999	0.7999	6.4932
3	15.0335	26.22	265.8641	0.6001	1.4999	0.7985	6.4637
4	15.0437	26.23	265.7850	0.6001	1.4999	0.7999	6.4999
5	15.0301	26.21	265.8899	0.6001	1.4999	0.7980	6.4523
6	15.0396	26.22	265.8190	0.6001	1.4987	0.7999	6.4999
7	15.0384	26.22	265.8259	0.6001	1.4987	0.7997	6.4999
8	15.0079	26.18	266.0586	0.6001	1.4999	0.7949	6.3776
9	15.0102	26.18	266.0569	0.6001	1.4933	0.7985	6.4637
10	15.0048	26.18	266.0829	0.6001	1.4999	0.7944	6.3669
11	15.0028	26.18	266.0975	0.6001	1.4999	0.7941	6.3604
12	14.9994	26.16	266.1442	0.6001	1.4912	0.7980	6.4523
13	15.0130	26.18	266.0175	0.6001	1.4933	0.7985	6.4999
14	15.0266	26.20	265.8926	0.6001	1.4987	0.7975	6.4932
15	15.0066	26.17	266.0653	0.6001	1.4920	0.7982	6.4999
16	14.9775	26.15	266.2910	0.6001	1.4999	0.7905	6.2748
17	14.9841	26.14	266.2788	0.6001	1.4831	0.7999	6.4999
18	15.0030	26.16	266.0923	0.6001	1.4912	0.7980	6.4999
19	14.9716	26.14	266.3354	0.6001	1.4999	0.7897	6.2551
20	15.0127	26.19	265.9838	0.6001	1.4999	0.7947	6.4498
Recommended value range			Min	0.60	1.49	0.79	6.3
			Max		1.50	0.80	6.5

Table 8-1 shows the input parameter values and output parameter values of the top 20 solutions in climatic sub-region A1. The optimal sunroom depth should be 0.6m; the value of external wall heat transfer coefficient varies from 1.49W/(m²·K) to 1.50W/(m²·K), which equivalent to adding 9mm thick EPS insulation material to the exterior wall; the value of roof heat transfer coefficient varies from 1.49W/(m²·K) to 1.50 W/(m²·K), which is adding 32mm thick EPS insulation material on the original roof; the value of window heat transfer coefficient varies from 6.3W/(m²·K) to 6.5 W/(m²·K).

With the optimal solutions of the passive design strategies, the building annual thermal loads varies from 14.9896kWh/m² to 15.0437kWh/m², the percentage of uncomfortable hours ranges from 26.15% to 26.23%, and the initial investment of the passive design strategy varies from 265.7850CNY/m² to 266.3354CNY/m².

(2) Optimal solution set in climatic sub-region A2.

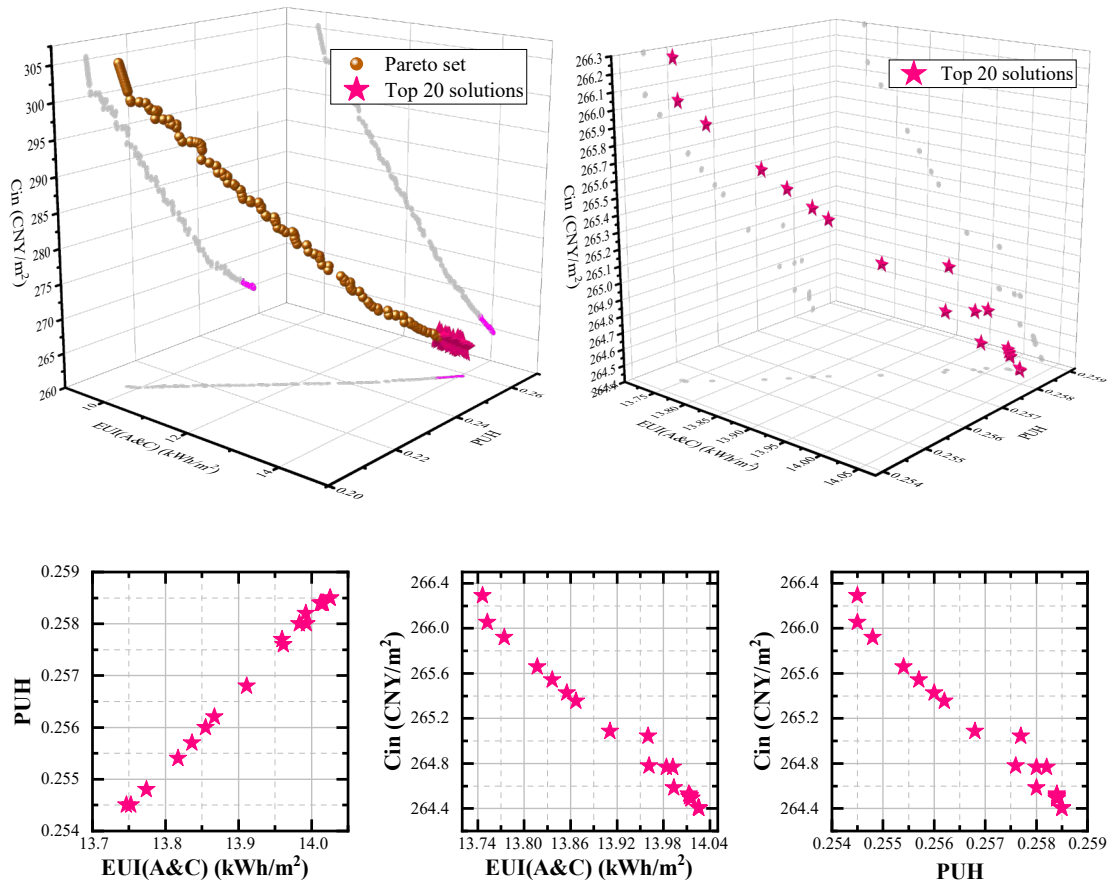


Figure 8-4. Distribution of TOPSIS decision results in Pareto for the climatic sub-region A2

Figure 8-4 and Table 8-2 show the passive design parameters and output dependent variables of the top 20 solutions in climatic sub-region A2. The optimal sunroom depth should be 0.6m; the value of external wall heat transfer coefficient varies from 1.49W/(m²·K) to 1.50 W/(m²·K), which equivalent to adding 9mm thick EPS insulation material to the exterior wall; the value of roof heat transfer coefficient varies from 0.74W/(m²·K) to 0.80 W/(m²·K), which is adding

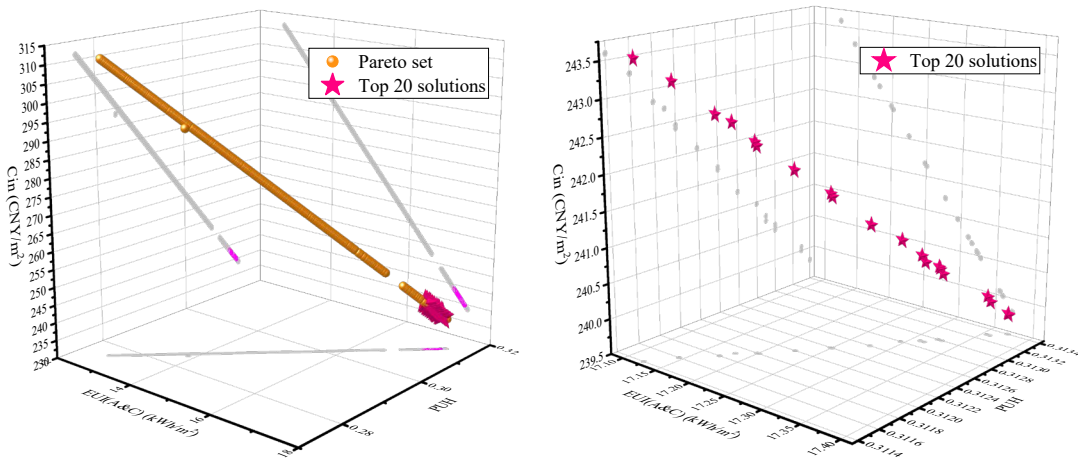
32mm~37mm thick EPS insulation material on the original roof; the value of window heat transfer coefficient varies from 6.20W/(m²·K) to 6.50W/(m²·K).

With the optimal solutions of the passive design strategies, the building annual thermal loads varies from 13.7464kWh/m² to 14.0257kWh/m², the percentage of uncomfortable hours ranges from 25.45% to 25.85%, and the initial investment of the passive design strategy varies from 264.4011CNY/m² to 266.2902CNY/m².

Table 8-2. The top 20 optimal renovation plans in climatic sub-region A2

Rank	EUI _{H&C} kWh/m ²	P _{uh} %	C _{in} CNY/m ²	SD m	EWHTC W/(m ² ·K)	RHTC W/(m ² ·K)	WHTC W/(m ² ·K)
1	13.9921	25.82	264.7657	0.6001	1.4893	0.7999	6.4416
2	14.0257	25.85	264.4011	0.6001	1.4999	0.7992	6.4814
3	14.0251	25.85	264.4073	0.6001	1.4999	0.7991	6.4787
4	14.0125	25.84	264.5291	0.6001	1.4961	0.7991	6.4787
5	14.0163	25.84	264.4931	0.6001	1.4999	0.7975	6.4416
6	14.0141	25.84	264.5148	0.6001	1.4999	0.7972	6.4322
7	14.0155	25.84	264.4864	0.6001	1.4966	0.7992	6.4999
8	14.0134	25.84	264.5053	0.6001	1.4961	0.7991	6.4999
9	13.9836	25.80	264.7671	0.6001	1.4893	0.7975	6.4999
10	13.9599	25.77	265.0428	0.6001	1.4999	0.7876	6.2039
11	13.9933	25.80	264.5830	0.6001	1.4999	0.7921	6.4999
12	13.9614	25.76	264.7776	0.6001	1.4999	0.7852	6.4999
13	13.9111	25.68	265.0844	0.6001	1.4999	0.7744	6.4999
14	13.8670	25.62	265.3533	0.6001	1.4999	0.7649	6.4999
15	13.8552	25.60	265.4256	0.6001	1.4999	0.7624	6.4999
16	13.8362	25.57	265.5416	0.6001	1.4999	0.7583	6.4999
17	13.8171	25.54	265.6579	0.6001	1.4999	0.7542	6.4999
18	13.7742	25.48	265.9199	0.6001	1.4999	0.7450	6.4999
19	13.7464	25.45	266.2902	0.6001	1.4999	0.7411	6.2681
20	13.7525	25.45	266.0521	0.6001	1.4999	0.7403	6.4999
Recommended value range			Min	0.60	1.49	0.74	6.20
			Max		1.50	0.80	6.50

(3) Optimal solution set in climatic sub-region B1.



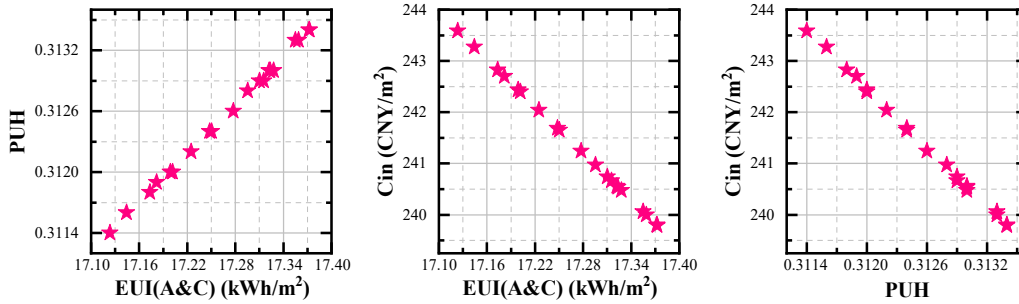


Figure 8-5. Distribution of TOPSIS decision results in Pareto for the climatic sub-region B1

Figure 8-5 and Table 8-3 show the passive design parameters and output dependent variables of the top 20 solutions in climatic sub-region B1. The optimal sunroom depth is 0.60m; the value of external wall heat transfer coefficient is 0.98W/(m²·K), which equivalent to adding 50mm thick EPS insulation material to the exterior wall; the value of roof heat transfer coefficient ranges from 0.69W/(m²·K) to 0.70W/(m²·K), which is adding 16mm thick EPS insulation material on the original roof; the value of window heat transfer coefficient varies from 3.90 W/(m²·K) to 4.10 W/(m²·K).

With the optimal solutions of the passive design strategies, the building annual thermal loads varies from 17.1236kWh/m² to 17.3726kWh/m², the percentage of uncomfortable hours ranges from 31.14% to 31.34%, and the initial investment of the passive design strategy varies from 243.5862CNY/m² to 239.7931CNY/m².

Table 8-3. The top 20 optimal renovation plans in climatic sub-region B1

Rank	EUI _{H&C} kWh/m ²	P _{uh} %	C _{in} CNY/m ²	SD m	EWHTC W/(m ² ·K)	RHTC W/(m ² ·K)	WHTC W/(m ² ·K)
1	17.1236	31.14	243.5862	0.6001	0.9801	0.6915	3.9165
2	17.1444	31.16	243.2684	0.6001	0.9801	0.6920	3.9278
3	17.1735	31.18	242.8260	0.6001	0.9801	0.6926	3.9435
4	17.1816	31.19	242.7023	0.6001	0.9801	0.6928	3.9479
5	17.1989	31.20	242.4386	0.6001	0.9801	0.6932	3.9573
6	17.2016	31.20	242.3968	0.6001	0.9801	0.6933	3.9588
7	17.2250	31.22	242.0413	0.6001	0.9801	0.6938	3.9714
8	17.2482	31.24	241.6876	0.6001	0.9801	0.6943	3.9840
9	17.2505	31.24	241.6525	0.6001	0.9801	0.6944	3.9853
10	17.2777	31.26	241.2387	0.6001	0.9801	0.6950	4.0000
11	17.2953	31.28	240.9705	0.6001	0.9801	0.6954	4.0096
12	17.3104	31.29	240.7401	0.6001	0.9801	0.6957	4.0178
13	17.3155	31.29	240.6632	0.6001	0.9801	0.6959	4.0205
14	17.3223	31.30	240.5596	0.6001	0.9801	0.6960	4.0242
15	17.3236	31.30	240.5390	0.6001	0.9801	0.6960	4.0249
16	17.3278	31.30	240.4758	0.6001	0.9801	0.6961	4.0272
17	17.3550	31.33	240.0604	0.6001	0.9801	0.6968	4.0419
18	17.3590	31.33	239.9994	0.6001	0.9801	0.6969	4.0441
19	17.3720	31.34	239.8019	0.6001	0.9801	0.6971	4.0511
20	17.3726	31.34	239.7931	0.6001	0.9801	0.6972	4.0515
Recommended value range			Min			0.69	3.90
			Max	0.60	0.98	0.70	4.10

(4) Optimal solution set in climatic sub-region B2.

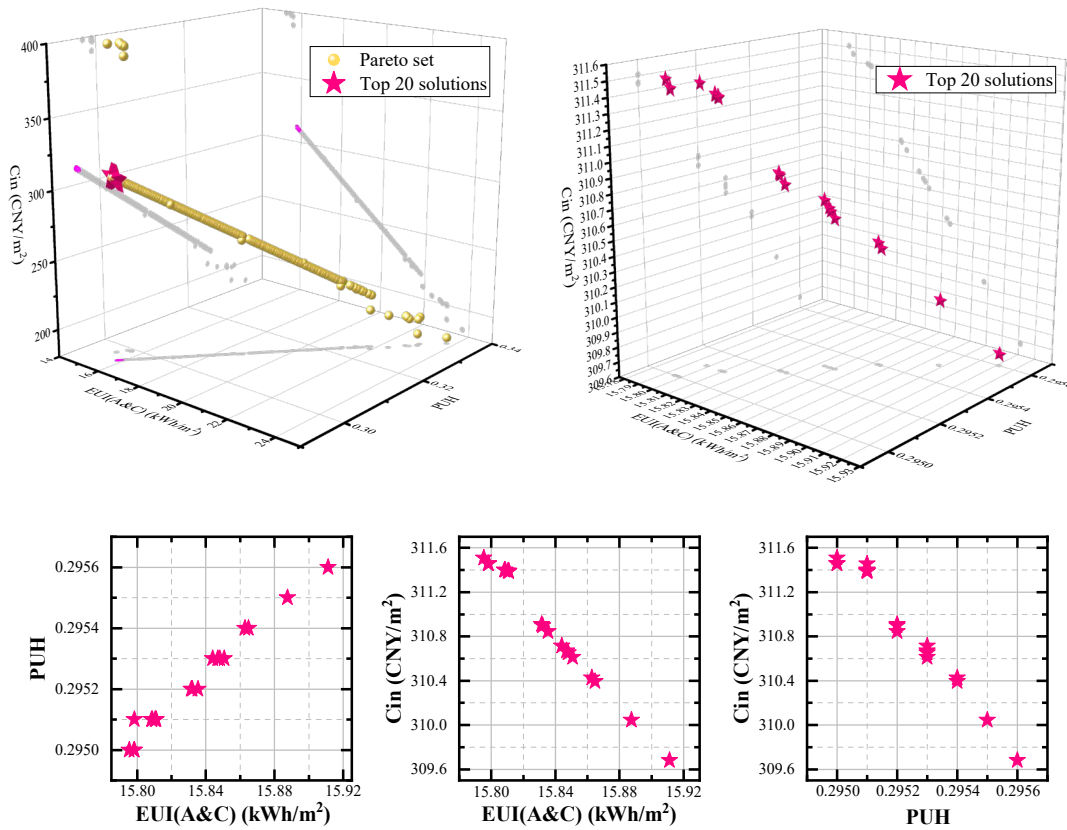


Figure 8-6. Distribution of TOPSIS decision results in Pareto for the climatic sub-region B2

Table 8-4. The top 20 optimal renovation plans in climatic sub-region B2

Rank	EUI _{H&C} kWh/m ²	P _{uh} %	C _{in} CNY/m ²	SD m	EWHTC W/(m ² ·K)	RHTC W/(m ² ·K)	WHTC W/(m ² ·K)
1	15.8105	29.51	311.3907	0.6035	0.4421	0.5904	1.5098
2	15.8110	29.51	311.3869	0.6042	0.4425	0.5901	1.5117
3	15.8109	29.51	311.3872	0.6042	0.4425	0.5901	1.5116
4	15.8088	29.51	311.3986	0.6036	0.4421	0.5901	1.5101
5	15.8084	29.51	311.4006	0.6035	0.4421	0.5901	1.5098
6	15.7954	29.50	311.5082	0.6009	0.4401	0.5901	1.5025
7	15.7982	29.50	311.4575	0.6009	0.4405	0.5901	1.5001
8	15.7984	29.51	311.4549	0.6009	0.4405	0.5901	1.5025
9	15.7984	29.50	311.4551	0.6009	0.4405	0.5901	1.5025
10	15.8875	29.55	310.0450	0.6001	0.4508	0.5921	1.5512
11	15.8315	29.52	310.9073	0.6001	0.4443	0.5909	1.5205
12	15.8321	29.52	310.8981	0.6001	0.4444	0.5909	1.5208
13	15.8355	29.52	310.8456	0.6001	0.4448	0.5910	1.5227
14	15.8441	29.53	310.7140	0.6001	0.4458	0.5911	1.5274
15	15.8470	29.53	310.6697	0.6001	0.4461	0.5912	1.5289
16	15.8481	29.53	310.6516	0.6001	0.4463	0.5912	1.5296
17	15.8508	29.53	310.6107	0.6001	0.4466	0.5913	1.5310
18	15.8628	29.54	310.4262	0.6001	0.4480	0.5916	1.5376
19	15.8648	29.54	310.3948	0.6001	0.4482	0.5916	1.5387
20	15.8877	29.55	310.0329	0.6001	0.4511	0.5922	1.5501
Recommended value range			Min		0.44		1.50
			Max	0.60	0.45	0.59	1.55

Figure 8-6 and Table 8-4 show the passive design parameters and output dependent variables of the top 20 solutions in climatic sub-region B2. The optimal sunroom depth ranges from 1.83m to 0.60m; the value of external wall heat transfer coefficient should be 0.44W/(m²·K) to 0.45 W/(m²·K), which equivalent to adding 50mm thick EPS insulation material to the exterior wall; the value of roof heat transfer coefficient should be 0.59W/(m²·K), which is adding 50mm thick EPS insulation material on the original roof; the value of window heat transfer coefficient varies from 1.50 W/(m²·K) to 1.55 W/(m²·K). With the optimal solutions of the passive design strategies, the building annual thermal loads varies from 15.7954kWh/m² to 15.8877kWh/m², the percentage of uncomfortable hours ranges from 29.50% to 29.55%, and the initial investment of the passive design strategy varies from 310.0329CNY/m² to 311.5082CNY/m².

(5) Optimal solution set in climatic sub-region C.

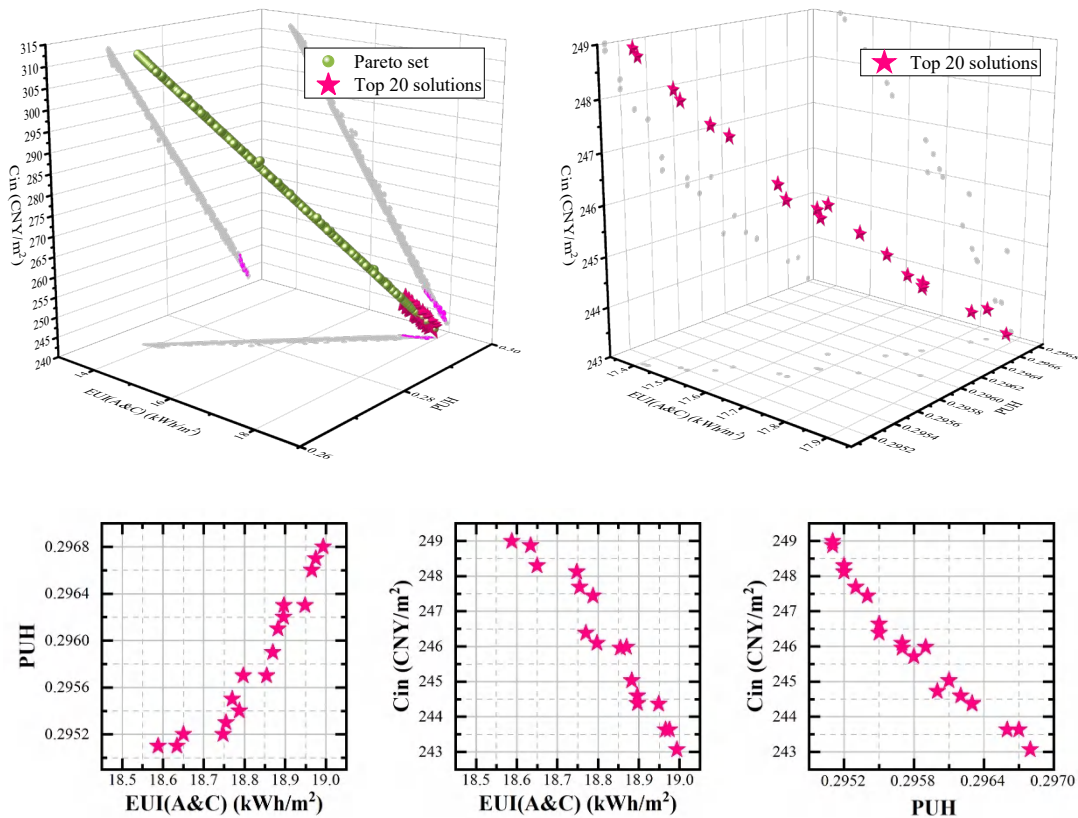


Figure 8-7. Distribution of TOPSIS decision results in Pareto for the climatic sub-region C

Figure 8-7 and Table 8-5 show the passive design parameters and output dependent variables of the top 20 solutions in climatic sub-region C. The optimal sunroom depth should be 0.6m; the value of external wall heat transfer coefficient is 0.98W/(m²·K), which equivalent to adding 0mm thick EPS insulation material to the exterior wall; the value of roof heat transfer coefficient should be 0.59W/(m²·K), which is adding 50mm thick EPS insulation material on the original roof; the value of window heat transfer coefficient varies from 1.5W/(m²·K) to 4.5W/(m²·K). With the optimal solutions of the passive design strategies, the building annual

thermal loads varies from 18.4953kWh/m² to 18.9933kWh/m², the percentage of uncomfortable hours ranges from 29.51% to 29.68%, and the initial investment of the passive design strategy varies from 243.0693CNY/m² to 248.9948 CNY/m².

Table 8-5. The top 20 optimal renovation plans in climatic sub-region C

Rank	EUI _{H&C} kWh/m ²	P _{uh} %	C _{in} CNY/m ²	SD m	EWHTC W/(m ² ·K)	RHTC W/(m ² ·K)	WHTC W/(m ² ·K)
1	18.8700	29.58	245.7121	0.6001	0.9801	0.5941	4.6032
2	18.9750	29.60	244.7216	0.6001	0.9801	0.5941	5.5461
3	18.7475	29.55	246.6376	0.6001	0.9801	0.5901	3.7943
4	18.4953	29.51	248.9948	0.6001	0.9801	0.5901	1.5001
5	18.5086	29.51	248.8699	0.6001	0.9801	0.5901	1.6190
6	18.5696	29.52	248.2933	0.6001	0.9801	0.5901	2.1679
7	18.5883	29.52	248.1169	0.6001	0.9801	0.5901	2.3358
8	18.6345	29.53	247.6816	0.6001	0.9801	0.5901	2.7502
9	18.7696	29.55	246.3830	0.6001	0.9801	0.5901	3.9326
10	18.6503	29.54	247.4371	0.6001	0.9801	0.5901	2.7664
11	18.7878	29.57	246.0950	0.6001	0.9801	0.5901	3.9434
12	18.7970	29.57	245.9492	0.6001	0.9801	0.5901	3.9488
13	18.7550	29.59	245.9841	0.6001	0.9801	0.5901	3.1022
14	18.8549	29.61	245.0300	0.6001	0.9801	0.5901	3.9832
15	18.8825	29.62	244.5928	0.6001	0.9801	0.5901	3.9995
16	18.8957	29.63	244.3831	0.6001	0.9801	0.5901	4.0073
17	18.8971	29.63	244.3619	0.6001	0.9801	0.5901	4.0081
18	18.9487	29.66	243.6304	0.6001	0.9801	0.5901	4.1526
19	18.9654	29.67	243.6297	0.6001	0.9801	0.5933	4.0316
20	18.9933	29.68	243.0693	0.6001	0.9801	0.5901	4.3706
Recommended value range			Min	0.60	0.98	0.59	1.50
			Max				4.50

(6) Optimal solution set in each climatic sub-region in Qinba mountainous area.

Through the above analysis, it can be seen that the multi-objective optimization schemes of the passive design strategy renovation of the traditional dwellings' present different optimal solutions in various climatic sub-regions. Table 8-6 summarizes the optimal multi-objective optimization results for the 5 climatic sub-regions in Qinba mountainous area.

For the climatic sub-region A1 to C, the minimum value of 0.6m is applied to the attached sunroom depth. In this case, the sunroom is only used as a heat collection space, not as a usable space. For sub-region A1 and A2, the values of the external wall heat transfer coefficient and the roof heat transfer coefficient should set at the maximum value specified by design standards, which are 1.50W/(m²·K) and 0.80W/(m²·K), respectively. For the sub-region B1 and C, the exterior wall doesn't need to be renovated, as it has good thermal insulation performance. For sub-region B2, the values of the external wall heat transfer coefficient should be as small as possible with the value of 0.44W/(m²·K). The roof in sub-region B1, B2, and C need to be renovated with the value of 0.70 W/(m²·K), 0.59 W/(m²·K), 0.59 W/(m²·K), respectively. The sub-region A1 and A2 could apply the most economical window type, with the heat transfer coefficient of 6.50 W/(m²·K). While for sub-regions B1, B2, and C, windows with smaller heat

transfer coefficients could be selected.

Table 8-6 The optimal multi-objective optimization results for the 5 climatic sub-regions in Qinba mountainous area

Sub-region	Value range						
	$EUI_{H\&C}$ kWh/m ²	P_{uh} %	C_{in} CNY/m ²	SD m	$EWHTC$ W/(m ² ·K)	$RHTC$ W/(m ² ·K)	$WHTC$ W/(m ² ·K)
A1	14.99~15.04	26.15~26.23	265.79~266.34	0.60	1.49~1.50	0.79~0.80	6.30~6.50
A2	13.75~14.03	25.45~25.85	264.40~266.29	0.60	1.49~1.50	0.74~1.80	6.20~6.50
B1	17.12~17.37	31.14~31.34	243.59~239.79	0.60	0.98	0.69~0.70	3.90~4.10
B2	15.80~15.89	29.50~29.55	310.03~311.51	0.60	0.44~0.45	0.59	1.50~1.55
C	18.50~18.99	29.51~29.68	243.07~248.99	0.60	0.98	0.59	1.50~4.50

8.4.3. Thermal loads simulation of the optimized dwelling

The optimal solutions obtained by applying the TOPSIS decision method in each climatic sub-region were selected for computer energy consumption simulation. The differences between the data of the NSGA2 fitting equation and the actual simulation data were presented in Table 8-7 and 8-8.

Table 8-7 The energy consumption calculation of the optimal solution by NSGA-2

Sub-region	$EUI_{H\&C}$ kWh/m ²	P_{uh} %	C_{in} CNY/m ²	SD m	$EWHTC$ W/(m ² ·K)	$RHTC$ W/(m ² ·K)	$WHTC$ W/(m ² ·K)
A1	14.9896	26.15	266.2672	0.60	1.49	0.80	6.42
A2	13.9921	25.82	264.7657	0.60	1.49	0.80	6.44
B1	17.1236	31.14	243.5862	0.60	0.98	0.69	3.92
B2	15.8105	29.51	311.3907	0.60	0.44	0.59	1.51
C	18.8700	29.58	245.7121	0.60	0.98	0.59	4.60

Table 8-8 The energy consumption simulation of the optimal solution

Sub-region	$EUI_{H\&C}$ kWh/m ²	P_{uh} %	C_{in} CNY/m ²	SD m	$EWHTC$ W/(m ² ·K)	$RHTC$ W/(m ² ·K)	$WHTC$ W/(m ² ·K)
A1	14.8530	25.39	272.1177	0.60	1.49	0.80	6.42
A2	13.8330	25.21	269.5091	0.60	1.49	0.80	6.44
B1	17.6259	30.98	243.3185	0.60	0.98	0.69	3.92
B2	15.9412	28.80	310.4284	0.60	0.44	0.59	1.51
C	18.3350	29.36	245.1238	0.60	0.98	0.59	4.60

The computer simulation results were compared with the NSGA2 fitting equation calculation result, and the errors for building annual thermal loads in sub-region A1, A2, B1, B2, and C were 0.92%, 1.15%, -2.85%, -0.82%, and 2.92%, respectively. The errors for proportion of uncomfortable hours in sub-region A1, A2, B1, B2, and C were 2.98%, 2.40%, 0.51%, 1.23%, and 0.74%, respectively. The errors for renovation investment in sub-region A1, A2, B1, B2, and C were -2.15%, -1.76%, 0.11%, 0.31%, and 0.24%, respectively. The errors of the fitting equation were within an acceptable range, indicating the optimization results were accurate.

Table 8-9 Building annual thermal loads before and after renovation

Sub-region	EUI _{H&C} before renovation	EUI _{H&C} after renovation	Energy-efficiency rate
	kWh/m ²	kWh/m ²	%
A1	37.879	14.990	60.43
A2	33.328	13.992	58.02
B1	45.424	17.124	62.30
B2	44.631	15.810	65.12
C	50.440	18.870	62.59

Table 8-9 shows the value of passive design parameters before and after renovation, the building annual thermal loads before and after renovation, and the energy efficiency rates of the renovated dwelling. The annual building thermal loads of the traditional dwellings after renovation in climatic sub-regions A1 to C, are 14.990kWh/m², 13.992kWh/m², 17.124kWh/m², 15.567kWh/m², 18.870kWh/m², respectively, which is reduced by 60.43%, 58.02%, 62.30%, 65.12%, and 62.59% than the value of 37.879kWh/m², 33.328kWh/m², 45.424kWh/m², 44.631kWh/m², and 50.440kWh/m² before renovation.

8.4.4. Thermal comfort improvement of the optimized dwelling

To verify the impact of the passive design parameters on the indoor air temperature, mean radiant temperature and relative humidity of the optimized dwelling, this study simulated the indoor air temperature, mean radiant temperature, and relative humidity of the target model before and after renovation. Without the use of cooling and heating installation, the fluctuation curves of the indoor mean radiant temperature, and relative humidity before and after renovation are shown in Figure 8-8 to 8-17.

(1) Indoor temperature simulation.

Figure 8-8 to Figure 8-12 show the variation trend of the outdoor air temperature, indoor air temperature and indoor mean radiant temperature in the 5 climatic sub-regions in Qinba mountainous area.

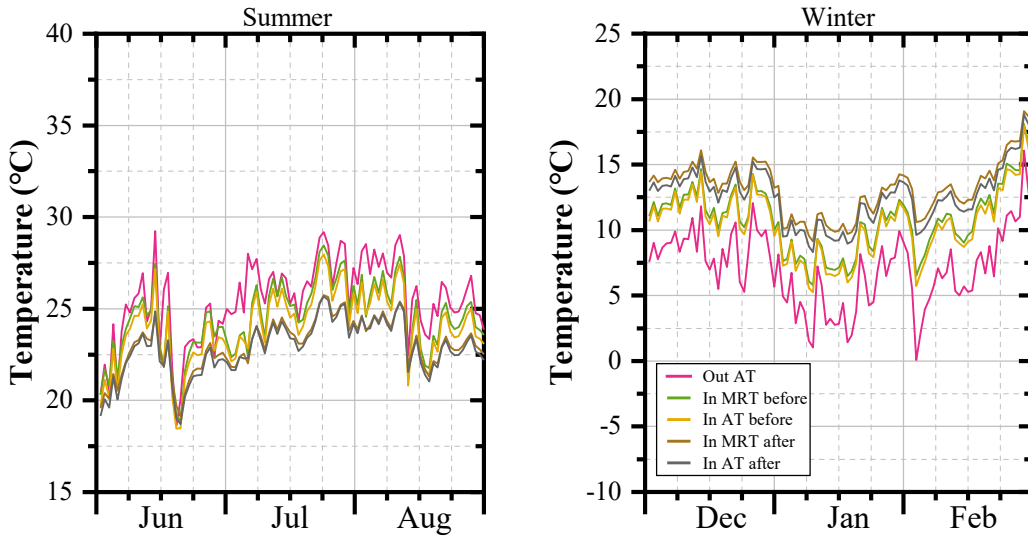


Figure 8-8. The temperature variation before and after renovation in climatic sub-region A1

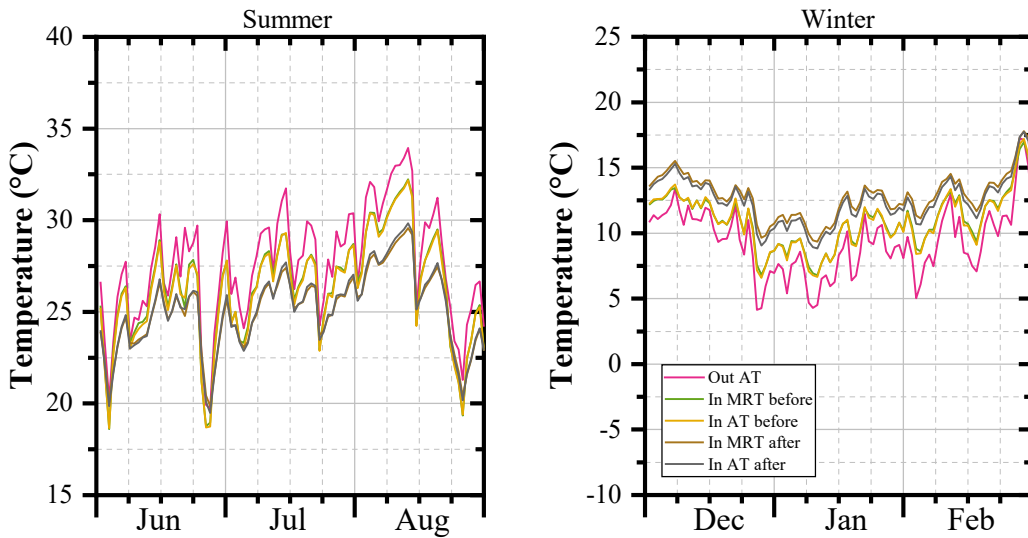


Figure 8-9. The temperature variation before and after renovation in climatic sub-region A2

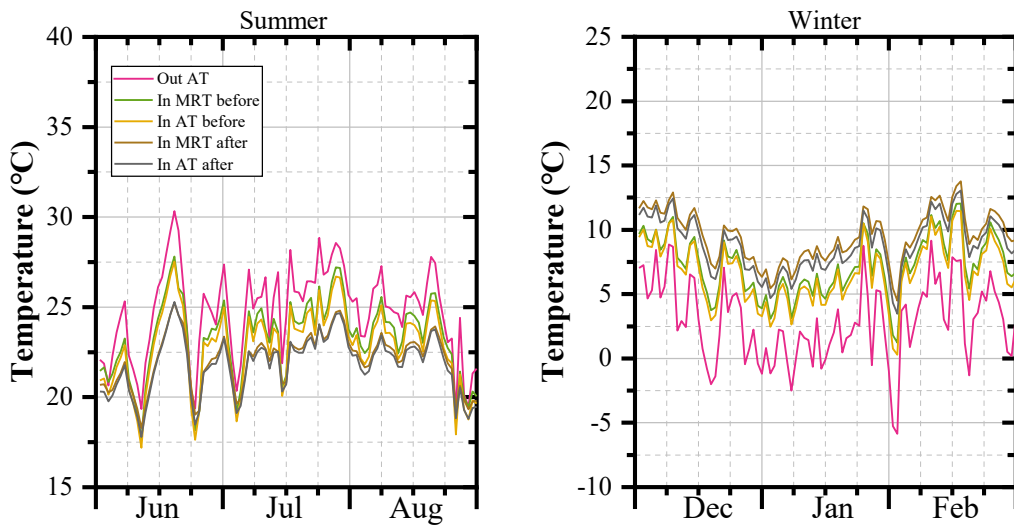


Figure 8-10. The temperature variation before and after renovation in climatic sub-region B1

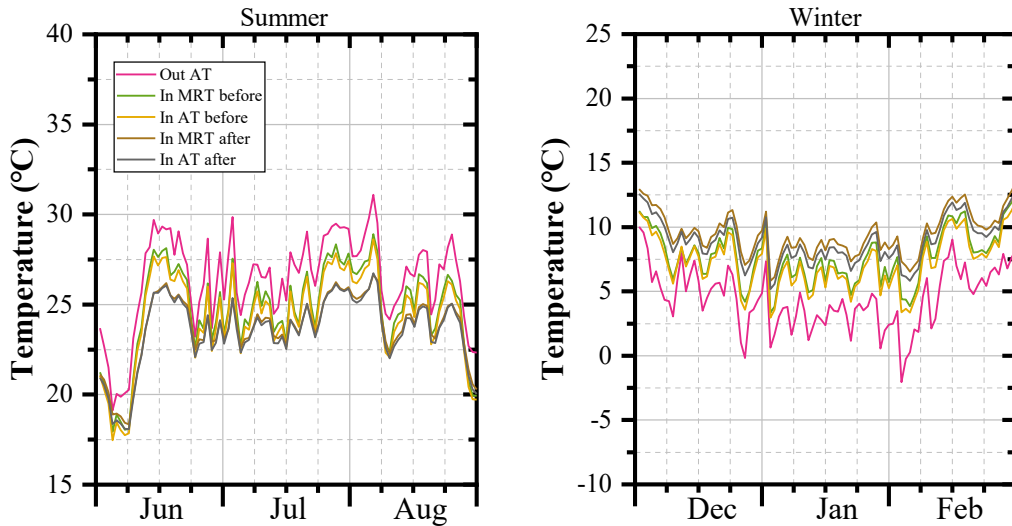


Figure 8-11. The temperature variation before and after renovation in climatic sub-region B2

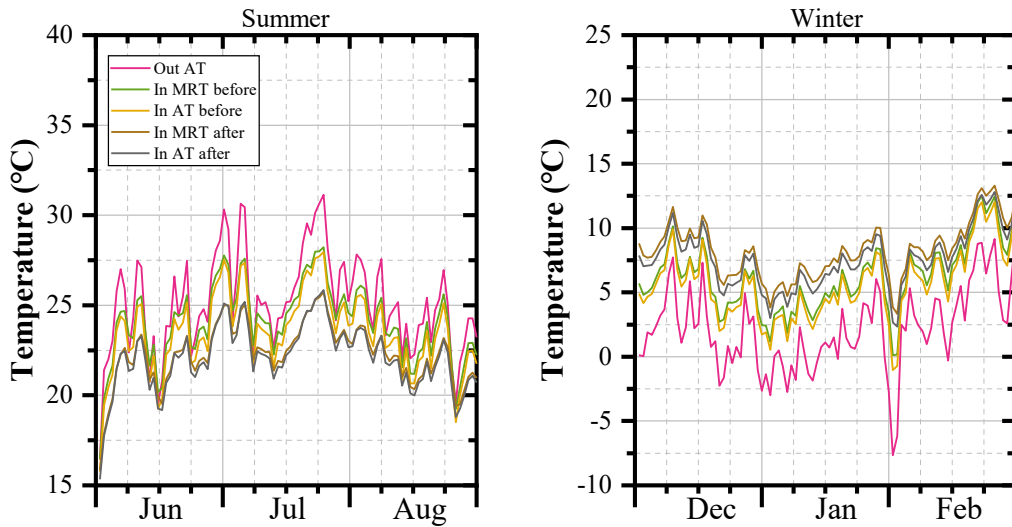


Figure 8-12. The temperature variation before and after renovation in climatic sub-region C

And based on the variation trend of the temperatures, Table 8-10 and Table 8-11 shows the variation ranges and mean values of the outdoor temperature, indoor air temperature, and indoor mean radiant temperature in winter and summer, respectively.

Table 8-10. The temperature variation before and after renovation in winter

Sub-region	Outdoor air temperature		Indoor air temperature				Indoor mean radiant temperature			
			Before		After		Before		After	
A1	7.1	0.1~16.1	10.4	5.3~18.0	13.3	8.3~18.8	10.8	5.8~18.1	13.9	9.1~19.1
A2	9.4	4.1~17.3	10.9	6.6~17.2	13.5	8.8~17.8	11.0	6.8~16.9	13.8	9.3~17.8
B1	2.9	-5.8~9.2	6.7	0.3~11.5	9.8	3.5~13.1	7.2	1.2~12.0	10.5	4.5~13.8
B2	4.5	-2.0~10.0	7.1	3.0~12.0	10.6	5.2~12.9	7.5	3.3~12.7	11.3	5.8~13.5
C	2.1	-7.6~9.6	5.6	-1.0~12.0	8.9	2.3~12.8	6.2	0.11~12.5	9.6	3.3~13.3

1) Temperature in winter. As shown in Table 8-10, the variation ranges of the outdoor air temperature are 0.1°C~16.1°C, 4.1°C~17.3°C, -5.8°C~9.2°C, -2.0°C~10.0°C, -7.6°C~9.6°C, with the mean value of 7.1°C, 9.4°C, 2.9°C, 4.5°C, and 2.1°C in sub-region A1 to C, respectively. After renovation, the variation ranges of the indoor mean radiant temperature are 9.1°C~19.1°C, 9.3°C~17.8°C, 4.5°C~13.8°C, 5.8°C~13.5°C, 3.3°C~13.3°C compared with that before the renovation of 5.8°C~18.1°C, 6.8°C~16.9°C, 1.2°C~12.0°C, 3.3°C~12.7°C, 0.11°C~12.5°C in sub-region A1 to C, respectively. The average values of mean radiant temperature are 13.9°C, 13.8°C, 10.5°C, 11.3°C, and 9.6°C after renovation, compared with the value of 10.8°C, 11.0°C, 7.2°C, 7.5°C, and 6.2°C before renovation. The renovated dwellings' indoor mean radiant temperatures have been raised 3.1°C, 2.9°C, 3.3°C, 3.8°C, 3.4°C compared with that before the renovation. The variation trend and amplitude of the indoor air temperature and mean radiant temperature are similar.

Table 8-11. The temperature variation before and after renovation in summer

Sub-region	Outdoor air temperature		Indoor air temperature				Indoor mean radiant temperature			
			Before		After		Before		After	
A1	25.4	18.6~29.2	24.0	18.5~28.0	22.8	18.7~25.7	24.5	18.8~28.5	23.0	19.1~25.7
A2	27.6	19.7~33.9	26.2	18.6~32.2	25.1	19.5~29.8	26.3	18.6~32.2	25.4	19.9~29.6
B1	24.7	19.1~30.3	22.8	17.2~27.5	21.8	17.7~25.3	23.2	17.6~27.8	22.1	18.3~25.2
B2	26.4	19.1~31.1	24.4	17.4~28.6	23.3	18.1~26.7	24.7	17.9~28.9	23.4	18.3~26.7
C	25.1	16.4~31.1	23.5	15.8~27.9	22.4	15.3~25.8	24.0	16.5~28.2	22.7	15.8~25.7

2) Temperature in summer. The Table 8-11 show that, the variation ranges of the outdoor air temperature are 18.6°C~29.2°C, 19.7°C~33.9°C, 19.1°C~30.3°C, 19.1°C~31.1°C, 16.4°C~31.1°C, with the mean value of 25.4°C, 27.6°C, 24.7°C, 26.4°C, and 25.1°C in sub-region A1 to C, respectively. After renovation, the variation ranges of the indoor mean radiant temperature are 19.1~25.7°C, 19.9~29.6°C, 18.3~25.2°C, 18.3~26.7°C, 15.8~25.7°C compared with that before the renovation of 18.8~28.5°C, 18.6~32.2°C, 17.6~27.8°C, 17.9~28.9°C, 16.5~28.2°C in sub-region A1 to C, respectively. The average values of mean radiant temperature are 23.0°C, 25.4°C, 22.1°C, 23.1°C, and 22.7°C after renovation, compared with the value of 24.5°C, 26.3°C, 23.2°C, 24.7°C, and 24.0°C before renovation. The renovated dwellings' indoor mean radiant temperatures have been decreased by 1.5°C, 0.9°C, 1.1°C, 1.3°C, 1.3°C compared with that before the renovation. The variation trend and amplitude of the indoor air temperature and mean radiant temperature are similar.

The passive design strategy applied on the traditional dwelling has a more obvious effect on the indoor air temperature and mean radiant temperature in winter than in summer, and the passive design strategies can significantly improve the indoor thermal environment of traditional dwellings in each climatic sub-region in Qinba mountainous area.

(2) Relative humidity simulation.

Figure 8-13 to Figure 8-17 show the variation trend of the outdoor and indoor relative humidity in the 5 climatic sub-regions in Qinba mountainous area.

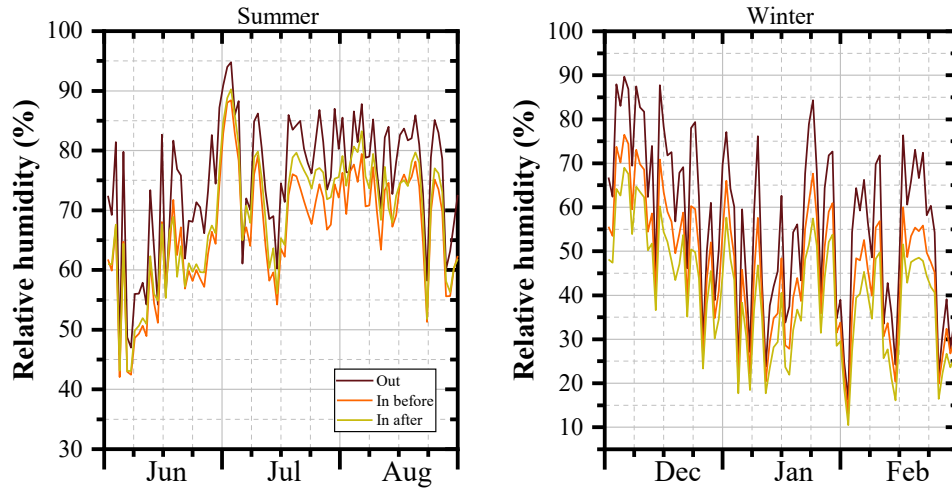


Figure 8-13. The relative humidity variation before and after renovation in climatic sub-region A1

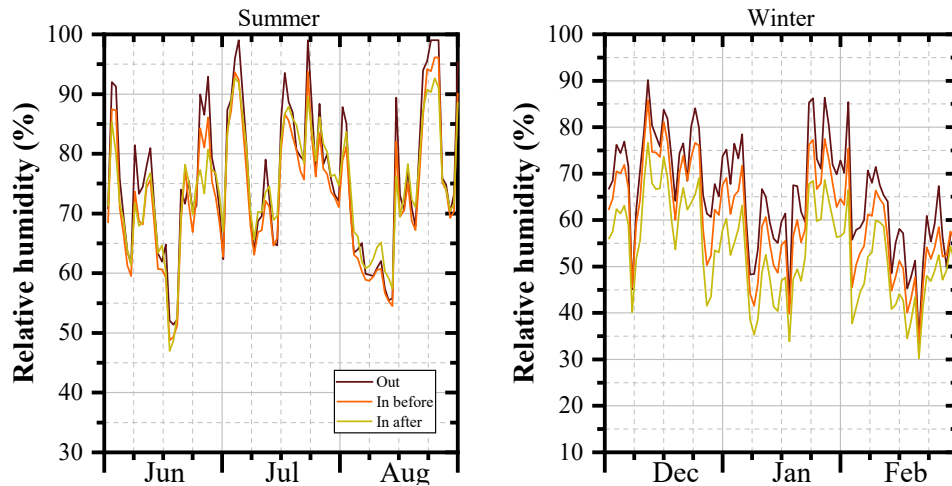


Figure 8-14. The relative humidity variation before and after renovation in climatic sub-region A2

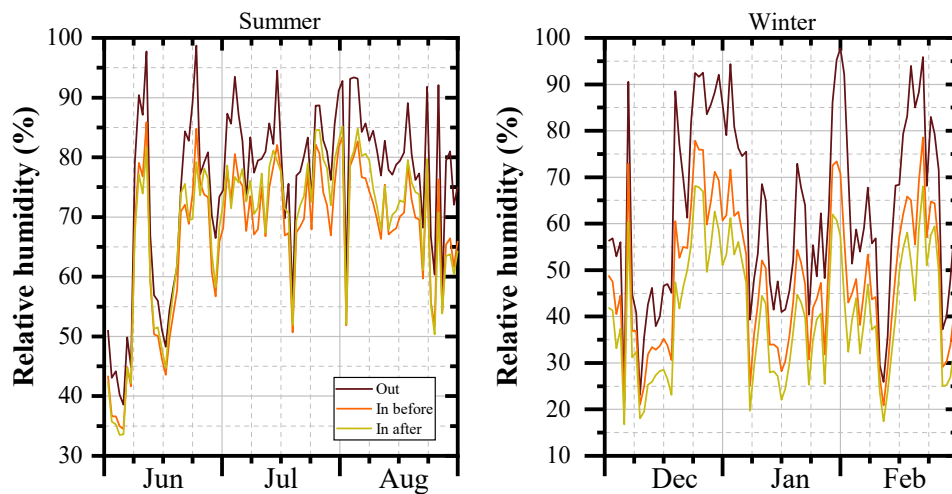


Figure 8-15. The relative humidity variation before and after renovation in climatic sub-region B1

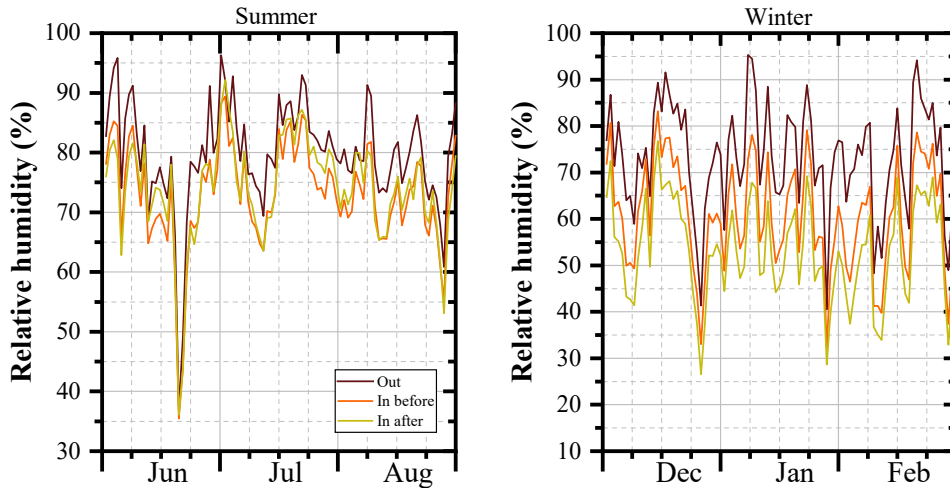


Figure 8-16. The relative humidity variation before and after renovation in climatic sub-region B2

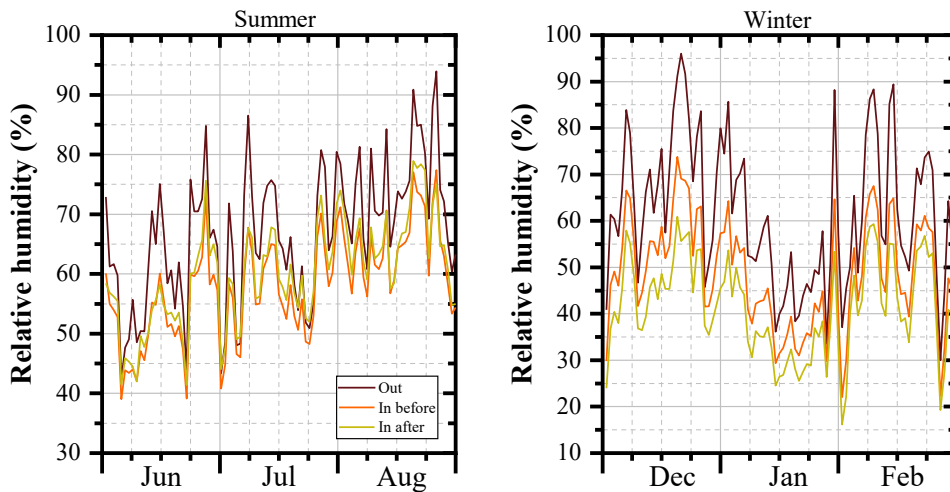


Figure. 8-17. The relative humidity variation before and after renovation in climatic sub-region C

And based on the variation trend of the relative humidities, Table 8-12 and Table 8-13 shows the variation ranges and mean values of the outdoor and indoor relative humidity in winter and summer, respectively.

Table 8-12. The relative humidity variation before and after renovation in winter

Sub-region	Outdoor relative humidity		Indoor relative humidity			
			before renovation		After renovation	
A1	57.1	16.3~89.7	46.7	13.1~76.5	40.4	10.5~69.0
A2	66.0	34.1~90.2	60.5	33.3~85.9	53.3	30.2~76.7
B1	63.4	21.7~97.8	48.8	20.3~78.6	41.3	16.8~68.2
B2	73.2	40.5~95.3	60.8	32.4~83.2	53.2	26.6~76.8
C	61.6	30.0~96.1	48.6	22.1~73.8	41.4	16.2~61.0

1) Relative humidity in winter. As illustrated in Table 8-12, the mean values of the outdoor relative humidity are 57.1%, 66.0%, 63.4%, 73.2%, and 61.6% in sub-region A1 to C. After renovation, the mean values of the indoor relative humidity are 40.4%, 53.3%, 41.3%, 53.2%, and 41.2% compared with that before the renovation of 46.7%, 60.5%, 48.8%, 60.8%, 48.6% in sub-region A1 to C, respectively. In winter, the indoor relative humidity has a certain degree of improvement after renovation, as the indoor relative humidity decreased by 6.3%, 7.2%, 7.5%, 7.6%, and 7.2% than that before renovation in sub-region A1 to C. In most of time in winter, the indoor relative humidity after renovation can meet the human comfort requirement of the relative humidity less than 70%.

Table 8-13. The relative humidity variation before and after renovation in summer

Sub-region	Outdoor relative humidity		Indoor relative humidity			
			before renovation		After renovation	
A1	75.1	45.8~94.8	66.8	42.1~88.4	68.9	43.1~90.3
A2	75.9	51.4~99.0	73.0	48.7~96.2	74.4	74.6~92.7
B1	75.9	38.6~98.7	67.2	34.5~85.9	68.5	33.5~85.2
B2	79.8	36.9~96.3	73.1	35.5~89.4	74.1	36.1~92.2
C	66.9	42.4~93.9	58.1	39.1~77.4	60.2	41.4~78.9

2) Relative humidity in summer. The Table 8-13 shows that the mean values of the outdoor relative humidity are 75.1%, 75.9%, 75.9%, 79.8%, and 66.9% in sub-region A1 to C. After renovation, the mean values of the indoor relative humidity are 68.9%, 74.4%, 68.5%, 74.1%, and 60.2% compared with that before the renovation of 66.8%, 73.0%, 67.2%, 73.1%, 58.1% in sub-region A1 to C, respectively.

In summer, there is no significant difference between the indoor relative humidity before and after renovation. The traditional dwelling can reduce the relative humidity to a certain extent, however, the outdoor relative humidity in the study area in summer is very high, the indoor relative humidity still has 51.1%, 68.5 %, 62.0 %, 72.8 %, and 14.1% of the time greater than 60%.

The passive design strategy applied on the traditional dwelling also has a more obvious effect on the indoor relative humidity in winter than in summer, and the passive design strategies can significantly improve the indoor humidity environment of traditional dwellings in winter. However, further research should continue to pay attention to improving the indoor humidity in summer by using dehumidification equipment.

8.5. Summary

In this chapter, by using the computer simulation, statistical analysis, NSGA-2, and TOPSIS method, the multi-objective optimization approaches to enhance the building energy efficiency, thermal comfort, and cost-effectiveness of passive design strategies for traditional dwellings in the 5 climatic sub-regions of Qinba mountainous area were obtained. The proposed process enables decision-makers to assess and compare hundreds of design solutions and prioritize alternative options in order to identify the most suitable one while balancing energy, comfort, and cost objectives. As a result, the strategy of achieving “low energy consumption with high thermal comfort and balanced economy” can be applied to buildings in other climate zones. The main conclusions of this chapter are as follows:

1) In this chapter, multiple regression equations based on passive design strategies (including sunroom depth, external wall heat transfer coefficient, roof heat transfer coefficient, and window heat transfer coefficient) were fitted to obtain the building annual thermal load, proportion of uncomfortable hours, and renovation investment for each climatic sub-region. By inputting the passive design parameters into the energy simulation software, the simulated outputs have small errors compared to the data obtained by NSGA2 through multiple regression equations. The high reliability of the optimal solution set data can be ensured.

2) This section proposes a multi-objective optimization model based on the TOPSIS method, NSGA2 genetic algorithm, and multiple regression analysis, with the goals of “energy efficiency”, “thermal comfort”, and “cost-effectiveness”. The model can obtain the optimal solution for the passive design parameters of traditional dwellings in Qinba mountainous area after balancing the three objectives. By using this model, 20 optimal solutions for the three-objective optimization of passive design parameters in the 5 climatic sub-regions of the Qinba mountainous area have been obtained.

3) This study also selects the optimal solutions for each climatic sub-region and simulates the building annual thermal loads of the optimal solutions using energy simulation software. The annual building thermal loads of the traditional dwellings after renovation in climatic sub-regions A1 to C are 14.990kWh/m², 13.992kWh/m², 17.124kWh/m², 15.567kWh/m², 18.870kWh/m², respectively, which is reduced by 60.43%, 58.02%, 62.30%, 65.12%, and 62.59% than the value of 37.879kWh/m², 33.328kWh/m², 45.424kWh/m², 44.631kWh/m², and 50.440kWh/m² before renovation.

4) The optimal solution was selected for simulation, and the indoor temperature and relative humidity before and after renovation were obtained without the use of cooling and heating equipment. The renovated dwellings' indoor mean radiant temperatures have been raised 3.1°C, 2.9°C, 3.3°C, 3.8°C, 3.4°C compared with that before the renovation in winter, and it have been decreased by 1.5°C, 0.9°C, 1.1°C, 1.3°C, 1.3°C compared with that before the renovation in summer. The indoor relative humidity decreased by 6.3%, 7.2%, 7.5%, 7.6%, and 7.2% than that before renovation in sub-region A1 to C in winter, but there is no significant difference

between the indoor relative humidity before and after renovation in summer. The passive design strategy applied on the traditional dwelling has a more obvious effect on the indoor air temperature, mean radiant temperature, and relative humidity in winter than in summer, and the passive design strategies can significantly improve the indoor physical environment of traditional dwellings in each climatic sub-region in Qinba mountainous area.

References

- [1] S. El Ahmar, F. Battista, and A. Fioravanti, "Simulation of the thermal performance of a geometrically complex Double-Skin Facade for hot climates: EnergyPlus vs. OpenFOAM," in *Building Simulation*, 2019, vol. 12, pp. 781-795: Springer.
- [2] G. A. Seber and A. J. Lee, *Linear regression analysis*. John Wiley & Sons, 2003.
- [3] L. Yang, L. Hou, H. Li, X. Xu, and J. Liu, "Regression models for energy consumption prediction in air-conditioned office building," *Journal of Xi'an University of Architecture and Technology (Natural science edition)*, vol. 47, no. 05, pp. 707-711, 2015.
- [4] K. Deb, M. Mohan, and S. Mishra, "A fast multi-objective evolutionary algorithm for finding well-spread pareto-optimal solutions," *KanGAL report*, vol. 2003002, pp. 1-18, 2003.
- [5] X. Cao et al., "A three-stage decision-making process for cost-effective passive solutions in office buildings in the hot summer and cold winter zone in China," *Energy and Buildings*, vol. 268, p. 112173, 2022.
- [6] E. Zitzler and L. Thiele, "Multiobjective evolutionary algorithms: a comparative case study and the strength Pareto approach," *IEEE transactions on Evolutionary Computation*, vol. 3, no. 4, pp. 257-271, 1999.
- [7] A. Ghosh and S. Neogi, "Effect of fenestration geometrical factors on building energy consumption and performance evaluation of a new external solar shading device in warm and humid climatic condition," *Solar Energy*, Article vol. 169, pp. 94-104, Jul 15 2018.
- [8] Y. Yu, Y. Luo, and J. An, *Probability and statistics with SPSS application*. Xi'an, China: Xi'an Jiaotong University Press, 2009.
- [9] X. He, *Applied multivariate statistical analysis*. Beijing, China: China Statistics Press, 2010.
- [10] K. Deb, S. Agrawal, A. Pratap, and T. Meyarivan, "A fast elitist non-dominated sorting genetic algorithm for multi-objective optimization: NSGA-II," in *Parallel Problem Solving from Nature PPSN VI: 6th International Conference Paris, France, September 18–20, 2000 Proceedings 6*, 2000, pp. 849-858: Springer.
- [11] H. H. Hosamo, M. S. Tingstveit, H. K. Nielsen, P. R. Svennevig, and K. Svidt, "Multiobjective optimization of building energy consumption and thermal comfort based on integrated BIM framework with machine learning-NSGA II," *Energy and Buildings*, vol. 277, p. 112479, 2022.
- [12] P. Kumar and P. Sarkar, "A comparison of the AHP and TOPSIS multi-criteria decision-making tools for prioritizing sub-watersheds using morphometric parameters' analysis," *Modeling Earth Systems Environment*, vol. 8, no. 3, pp. 3973-3983, 2022.
- [13] H.-Q. Nguyen, V.-T. Nguyen, D.-P. Phan, Q.-H. Tran, and N.-P. Vu, "Multi-criteria decision making in the PMEDM process by using MARCOS, TOPSIS, and MAIRCA methods," *Applied sciences*, vol. 12, no. 8, p. 3720, 2022.
- [14] B. Ceballos, M. T. Lamata, and D. A. Pelta, "A comparative analysis of multi-criteria

decision-making methods,” *Progress in Artificial Intelligence*, vol. 5, pp. 315-322, 2016.

[15] X. Cao et al., “Energy-quota-based integrated solutions for heating and cooling of residential buildings in the Hot Summer and Cold Winter zone in China,” *Energy and Buildings*, vol. 236, p. 110767, 2021.

[16] N. Delgarm, B. Sajadi, and S. Delgarm, “Multi-objective optimization of building energy performance and indoor thermal comfort: A new method using artificial bee colony (ABC),” *Energy and Buildings*, vol. 131, pp. 42-53, 2016.

Chapter 9

CONCLUSION AND PROSPECT

CHAPTER NINE: CONCLUSION AND PROSPECT

CONCLUSION AND PROSPECT..... 1

9.1. Conclusion..... 1

9.2. Prospect 5

9.1. Conclusion

Given China's goal of achieving a carbon peak by 2030, as well as the pressing energy consumption and environmental challenges, reducing building energy use has become an urgent priority. Passive design is an effective climate adaptive approach that can help to save energy, reduce emissions, and enhance indoor thermal comfort without relying on artificial energy resources. It is also essential to consider local climate conditions when developing passive design strategies. Climate zoning can aid in the formulation of building energy conservation standards and the adaptation of energy conservation technologies according to the region. Furthermore, given that rural regions in China account for 34% of the building area and 22% of total building energy consumption as of 2020, improving indoor thermal comfort and reducing energy consumption in traditional rural dwellings is of paramount importance. With a large number of rural dwellings and an increasing demand for thermal comfort and energy efficiency, utilizing passive strategies that leverage climate adaptability is crucial. The main works and results in this research can be summarized as follows:

CHAPTER 1, RESEARCH BACKGROUND AND PURPOSE OF THE STUDY. This chapter introduced the China's urbanization process and carbon emissions, the status of energy consumption in rural residential buildings in China, the ecological architecture and passive design strategy, and the climate adaptability of traditional dwellings. Against the backdrop of large stock of rural dwellings, continuously increasing demand for residents' thermal comfort and building energy consumption, utilizing traditional dwellings' climate adaptability (passive strategies) to improve the indoor thermal comfort and reduce building energy consumption in rural areas has significant implications.

CHAPTER 2, LITERATURER REVIEW. In this chapter, the relevant research of this paper is well reviewed, including the literature review of climatic subdivision, thermal comfort, and passive design strategy. The previous studies of climatic subdivision and China's current climate zoning standards have been discussed in the climatic subdivision section. The previous studies and evaluation indicators of thermal comfort have been reviewed in the thermal comfort section. The previous studies and types of passive design strategies have been described in the passive design strategy section. Through the previous research on climate-adaptive and energy-saving strategies in recent years, it has been found that most studies focus on the existing climate zones and pay attention to single aspects such as residential thermal environment, thermal comfort, and energy consumption. And there is less research on the behavior adjustment methods in thermal adaptation, especially in the studies on the relationship between climate adaptation and thermal comfort renovation, which mostly provide qualitative descriptions. There is also a lack of passive design methods and technical strategies for climate adaptation in the design stage. Therefore, it is worth studying the indoor thermal comfort improvement of traditional residential buildings in the Qinba mountainous area based on the investigation of thermal comfort under the background of climate subdivision.

CHAPTER 3, RESEARCH METHODOLOGY. The primary focus of this paper is to investigate the climatic subdivision of the Qinba mountainous area, assess residents' thermal comfort, and optimize passive design strategies for dwellings in the region. In this chapter, we provide an overview of the methodologies employed in the research, including the spatial interpolation method, field survey method, computer simulation method, statistical analysis method, and multi-objective optimization genetic algorithm method. These methods were used to organize and classify meteorological data, calculate thermal comfort indicators, simulate building energy consumption before and after implementing passive design strategies, and ultimately obtain the optimal optimization solutions for each climatic sub-region. By employing these methods, we were able to effectively optimize passive design strategies to enhance energy efficiency and thermal comfort for dwellings in the Qinba mountainous area.

CHAPTER 4, CLIMATIC SUBDIVISIONS IN QINBA MOUNTAINOUS AREA. In this chapter, by using Co-Kriging spatial interpolation and computer simulation method, the Qinba mountainous area are subdivided into 5 climatic sub-regions, and the climatic supplementary elements are also classified to describe the climatic characteristics of the region. Firstly, based on Co-Kriging spatial interpolation method, by applied the value of HDD18 and CDD26 from 2011 to 2020, the Qinba mountainous area are divided in 5 climatic sub-regions: sub-region A1 ($1000^{\circ}\text{C}\cdot\text{d} < \text{HDD18} < 1600^{\circ}\text{C}\cdot\text{d}$, $60^{\circ}\text{C}\cdot\text{d} < \text{CDD26} < 200^{\circ}\text{C}\cdot\text{d}$); sub-region A2 ($1000^{\circ}\text{C}\cdot\text{d} < \text{HDD18} < 1600^{\circ}\text{C}\cdot\text{d}$, $60^{\circ}\text{C}\cdot\text{d} < \text{CDD26} < 200^{\circ}\text{C}\cdot\text{d}$); sub-region B1 ($1600^{\circ}\text{C}\cdot\text{d} < \text{HDD18} < 2200^{\circ}\text{C}\cdot\text{d}$, $0^{\circ}\text{C}\cdot\text{d} < \text{CDD26} < 60^{\circ}\text{C}\cdot\text{d}$); sub-region B2 ($1600^{\circ}\text{C}\cdot\text{d} < \text{HDD18} < 2200^{\circ}\text{C}\cdot\text{d}$, $60^{\circ}\text{C}\cdot\text{d} < \text{CDD26} < 200^{\circ}\text{C}\cdot\text{d}$); sub-region C ($2200^{\circ}\text{C}\cdot\text{d} < \text{HDD18} < 3200^{\circ}\text{C}\cdot\text{d}$, $0^{\circ}\text{C}\cdot\text{d} < \text{CDD26} < 60^{\circ}\text{C}\cdot\text{d}$). Then, by using Co-Kriging method, the 5 climatic sub-regions were added the supplementary meteorological information such as relative humidity, wind speed, and solar radiation. Finally, the climatic conditions and building annual thermal loads of the representative counties in the 5 climatic sub-regions were analyzed, the result shows that the change law of air temperatures and building annual thermal loads in the 5 representative counties in each climatic sub-regions conform to the climate subdivision logic of Qinba mountainous area.

CHAPTER 5, FIELD SURVEY AND TRADITIONAL DWELLING' ENVIRONMENTAL MEASUREMENT IN THE CLIMATIC SUB-REGIONS. In this chapter, by using the field survey method, the characteristics of traditional settlements, courtyards, and residential dwellings were summarized, and the environmental parameters measurement of 5 sub-climatic sub-regions were conducted. Firstly, according to the mountain geomorphic environment and settlement location in Qinba mountainous area, the settlements could be divided into 3 types, which are settlement in the gully, settlement leaning against the mountain, and settlement on the mountain slope. Then, the building layout of traditional dwellings in the study area can be divided into 4 types, the "I"-shaped dwelling, the "L"-shaped dwelling, the "U"-shaped dwelling, and the "□"-shaped building, accounting for 52.0%, 23.5%,

12.0% and 12.5% of the total sample size, respectively. According to the architectural form, the courtyards are divided into 3 types: open courtyards, semi-open courtyards, and closed courtyards, accounting for 75.5%, 12%, and 12.5% of the total sample size, respectively. Finally, the research team also conducted multiple investigations on traditional dwellings in the 5 climatic sub-regions during winter and summer. The survey results indicate that the study area is generally cold and humid in winter, failing to meet the requirements of human comfort. During summer, the overall relative humidity tends to be high. However, except for some areas where the indoor temperature occasionally exceeds human comfort requirements, the indoor temperature remains moderate for most of the time. In general, the variation range of indoor temperature and humidity in traditional dwellings is smaller than that outdoors, indicating that the traditional dwellings have a certain regulating effect on the indoor physical environment.

CHAPTER 6, THERMAL COMFORT INVESTIGATION OF THE CLIMATIC SUB-REGIONS. In this chapter, by using field survey, statistical analysis, and computer simulation method, the indoor thermal environment of traditional dwellings in the 5 climatic sub-regions in Qinba mountain area was compared, the thermal sensation of residents was investigated. Firstly, the outdoor and indoor environmental parameters' measurement and residents' thermal sensation questionnaire research were conducted. Then, the linear regression analysis was applied to the mean thermal sensation voting (MTS) and the indoor operating temperature (Top) to obtain the thermal comfort equations in each climatic sub-region, and the neutral temperatures and thermal comfort ranges in each climatic sub-region were calculated. The neutral temperatures of residents are 15.8°C, 15.8°C, 14.3°C, 14.3°C, 13.4°C in winter and 26.6°C, 27.3°C, 26.6°C, 27.3°C, and 26.6°C in summer respectively. And the thermal comfort ranges are 13.9~17.6°C, 13.9~17.6°C, 12.6~16.0°C, 12.6~16.0°C, and 11.4~15.4°C in winter and 21.4~31.7°C, 21.4~33.2°C, 21.4~31.7°C, 21.4~33.2°C, 21.4~31.7°C in summer, respectively. In winter, the predicted indoor neutral temperatures are higher than the measured thermal neutral temperature, and in summer, the predicted indoor neutral temperatures are lower than the measured thermal neutral temperature, indicating that the residents have certain adaptability to the actual thermal environment. Finally, the annual building thermal loads of typical traditional dwellings in the 5 climatic sub-regions' representative counties based on standard requirements and measured neutral temperature are simulated. The annual thermal loads based on the measured neutral temperature are 37.86 kWh/m², 33.33 kWh/m², 45.42 kWh/m², 44.61 kWh/m², and 50.44 kWh/m² from climatic sub-region A1 to C, respectively, which is 31.32 %, 35.28 %, 37.86 %, 39.37 %, and 41.82 % lower than that based on the standard requirements of 54.87 kWh/m², 50.50 kWh/m², 73.09 kWh/m², 73.58 kWh/m², and 86.69 kWh/m².

CHAPTER 7, EFFECTIVENESS STUDY OF PASSIVE DESIGN PARAMETERS FOR TRADITIONAL DWELLING. In this chapter, by using computer simulation, statistical analysis, and orthogonal arrays method, the effectiveness of passive design parameters was

evaluated in each sub-region and the single-objective optimization approaches to enhance the building energy efficiency of the passive design strategies in climatic sub-region A1 were obtained. Firstly, for the single controlled variable study, the energy consumption analysis and relative sensitivity coefficient calculation of 11 passive design parameters were simulated in 5 climatic sub-regions in Qinba mountainous area, and the 4 effective passive renovation parameters for traditional dwellings were sunroom depth, exterior wall heat transfer coefficient, roof heat transfer coefficient and window heat transfer coefficient as the average relative sensitivity coefficient (ω_i) of these 4 parameters 19.16%, 23.50%, 32.23%, and 19.53%, respectively. Then, for the multi controlled variable study, this research applied the orthogonal arrays analysis to evaluate 4 effective parameters to obtain the optimal combination. Finally, the building annual thermal loads of the optimal renovated dwelling in climatic sub-region A1 were simulated through energy simulation software. The result shows that the optimal combination could reduce the annual energy consumption of the simulated dwelling by 65.1% compared with that of the original one.

CHAPTER 8, MULTI-OBJECTIVE OPTIMIZATION OF COST-EFFECTIVE PASSIVE STRATEGIES FOR TRADITIONAL DWELLING. In this chapter, by using the computer simulation, statistical analysis, NSGA-2, and TOPSIS method, the multi-objective optimization approaches to enhance the building energy efficiency, thermal comfort, and cost-effectiveness of passive design strategies for traditional dwellings in the 5 climatic sub-regions of Qinba mountainous area were obtained. Firstly, the multiple regression equations based on the 4 effective passive design parameters (including sunroom depth, external wall heat transfer coefficient, roof heat transfer coefficient, and window heat transfer coefficient) were fitted to obtain the building annual thermal load, proportion of uncomfortable hours, and renovation investment for each climatic sub-region. In addition, the NSGA-2 genetic algorithm has been used to find the Pareto optimal solution set based on a multi-regression equation with the three objectives (energy efficiency, thermal comfort, and cost-effectiveness). Then, based on the Euclidean distance of the TOPSIS method, 20 optimal solutions for the three-objective optimization in the Pareto set in the 5 climatic sub-regions of the Qinba mountainous area have been obtained. Finally, the building annual thermal loads and indoor comfort values of the optimal renovated dwelling in each climatic sub-region were simulated through energy simulation software. The result shows that the annual building thermal loads of the traditional dwellings after renovation in climatic sub-regions A1 to C are 14.990kWh/m², 13.992kWh/m², 17.124kWh/m², 15.567kWh/m², 18.870kWh/m², respectively, which is reduced by 60.43%, 58.02%, 62.30%, 65.12%, and 62.59% than the value of 37.879kWh/m², 33.328kWh/m², 45.424kWh/m², 44.631kWh/m², and 50.440kWh/m² before renovation. The renovated dwellings' indoor mean radiant temperatures have been raised 3.1°C, 2.9°C, 3.3°C, 3.8°C, 3.4°C compared with that before the renovation in winter, and it have been decreased by 1.5°C, 0.9°C, 1.1°C, 1.3°C, 1.3°C compared with that before the renovation in summer. The indoor relative

humidity decreased by 6.3%, 7.2%, 7.5%, 7.6%, and 7.2% than that before renovation in sub-region A1 to C in winter, but there is no significant difference between the indoor relative humidity before and after renovation in summer. The passive design strategy applied on the traditional dwelling has a more obvious effect on the indoor air temperature, mean radiant temperature, and relative humidity in winter than in summer, and the passive design strategies can significantly improve the indoor physical environment of traditional dwellings in each climatic sub-region in Qinba mountainous area. As a result, the strategy of achieving “low energy consumption with high thermal comfort and balanced economy” can be applied to buildings in other climate zones.

CHAPTER 9, CONCLUSION AND PROSPECT. In this chapter, a concise summary of each preceding chapter is provided.

In conclusion, the Qinba mountainous area is vast, with complex terrain and diverse climate. In order to better match different thermal comfort ranges, passive design strategies, and their parameters, a detailed climate zoning is required. Studies have shown that residents’ heat demand varies across climatic sub-regions in Qinba mountainous area. Therefore, setting the cooling and heating set points based on different heat demands can effectively reduce energy consumption. Furthermore, the additional sunroom, external wall heat transfer coefficient, roof heat transfer coefficient, and window heat transfer coefficient are effective passive strategies in all of the climatic sub-regions in Qinba mountainous area. However, the passive design parameters’ values based on multi-objective (energy efficiency, thermal comfort, and cost-effectiveness) optimization are different in each climatic sub-region. Adopting a multi-objective optimization strategy can help to screen out the optimal passive design strategy for each sub-region. Applying the optimal solution can effectively reduce building energy consumption and improve indoor thermal comfort, under the premise of low renovation costs. The findings of the study will serve as a reliable reference for building designers, as well as for the modification of energy efficiency design guidelines for the selection of building energy saving schemes.

9.2. Prospect

This study focuses on the climatic subdivision of the Qinba mountainous area, conducting an investigation into the thermal comfort of traditional dwellings, and implementing a multi-objective optimization of passive design strategies. Rural residential buildings make up a large proportion of the residential buildings in Qinba mountainous area, with not only traditional dwellings but also a significant number of newly constructed rural self-built residential buildings in recent years. Due to outdated design concepts, construction technology, and insufficient building funds, the indoor thermal comfort of the new construction is poor, requiring high energy consumption to maintain a relatively comfortable indoor environment. Therefore, the next steps in this research will mainly focus on the design strategies for newly

constructed rural homes, including:

(1) Further research should focus on exploring and simulating the orientation, functional layout, and form of newly constructed rural residential buildings, designing building modules that are suitable for different family sizes and functional needs, and providing guidance for the concept design of new rural residential buildings.

(2) Further research also needs to concentrate on studying the impact of local building materials on building energy consumption, thermal comfort, and construction cost, and seeking environmentally friendly building materials with good thermal insulation performance, low cost, and the ability to retain the regional characteristics of rural homes, in order to improve indoor thermal comfort while reducing energy consumption.

(3) At the same time, researches should apply the logic and methods of this study to other areas, explore the climate zoning and climate suitability improvement strategies for rural areas in hot summers and cold winter zone.